The Hashemite Kingdom of Jordan
Scientific Research Support Fund
The Hashemite University

JJEES

Jordan Journal of Earth and Environmental Sciences

Indexed by Scopus
ELSEVIER

Volume (14) Number (2)

Cover photo © Prof. Eid Al Tarazi

JJEES is an International Peer-Reviewed Research Journal

ISSN 1995-6681 jjees.hu.edu.jo June 2023

Jordan Journal of Earth and Environmental Sciences (JJEES)

JJEES is an International Peer-Reviewed Research Journal, Issued by Deanship of Scientific Research, The Hashemite University, in corporation with, the Jordanian Scientific Research Support Fund, the Ministry of Higher Education and Scientific Research.

Editorial Board:

Associate Editorial Board: (Arranged Alphabetically)

International Advisory Board: (Arranged Alphabetically)

Editorial Board Support Team:

Submission address:

Manuscripts should be submitted electronically to the following e-mail:

jjees@hu.edu.jo

For more information and previous issues:

www.jjees.hu.edu.jo

Hashemite Kingdom of Jordan

Scientific Research Support Fund

Hashemite University

Jordan Journal of Earth and Environmental Sciences

JJEES

An International Peer-Reviewed Scientific Journal

Financed by the Scientific Research Support Fund

Volume 14 Number (2)

http:// jjees.hu.edu.jo/

ISSN 1995-6681

*Water Harvesting - Wadi Mushash - Muwaqqar Area, Jordan 2023.
Photographed by Prof. Eid Al Tarazi

JJEES
Jordan Journal of Earth and Environmental Sciences

PAGES	PAPERS
83 - 90	Flood Disaster Preparedness and Capacity Assessment Among Crop Farmers in Edo State, Nigeria. *Odiana S., Mbee D. M and Akpoghomeh O. S*
91 - 102	Mineralogy and Geochemistry of Beryl-Bearing Prgmatite Dykes from Gbayo, Southwestern Nigeria *Razak O. Jimoh, Akinade S. Olatunji, Jimoh Ajadi and Adegoke O. Afolabi*
103 - 112	Assessing The Extent of Public Participation in Planning and Management of Conservation Areas in Nigeria *Hassan Abdulaziz, Shuaibu Abdul-Wahab and Ibrahim Jibrin Abubakar*
113- 125	Hydrogeological Modeling of the Sandstone Aquifer of Mostaganem Plateau (North-West Algerian) and Perspectives on the Evolution of Withdrawals *Bentahar Fatiha, Mesbah Mohamed and Ribstein Pierre*
126 -134	Geochemistry of Detrital Chromite from Gercus Formation (M. Eocene), Northern Iraq: Implications for the Provenance and Paleotectonic *Zahraa J. Al-Jubory, Falah A. Al-Miamary, Safwan F. Al-Lhaebi and Harvey E. Belkin*
135 - 145	Effect of Irrigation with Treated Wastewater on Potatoes' Yields, Soil Chemical, Physical and Microbial properties *Hasan Alkhaza'leh, Ahmad Abu-Awwad and Mohammed Alqinna*
146 - 157	Geochemistry and Tectonic Setting of the Metagabbros of Penjween Ophiolite Complex, Northeastern Iraq *Omar S. Al-Taweel, Flyah H. Al-Khatony, Mohammed A. Al-Jboury and Shareef Th. Al-Hamed*
158 - 174	Integrated evaluation of soil erosion-prone areas based on the GIS technique and the analytic hierarchy process on hillside slopes, northwest of Jordan *Noah Mohammad Ali Al-Sababhah and Mohammad Mahmoud Al maqablah*

JJEES

JJEES (2023) 14 (2): 83-90
ISSN 1995-6681

Jordan Journal of Earth and Environmental Sciences

Flood Disaster Preparedness and Capacity Assessment Among Crop Farmers in Edo State, Nigeria.

Odiana S.,[1] Mbee D. M[2], Akpoghomeh O. S.[3]

[1]Department of Environmental Management and Toxicology, Faculty of Life Sciences, University of Benin, P.M.B. 1154, Benin City, Edo State, Nigeria.
[2,3] Department of Geography and Environmental Management, Faculty of Social Sciences, University of Port Harcourt. P.M.B. 5323, Port Harcourt, Rivers State, Nigeria.

Received 7th February 2022; Accepted 26th September 2022

Abstract

Flood occurs when there is an overflow of any area which is not normally covered with water. It has claimed many lives, displaced millions, and destroyed crops and farmlands. It is more pronounced in developing nations where the level of preparedness and coping capacity are low in comparison with developed ones. It is against this background that this study evaluated flood disaster preparedness and capacity assessment among crop farmers in Edo State Nigeria. The sample size was determined using the Taro Yammane formula. A total of 400 crop farmers were drawn as the sample size. The study used survey research techniques where questionnaires designed on a Likert scale were distributed to the crop farmers obtained using a multistage sample technique. Key informant interview was also carried out with the staff of the Edo State Agricultural Development Programme. The data obtained were analyzed using mean and standard deviation. The result obtained revealed that most of the crop farmers were in their economically productive age, literate, and had poor coping capacity. The findings also revealed that though they applied some forms of preparedness measures but were still not better prepared for the disaster. They were also faced with challenges concerning coping and preparedness to flood disasters. Therefore, crop farmers in Edo State have poor coping capacity and are not effectively prepared against flooding. Government at all levels should intensify flood control measures and provide poverty alleviation programs that will be beneficial to crop farmers.

Keywords: *Flooding, Crop, Farmers, Preparedness, Coping, Challenges*

1. Introduction

Flooding is expressed as the surplus of water in a place that is naturally dry (Stephen, 2011). It might be seen as a relative spill of water over the banks of surface water bodies like rivers. Flooding can also be considered as an outpouring of water that comes from a river, reservoirs, lakes, etc, and bring about destruction to lives and properties. (Ojo, 2007). It is a condition of partial or whole submergence of an area due to spillover from the sporadic and speedy buildup of runoff (Onuigbo *et al.,* 2017). It is probably the most damaging, common, and frequent natural hazard in the world (Al Azzam and Al Kuisi, 2021). A flood happens as soon as the water in a river or any water body flows out of its boundaries and submerges nearby areas (Stephen, 2011). Some of the factors resulting in flood disasters include the throwing away of solid wastes in drains and on the floodplain (Sarah 2007) cited in Okeleye (2016). James (2000) reported that uncontrolled urbanization such as building along flood plains, and unrestrained advancement of structures into flood plains alongside massive road construction with large-scale land recovery result in flood disaster. Ajayi (2012) cited in Okeleye (2016) stated that raising infrastructures along the riverway caused major flooding in Oyo State. Farmers are usually challenged and ascertaining the damage caused to farmers may not be easy but it is believed to be a problem to their livelihood (Alade and Ademola 2013). In Nigeria, flooding has brought about an increase in the prices of food crops, leading to an inflation upsurge of 2% (Onwuka *et al.,* 2015). There is therefore the need for preparedness and coping.

World Health Organisation (2007), opined that preparedness is activities carried out by individuals or communities to enable them to take better actions in the case of emergency and disaster conditions. Preparedness is seen as actions geared towards enhancing coping potentials. Disaster preparedness is a vital constituent of any disaster management because it reduces detrimental outcomes (Odunola and Balogun, 2015). Capacity assessment on the other hand is the way the capacity of a group or individual is evaluated against anticipated goals, where prevailing capacities are known for maintenance and capacity gaps are set apart for further action (UNDRR, 2017). Coping capacity can be influenced by a high incidence of urban poverty. Poverty is a major militating factor in Nigeria (Lame and Yosoff, 2015; Ike and Uzokwe 2015). It is against this background that this study was carried out to evaluate the preparedness and coping capacity of crop farmers in Edo State, Nigeria.

2. Methodology

This study was carried out in Edo State Nigeria as shown in Figure 1, comprising Edo South, Central, and North Senatorial Districts. Edo state which was created in 1991 out of the old Bendel state is one of the Niger Delta States. It

* Corresponding author e-mail: odiana09@yahoo.com

has a population of 3218332 comprising 1640461 males and 1577871 females based on the 2006 census. The state covers a land mass of about 19638SqKm. Common food crops grown in the State include cassava, yam, maize, rice, and plantain. The State is divided into three (3) agro-ecological zones namely Edo North, Edo Central, and Edo South to Edo State Agricultural Development Programme (ADP) delineation (Edo State government, 2013; Erie, 2007) cited in Alufohai *et al* (2015).

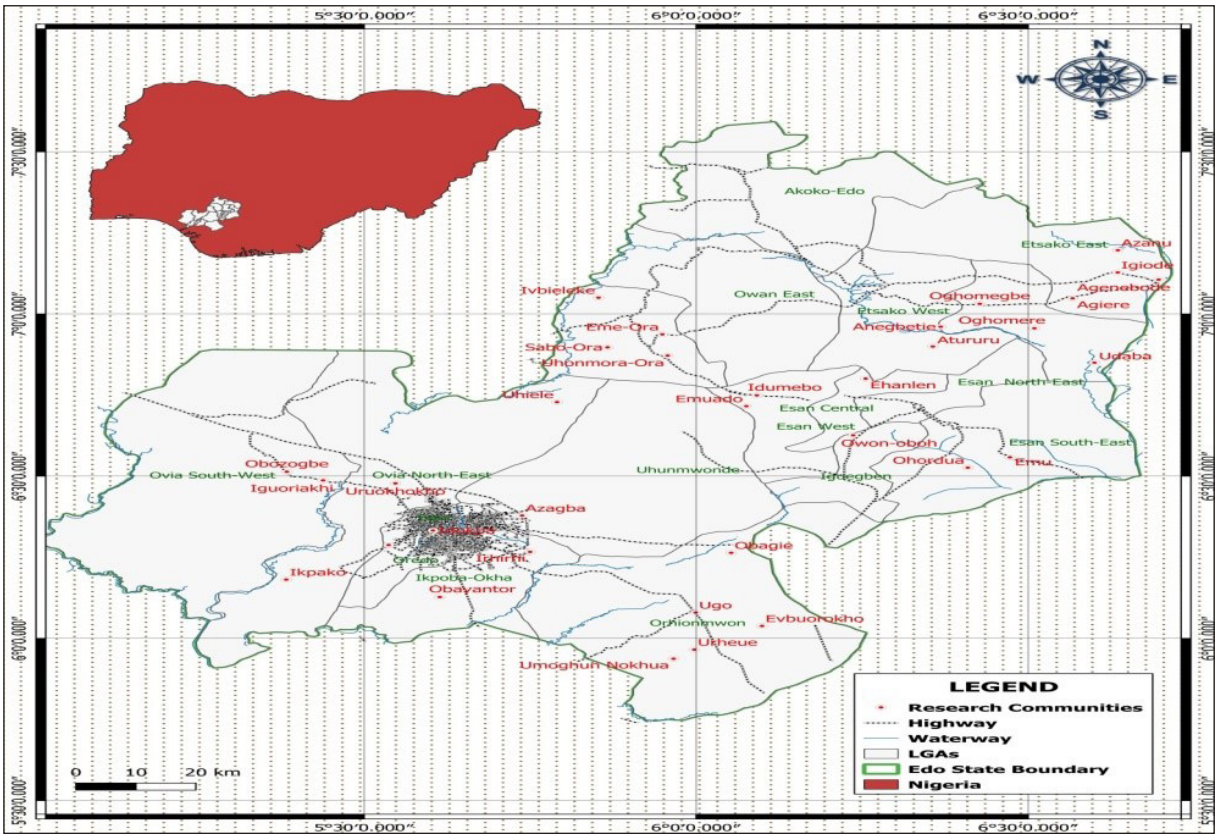

Figure 1. Map of Edo State showing the farming communities studied

2.1 Sample Size Determination

The study drew a sample size of 400 from a total of 91000 crop farmers in Edo State. The sample size was determined using the formula for sample size determination as given by Yamane (1967) as

$$n = \frac{N}{1 + N(e)^2}$$

Where

n = sample size

N = population size (number of crop farmers in Edo State)

e = acceptable sampling error margin ie 0.05

1 = constant

2.2 Sampling Techniques

A multistage sampling technique was used to select four hundred (400) crop farmers for this study. Firstly, ten (10) agricultural blocks were randomly selected. In each agricultural block and with the assistance of the Extension Services Department, farming communities/cells were identified, from which four (4) communities/cells were randomly selected making a total of forty (40) communities/cells for the study. In each selected community/cell, with the assistance of Extension Agents, ten (10) crop farmers were randomly selected, bringing the total sampled respondents to four hundred (400) for the study.

2.3 Methods of Data Collection and Analysis

Questionnaires designed on the Likert scale as well as interviews with Staff of the Edo State Agricultural Development Programme were used to obtain information for this study. The data collected were subjected to descriptive statistics such as mean and standard deviation. Other descriptive statistical methods that were employed were simple frequency, percentages, charts, and graphs where necessary.

3. Results

3.1 Demographic Characteristics of the Crop Farmers

The gender, age, marital status and educational level of the crop farmers are shown in Table 1 below. There were 71.3% male and 28.8% female which means that most of the crop farmers were male. In terms of age, 10.5% were less than 30 years, 35.3% were between 31-40 years, 34.8% were between 41-50 years 19.5% were over 50 years. This showed that most of the crop farmers were in their economically productive age. This is beneficial because young age farmers could have higher tendencies to cope and prepare for flooding than the much-aged ones. As shown in the table, 84.3% were married, 11.5% were single, 2.8% were widows/widowers and others made up 1.5% indicating that they were mostly married persons. This could enhance their preparedness as married farmers would have immediate family members that can render some needed assistance. The result also revealed

that 33.5% had only primary school education, 49.0% had secondary education, 11.5% had tertiary education and 6.0% had no formal education signifying that most of the crop farmers were literate. Being mostly literate connotes that accepting innovations that could help in improving their capacity and preparedness for flooding would not be difficult.

Table 1. Demographic characteristics of the crop farmers

Characteristics	Components	Frequency	Percentage (%)
Gender	Male	285	71.2
	Female	115	28.8
	Total	400	100.0
Age	30 or less	42	10.5
	31-40	141	35.3
	41-50	139	34.8
	50 and above	78	19.5
	Total	400	100.0
Marital Status	Married	337	84.3
	Single	46	11.5
	Widow or widower	11	2.8
	Others	6	1.5
	Total	400	100.0
Educational Level	Primary	134	33.5
	Secondary	196	49.0
	Tertiary	46	11.5
	No formal education	24	6.0
	Total	400	100.0

Source: Researcher's computation, 2021

3.2 Coping Capacity of Crop Farmers to Flood Hazard

The mean of the result on the coping capacity of crop farmers to flooding, as shown in Table 2 below, revealed that the crop farmers agreed to only one item analyzed. That is, people living with you have one another's contacts to call should a flood disaster occur. They were however in disagreement with other items. Therefore, from the result, it can be deduced that the crop farmers had poor coping capacity to flood disasters.

Table 2. Coping capacity of crop farmers to flood hazard

	N	Sum	Mean	SD
having a different savings food is being practiced by you	400	771	1.93	.827
Planning for flood disasters is being practiced by you	400	887	2.22	1.041
There is a place where people are to meet should flooding occur	400	857	2.14	.911
Ways of how to search for any missing person should flooding occur are put in place	400	882	2.20	.797
People living with you have one another's contacts to call should a flood disaster occur.	400	1144	2.86	.760

Source: Field survey, 2021

3.3 Crop Farmers' Preparedness Measures for Flood Disaster

The mean of the result on preparedness measures of crop farmers for flood disasters as shown in Figure 2 below indicated that the crop farmers agreed with the items analyzed. Therefore, it can be inferred that the crop farmers applied flood preparedness strategies to ameliorate the effects of flooding.

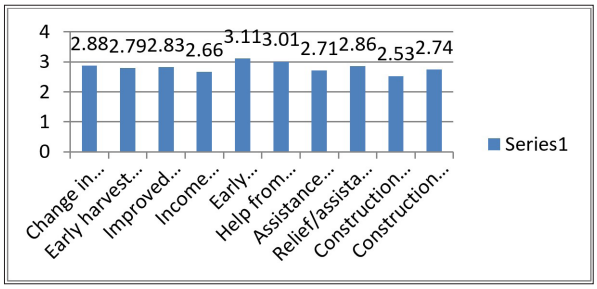

Figure 2. Crop farmers' preparedness measures to flood disaster

3.4 Effectiveness of Preparedness Strategies for Flood Disaster

The mean of the result on how effective the preparedness measures applied by the crop farmers as shown in Figure 3 below revealed that the preparedness measures were slightly effective.

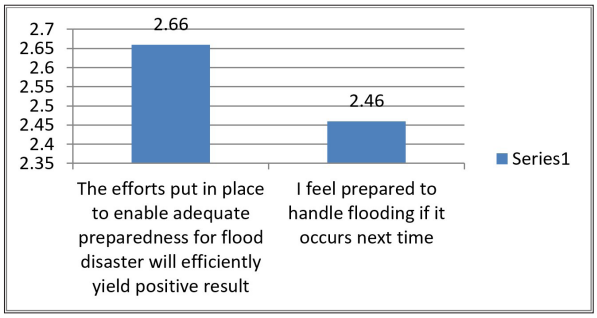

Figure 3. Effectiveness of preparedness strategies to flood disaster

3.5 Constraints to Flood Disaster Preparedness

The mean of the result on constraints to flood disaster preparedness faced by the crop farmers as shown in Figure 4 below indicated that the crop farmers expressed disagreement only to the size of farmland as a constraint to flood preparedness. They were however in agreement with other items. Therefore, it can be deduced that the crop farmers had some challenges in preparing and coping with the flood disaster.

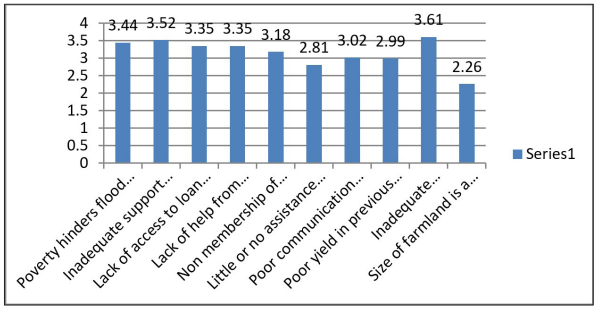

Figure 4. Constraints to flood disaster preparedness

4. Discussion

4.1 Demographic Characteristics of the Crop Farmers

The result revealed that most of the farmers in the study area were males which attests to the fact that there are more males in farming in Nigeria (Kasali *et al.,* 2009). This could be attributable to the fact that women have smaller plots of land, less access to physical inputs such as fertilizer and herbicide, and low labor (Oseni *et al.,* 2013). Women are also

mostly not opportune to own farms due to cultural biases (Fasina, 2013). The finding obtained in this study is coherent with those stated by Okeleye *et al.,* (2016); Umar and Muazu, (2017). This result showed that most of the crop farmers were in their economically productive age of fewer than 50 years of age which corroborates with the findings of Oronye (2012); Oyatayo *et al* (2016) Umar and Muazu (2017); Salami *et al.,* (2017). Having the majority of the crop farmers at an age of less than 50 can be ascribed to farmers' productivity being decreased as they age. Similarly, their level of physical involvement and consequentially their agricultural productivity would have been detrimentally affected as they age (Fasina, 2013). It is worth noting that older farmers are more vulnerable to the outcome of disasters like flooding as a result of challenges they may have in preparedness and recovery. This agrees with the work of Maltais (2019) who reported that throughout the world, floods have sadly disturbed many people over the age of 65. Some had serious injuries, others died, and sadly, many could not bear the menace.

Most of the crop farmers were married. This is in line with Owolabi (2013); Okeleye (2016). Married farmers could benefit from the support they get from their spouses. This is in agreement with Fasina (2013) who reported that the fact that the majority of their respondents are married could infer that couples are involved in cooperative efforts in farming activities. Those married could also have persons that could assist if a disaster like flooding occurs thereby enhancing their preparedness and coping capacity. This is consistent with the report of Owolabi (2013). Most of the crop farmers were literate which corroborates with Ahile and Adityavyar (2014); Oyatayo *et al.,* (2016). Their level of education is encouraging as it will help in embracing innovations and developments geared towards enhancing their preparedness and coping capacity to flood disasters. This is in line with Muttarak and Pothisiri (2013), which stated that the educational level of residents could influence their level of preparedness for disaster.

4.2 Coping Capacity of Crop Farmers to Flood Hazard

The farmers in this study were in the affirmative that they had poor coping capacity which is coherent with the outcome of Okeleye *et al.,* (2016) in their study on the impact assessment of flood disasters on the livelihoods of farmers in selected farming communities in Oke-Ogun region of Oyo State, Nigeria. The outcome of the interview also confirms that the farmers are faced with poor coping capacity. This relatively low coping capacity of the farmers makes them vulnerable to the effects of flooding. Better coping capacity would have made them to be resilient thereby not discouraged with farming. Their discouragement could affect food security and aggravate hunger and poverty. Attaining better coping capacity in the study area would not have been a difficult task to achieve because of their literacy level as the majority had secondary education and above. Boakye *et al* (2018) opined that one key factor that influences the adaptive capacity of any society is the literacy level appraised by the level of educational attainment. According to Brooks *et al* (2004), one's adaptive capacity is largely determined by one's level of education. This is because; high literacy enhances the spreading and assimilation of information. During an assessment of the adaptive capacity of Nigeria, Adejuwom (2005) observed that education was a major determinant of adaptive capacity. Accordingly, the study concluded that people with lower levels of education have lesser adaptive capacity.

The farmers in this study were aware of flooding and the danger it could cause. Yet their coping capacity was poor which infers that though their awareness of flooding is sufficient enough they lack adequate capacity in other relevant areas to effectively cope with flooding. This proposition agrees with Boakye *et al.,* (2018). It can be inferred from the study that the farmers react to the outcomes of flood disaster when it occurs, but cannot cope adequately to ameliorate the challenges posed by it thereby affecting crop production and their livelihood. This has serious consequences on food security in the long run.

4.3 Crop Farmers' Preparedness Measures for Flood Disaster

The outcome of this study revealed that the crop farmers applied flood preparedness strategies to ameliorate the menace of flooding in the study area but how effective are they is another point of concern. This finding conforms with Odunlola and Balogun (2015); Okeleye *et al.,* (2016); Akukwe (2019). However, it was contrary to that of Salami *et al.,* (2017) who reported that most of their respondents never practiced any preparedness measures. Ezemonye and Emeribe (2014) affirm that a flood preparedness plan is about putting in place a set of appropriate arrangements in advance for an effective response to floods. The need for preparedness is important because sometimes natural hazards like flooding may not be prevented but can be managed through preparedness. This conforms to the proposition of Tierney, Lindell, and Perry, (2001). Change in planting season and early harvest are among the preparedness strategies that the crop farmers were affirmative to. These strategies buttressed by interview of staff of Edo State ADP enables the farmers to have some harvest at the end of the farming season. This is because a change in planting season will enable the farmers to either plant early or late as the case may be to manage the effects associated with flood disasters. Likewise in early harvest, the farmers can reap before the flood comes. This however may not be free from harvesting crops that are not adequately matured. These strategies depend on weather variability and the use of improved crop varieties that mature quickly. To some extent, the application of these strategies is based on intuition concerning the observation of weather and prediction of flood disasters by the farmers. This is in agreement with Akukwe (2019). The use of improved varieties to enhance preparedness for flooding was agreed upon by the farmers in this study which is similar to the findings of Ajibade *et al.,* (2019). This however depends on the education level of the farmers. According to Okeleye *et al.* (2016), education enhances the translation of information into meaningful usage and it is very essential in taking any informed decision.

Early warning is also helping the farmers in this study to prepare ahead of flood disasters as affirmed by the crop farmers which corroborates with that of Okeleye *et al*.,(2016).

Early warning enables the farmers to have information about impending disasters like flooding. The proper application of early warning signs will help the farmer to manage the flooding should it occur thereby avoiding or minimizing its effects. This agrees with Ashraf *et al*. (2013), which argue that effective communication systems and accessibility to early warning systems lessen vulnerability as they make people respond and prepare for disaster.

In this study, income diversification was agreed by the farmers to be essential in preparedness for flooding should it occur. This strategy was also reported in Okeleye *et al*.,(2016); Akukwe (2019). The involvement of the farmers in other sources of income away from their farming activities will limit the socio-economic impact of the flood on them as it helps to cushion the outcome of flooding on the farm or crops. According to Gautam and Anderson (2016), livelihood diversification has been a commonly adopted strategy for coping with shocks in various communities. Similarly, Ashraf *et al*. (2013) argue that involvement in other non-farming activities will lessen farmers' vulnerabilities to the outcome of disasters like flooding.

The farmers were in the affirmative that assistance from cooperative society and the government will enable preparedness for flooding as they help to cushion the effects and to enhance recovery. According to Arukwe (2019), group membership has been adduced to provide social capital in terms of shock. The farmers in the study area have a cooperative group they belong to, but relief from the cooperatives and the government according to the farmers has been inadequate. Furthermore, the Construction of a drainage system was also agreed upon by the farmers to enhance their preparedness. Properly constructed and adequate drainage system aid in conveying overflowing water to safe destinations thereby reducing the potential of the flood to cause any danger to the farmers. Ibrahim, Ndatsu, and Yisa (2020) also reported the use of flood diversion trenches as a preparedness measure for flooding in their study.

4.4 Effectiveness of Preparedness Strategies for Flood Disaster

The study revealed that crop farmers were not effectively prepared against flooding should it occur. This is in agreement with the proposition of Oruonye (2013); Odunola and Balogun (2015); Oluchi *et al* (2017). The outcome of the interview conducted revealed the high tendency of floods to cause damage. This infers that the crop farmers were not effectively prepared against flooding in the study area. It, therefore, means that farmers in this study area are vulnerable to the effects of flooding despite having one form of preparedness measures applied. This deduced danger to crops and farmers' livelihood which could affect food security and exacerbate poverty and hardship in the study area. The poor effectiveness of preparedness to flood disasters in the study area indicates inadequate flood management by the government, cooperatives, communities, and other relevant agencies. It could also infer that the farmers were not adequately proactive to avoid being affected by floods thus they wait until it is too late for them to do anything. This aligns with the findings of Oluchi *et al.,* (2017).

4.5 Constraints to Flood Disaster Preparedness

This study also revealed that the farmers in the study area were faced with some challenges in preparing and coping with flood disasters. This finding is in line with Oruonye (2013). The constraints could hinder effective preparedness and coping with the flood disaster thereby enhancing the farmers' vulnerability to it and consequently damage to crops and the general wellbeing of the crop farmers. The farmers in this study affirmed that poverty is a challenge hindering their preparedness for flood disasters. This factor was also reported in Kundzewicz (2002); Mondal (2010); Lawal *et al* (2011); Salami *et al.,* (2017). As a result of the paucity of funds, the farmers would not be able to spend sufficiently on measures that will enable them to prepare and bear with the disaster. This agrees with the findings of Adegboye (2011) who opined that insufficient money limits the application of flood control measures. Lack of funds could also make them farm in highly flood-prone areas because of some advantages it may naturally provide which they may not be able to afford if they should go to a safer place. For instance, good farming potentials and availability of water along river banks and close to detention ponds made some of their farms in those areas in expectation of better yields. This proposition is consistent with Bariweni *et al.,* (2012); Hallagatt *et al.,* (2020). Poverty also affects the tendency of the farmers to recover from flood disasters when it hits them. They, therefore, find it difficult to recover any time flooding occurs. This agrees with Erman *et al* (2019) and Erman *et al.* (2020).

The farmers agreed that inadequate support from the government and relevant authorities was among the challenges that affect their capacity to prepare for flooding in the study area. This is a serious factor because government at different levels has the statutory obligation to put preventive measures in place to minimize future flood risks. In a similar study in Taraba State, Oruonye (2012) argues that various disaster management stakeholders in the state have a weak capacity to respond adequately to emergency disaster situations. Also, UNDRR (2014) stated that poor involvement of the government in preparing vulnerable communities affect their preparedness. Similarly, limited inter-agency coordination, as well as the absence of political commitment and will to embolden preparedness activities, due to the political and institutional mindset of post-disaster relief instead of risk mitigation strategies, often create hurdles to preparedness capacities among the key government stakeholders Perera *et al* (2020).

Lack of help from cooperatives and non-membership of any association was considered by the crop farmers as a constraint to flood preparedness in the study area. Cooperatives as recommended by Edo State ADP were established among the crop farmers to serve as a medium of reaching the government and assisting members. The farmers were supposed to be members of cooperatives available in their communities. But some farmers did not join any of the cooperatives at the time the researcher was carrying out this study. Others were members but were not financially contributing to the cooperatives. These attitudes

most times affect the effectiveness of the cooperatives to serve the purposes for which they were established. Support from cooperatives could enable the farmers to cushion the effects of flood disasters. Therefore, lack or inadequate support from cooperative or non-membership at all could pose some challenges to crop farmers in the study area to prepare and cope with the outcomes of flooding. This finding is in agreement with that of Lawal *et al.,* (2011) who stated that scanty support among other factors were major hiccups confronted by farmers in the application of flood control measures. Similarly, little or no assistance from other community members who particularly were not farmers was considered a challenge to flood preparedness among the crop farmers. When flooding occurs, crop farmers particularly those who have no other sources of income outside farming, are usually affected the most. Therefore, support from other community members is helpful to their preparedness and enhancement of their coping capacity. This is in line with Ibrahim *et al.,* (2020).

Furthermore, poor communication network was also agreed upon by the crop farmers as a factor that hinders flood preparedness in the study area which agrees with Ibrahim *et al.,* (2020). Communication is very important to crop farmers in times of flooding because they need to know what to do, the safer locations to relocate to if need be, the roads that are safe to pass, and where to get medical attention in case of injuries or food as the event last. Extension officers from Edo State ADP were on the ground in the various communities in the state to supply crop farmers with the necessary information they need to enhance their coping capacity and preparedness for flooding. The use of extension officers to communicate with farmers was also reported by Okwu and Umoru (2009); Adegboye *et al* (2013).

4. Conclusions

Flooding is one form of disaster capable of destroying lives, property, and livelihood. Crop farmers like other persons are vulnerable to the effects of flooding because it affects their crops, farmland, and general well-being. To a large extent, preventing floods, particularly in developing nations like Nigeria may be difficult to achieve. Therefore, preparedness and coping with the menace could be considered appropriate management measures.

This study concluded that the crop farmers had poor coping capacity which increases their susceptibility to the effects of flooding. A better coping capacity would mean that the crop farmers in Edo State could be able to absorb the shock should the disaster occurs. They applied preparedness measures like change in the planting season, diversification of income, construction of drainages, early warning, early harvest, etc to ameliorate the effects of flooding but were still not effectively prepared. This implied that flooding continues to be one of the problems the farmers are facing. They are however challenged with hindrances like poverty, and inadequate support from the government and relevant authorities, among others as they prepare and cope. The constraints increase the farmers' susceptibility to flooding in the study area and consequently damage crops and their general well-being. Therefore, the crop farmers in Edo State have poor coping capacity and are not better prepared for flood disasters.

Recommendations

1. The crop farmers should be encouraged to practice some coping strategies like saving money and farm produce to sustain in case a flood occurs in subsequent years

2. The crop farmers should belong to the cooperative available in their communities and pay their dues regularly. This is to enable the cooperatives to render some assistance that could help in enhancing their coping and preparedness for flooding.

3. The crop farmers should be encouraged to take up other sources of income to complement income from farming. This is to enable them to cushion the effects of flood any time it occurs.

4. Government should provide poverty alleviation programs that will be beneficial to crop farmers. This is to enable them to overcome the challenges posed by poverty to flood disaster preparedness.

5. Support from the government and other relevant agencies should reach the farmers timely anytime a flood occurs. This is to enhance quick recovery from flood disasters by crop farmers.

6. Relevant government agencies like Nigerian Meteorological Agency and Nigerian Hydrological Service Agency should provide effective and adequate early warning signals to enhance the farmers' preparedness and coping capacity for flooding.

7. Agricultural Extension Officers should be adequately motivated to enhance frequent and effective contact with the crop farmers. This is to enable the timely passage of necessary information needed to improve the farmers coping capacity and preparedness for flooding.

References

Al Azzam N. and Al Kuisi M. (2021) Determination of flash floods hazards and risks for Irbid Governorates using hydrological and hydraulic modelling. *Jordan Journal of Earth and Environmental Sciences,* 12(1): 81-91.

Adegboye, G. A. (2011). The Effect of Extension Information on Output and Income of Women Maiza Farmers in Soba Local Government Area, Kaduna State. An Unpublished MSc. Thesis, Department of Agricultural Economics and Rural Sociology, Ahmadu Bello University, Zaria, Kaduna State.

Adegboye, G. A., Oyinbo, O., Owolabi, J. O., & Hassan, O. S. (2013). Analysis of the sources and effect of extension information on output of women maize farmers in Soba Local Government Area of Kaduna State, Nigeria. *European Scientific Journal 9*(9), 210-217

Adejuwon, J. O. (2005): Food crop production in Nigeria. Present effects of climate variability. *Climate Research*. 30, 53–60.

Ahile, S.I. & Andityavyar, E.M. (2014). Household perception and preparedness against flooding in Makurdi town, Benue State, Nigeria. *IOSR Journal of Environmental Science, Toxicology and Food Technology, 8*(11), 1-6.

Ajibade, E.T., Babatunde, R.O., Ajibade, T.B. & Akinsola, G.O (2019). Empirical analysis of adaptation strategies used in mitigating flood related losses by rice farmers in Kwara State,

Nigeria. *Agrosearch, 19*(1), 59-71.

Akukwe (2019). *Spatial analysis of the effects of flooding on food security in agrarian communities of South Eastern Nigeria*. Retrieved from www. rerepository.uonbi.ac.ke.

Alade O.A. & A.O. Ademola, 2013. "Perceived Effect of Climate Variation on Poultry Production in Oke Ogun Area of Oyo State." Journal of Agricultural Science. 5(9): 176-182.

Alufohai, G. O., Ugolor, D., Edemhanria, I. I. (2015). Beneficiaries' perception of the effect of ifad-community based natural resource management programme on their livelihood in edo state, Nigeria. *Nigerian Journal of Rural Sociology 15*(2), 7-12

Ashraf M. Y., Rafique N., Ashraf M., Azhar N.& Marchand M., (2013): "Effect of supplemental potassium on growth, physiological and biochemical attributes of wheat grown under saline conditions". *Journal of Plant Nutrition, 36* (3), 253-259.

Bariweni P. A. Tawari C.C. & Abowei J.F.N. (2012) Some environmental effects of flooding in the Niger Delta Region of Nigeria *International Journal of Fisheries and Aquatic Sciences,* 1(1), 35-46.

Boakye W. A., Bawakyillenuo S. & Agbelie I (2018). Diagnoses of the adaptive capacity of urban households to floods: The Case of Dome Community in the Greater Accra Region of Ghana. Ghana Journal of Geography, 10(2), 1–22.

Brooks, N., Adger, W. N., & Kelly, P. M. (2005). The determinants of vulnerability and adaptive capacity at the national level and the implications for adaptation. *Global environmental change, 15*(2), 151-163.

Erman A, Motte E, Goyal R, Asare A, Takamatsu S, Chen X, Malgioglio S, Skinner A, Yoshida N, & Hallegatte S (2020). The road to recovery: the role of poverty in the exposure, vulnerability and resilience to floods in Accra. *Economics of Disasters and Climate Change, Springer, 4*(1), 171-193

Erman A, Tariverdi M, Obolensky M, & Hallegatte S (2019). Flooded in Dar Es Salaam – The Role of Poverty in Disaster Risk. Policy Research Working Paper 8976. World Bank, Washington, DC. Refrieved from www. openknowledge. worldbank.org.

Ezemonye, M. N & Emeribe, C.N. (2014). Flooding and household preparedness in Benin City, Nigeria. *Mediterranean Journal of Social Sciences, 5*(1), 2039-2117

Fasina O. O. (2013). Farmers perception of the effect of aging on their agricultural activities in Ondo State, Nigeria. *The Belogradchik Journal for Local History, Cultural Heritage and Folk Studies, 4*(3), 371-387

Gautam Y.& Anderson P. (2016) Rural livelihood diversification and household wellbeing: insight fron Humla, Nepal. *Journal of Rural Studies,* 44, 239-249.

Hallegatte, S., Vogt-Schilb, A., Rozenberg, J. Bangalore M. & Beaudet C. (2020) From poverty to disaster and back: a review of the literature. *Economics of Disasters and Climate Change,* 4, 223–247.

Ibrahim, M., Ndatsu, J. A & Yisa, K. M (2020). Effects of flood on crop farmers in riverine area in Niger State Nigeria. *ATBU Journal of Science, Technology and Education, 8*(2):311-319.

Ike, P.C. & Uzokwe, U.N., (2015). Estimation of poverty among rural farming households in Delta State. *Journal of Poverty, Investment and Development,* 11, 86–93.

James M. W., (2000). "The nation's responses to flood disasters: An historical account by the association of state of floodplain manager", U.S.A. Paul Osmanllinois Publication.

Kasali R., Ayanwale., & Williams S. B., (2009). "Farm location and determinants of agricultural productivity in the Oke-Ogun Area of Oyo State, Nigeria". *Journal of Sustainable Development in Africa, 11*(2), 1-19.

Kundzewicz, Z. W. (2002). Non-structural flood protection and sustainability. *Water International, 27*(1), 3-13.

Lame, S.M. & Yusoff, W.F.W. (2015). Poverty reduction in Nigeria: The role of entrepreneurship education. *Journal of Educational and Literature, 3*(2), 63–71.

Lawal, J. O., Omonona, B. T. & Oyinleye, O. D, (2011). Effects of livelihood assets on poverty status of farming households in South Western Nigeria. *Journal of Challenges for Agriculture, food and Natural Resources, 7*(1), 1 - 8.

Maltais D. (2019). Elderly people with disabilities and natural disasters: Vulnerability of seniors and post trauma *HSOA Journal of Gerontology and Geriatric Medicine, 5*(4), 1-7.

Mondal M. H. (2010): Crop agriculture of Bangladesh: Challenges and opportunities. *Bangladesh Journal of Agricultural Research, 35*(2), 235-245

Muttarak, R. & Pothisiri, W. (2013). The role of education on disaster preparedness: case study of 2012 Indian Ocean Earthquakes on Thailand‟s Andaman Coast. *Ecology and Society, 18*(4), 51-66.

Odunola, O. O. & Balogun, F. A. (2015). Analyzing household preparedness on flood management in riverside: a focus on Apete Community in Ibadan, Nigeria. *IOSR Journal Of Humanities And Social Science, 20*(9), 07-32.

Ojo, O. O., and Adejugbagbe J. A. (2017). "Solid waste disposal attitude in Sango Ota, Ogun State: implication for sustainable city development in Nigeria." *Journal of Environment and Waste Management, 4* (3), 253–260.

Okeleye S. O., Olorunfemi F. B. , S Ogbedji J. M. & Aziadekey M. (2016). Impact assessment of flood disaster on livelihoods of farmers in selected farming communities in Okeogun region of Oyo State, Nigeria. *International Journal of Scientific and Engineering Research, 7*(8), 67-83

Okwu, O. J. & Umoru, B. I. (2009). A study of women farmers' agricultural information needs and accessibility: A case study of Apa Local Government Area of Benue State, Nigeria. *African Journal of Agricultural Research, 4* (12), 1404-1409.

Oluchi E. B., Chinwe A. N., James N. & Dickson R. S. (2017). Effective management of flooding In Nigeria (a Study Of Selected Communities In Anambra State). *Nigerian Journal of Management Sciences, 6*(1), 42-50.

Onuigbo, I.C.; Ibrahim, P.O.; Agada, D.U.; Nwose, I.A. & Abimbola, I.I. (2017). Flood vulnerability mapping of Lokoja Metropolis using Geographical Information System Techniques. *Journal of Geosciences and Geomatics*, *5,* 229–242.

Onwuka, S. U.; Ikekpeazu, F. O. & Onuoha, D. C. (2015). Assessment of the causes of 2012 floods In Aguleri And Umuleri, Anambra East Local Government Area of Anambra State, Nigeria. *British Journal of Environmental Sciences, 3* (1), 43-57.

Oruonye, E.D. (2013) An assessment of food risk perception and response in Jalingo Metropolis. Jalingo Taraba State. *International Journal of Forest, Soil and Erosion, 3*(4), 113-117.

Oseni G., Goldstein M., & Utah A, (2013). *Gender dimensions in Nigerian agriculture*. Retrieve from www. openknowledge. worldbank.org.

Owolabi, B (2013). Coping strategies of vulnerable people in flood disaster prone areas in Ibadan metropolitan city of Oyo state Nigerian. *Journal of Rural Sociology, 13* (3), 19-26.

Oyatayo, K.T., Songu, G.A., Adi, T.A., Jidauna, G.G. & Ndabula, C. (2016). Assessment of People's awareness and perception of flooding in Donga Town, Taraba State, Nigeria. *Journal of Geoscience and Environment Protection, 4*, 54-62.

Perera D., Agnihotri J., Seidou O. & Djalante R (2020). Identifying societal challenges in flood early warning systems. *International Journal of Disaster Risk Reduction, 51*, 1-9.

Salami, R.O., Von Meding, J.K. & Giggins, H., (2017) 'Vulnerability of human settlements to flood risk in the core area of Ibadan metropolis, Nigeria'. *Jàmbá Journal of Disaster Risk Studies, 9*(1), 1-14.

Stephen, A. (2011) "River Systems & Causes of Flooding". Tulane University, EENS 2040.

Tierney, K. T., Lindell, M. K., and Perry,R. W. (2001): Facing hazards and disasters: Understanding human dimensions. Joseph Henry Press, Washington.

Umar N. K. & Muazu A. (2017). Community perception and adaptation strategies toward flood hazard in Hayin-Gada, Dutsin-Ma Local Government Area, Katsina State, Nigeria). *Dutse Journal of Pure and Applied Sciences, 3*(1), 444-457.

United Nations International Strategy for Disaster Reduction (UNISDR) (2014). Progress and challenges in disaster risk reduction: A contribution towards the development of policy indicators for the Post- 2015 Framework on Disaster Risk Reduction. Geneva, Switzerland.

United Nations Office for Disaster Risk Reduction (UNDRR) (2017). *UNDRR Terminology on disaster risk reduction 2017.* Retrieve from www.unisdr.org. Accessed on 10/10/21.

World Health Organisation (WHO) (2007). Risk reduction and emergency preparedness. The WHO six-year Strategy for the Health Sector and Community Capacity Development, Switzerland: WHO Document production Service p.4-20.

Yamane, T. (1967). Statistics, an introductory analysis, 3rd Ed., Harper and Row Publishers, New York. p. 886.

JJEES

JJEES (2023) 14 (2): 91-102
ISSN 1995-6681

Jordan Journal of Earth and Environmental Sciences

Mineralogy and Geochemistry of Beryl-Bearing Prgmatite Dykes from Gbayo, Southwestern Nigeria

*Razak O. Jimoh[1], Akinade S. Olatunji[2], Jimoh Ajadi[3], Adegoke O. Afolabi[4]

[1]Department of Chemical and Geological Sciences, Al-Hikmah University, P. M. B. 1601, Ilorin, Nigeria
[2]Department of Geology, University of Ibadan, Ibadan, Nigeria
[3]Department of Geology and Mineral Science, Kwara State University, Ilorin, Nigeria
[4]Department of Earth Sciences, Ladoke Akintola University of Technology, Ogbomoso, Nigeria

Received 23rd March 2022; Accepted 26th September 2022

Abstract

The Gbayo granitic beryl-bearing pegmatites occur as discontinuous dykes, intruding into the host rock of mica schist. This study was aimed at appraising the geochemistry and mineralization potentials of the pegmatites. Systematic geological mapping to ascertain the relationships between the pegmatites and their host rocks was undertaken. Fresh pegmatite samples were collected for both petrographic and geochemical studies. Analytical results showed high SiO_2 (64.88 to 81.94%) and Al_2O_3 (11.54 to 19.11%,), and fair concentrations of Na_2O (av. 4.10%) and K_2O (av. 3.58%). The relatively high aluminum and alkaline compositions have promoted beryl crystallization from the pegmatitic melt. Incompatible elements are fairly concentrated in most of the analyzed samples, except for Rb which has the highest and greatest variability, with values ranging from 30.10 to 1,528.40ppm which could be indicative of the high degree of melts fractionation, resulting from long travel distance of pegmatite-forming melts. The K/Rb ratios for most of the analyzed beryl-bearing pegmatite samples are less than 100, with a mean value of 75.11, which is indicative of mineralization. Elevated Be values (>142ppm) were observed for some samples, indicating some levels of beryl mineralization. The dominance of Fe chromophore in the pegmatites accounts for the manifestations of aquamarine.

Keywords: *Gbayo, Pegmatites, Beryl-bearing, Mineralisations, Aquamarine.*

1. Introduction

Granitic pegmatites form an intrinsic and genetically important part of granitic intrusions in most orogenic belts (Cerny et al., 2012a), and as such have their mineralogy similar to those of the granites, consisting mainly of quartz, feldspar, and muscovite. They are characterized by anomalous enrichment in incompatible lithophile elements such as Rb, Cs, Li, Be, and Sn and are often associated with Nb-Ta-Sn-W mineralizations (Linnen et al., 2012). These occasional enrichments in the unusual trace elements will also result in the crystallization of equally unusual and rare minerals such as beryl, tourmaline, etc. This distinctiveness has made the study of pegmatites a subject of interest to many authors all over the world, particularly in Nigeria. Beryl, the most common beryllium-bearing mineral in the earth's crust, occurs in granite pegmatites and may form at different stages of pegmatite consolidation and crystallization, by auto-metasomatic processes, and during hydrothermal events (Cerny 2002; Wang et al. 2009).

Pegmatites within the Precambrian Basement Complex rocks of Nigeria have been categorized in terms of rare elements (e.g. Nb, Ta, Li, W, Sn, Be, B, Cs, Rb) mineralization as mineralized and non-mineralized (Adetunji et al, 2016). Matheis and Caen-Vachette (1983), while working on the pegmatites of the Pan-African reactivation zone, covering areas of Egbe, Ijero, and Wamba, distinguished them as barren and mineralized. In the Nasarawa area of Central Nigeria, Akintola and Adekeye (2008) also categorized the pegmatites in the area into two; the simple, barren quartz-feldspar and the complex rare-metal pegmatites. Jimoh and Olatunji (2020), in classifying the Olode groups of pegmatites as mineralized and barren, suggested the same parental source for the two varieties but believed that the differences, particularly in their mineralization potentials, might have resulted from their varied degree of fractionation and evolutionary trends. The Nigerian pegmatites were formed during the time of 562–534 Ma, indicating emplacement related to the end of the Pan-African magmatic activity, and have been sources of cassiterite and columbite–tantalite production (Garba 2003). They occur mostly as dyke-like intrusions, which vary from a few meters to several kilometers in length and a few centimeters to meters in width (Okunlola and Akintola 2007).

Mining activities have been going on in various parts of Gbayo, (Latitudes 7^0 11' to 7^0 14' and Longitudes 3^0 55' to 3^0 58' 30) for some time now, taking out various quality grades of beryl, including top facet grades from the beryl-bearing pegmatite dykes. Several tons of high-grade gem beryls, particularly aquamarine are being exploited from

* Corresponding author e-mail: rojgems@yahoo.com

the different mines in the area. Metallic minerals such as columbite-tantalite and some rock-forming minerals which are valuable like feldspar are also included in the mineral resources that are being mined for economic purposes in the area. The mineralogy and geochemistry of the Gbayo beryl-bearing pegmatite dykes were studied to appraise their nature of mineralization.

2. Research Methods

A geological mapping exercise was undertaken in Gbayo and the surrounding area to unravel the geology of the area. Representative fresh samples of beryl-bearing pegmatites were collected from various mines for both petrographical and geochemical studies. Ten of the samples were each cut into slides, from which the mineralogical contents were determined with the aid of the petrological microscope using transmitted polarized light. Due to the coarse-grained nature of pegmatites' mineral contents, large enough samples were taken to characterize the whole rock geochemistry. Ten such samples were individually pulverized and subjected to major, trace, and rare elements analysis, using the technique of Inductively Coupled Plasma - Mass Spectrometry (ICP-MS) after fusion with $LiBO_2$, at the ACME Analytical Laboratories Ltd, Vancouver, Canada. The detection limits for major elements range from 0.002 to 0.04%, and 0.02 to 1ppm for trace elements. For the elemental determinations, 0.2gm each of powdered samples and 1.5gm LiBO2 flux were mixed in a graphite crucible and subsequently heated to 1050^0C for 15 min. The molten samples were then dissolved in 5% HNO3. The sample solution was typically introduced into the ICP plasma as an aerosol, it is completely dissolved and the elements in the aerosol are converted first into gaseous atoms and then ionized towards the end of the plasma. They are then brought into the mass spectrometer via the interface cones. The interface region in the ICP-MS transmits the ions traveling in the argon sample stream at atmospheric pressure into the low-pressure region of the mass spectrometer. Once the ions enter the mass spectrometer, they are separated by their mass-to-charge ratio. They are then detected by a suitable detector which translates the number of ions striking the detector into an electrical signal that can be measured and related to the number of atoms of that element in the sample via the use of calibration standards.

3. Geological Setting

Gbayo and the surrounding areas are underlain by crystalline rocks of the southwestern Nigerian Basement Complex. The crystalline rocks in Nigeria are divided into three main groups; the Basement Complex (Pan-African and Older (Precambrian), > 600 Ma), Younger Granites (Jurassic, 200 – 145 Ma), and Tertiary to Recent volcanic (Fig. 1). The Basement Complex of Nigeria, of which the Southwestern Nigeria Basement Complex is part, forms a part of the African crystalline shield, which occurs within the Pan-African mobile belt that lies between the West African and Congo Cratons, and south of the Tuareg Shield (Black, 1980). It has a complex geologic history, resulting from different episodes of rock formation spanning the Achaean to Lower Proterozoic. Within the Basement Complex, Obaje (2009) distinguished four petro-lithological units; the Migmatite-Gneiss Complex, the Schist Belts, the Older Granites, and the Undeformed Acid and Basic Dykes.

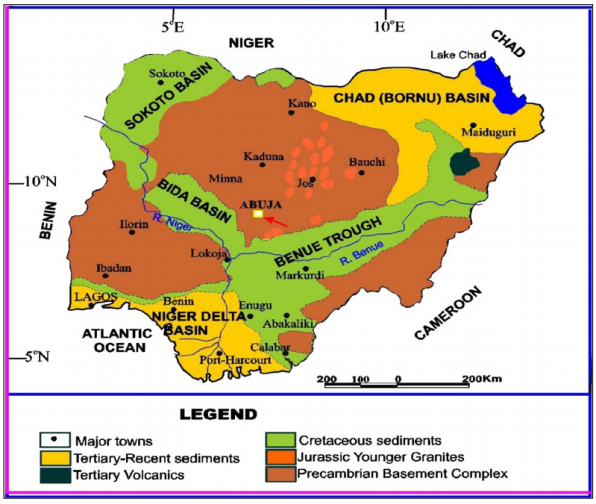

Figure 1. Generalized geological map of Nigeria showing the three lithological units (After Obaje, 2009).

The Migmatite-Gneiss Complex has a heterogeneous assemblage, comprising migmatites, orthogneisses, paragneisses, and a series of basic and ultrabasic metamorphosed rocks. Petrographic evidence indicates that the Pan-African reworking led to the re-crystallization of many of the constituent minerals of rocks of the Migmatite-Gneiss Complex by partial melting with the majority of the rock types displaying medium to upper amphibolites facies metamorphism. The rocks of the Schist Belts are best developed in the western half of Nigeria, west of 8^0E longitude, and are Upper Proterozoic supracrustal assemblages of low to medium-grade metasediments-dominated belts (Annor et al., 1996). They generally trend North-South and have been in-folded into the Migmatite-Gneiss-Quartzite Complex. Lithologically, the Schist Belts consist of quartzites, amphibolites, pelitic and mica-schists, calc-silicate rocks, marbles, phyllites, meta-conglomerate iron formations, and subordinate meta-igneous rocks (Elueze, 1992). The Older Granites, otherwise known as the Pan-African Granitoids are believed to have been emplaced during the Pan-African orogeny and occur intricately with the Migmatite-Gneiss Complex and the Schist Belts into which they are generally intruded (Harper et al., 1973). The Pan-African intrusive suite comprises mainly granites and granodiorite, with subordinate pegmatite and aplites. Affiliated rocks include charnockites, syenites, tonalites, adamellites, quartz monzonites, and gabbro. The Undeformed acid and basic dykes often observed to crosscut the rocks of the Migmatite-Gneiss Complex, the Schist Belts and the Older Granites are late to post-tectonic Pan-African. They include the felsic dykes, such as the muscovite, tourmaline- and beryl-bearing pegmatites, and the basic dykes such as dolerite dykes which are believed to belong to the terminal stage of the Pan-African orogenic event in Nigeria (Olarewaju, 1999).

4. Field Relationships

Although rocks are poorly exposed in major parts of Gbayo, field observations have shown that the geology of the area is dominated by mica schist, pegmatite, and aplite, with

the schist being the oldest and the host to the other rock types in the area (Fig. 2). The mica schist generally served as the host rock to the beryl-bearing pegmatites in virtually all the mining excavations in the area (Fig. 3). The poor exposure of the host mica schist in the area could have resulted from its high susceptibility to weathering. Over three-quarters of the map, area is underlain by the Precambrian pegmatites, ranging from huge intrusive bodies to small pockets of pegmatitic intrusions intermittently observed in the area.

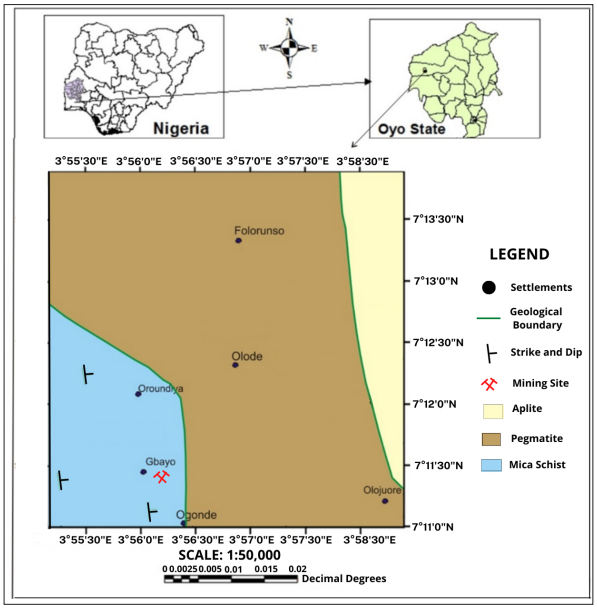

Figure 2. Geological map of Gbayo, the study area.

Figure 3. Photograph shows beryl-bearing pegmatite generally hosted by the micaceous schist in Picnine mines, Gbayo.
Latitude 07^0 11' 25.6" N, Longitude 003^0 55' 39.2" E

The central portion of the map area is predominantly underlain by pegmatites that have intruded the older mica-schist discordantly, making pegmatites the most prominent visible rock type in the area. In most instances they occur as low-lying intrusive bodies, while in many others they are found as flat-lying veins and dikes, either crosscutting each other or with quartz veins. These pegmatites belong to the early Precambrian pegmatites, classified by Rahaman (1988) as members of the Older Granite suite, believed to have been emplaced during the Pan-African orogeny (Harper et al, 1973). Megascopically, pegmatite is deficient in muscovite but mainly contains orthoclase feldspar and quartz with schorl and garnet crystals as accessory minerals. Bordering the Pan-African pegmatites to the northeast of the map area is aplite, which is similar in composition to the pegmatite but with finer grain sizes. Just like the pegmatites the aplites also bear some euhedral crystals of schorl and garnet disseminated within the matrix.

In all the mining excavations observed in the study area, pegmatites occur as dykes of varying widths, trending NE-SW and intruding into the host mica schist. These pegmatite dykes are lithologically and chronologically different from the Precambrian pegmatites in the central portion of the map area. They are the NE-SW trending beryl-bearing pegmatite dykes, which are highly rich in muscovite, and have been described by Dada (2006) as members of the felsic dykes, belonging to the Un-deformed acid and basic dykes. They are believed to be late to post-tectonic Pan African, whose ages range between 580 and 535 Ma using Rb-Sr studies on whole rocks (Matheis and Caen-Vachette, 1983; Dada, 2006). Adetunji et al. (2016) recently obtained U-Pb zircon age of 709 +27/-19 Ma established for the Ede pegmatites to represent the oldest Pan African magmatic event so far reported in southwestern Nigeria. Ball (1980) believed that a conjugate fracture system of the strike-slip faults that is believed to have marked the end of the Pan-African tectonic event probably controlled the emplacement of the NE-SW trending beryl-bearing pegmatite.

5. Petrography

The mineralogy of the beryl-bearing pegmatite dyke is simple, consisting of quartz, feldspar, and muscovite with beryl and occasional metallic oxides, including columbite-tantalite ($(Fe, Mn)(NB, Ta)_2O_6$), and rarely cassiterite (SnO_2). The petrographic study of the beryl-bearing pegmatite samples reveals they contain plagioclase feldspar (30-35%), orthoclase feldspar (15-20%), microcline (5-10%), quartz (15-20%), muscovite (10-15%), and other accessory minerals which may include beryl and columbite-tantalite (Fig. 4 and 5). As shown in the photomicrographs, most of the quartz crystals display granophyric textures, owing to their intergrowth with alkali feldspar, even though their outlines are visible due to their slightly different reliefs. The polysynthetic twinning in plagioclase distinguishes it from tartan or cross-hatched twinning, which is diagnostic of microcline, particularly under crossed polar. However, most of the feldspar crystals are microperthitic in nature (Fig. 5a and 5b), as both the plagioclase and alkali feldspars have intergrown together. No twinning is visible in the field of alkali feldspar. It is therefore most appropriate to name these minerals orthoclase-microperthite.

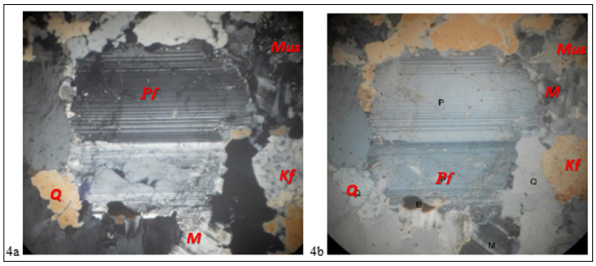

Figure 4. Figures 4a&b. Photomicrographs of the beryl-bearing pegmatite sample from Picnine mines in Gbayo; in transmitted light, Pf =Plagioclase feldspar, Kf = Potassium feldspar, Q = quartz, Mus = Muscovite, M = Microcline (X40).

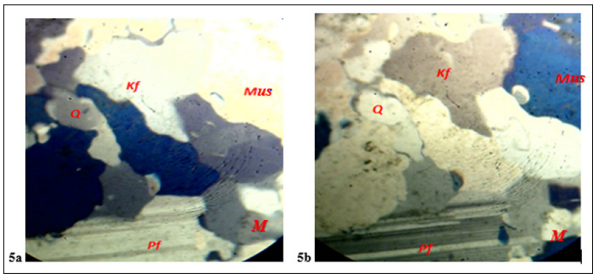

Figures 5a and **b**. Photomicrographs of the beryl-bearing pegmatite sample from Otoki mines in Gbayo; (4a) under plane-polarized light (ppl) & (4b) under crossed polars (xpl), Pf =Plagioclase feldspar, Kf = Potassium feldspar, Q = quartz, Mus = Muscovite, M = Microcline (X40).

Interesting economic mineralization, consisting of huge gem potentials of beryl, particularly aquamarine accompanied by metallic minerals such as columbite-tantalite and cassiterite, is prevalent within the beryl-pegmatite dykes. Where visible, these pegmatite dykes often bear crystals of blue, colorless, and occasionally yellow beryl, occurring either within quartz-muscovite assemblages along the contacts between these pegmatites and the host mica schist, or in miarolitic cavities within the pegmatites (Fig. 6). Columnar pale blue beryl crystals with simple morphology commonly occur in blocky pegmatite units, in close association with quartz, microcline, and muscovite, where they reach several centimeters to meters in length. In most gem-mineral deposits of southwestern Nigeria, tourmaline and beryl which are usually associated with other gem minerals alongside other rock-forming minerals such as feldspars, quartz, and muscovite, occur in miarolitic cavities within granitic pegmatites, and along the contacts which these pegmatites make with their host rocks (Jimoh, 2018). Beryl mostly occurs as euhedral to subhedral crystals of aquamarine ($Be_3Al_2Si_6O_{18}$) (Fig. 7) and goshenite ($Be_3Al_2SiO_6$) of varied diameters embedded in the beryl-bearing granitic pegmatite dykes crosscutting the micaceous schist in the area. Several tons of gem-quality aquamarine crystals have been exploited from the different mines in the area (Jimoh, 2018). Although most of the beryl crystals are fractured and opaque, a lot of clear and transparent crystals were also found, and have been cut into good-quality pieces of jewelry. Other economic minerals usually found associated with the beryl crystals which are also being exploited include metallic minerals such as columbite-tantalite and cassiterite, and rock-forming minerals like feldspar and quartz.

Figures 6. Photograph shows a miarolitic cavity within the NE-SW beryl-bearing pegmatite form which crystals of beryl have been evacuated.

Figures 7. Photograph shows a miarolitic cavity within the NE-SW beryl-bearing pegmatite form which crystals of beryl have been evacuated.

6. Geochemistry

6.1. Major elements

The chemical compositions of the analyzed samples of the Gbayo beryl-bearing pegmatite dykes, which are the direct reflections of their modal compositions, have major oxides constituting more than 99% of their entire chemical compositions (Table 1). Results from the geochemical analysis show high enrichments in SiO_2 and Al_2O_3, fair enrichments of the alkali metal oxides, Na_2O and K_2O, but depletion in the remaining major oxides. While SiO_2 values ranged from 64.88% to 81.94%, with a mean value of 75.05% and a standard deviation of ±5.81, the Al_2O_3 values ranged from 11.54% to 19.11%, with an average value of 14.97% and a standard deviation of ±2.44 (Table 2). The alkali metal oxides, Na_2O and K_2O are fairly enriched in most of the sampled pegmatites with their mean values of 4.10% and 3.58% respectively, which could be due to the high feldspar content of the pegmatites. The relatively high aluminum and alkaline compositions might have promoted beryl crystallization from the pegmatitic melt. London and Evensen (2002) observed that high aluminum and alkaline compositions are the main conditions required for beryl crystallization, especially in pegmatites. The aluminum saturation indices (ASI) for the sampled pegmatites are greater than one (A/CNK > 1 and A/NK > 1, where A = Al_2O_3, CNK= $CaO+Na_2O+K_2O$ and NK = Na_2O+K_2O), indicating that all the investigated rocks are per-aluminous. Their provenances are therefore believed to be peraluminous and belong to the Lithium - Cesium - Tantalum (LCT) family pegmatites, as Cerny (1982) found pegmatites of the LCT family to be of mild to extremely per-aluminous parent granitic compositions. The highly siliceous and per-aluminous compositions provided the silicic and acidic environments necessary for beryl formation (Jimoh, 2018). Beryllium saturation levels in melts are mostly affected by temperature but also decrease with increasing alumina and silica activity (London and Evensen, 2002), which explains the empirical association of beryl with silica-rich peraluminous magmas. Most beryl occurrences, particularly economic beryl deposits, are in pegmatites derived from peraluminous magmas (Groat et al, 2005). Turpin et al. (1990) pointed out that peraluminous granites are generally considered to be generated through the partial melting of upper crustal rocks, especially during continent-continent collision events.

Table 1. Representative pegmatite compositions from Gbayo.

Sample	R01	R02	R03	R04	R05	R06	R07	R08	R09	R10
Major Oxides (wt%)										
SiO_2	80.50	81.94	74.89	75.88	65.00	74.71	76.27	64.88	78.38	78.05
Al_2O_3	12.49	11.54	14.72	14.72	19.01	15.27	14.29	19.11	13.88	14.22
Fe_2O_3	0.62	0.79	0.64	0.41	0.32	0.65	0.43	0.40	1.08	1.12
MgO	0.08	0.10	0.06	0.02	0.01	0.05	0.02	0.01	0.10	0.10
CaO	0.17	0.17	1.10	0.45	0.04	1.10	0.54	0.04	0.11	0.09
Na_2O	2.78	1.86	6.51	5.43	2.68	6.60	5.40	2.74	0.92	0.87
K_2O	2.08	2.21	0.44	1.88	12.62	0.42	1.78	12.50	3.44	3.58
TiO_2	0.02	0.03	0.02	0.01	0.01	0.01	0.01	0.01	0.03	0.03
P_2O_5	0.02	0.03	0.04	0.39	0.19	0.04	0.46	0.19	0.06	0.05
MnO	0.02	0.02	0.73	0.07	0.01	0.70	0.08	0.01	0.03	0.03
Cr_2O_3	0.002	0.001	0.001	0.001	0.001	0.001	0.001	0.001	0.001	0.001
LOI	1.2	1.3	0.4	0.7	0.1	0.4	0.7	0.1	1.9	1.8
Sum	99.99	99.94	99.97	99.99	99.99	99.98	99.99	99.99	99.93	99.92
A/NK	2.57	2.84	2.18	2.01	1.24	2.18	1.99	1.25	3.18	3.20
A/CNK	2.48	2.72	1.88	1.90	1.24	1.88	1.85	1.25	3.11	3.12
Trace Elements (ppm)										
Ba	20	28	67	17	50	66	15	51	24	26
Be	31	174	33	32	5	32	32	6	142	170
Co	0.5	0.5	0.7	0.1	0.3	0.6	0.3	0.3	0.3	0.5
Cs	13.1	6.5	1.1	4.7	30.8	1	4.5	30.3	22.8	24.3
Ga	23.0	22.1	16.7	18	12.7	16.4	15.9	12.6	37.9	38
Hf	0.4	0.5	2.5	1.6	0.1	3.1	1.4	0.1	1.2	7.4
Nb	38.0	54.9	8.3	17.1	0.4	6.6	14.5	0.4	98.6	85.9
Rb	232.4	213.1	31.9	224.8	1528.4	30.1	197.3	1523.3	661.1	628.8
Sn	10	9	4	3	0.5	3	2	0.5	29	31
Sr	20.4	18.2	177.3	27.3	42	171.1	26.9	41.1	8.9	9.1
Ta	19.3	25.7	5.5	4.8	0.2	3.1	4	0.2	23.5	20.1
Th	2.2	1	4.8	2.6	0.1	3.1	2.3	0.1	1.2	0.6
U	0.7	0.7	2.2	4.9	0.2	2	5.7	0.1	1	2.1
V	*4*	12	4	4	4	4	4	4	4	15
W	0.6	1.3	0.3	0.3	0.3	0.3	0.3	0.3	2.2	1.8
Zr	4.9	4.8	24.7	17.4	1.3	26.6	15	0.7	12	70.1
K	17267	18345	3652	15606	104759	3486	14776	103763	28555	29718
K/Rb	74.3	86.1	114.5	69.4	68.5	112.8	74.9	68.1	43.2	47.3
Nb/Ta	1.97	2.14	1.51	3.56	2.00	2.13	3.63	2.00	4.19	4.27
Ta/Nb	0.51	0.47	0.66	0.28	0.5	0.47	0.27	0.5	0.24	0.23
Y	0.6	1.3	3.7	0.6	0.1	3.1	0.8	0.1	1.9	1.9
La	0.4	1.5	1.7	1	0.4	0.9	0.7	0.3	1.2	2.6
Ce	1.3	2.1	2.5	1	0.2	2	0.9	0.1	2	2.2
Pr	0.11	0.32	0.26	0.07	0.01	0.2	0.06	0.01	0.28	0.23
Nd	0.7	1	1	0.2	0.2	0.8	0.2	0.3	0.8	0.8
Sm	0.13	0.34	0.32	0.06	0.03	0.29	0.06	0.03	0.3	0.32
Eu	0.01	0.07	0.11	0.01	0.01	0.09	0.02	0.01	0.04	0.05
Gd	0.17	0.33	0.37	0.08	0.03	0.37	0.09	0.03	0.31	0.28
Tb	0.01	0.05	0.09	0.02	0.01	0.08	0.02	0.01	0.06	0.06
Dy	0.08	0.29	0.52	0.07	0.03	0.41	0.14	0.03	0.29	0.35
Ho	0.01	0.05	0.1	0.01	0.01	0.07	0.01	0.01	0.04	0.06
Er	0.02	0.14	0.3	0.04	0.02	0.21	0.05	0.02	0.14	0.14
Tm	0.01	0.02	0.04	0.01	0.01	0.03	0.01	0.01	0.02	0.03
Yb	0.03	0.12	0.32	0.03	0.03	0.22	0.06	0.03	0.11	0.19
Lu	0.01	0.02	0.04	0.01	0.01	0.03	0.01	0.01	0.01	0.03

Table 2. Statistical summary of major oxide compositions of Gbayo beryl-bearing pegmatites.

Major Oxides	Range	Mean ± S.D	Standard Deviation (S.D)
SiO_2	64.88 - 81.94	75.05	± 5.81
Al_2O_3	11.54 - 19.11	14.97	± 2.44
Fe_2O_3	0.32 - 1.12	0.65	± 0.28
MgO	0.01 - 0.10	0.05	± 0.04
CaO	0.04 - 1.10	0.38	± 0.41
Na_2O	0.87 - 6.60	3.58	± 2.21
K_2O	0.42 - 12.62	4.10	± 4.58
TiO_2	0.01 - 0.03	0.02	± 0.01
P_2O_5	0.02 - 0.46	0.15	± 0.16
MnO	0.01 - 0.73	0.17	± 0.29

It is therefore believed that the Gbayo beryl-bearing pegmatite dykes from the study area have resulted from the partial melting of un-depleted upper to middle crustal materials. Matheis (1987) argued that rare-metal pegmatites of Nigeria are products of high-grade metamorphic conditions, which were emplaced along a deep-seated continental lineament and enhanced by high crustal heat flow and the addition of fluid phases. He reinstated that the host rock contributed significantly to the individual characteristics of each pegmatite occurrence, as demonstrated by the marked differences between the pegmatite fields of southwest and central Nigeria. The fluids precipitating the beryl-bearing pegmatites are probably a mixture of expelled magmatic and hydrothermal melts from some plutons and mobilized metamorphic fluids from the surrounding metasedimentary rocks of the host mica schist.

The inter-oxide associations existing between the major oxides of the beryl-bearing pegmatites as expressed by Pearson correlation coefficients revealed some significant levels of positive and negative correlations (Table 3). SiO_2 exhibits strong negative correlations with Al_2O_3 (-0.99), an amphoteric oxide, and K_2O (-0.84), an alkali metal oxide, while it is positively correlated with the basic oxides; SiO_2-MgO (0.81), SiO_2-TiO_2 (0.69), SiO_2-Fe_2O_3 (0.62), significant in most cases. The weak correlation existing between SiO_2 and CaO (0.11) is an indication of magmatic origin for the beryl-bearing pegmatites (Frondel and Collette, 1957). The Harker plots of; SiO_2 versus MgO (Fig. 8A) yielded a well-defined positive trend, reflecting the positive correlation between the two oxides, while SiO_2 versus Al_2O_3 (Fig. 8B) shows a discernible negative trend, confirming an inverse correlation between the two oxides. This negative correlation between SiO_2 and Al_2O_3, coupled with the high enrichments of the pegmatite samples in SiO_2 in preference to Al_2O_3 are necessary conditions required for beryl crystallizations in pegmatites (London and Evensen, 2002).

Table 3. Statistical correlation coefficients for major oxides of analyzed Gbayo beryl-pegmatite samples.

	SiO_2	Al_2O_3	Fe_2O_3	MgO	CaO	Na_2O	K_2O	TiO_2	P_2O_5	MnO
SiO_2	1									
Al_2O_3	-.99**	1								
Fe_2O_3	.62	-.55	1							
MgO	.81**	-.77**	.91**	1						
CaO	.11	-.09	-.13	-.09	1					
Na_2O	-.12	.11	-.54	-.48	.89**	1				
K_2O	-.84**	.82**	-.40	-.54	-.61	-.41	1			
TiO_2	.69*	-.67*	.91**	.97**	-.19	-.58	-.39	1		
P_2O_5	-.28	.26	-.61	-.71*	-.02	.35	.13	-.71*	1	
MnO	.01	.02	-.01	.01	.94**	.75*	-.47	-.06	-.29	1

***. Correlation is significant at the 0.01 level (2-tailed).*

**. Correlation is significant at the 0.05 level (2-tailed)*

Since aluminum is a major component that is usually immobile during most geological processes such as metamorphic and hydrothermal processes, variation diagrams of different element oxides plotted against Al_2O_3 may assist in defining the behavior of these oxides in geological materials. While Al_2O_3 is negatively correlated with most of the basic oxides, it is positively correlated with the alkali metal oxides, confirming the necessity for adequate concentrations of aluminum and alkaline for beryl crystallization in pegmatites (London and Evensen, 2002). The negative correlations between Al_2O_3 and most of the basic oxides are possible indications of cations substitutions within the respective mineral crystal lattices within the pegmatite. The higher the negative correlation coefficients, the greater the ease with which substitutions take place between the concerned cations. The Al elements show a general negative correlation to other elements that substitute for it (Jimoh, 2018). The binary plot of Al_2O_3 versus MgO (Fig. 8C) yielded a negative trend, while that of Al_2O_3 against K_2O (Fig. 8D) presented a positive trend.

Significant positive correlations were established among most of the basic oxide pairs; Fe_2O_3-MgO (0.91), Fe_2O_3-TiO_2 (0.62), MgO-TiO_2 (0.97), and CaO-MnO (.94). The degree of positive correlation is indicative of the level of affinity among the cations in the respective pair. The binary plots of Fe_2O_3 against MgO (Fig. 8E) and that of Fe_2O_3 versus TiO_2 (Fig. 8F) all yielded visible positive trends, indicating positive correlations between the respective basic oxides. The high positive correlations among the basic oxides might probably be due to the petrogenetic influence of the dominant host mica schist on the pegmatites. The Gbayo beryl-bearing pegmatite dykes are believed to have crystallized from fluid-rich melts resulting from fractional crystallization and partial melting of their metamorphic rock. The rare metal pegmatites of Nigeria are products of high-grade metamorphic conditions (Matheis, 1987), whereby the host rocks to the individual pegmatites contributed immensely to their occurrences, through partial melting.

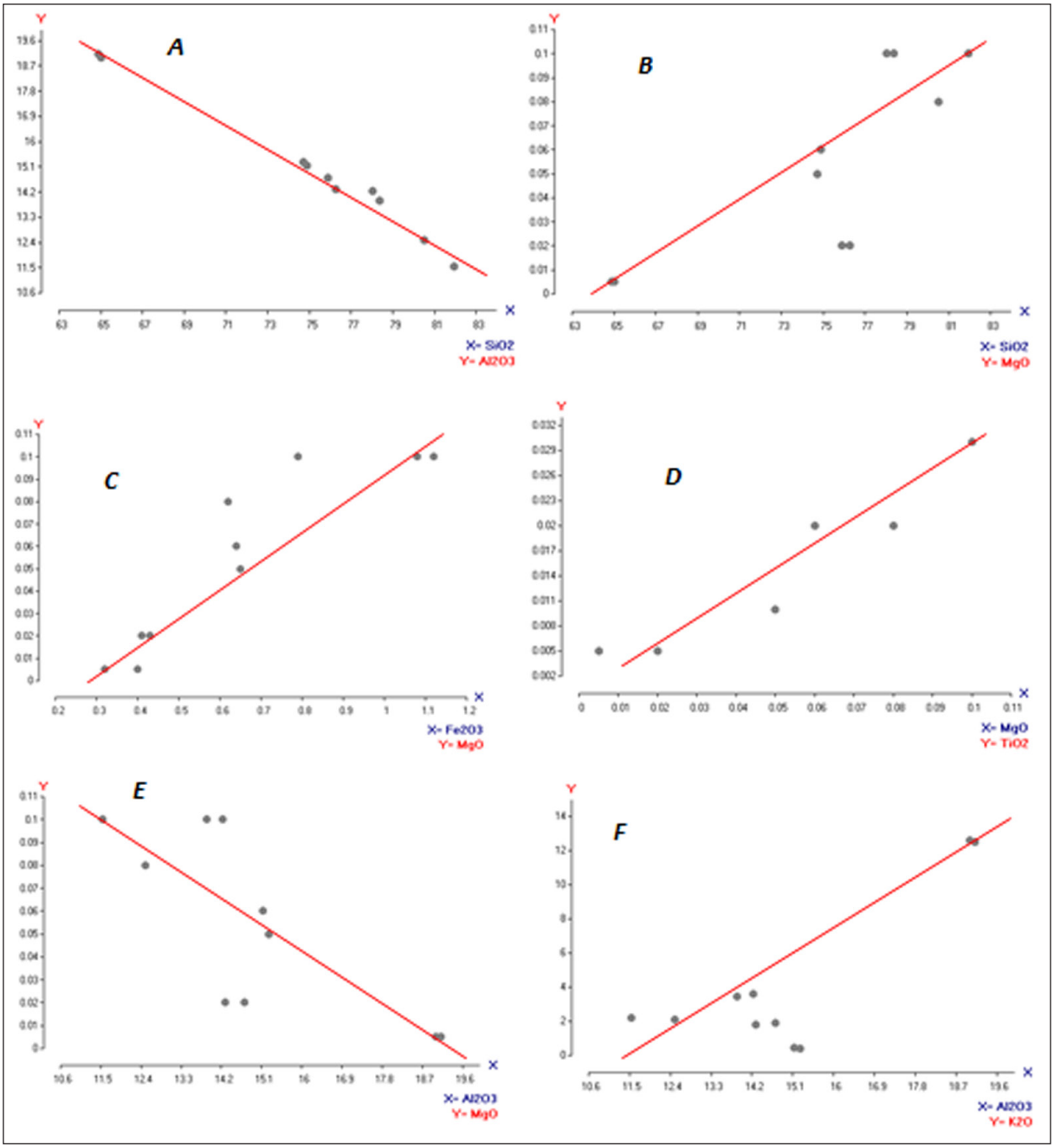

Figures 8A-F. Binary plots of; **A)** SiO_2 versus Al_2O_3, **B)** SiO_2 against MgO, **C)** Fe_2O_3 versus MgO, **D)** Fe_2O_3 against TiO_2, **E)** Al_2O_3 versus MgO, and **F)** Al_2O_3 against K_2O

6. Trace elements

Trace element contents of the Gbayo beryl-bearing pegmatite dykes vary over several orders of magnitude across the analyzed samples with their median values generally varying between 0.30ppm (W) and 228.60ppm (Rb) (Table 4). Incompatible elements are fairly enriched in most of the samples, except for Rb which shows high enrichment. The highest concentration and greatest variability in compositions were observed for Rb, with values ranging from 30.10ppm to 1,528.40ppm, a mean and standard deviation values of 533.52, and ±571.04 ppm respectively. These observed variations in the pegmatites' composition, coupled with the high enrichment, particularly in Rb could be indicative of a high degree of melts fractionation and evolution, resulting from the long traveling distance of the pegmatite forming melt from its parental source (Cerny, 1992). This indicates weak mineralization of the pegmatites. Although Rb is not known to form any ore mineral of its own, it is a common constituent of cesium and lithium ore minerals such as lepidolite ($K(Li, Al)_3(Al, Si, Rb)_4O_{10}(F, OH)_2$), pollucite ($(Cs, Na)_2Al_2Si_4O_{12}.2H_2O$), tourmaline ($Na(Mg, Fe)_3Al_6(BO_3)_3(Si_6O_{18}(OH)_4$ and beryl ($Be_3Al_2(SiO_3)_6$ (Jimoh, 2018). Rb, being a trace element may not be observed in some of the chemical formulae of these minerals, it is however a common substituting element.

Table 4. Summary of some trace element compositions of studied Gbayo beryl-bearing pegmatites (ppm)

Elements	*Range*	*Mean ± S.D*	*Median*
Ba	15.00 – 67.00	36.40 ± 20.13	27.00
Be	5.00 – 174.00	65.70 ± 67.79	32.00
Co	0.10 – 0.70	0.41 ± 0.18	0.40
Cs	1.00 – 30.80	13.91 ± 12.02	9.80
Ga	12.60 – 38.00	21.33 ± 9.39	17.35
Hf	0.05 – 7.40	1.82 ± 2.21	1.30
Nb	0.40 – 98.60	32.47 ± 35.95	15.80
Rb	30.10 – 1528.40	533.52 ± 571.04	228.60
Sn	0.50 – 31.00	9.20 ± 11.43	3.50
Sr	8.90 – 177.30	54.23 ± 64.23	27.10
Ta	0.20 – 25.70	10.64 ± 10.20	5.15
Th	0.10 – 4.80	1.80 ± 1.49	1.70
U	0.10 – 5.70	1.96 ± 1.93	1.50
V	4.00 – 15.00	5.90 ± 4.07	4.00
W	0.30 – 2.20	0.77 ± 0.73	0.30
Zr	0.70 – 70.10	17.75 ± 20.55	13.50

Trace elements like Be, Sr, Ba, Nb, Ga, Zr, Cs, Ta, and Sn are fairly distributed in most of the analyzed pegmatite samples with mean values of; 65.70ppm, 54.23ppm, 36.40ppm, 32.47ppm, 21.33ppm, 17.75ppm, 13.91ppm, 10.64ppm and 9.20ppm respectively. Be, Nb, Ta and Sn however show consistent enrichments in some pegmatite samples, indicating possible association with beryl, tantalite-columbite, and tin mineralization in the pegmatites. It is noteworthy that where mineralization is present in a pegmatite, there are usually elevated levels within the analyzed pegmatite samples of elements related to such mineralization. Consequently, samples R02, R09, and R10 which contain relatively high quantities of Be; 174ppm, 142ppm, and 170ppm respectively, indicate some level of beryl mineralization, and so are most likely to contain aquamarine or any other beryl minerals within their parent pegmatites. These values, although not exceptional, are significant and could be considered encouraging. Beryllium is a relatively rare element in the Earth's crust, ranking 47th most abundant. It averages approximately 3 ppm in the upper crust, which is elevated compared to 60 ppb inferred in the primitive mantle (Grew 2002). It can thus be inferred that some of the Gbayo pegmatite dykes are highly mineralized in terms of beryl, particularly aquamarine and goshenite mined from the area. Beryl mineral types that occur within the Gbayo beryl-bearing pegmatite dykes include aquamarine, goshenite, and very rarely heliodor ($Be_3Al_2Si_6O_{18}$). The relatively high Fe_2O_3 mean value of 0.65% in the analyzed pegmatite samples is possibly responsible for these occurrences. The chromophores for many beryl minerals include Cr ± V in green emerald, Mn in pink morganite, Fe^{3+} in yellow heliodor, and Fe^{2+} in blue aquamarine (Vianna et al. 2002a, b; Mihalynuk and Lett 2003), although Figueiredo et al. (2008) noted variable Fe^{3+}/Fe^{2+} in aquamarine. The depletion of the element, V and oxides; Cr_2O_3 and MnO in the analyzed pegmatite samples, with the elements getting below their detection limits of the LA-ICP-MS technique in some, are responsible for the non-occurrences of emerald and morganite in the Gbayo beryl-bearing pegmatite dykes. Cr, V, and Mn generally do not occur in sufficient concentrations in granitic rocks, and the geological conditions needed to bring Be into contact with Cr and/or V are typically absurd. The only dominant beryl chromophore within Gbayo beryl-bearing pegmatites is Fe, which accounts for the manifestations of aquamarine, goshenite, and rarely heliodor beryl types in the pegmatites of the area.

The geochemical data presented indicated that Be enrichment tends to coincide with enrichments in Ta, Nb, Sn, and Zr (Table 1). The primary mineralization of Ta, Nb, Sn, Be and Li is usually hosted in quartz-feldspar-muscovite pegmatites (Kinnaird, 1984). The Be is best enriched in magma through the process of fractional crystallization whereby the element behaves incompatibly, and so is not taken up in crystallizing rock mineral phases, and is thereby enriched in the residual melt fraction. Many high-field strength elements such as Ta and Nb, as well as halogens (Cl and F) and other small ions are also typically enriched in residual melts, and play a role in depressing the solidus (London et al., 1996) such that Be enrichments continue to take place, even at low temperatures with low percentages of remaining melt. In the same vein, beryl mineralization in Gbayo beryl-bearing pegmatites is generally associated with elevated Ta, Nb, Sn, and Zr contents, indicating tantalite-columbite, cassiterite, and zircon mineralization, and thus can serve as an exploration guide for these minerals. Beus (1966) established that ≥ 20ppm Ta concentrations are characteristic of columbo-tantalite pegmatites. It is also apparent to note that the target commodity deposit types in the area include beryl, tantalite-columbite, and cassiterite.

Based on the known mineralogy and geochemistry

of the investigated Gbayo beryl-bearing pegmatites, the pegmatites can be classified as beryl-columbite pegmatites, as defined by Cerny (1991). Beryl represents the most abundant Be phase in the earth's lithosphere. It is the first of the truly exotic, rare-element minerals to crystallize in the evolutionary sequence of LCT rare-element pegmatites. It is a characteristic phase in the relatively less fractionated granitic pegmatites of the beryl-columbite subtype, lacking Li and Cs minerals, but commonly occurs with Nb-Ta oxide minerals, especially with members of the columbite group, e.g columbite-tantalite (Cerny, 2000). Such pegmatite populations are usually closely connected with their parental granitic rocks; the pegmatite dykes are usually situated within the granites or in adjacent metamorphic rocks, near parent granite. In the case of the Gbayo pegmatites, they occur as pegmatite dykes situated within the metamorphic rocks of mica schist, adjacent to their parent granitic rocks.

Very strong positive correlations exist between some trace element pairs; Be-Ta (0.87), Be-Nb (0.89), Be-Sn (0.81), Nb-Ta (0.89), Nb-Sn (0.96) and Sn-Ta (0.77) (Table 5). These are demonstrated by the correlation plots of the element pairs (Fig. 9A - F). The high positive correlations between these elements reflect their associations in the formation of rare metal ores from the pegmatitic melts.

Table 5. Statistical correlation coefficients for trace elements of analyzed Gbayo beryl-pegmatite samples.

	Ba	Be	Co	Cs	Ga	Hf	Nb	Rb	Sn	Sr	Ta	Th	U	V	W	Zr
Ba		1														
Be		-.38	1													
Co		.55	.18	1												
Cs		-.03	.06	-.35	1											
Ga		-.45	.82**	.08	.23	1										
Hf		.02	.45	.36	-.06	.56	1									
Nb		-.52	.89**	.03	.22	.97**	.41	1								
Rb		.15	-.18	-.42	.93**	-.12	-.24	-.11	1							
Sn		-.39	.81**	.10	.31	.99**	.58	.96**	-.03	1						
Sr		.85**	-.40	.64*	-.52	-.42	.13	-.51	-.36	-.41	1					
Ta		-.51	.87**	.21	.02	.81**	.20	.89**	-.28	.77**	-.47	1				
Th		.28	-.28	.46	-.84**	-.21	.12	-.29	-.80**	-.26	.73*	-.19	1			
U		-.40	-.14	-.31	-.59	-.10	.24	-.15	-.53	-.16	.02	-.26	.47	1		
V		-.25	.81**	.26	.13	.55	.63	.58	-.04	.57	-.33	.60	-.36	-.12	1	
W	-.41	.90**	.04	.31	.94**	.37	.98**	.01	.94**	-.48	.85**	-.37	-.26	.59	1	
Zr	-.02	.45	.33	-.06	.56	.99**	.42	-.24	.59	.10	.20	.12	.27	.63	.38	1

***. Correlation is significant at the 0.01 level (2-tailed).*

**. Correlation is significant at the 0.05 level (2-tailed).*

The binary plots of the individual pair of trace elements in the pegmatites highlight compositional variations, and mineralization trends, and suggest geochemical tools for future geochemical sampling procedures. Each plot exhibits well discernible positive trend, signifying positive correlations between the element pair. Rb, Cs, and K_2O show consistent enrichments in the analyzed pegmatite samples with their highest values of 1,528.4ppm, 30.8ppm, and 12.62% respectively. The highest values were observed in sample R05, while the lowest respective values of 30.1ppm, 1.0ppm, and 0.42% were observed in sample R06. Very strong positive correlations, therefore, exist among the three elements. The binary plots of Rb versus Cs and Rb against K_2O (Figures 10a and b) both display discernable positive trends, showing positive correlations between each element pair. The values of the K/Rb ratios for most of the analyzed beryl-bearing pegmatites are less than 100 (Table 1) with a mean value of 75.11, which is indicative of mineralization (Tischendorf 1977). This indicates that the Gbayo beryl-bearing pegmatites are mineralized to some extent. It is remarkable to note that both samples R03 and R06 with K/Rb ratios greater than 100 are also most depleted in Rb and Cs, making them the least fractionated and mineralized part of the analyzed beryl-bearing pegmatites. It follows therefore that the studied Gbayo beryl-bearing pegmatites have varied degrees of fractionations and mineralization, and this is believed to be dependent on the travel distance of the pegmatites from their various parent sources (Cerny, 1992).

The investigated pegmatite samples are fairly more enriched in the light rare earth elements (LREE) than the heavy rare earth elements (HREE) (Fig. 11), suggesting a lower crust source for the pegmatitic melts. Most of the samples exhibit chondrites-normalized REE patterns, which virtually display slight LREE-enriched and HREE-depleted patterns and generally exhibit fractionated asymmetric concave-upward shapes, with well-pronounced negative Europium (Eu) anomalies, an indication for granite-related pegmatite. The negative Eu anomaly suggests fractionation and indicates a late metasomatic effect (Taylor et al., 1986). Two of the samples however show no detectable Eu anomaly. A few of the samples also exhibit negative Ce anomaly, which according to Garba (2003) indicates oxidizing conditions during mineralization and interaction between melt-fluids and host rocks over great distances.

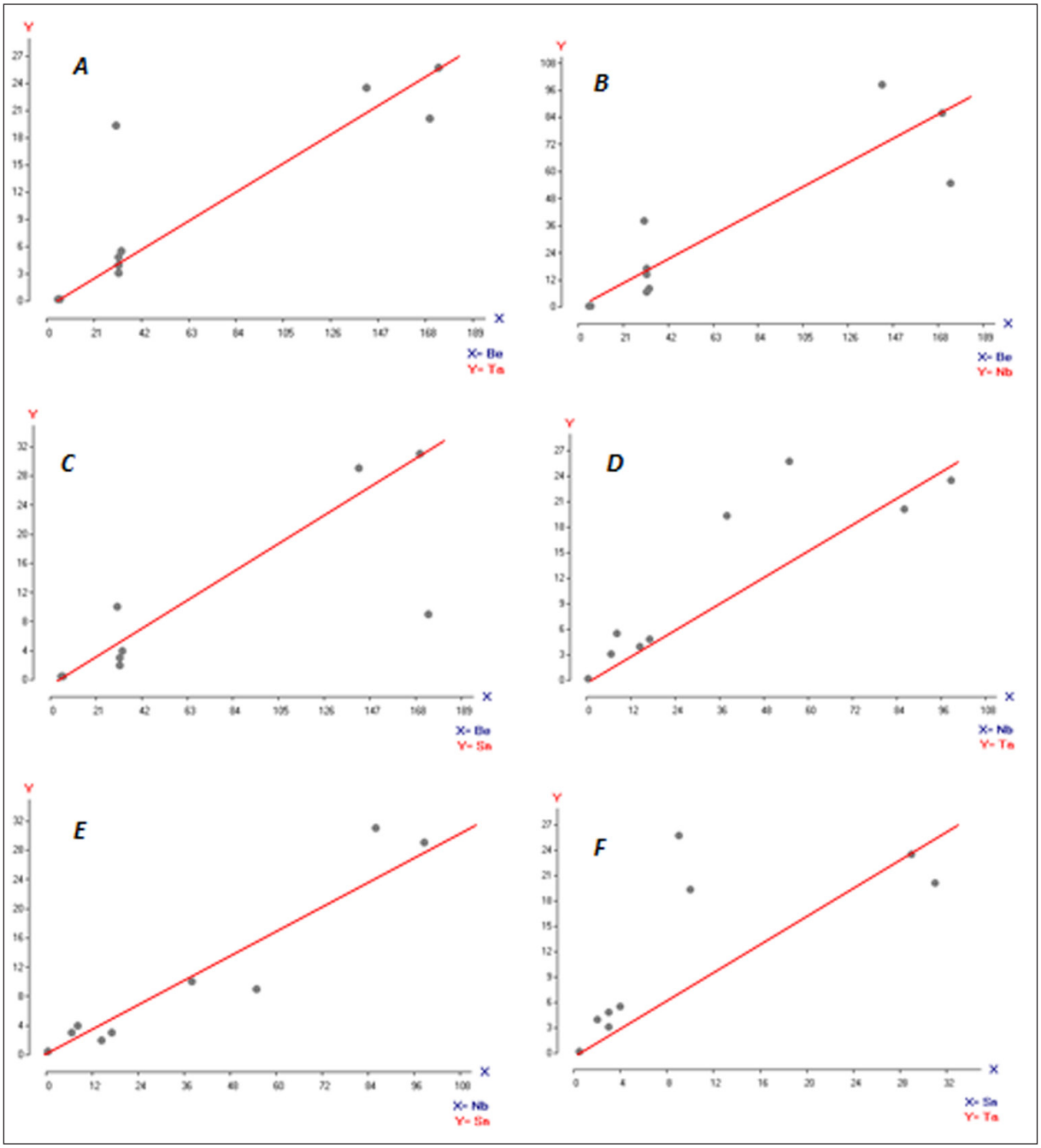

Figures 9A-F. Binary plots of; **A)** Be versus Ta, **B)** Be against Nb, **C)** Be versus Sn, **D)** Nb against Ta, **E)** Nb versus Sn and **F)** Sn against Ta

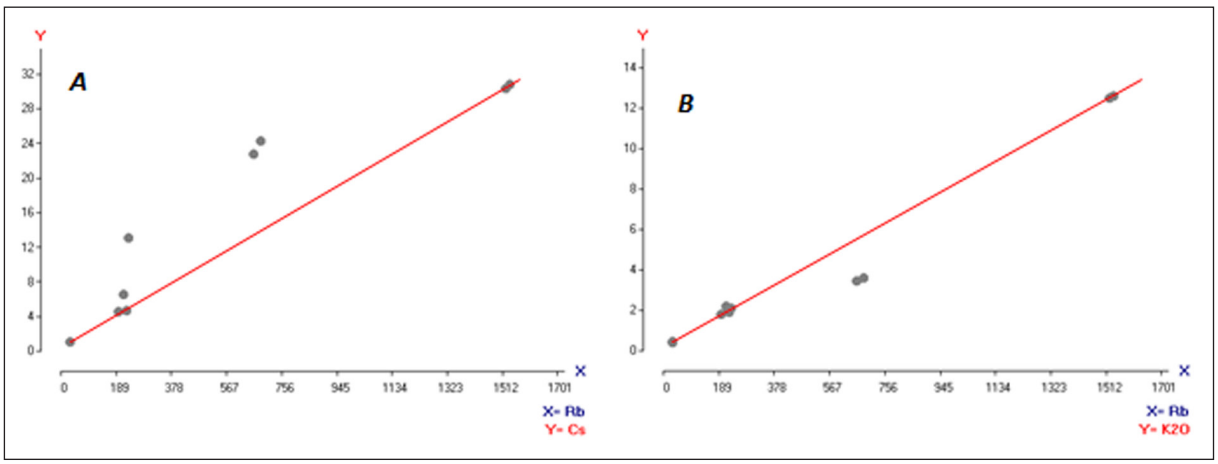

Figures 10A and **B.** Binary plots of; A) Rb versus Cs, B) Rb against K_2O.

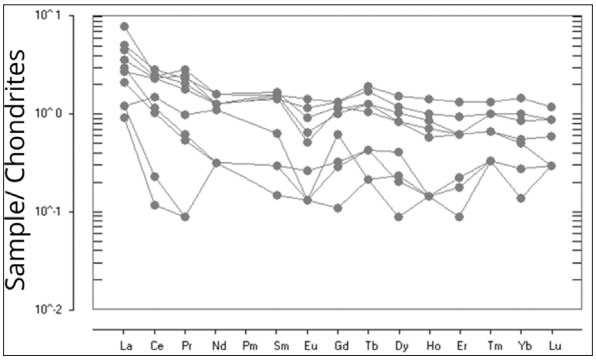

Figure 11. Chondrites-normalized REE patterns of the beryl-bearing pegmatite dyke samples from the Gbayo studied site, southwestern Nigeria. Chondrite values from Sun and McDonald (1989).

7. Conclusions

The studied Gbayo beryl-bearing pegmatite dykes comprise a simple mineralogy; feldspar, quartz, and muscovite, with beryl and occasionally some metallic oxides including tantalite-columbite and cassiterite, as accessory minerals. These pegmatite dykes have crystallized from fluid-rich melts resulting from fractional crystallization (residual pegmatitic melt) and partial melting (anatectic pegmatites). The fluids precipitating these minerals are probably a mixture of expelled magmatic fluids rich in water and some incompatible elements such as Be, Ta, and Nb, and mobilized metamorphic fluids from the surrounding meta-sedimentary rocks. Beryl represents a characteristic accessory mineral in the granitic pegmatites, and commonly occurs together with Nb–Ta oxide minerals, mainly members of the columbite group. Consequently, the mineral association, mineral chemistry, and petrologic features place these pegmatites within the beryl and beryl–columbite subtypes of the rare-element LCT family of pegmatites in the classification of Cerny and Ercit (2005).

References

Adetunji, A., Olarewaju, V.O., Ocan, O.O., Ganev, V.Y. and Macheva, L. (2016). Geochemistry and U-Pb zircon geochronology of the pegmatites in Ede area, southwestern Nigeria: A newly discovered oldest Pan African rock in southwestern Nigeria. Journal of African Earth Sciences. 115: 177-190.

Akintola, O.F. and Adekeye, J.I.D. (2008). Mineralization potentials of pegmatites in the Nasarawa area of Central Nigeria. Earth science research journal. 12 (2): 213-234.

Annor, A.E., Olobaniyi, S.B., Mucke, A., (1996): A note on the Geology of Isanlu area, in the Egbe-Isanlu schist belt, S. W. Nigeria. Mining Geology. 32(1), pp. 47.

Ball, E. (1980). An example of very consistent brittle deformation over a wide intra-continental area: The late Pan-African Fracture system of the Tuareg and Nigerian Shield. Tectonophysics. 61,363-379.

Beus, A.A. (1966). Geochemical exploration for endogenic deposits of rare elements on the example of tantalum. Nedra, Moscow, Engl. Transl. GSE Libr, Ottawa.

Black, R. (1980). Precambrian of West Africa, Episodes, 4, 3-8.

Cerny, P. (1982). Mineralogy of Rubidium and Cesium. In: Granitic pegmatite in science and industry. Mineralogical Assoc. of Canada Short Course Handbook. P. Cerny (ed.), 8, 149 - 161.

Cerny, P. (1991). Rare-element granitic pegmatites, Part I: Anatomy and internal evolution of pegmatite deposits. Geoscience Canada. (Ore Deposit Models series) 18: 49-67.

Cerny, P. (1992). Geochemical and petrogenetic features of mineralization in rare-element granitic pegmatites in the light of current research. Applied Geochemistry 7: 393-416.

Cerny, P. (2000). Constitution, petrology, affiliations and categories of miarolitic pegmatites. Memorie della Societa Italiana di Scienze Naturali e del Civico di Storia Naturalle di Milano. 30, 5-12.

Cerny, P. (2002) Mineralogy of beryllium in granitic pegmatites. In: Grew ES (ed) Beryllium: Mineralogy, Petrology, and Geochemistry. Reviews in Mineralogy and Geochemistry 50 (1): 405–444.

Cerny P., and Ercit T.S. (2005). The classification of granitic pegmatites revisited. Canadian Mineralogist. 43: 2005–2026.

Cerny, P., London, D. and Novak, M. (2012a). Granitic pegmatites as reflections of their sources. Elements 8, 289–294.

Dada, S.S. (2006). Proterozoic Evolution of Nigeria. In: The Basement Complex of Nigeria and its Mineral Resource. Oshin, O. Ed. Akin Jinad and Co. Ibadan, Nigeria, pp24 – 44.

Elueze, A.A. (1992). Rift system for Proterozoic schist belts in Nigeria. Tectonophysics. 209:167-169.

Figueiredo, M.O., Pereira da Silva, T., Veiga, J.P., Leal Gomes, C., De Andrade, V. (2008). The blue coloring of beryls from Licungo, Mozambique: an X-ray absorption spectroscopy study at the iron K-edge. Mineral Mag 72: 175–178.

Frondel, C. and Collette, R.L. (1957). Synthesis of tourmaline by reaction of mineral grains with NaCl-H3BO3 solution, and its implications in rock metamorphism. American Mineralogist, 42, 754-758.

Garba, I. (2003). Geochemical discrimination of newly discovered rare-metal bearing and barren pegmatites in the Pan-African (600 ± 150 Ma) basement of northern Nigeria. Applied. Earth Sciences. 112: 287-292.

Grew, E.S. (2002) Mineralogy, petrology, and geochemistry of beryllium: an introduction and list of beryllium minerals. In: Grew ES (ed) Beryllium – Mineralogy, Petrology, and Geochemistry. Rev Mineral Geochem 50: 1–76.

Groat, L.A, Hart, C.J.R, Lewis, L.L., Neufeld, H.L.D (2005) Emerald and aquamarine mineralization in Canada. Geosciences Canadian. 32: 65–76.

Harper, C.T., Sherrer. G., McCurry, P. and Wright, J.B. (1973). K. Ar retention ages from the Pan- African of Northern Nigerian, Bulletin of Geological. Society of America. Pp. 919 – 926.

Jimoh, R.O. (2018). Geochemical characterization of tourmaline and beryl from selected gem-bearing pegmatites in southwestern Nigeria. Ph.D. thesis, University of Ibadan. Pp96.

Jimoh, R.O. and Olatunji, A.S. (2018). Geology, Mineralogy, and Geochemistry of Beryl from Falansa, Southwestern Nigeria. Centrepoint Journal (Science Edition). CPJ 2018009/24109. Vol. 24(1) 145 – 170.

Jimoh, R.O. and Olatunji, A.S. (2020). Geological and Geochemical Characterisation of Pegmatites around Olode, Southwestern Nigeria. Tanzania Journal of Science TJS. 46(3): 733-747.

Kinnaird, J.A. (1984). Contrasting styles of Sn-Nb-Ta-Zn mineralization in Nigeria. Journal of African Earth Sciences. 2(2), 81-90.

Linnen R.L., Van Lichtervelde M., and Cerny P. (2012) Granitic pegmatites as sources of strategic metals. Elements 8, 275–280.

London, D., Morgan, G. and Wolf, B. (1996). Boron in granitic rocks and their contact aureoles. In: Grew, E.S. & Anovitz, L.M. (eds.) Boron: mineralogy, petrology, and geochemistry. Reviews in Mineralogy 33, 299–330.

London, D. and Evensen, J.M. (2002). Beryllium in silicic magmas and the origin of beryl-bearing pegmatites in E.S. Grew, ed., Beryllium: Mineralogy, Petrology, and Geochemistry: Reviews in Mineralogy and Geochemistry. 50: 445-486.

Matheis, G. and Caen-Vachette, M. (1983). Rb-Sr isotopic study of rare metal bearing and barren pegmatites in the Pan-African reactivation zone of Nigeria. Journal of African Earth Sciences, 1: 35-40.

Matheis, G. (1987). Nigerian rare metal pegmatites and their lithological framework. Journal of Geology, 22: 271-291.

Mihalynuk, M.G, Lett, R. (2003). Composition of Logtung beryl (aquamarine) by ICPES/MS: a comparison of beryl worldwide. In: Geological Fieldwork 2003. Crown Publications Inc., British Columbia, pp 141–146.

Obaje, N.G. (2009). Geology and mineral resources of Nigeria. Lecture notes in earth sciences.

Okunlola, O.A. and Akintola, A.I. (2007). Geochemical featues and rare-metal (Ta-Nb) potentials of Precambrian pegmatites of Sepeteri area, Southwestern Nigeria. Ife Journal of Science. 9(2): 203-214.

Olarewaju, V.O. (1999). Fluid inclusion studies of Coarse-grained Charnockitic and hybrid rocks in Ukpilla area, Southwestern Nigeria. Journal of Mining. Geology 35 (1) 1- 8.

Rahaman, M.A. (1988). Recent advances in the study of the basement complex of Nigeria, In: Precambrian Geology of Nigeria. P.O. Oluyide, W.C. Mbonu, A.E. Ogezi, T.G. Egbuniwe, A.C. Ajibade, and A.C. umeji. Eds. Geological Survey of Nigeria. Kaduna pp. 11 – 41.

Sun, S.S. and McDonald, W.F. (1989). Chemical and isotopic systematics of oceanic basalts: Implications of mantle composition and processes. In: Saunders, A.D., Nurry, M.J., Eds, Magmatism in the ocean basins, Geological Society, London, Special Publication, 42, 313-345.

Taylor, S.R., Rudnick, R.L., McLennan, S.M. and Eriksson, K.A. (1986). Rare earth element patterns in Archean high-grade metasediments and their tectonic significance. Geochimica et Cosmochimica Acta 50(10): 2,267-2,279.

Tischendorf, G. (1977). Geochemical and petrographic characteristics of silicic magmatic rocks associated with rare metal mineralization. In: Stemprok, M., Burnol, L., Tischendorf, G. (Eds.), IGCP Mineralization Associated with Acid Magmatism, vol. 2. Geological Survey, Prague, pp. 41-98.

Turpin, B.J., Cary, R.A. and Huntzicher, J.J. (1990). An in-situ-Time resolved analyzer for aerosol organic and elemental carbon. Aerosol Science. Technology. 12(1): 161-171.

Vianna, P., da Costa, G., Grave, E., Evangelista, H., Stern, W. (2002a) Characterization of beryl (aquamarine variety) by Mössbauer spectroscopy. Phys Chem Miner 29: 78–86.

Wang, R.C., Che, X.D., Zhang, W.L., Zhang, A.C., Zhang, H. (2009) Geochemical evolution and late re-equilibrium of Na-Csrich beryl from the Koktokay pegmatite (Altai, NW China). European Journal of Minerals. 21: 795–809.

JJEES

Jordan Journal of Earth and Environmental Sciences

JJEES (2023) 14 (2): 103-112
ISSN 1995-6681

Assessing The Extent of Public Participation in Planning and Management of Conservation Areas in Nigeria

Hassan Abdulaziz[1*], Shuaibu Abdul-Wahab[2], Ibrahim Jibrin Abubakar[3]

[1&3]Department of Urban and Regional Planning, Faculty of Earth and Environmental Science, Bayero University Kano, Kano State, Nigeria.
[2]Department of Urban and Regional Planning, School of Environmental Science, Federal Polytechnic Nasarawa, Nasarawa State, Nigeria.

Received 6th June 2022; Accepted 7th February 2023

Abstract

Planning and management are critical stages in environmental/nature conservation in the 21st century for better performance and sustainability of the areas. This is important as conservation areas are made up of distinct ecological units of diverse nature providing ecological services beneficial to the environment and mankind at large. As such involving and determining the extent of community participation in the conservation of such areas is of paramount importance. This study is aimed at determining the extent of community participation in the conservation of natural areas. The study employs the mixed research design where two-staged sampling techniques were used to collect data to obtain an in-depth understanding of the extent of public participation in conservation planning and management. A questionnaire was used to collect quantitative data, while an interview was used to collect qualitative data. The Quantitative data collected were analyzed descriptively using simple percentages, mean, and inferentially using Pearson Chi-Square ($\chi 2$) and Cramer's V test; while qualitative data were transcribed, reported, and discussed concurrently with the quantitative results. The findings reveal that there is a significant difference in communication level between conservation managers and the public; understanding of conservation area boundaries, conservation area rules, and regulations across the sampled communities. On the other hand, public involvement of the communities in decision-making processes indicated that they were excluded, therefore unable to influence management decisions. The results also reveal that the planning and management approach adopted by the game reserve reflects that of a Top-Down rather than a collaborative approach.

Keywords: *Conservation areas, Collaboration, Public Participation, Local communities, Decision-making.*

1. Introduction

Planning and management have been identified as robust strategies in the quest for the attainment of sustainable outcomes (Ramirez, 2014). The strategy has so far extended to cover many areas of human livelihood ranging from transportation to industrialization, as well as in the conservation of natural/protected areas with the outlook assuming many dimensions. This is the same with the planning and the management of conservation areas which ensue at different stages from a different perspective including public participation in the planning and management phases of conservation areas. According to (Ribot et al, 2006) participation of the public, the indigenous, and local communities in the planning and management of conservation areas in the developing world have been neglected. This leads to the observation by (Carey, Dudley, and Stolton, 2000); as is partly responsible for the illegal exploitation, unsustainable human use, and degradation of such conservation areas as they are situated in human-dominated environments (Carey, Dudley, and Stolton, 2000); thereby, resulting in conflict and crisis between host communities and the government agencies (Kurdoglu and Cokcaliskan, 2011) responsible for the management. Conservation areas are major determinants of sustainability for both the built and natural environment and may as well offer support in the realization of the sustainable development goals particularly (SDG 15) with unlimited services to humans and the built environment.

Historically, local communities and indigenous people have been the inhabitants and custodians of conservation areas. They adopted local strategies and institutional arrangements in protecting the conservation areas which in turn resulted in the success and sustainable uses (Berkes et al, 1989) of such areas. This scenario later sees the government taking over the planning, control, and management of the conservation areas and converting them into institutionalized organs for better planning and management. This eventually ushers in the era of the Top-Down decision-making approach in the management of conservation areas. In the approach stakeholders in both the planning and management phases are all relegated (Lockwood, 2010; Brockington and Igoe, 2006; Webster and Osmaston, 2003), as such, the expected conservation goals became difficult to achieve as most of the conservation challenges are human-related. Ultimately, this leads to the failure of the Top-Down decision-making approach in achieving the primary objectives of protection and conservation (Ite, 1998; Ite and Adams, 1998; Poffenberger, 1990). Furthermore, the Top-Down decision-making approach was, however, disadvantageous as it fail to carry the indigenous and local people along making privileged knowledge and information that is relevant to sustainable planning and management of the conservation

* Corresponding author e-mail: ahassan.urp@buk.edu.ng

areas scares.

In Nigeria, the historical development of conservation areas is traced back to the colonial era when the British colonial government designated the first conservation area in 1899 (Lowe, 1984) covering an area of 97,125 hectares (0.01%), which by 1950 had expanded to 7,332,031 hectares (8%) and by 1980, the area of coverage made up of (11%). By 1975 a total of 35 game reserves have been established with the first National park known as Lake Kainji Game Park coming to the limelight in 1979 as well as adding two more game reserves coming on board by 1999. At inception, the management of the conservation areas was bestowed on traditional institutions and local people. This system in 1900 was changed as the government took over control of the conservation areas. Regarding the agencies that oversee the activities of the game reserves, the Department of Forestry was in charge of running their affairs in 1897, whereas laws and policies which restrict activities on game reserves first came on board by 1932 with the restriction of hunting activities of the traditional and the local people. This trend continued with the establishment of laws that protect the northern region's game reserves in 1963. By 1979 Decree No.46 of 1979, 1989 National Policy on Environment, 1992 Environmental Impact Assessment Decree (EIA) Decree No.86, and Decree 36 of 1991 was later set up to ensure proper management of conservation areas. The National Policy on Environment was later revised in 1999.

However, because some of the conservation areas are located in human-dominated areas, collaborating with public, indigenous, and local communities in and around the conservation areas becomes necessary. Public participation is a significant component of the planning process whereby involvement of the public particularly the indigenous and local communities in conservation area planning and management increases their awareness of the importance of biodiversity conservation and the tendency of the areas to be successfully managed (Gbadegesin and Ayileka, 2000; Stolton, 2004; Hyakumura, 2010; Vodouhe et al, 2010). This is in line with and anchored closely based on the theory of public participation and collaboration. Kurdoglu and Cokcaliskan (2011) and Nielsen (2012) emphasize that the non-involvement of public/local communities in the planning and management process of conservation areas can lead to more conflict, thereby leading to more environmental harm than good. Meanwhile, collaboration allows joint decision-making and setting priority in the planning, implementation, and evaluation process to resolve conflict, develop and advance a shared vision (Koontz, 2006; Selin and Chavez, 1995); where organizations and stakeholders agree on a common way of finding a lasting solution to the identified problem via available means and resources (Bockstael et al, 2016; Pfahl et al, 2015; Nakakaawa et al, 2015; Woodland and Hutton, 2012; Ezebilo and Mattsson 2010; World Bank, 1999; Gray, 1989). As such this process allows local communities, nation-states, and the private sector to have equal opportunities in the decision-making process (World Bank, 1999). As noted by (O'Riordan 1989; Nursey-Bray and Rist 2009; Dixon and Dougherty, 2010; Ezebilo and Mattsson 2010; Hyakumura, 2010; Berkes, 2010; Lockwood, 2010; Vodouhe et al., 2010; Davies and White, 2012; Nielsen, 2012); collaboration with public/local communities and indigenous people in conservation area management yields better outcome, successful management, and sustainability of the areas, resolve conflicts between local communities surrounding the areas and the managers, as well as ensuring equitable partnership between the two parties (Berkes, 2009; Nursey-Bray and Rist, 2009; Berkes et al, 1991; Parr et al, 2008; Ezebilo and Mattsson, 2010; Gray, 1989). As such, the need for proper planning and management of these areas becomes necessary. This paper aims to address the gap between theory and practice by assessing the extent of public participation in conservation planning and management.

2. Study Area

The study was conducted in three conservation areas of Bauchi State, Nigeria namely: Yankari Game Reserve, Sumu Wildlife Park, and Lame Burra Game Reserve. Bauchi is a state in the North Eastern part of Nigeria located between Latitude 9^0 3^1N and 12^0 3^1N and Longitude 8^0 50^1E 11^0 0^1E as shown in Figure 1. It has a total land mass of 49,933.87km^2 equivalent to 5.3% of the country's total landmass. It is bounded by Jigawa and Yobe to the North, Gombe to the East, Plateau to the South, Kaduna to the West, and Kano to the North-West. The state is among the leading states inhabiting a high number of conservation areas with 53 out of the 1021 conservation areas in the country (Hassan, *et al*, 2015). The conservation areas are under the custody of the state government, however, under different state-owned agencies. Yankari Game Reserve is located in the Sudan Savannah vegetation zone, while Sumu Wildlife Park and Lame Burra Game Reserve are located in the Guinea Savannah vegetation zone.

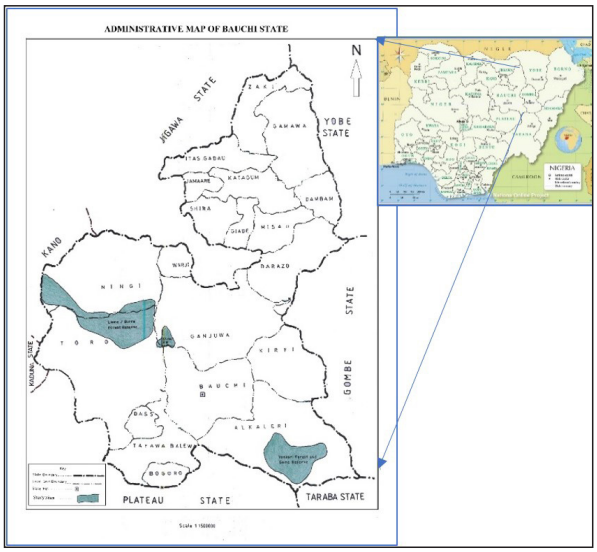

Figure 1. Map of Nigeria showing the location of the study area
Source: https://www.nationsonline.org/maps/nigeria-administrative-map.jpg

3. Methodology

This study adopted a mixed-method research design, where both quantitative and qualitative approaches were used in collecting relevant data for the study. The quantitative data were collected using a questionnaire, while the qualitative data were collected through the use

of interviews in line with the recommendation of the research design (Creswell, 2010; 2012). Indicators used in the questionnaire were sourced from the literature relating to public participation in environmental conservation and management.

3.1 Sampling technique and sample size

Two-staged sampling techniques were used to select samples. The first stage was stratified sampling, which was used to categorize the six communities under study as strata. The communities selected for the study are Minamaji and Duguri Communities neighboring Yankari Game Reserve, Kwange and Yuga Communities neighboring Lame Burra Game Reserve, and Sumu and Tafazuwa neighboring Sumu Wildlife Park. The second stage involves the use of a simple random sampling technique to draw samples from each of the strata.

Sample size always depends on population size. The population of the six sampled communities is presented in Table 1. However, literature revealed that studies involving statistical tests aimed at comparing groups may not necessarily take a sample concerning the population, but rather take a representative size across all the groups. According to Blaikie (2000), the minimum sample size required for a statistical test comparing between groups is 50 samples per group; while Denscombe (2007) recommended 30 samples per group. Therefore, this study adopts the recommendation of 50 samples per group, thereby totaling 300 samples for the six communities under study. The 300 sample size represents 10% of the population size. To overcome the issues of non-response rate and missing responses, 30% of the sample size was increased to the actual sample size in line with the recommendation of (Newing, 2011).

Table 1. Communities, Population, and Sample Size for the Communities.

Neighboring Conservation Area	Sampled Communities	Population	Sample Size
Yankari Game Reserve	Mainamaji	4,218	50
	Duguri	12,108	50
Lame-Burra Game Reserve	Yuga	4,983	50
	Kwange	4,081	50
Sumu Wildlife Park	Sumu	2,724	50
	Tafazuwa	2,317	50
Total		**30,431**	**300**

3.2 Questionnaire and interview administration

The questionnaire comprises two sections namely section I comprising of 8 questions relating to demographic profile, while section II comprises 5 questions measuring the extent of participation of the local communities in the planning and management of the conservation areas. Indicators in section II were sourced from previous research conducted in the field of public participation in environmental conservation and collaborative management of nature and conservation as presented in Table 2 below.

Table 2. Indicators Used in the Questionnaire.

S/N	Indicators	Source
1	There is regular communication between reserve managers and the local community	Parr *et al*. (2008),
2	The community members understand the conservation area boundary	Carey, Dudley, and Stolton (2000)
3	The community members understand the conservation area rules and regulations	Carey, Dudley, and Stolton (2000)
4	The community members are invited to a decision making about the conservation area	Berkes (2010), Parr *et al*. (2008), Mulongoy and Chape (2004), Thomas and Middleton (2003). Gbadegesin and Ayileka (2000), Berkes *et al*. (1991), Gray (1989)
5	The community members can influence management decision	Mulongoy and Chape (2004), Parr *et al*. (2008), Thomas and Middleton (2003)

In administering the questionnaire, ethical issues raised by Saunders *et al* (2016) such as the objectivity of the researcher, respect for communities' values, the voluntariness of the communities' members to participate, a promise of confidentiality and compliance with data management were taken into consideration before gaining access into the communities. The first point of the visit was the communities' heads of all communities, consent of the heads was obtained before administration. Each of the communities' leaders gives us an appointment that can be suitable to invite their members to participate and cooperate in responding to the questionnaire, and the meeting point is the communities' leaders' residence which serves as the muster point.

Respondents were then selected using the simple random technique where numbers were assigned to each member at the muster point, and a table of random numbers was used to select 50 samples in-line with the recommendation of (Newing, 2011; Creswell, 2012) that gives each member equal opportunity to be selected as sample. For those sampled respondents that were not literate, the researcher conducted self-administered questionnaires approach, where the respondents were asked questions, and their responses were entered into the questionnaire by the researcher.

Similarly, interviews were conducted with a community leader and two other stakeholders as shown in Table 3 below. Three interviewees were selected because no sample size was required but just depends on the level of saturation (Newing, 2011). The questions on the questionnaire were later modified to take the format of questions and used as an interview guide.

Table 3. Interviewees Profile.

S/N	Interviewee	Location
1	Community Leader	Duguri community neighboring Yankari Game Reserve
2	Stakeholder	Sumu community neighboring Sumu Wildlife Park Game Reserve
3	Stakeholder	Yuga community neighboring Lame-Burra Game Reserve

3.3 Data analysis

Quantitative data collected for the study were analyzed using simple percentages, charts, Chi-Square (χ^2), and Cramer's V test; while qualitative data were transcribed and reported, and discussed concurrently with the findings of quantitative. The implications of the findings were further discussed and recommendations were made based on the findings of the study.

4. Results

Data collected were analyzed and discussed based on the respondents' profiles and six parameters identified for assessing the extent of public participation in conservation planning and management. The analysis is presented in sub-sections below.

4.1 Respondents' profile

The study sampled 50 respondents from each of the six studied communities. Due to the cultural and traditional setting of the communities which are Muslim-dominated, the communities' leaders informed the researcher that the members can participate accordingly, but there is a restriction concerning the interaction of the researcher with females, in-line with their cultural and religious background. Therefore, all the respondents included in the study are males. The findings of the study revealed that the youngest respondent is 20 years old while the oldest is 65 years, with a mean age of 37.6 years as presented in Table 4. From the Table, the majority of the respondents were married. This is a typical character of African settings particularly in Muslims dominated communities where youths are encouraged to marry at an early stage to avoid social ills in society. The respondents have dependents ranging from 1 to 29 persons, with a mean of 9 dependents per person. Respondents' level of education is a typical reflection of a developing nation, particularly in a rural setting. For the studied communities, the majority constituting 70% attended non-formal education, which is Islamic knowledge, followed by a significant number that attended primary education, while those that attended secondary and tertiary are insignificant. The respondents' occupation is a reflection of their level of education. Due to their low level of education, the majority of the respondents were engaged in crop production, livestock rearing, and other forms of informal activities; with a negligible percentage engaged in service. All the communities under study are within a radius of 3km. The minimum duration of stay of the respondents in their respective communities is 4 years and the maximum is 65 years, with a mean of 31.78 years.

Table 4. Respondents' Profile.

Variable	Option		Frequency	Percentage %
Age	Minimum =	20 years		
	Maximum =	65 years		
	Mean =	37.60 years		
Marital Status	Single		30	10%
	Married		252	84%
	Divorced		8	2.7%
	Widow		10	3.3%
Number of Dependents	Minimum =	1 person		
	Maximum =	29 persons		
	Mean =	9 persons		
Highest Qualification	Non-Formal		210	70%
	Primary		67	22.3%
	Secondary		19	6.3%
	Tertiary		4	1.3%
Occupation	Civil Servant		8	2.7%
	Crop Producer		196	65.3%
	Livestock Rearer		47	15.7%
	Others		49	16.3%
Distance from Conservation Area	Minimum =	0.2km		
	Maximum =	2.5km		
	Mean =	1.12km		
Duration of stay in their community	Minimum =	4 years		
	Maximum =	65 years		
	Mean =	31.78 years		

4.2 Communication between staff and local communities

Communication is a medium through which information is shared between affected parties or from decision-makers to affected target people. Communication is an important tool/technique for effective environmental planning. It is a medium through which objectives and policies of environmental plans, specifically conservation area management plans can be communicated to the public, particularly community members surrounding the conservation areas. Adequate communication can also build trust and understanding between affected parties.

Results of the study as presented in Figure 2 revealed that the level of communication between conservation area managers and local communities surrounding them varies across the sampled communities, where some communities tend to indicate adequate communication while some indicated a low level of communication.g

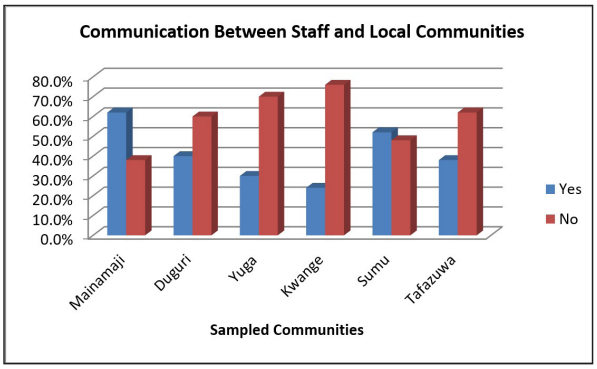

Figure 2. Level of communication between staff and local communities.

Furthermore, the Pearson Chi-Square statistic test revealed that there is a statistically significant difference in the level of communication between conservation managers of the respective conservation areas and members of local communities surrounding them with a Chi-Square Value (χ^2) = 20.298, df = 5 at $p<0.05$. Similarly, Cramer's V test with a value of 0.260 at $p<0.05$ also verified the result of the Chi-Square statistics, further indicating a statistically significant difference in the level of communication between conservation managers and local communities. This implies that the level of communication differs significantly across the sampled communities.

Findings of the interview with a community leader from Duguri around Yankari Game Reserve revealed that the communication between the conservation managers and the local communities is mainly in the form of extending management information or their request to the communities. If they notice any activity such as encroachment into the conservation area or if their managers chased any hunter in the conservation area and were not able to arrest him, they approach the communities for either investigation, inquiry, or support to arrest the poachers. This is slightly similar to the response of an interviewee from the Sumu community neighboring Sumu Wildlife Park, where he indicated that conservation managers do frequent their community to update them with information about the conservation area. In contrast, an interviewee from the Yuga community around Lame Burra Game Reserve revealed that managers of the conservation area only come to their community if their community is selected for any of the non-governmental organizations' projects, but not for the conservation area. The respondent further explained that they even engage in protecting the conservation area by preventing outsiders from carrying out illegal activities because they are aware of some of the benefits of the area. Also taking into consideration the limited number of staff in charge of protection and conservation activities in Lame-Burra Game Reserve.

4.3 Understanding of conservation area boundary

Demarcation of conservation area boundaries is important in conservation area planning because it is the first step towards better environmental protection and management. This allows the communities around them to understand where their jurisdiction ends so that communities do not trespass into the conservation areas. The variation in the level of understanding of conservation area boundary may not be unconnected to the level at which the public/ local communities are accommodated. Accommodating the public/local communities can encourage the community members to have a good understanding of the affairs of the conservation areas and feel a sense of belonging while neglecting the communities can pave the way for unwanted or prohibited activities in the conservation areas.

Analysis of the data collected conservation area boundary is presented in Figure 3 below. The result revealed that the communities are aware of the boundary of conservation areas neighboring them, except for the Kwange community neighboring Lame-Burra Game Reserve. This implies that most of the communities can operate within the limit of their communities without encroaching on the conservation area surrounding them. This is a significant achievement from the side of the management of the conservation areas. However, the situation is discouraging from the side of the Lame-Burra Game Reserve. From the result, it can be deduced that some communities around Lame-Burra Game Reserve are not aware of the boundary of the conservation area. This can threaten the conservation area as community members can encroach on or carry out unsustainable activities inside the conservation area.

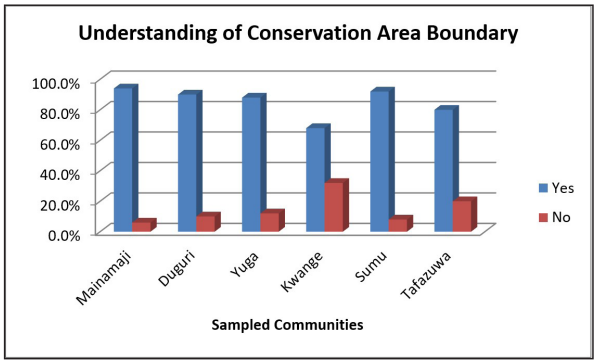

Figure 3. Extent of understanding of conservation area boundary.

Further statistical analysis using Pearson Chi-Square revealed that there is a statistically significant difference in the level of understanding of conservation area boundary across the sampled communities, with a Chi-Square value (χ^2) of 19.070, df = 5, at $p< 0.05$. Cramer's V test was also used

to validate the Chi-Square test, a value of 0.252 at $p<0.05$ was obtained, which indicates a similar pattern of statistically significant difference in understanding conservation area boundary across the studied communities. This implies that the level of understanding of conservation area boundaries differs across the sampled communities neighboring the three respective conservation areas under study.

Interview results revealed that community members neighboring Yankari Game Reserve are from time to time engaged in clearing and re-marking the boundary so that it can be clear to members and non-members of the communities. This has made community members around the conservation area to be aware of the boundary. The finding is similar in Sumu Wildlife Park where the conservation managers engage the community members in boundary demarcation, and as such, they are aware of the boundary. The finding is contrary in Lame Burra Game Reserve, where the interviewee indicated that managers do not engage them in boundary clearing or boundary demarcation. This according to him is difficult for the communities to understand exactly the location of the boundary. The communities can only show the boundary of the conservation area based on their perception.

4.4 Understanding of conservation areas rules and regulations

The result of the study relating to the understanding of conservation area rules and regulations is presented in Figure 4 below. The result revealed that communities neighboring Yankari Game Reserve indicated a high level of agreement to the understanding of the rules and regulations governing it, followed by Sumu Wildlife Park and Lame-Burra Game Reserve respectively. Nevertheless, the management of the conservation areas needs to speed up in creating awareness and educating the communities on the rules and regulations governing the conservation areas. This can go a long way in achieving conservation goals.

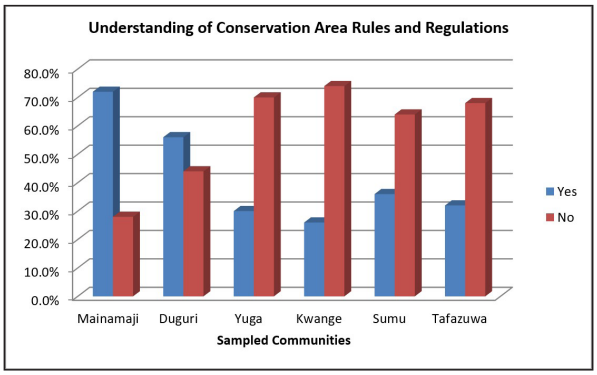

Figure 4. Extent of understanding of conservation area rules and regulations.

Inferential analysis using the Chi-Square test indicated that there is a statistically significant difference in the level of understanding of rules and regulations governing the conservation areas across the six sampled communities as indicated by a Chi-Square value of $(\chi^2) = 33.498$, df = 5, at $p< .05$. A follow-up test was conducted using Cramer's V statistics to substantiate the findings of the Chi-Square test, where a value of 0.334 at $p<0.05$ was obtained. This further validated the result of the Chi-Square thereby indicating a statistically significant difference in the level of understanding of conservation area rules and regulations across the sampled communities. This implies that the level of understanding of the conservation area rules and regulations across the sampled communities differs. The results of the interview across all the six respective communities under study revealed that the community members are aware of rules and regulations such as the prohibition of poaching, cutting down of trees, grazing, and farming activities inside the conservation areas. Interestingly, all the communities are aware of the basic rules of prohibited activities inside the conservation areas. Understanding these can contribute to the sustainability of the conservation areas.

4.5 Involvement of communities in decision-making

The key to successful planning and management is public participation in the planning and management processes. This is through the involvement of communities in the decision-making that affect them. The involvement of communities in the decision-making process can make the communities a sense of belonging and contribute actively to the protection activities. However, the findings are discouraging as the majority of the communities were not involved in decision-making. Therefore, the management of the conservation areas needs to re-strategize and give room for the participation of local communities in both the planning and management processes as required by the National Policy on Environment to achieve effective management. The findings of the United Nations Environment Programme (2007) have identified the participation of local communities in decision-making in natural resource management as an effective way of achieving successful protection of the ecosystem and improving communities' well-being.

Analysis of the level of involvement of members of local communities in decision-making about the conservation areas neighboring them is presented in Figure 5 below. The result revealed that communities neighboring all three respective conservation areas under study are not involved in decision-making about the conservation areas. This is not encouraging because the communities are neglected when it comes to decision-making. This is a clear indication of the Top-Down management approach where the public and members of communities are set aside in decision-making.

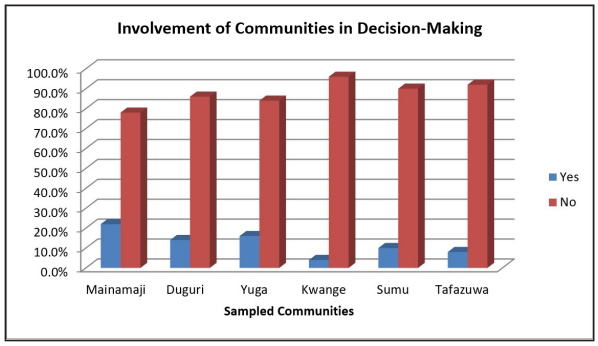

Figure 5. Level of involvement of communities in decision-making.

Further statistical analysis reveals that there is no significant difference in the level of involvement of communities in decision-making across the sampled communities, with a Chi-Square value of $(\chi^2) = 9.403$, df = 5, and $p< .05$. Similarly, Cramer's V test with a value

of 0.177 at p<0.05 validated the result of the Chi-Square indicating no statistically significant difference in the level of involvement of local communities in decision-making about the conservation areas. This indicates that the level at which members of the public, particularly local communities are involved in the decision-making process is the same across the respective communities. This is an indication that the local communities across all the sampled communities are neglected by the management when it comes to decision-making about the conservation areas.

Interview results have validated the findings of the questionnaire, where the respondents across the interviewed communities revealed that they were not involved in decision-making about the conservation areas. A respondent added that what some view as involvement in decision-making is just a mere notification and seeking the cooperation of members of the communities in complying with the instructions.

4.6 Ability of communities to influence management decision

The ability of local communities to influence management decisions of conservation areas neighboring them was determined in this study. The perceptions of the respondents across all the studied communities tend to be similar as they were unable to influence management decisions about the management of conservation areas neighboring them as in Figure 6 below.

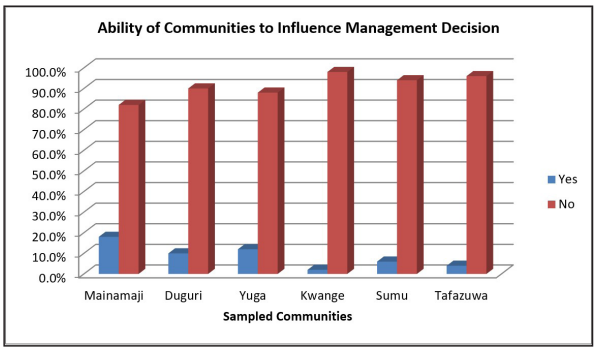

Figure 6. Ability of communities to influence management decision.

Analysis using Chi-Square statistics revealed that there is no statistically significant difference in the ability of the communities members in influencing management decisions across the sampled communities, with a Chi-Square value of (χ^2) = 10.949, df = 5, and p< .05. The result was further validated by a follow-up test using Cramer's V statistics, where a value of 0.191 at p<0.05, indicating that there is no statistically significant difference in communities' ability to influence management decisions about conservation areas neighboring them. Similarly, the findings of the interview also indicated that members of the communities around the three respective communities under study were not able to influence management decisions about the conservation areas.

5. Discussion

The findings of the study indicated differences in communication between conservation managers and local communities. This may be attributed to the location of the communities or the priority given to the communities by the respective conservation managers. It may also be since, managers cannot communicate directly with all members of the community, as the channel of communication may be through community leaders and stakeholders in each community, from there, the information can reach other members. The channel of communication is important because it has been identified by Bockstael *et al.* (2016) to be the main obstacle to successful collaboration itself. The disparities in the level of communication between members of local communities across communities may be also attributed to (i) staff strength/capacity, (ii) size of the conservation area, (iii) number of communities around the conservation areas, (iv) nature of the terrain where the conservation areas are located, (v) accessibility among others. This pattern of response is not surprising because, Yankari has 224,410 hectares of land, with 281 staff, Lame Burra has 205,767 hectares with 47 staff, and Sumu has 8,000 hectares with 53 staff. Based on the staff strength of the conservation areas, Yankari has more capacity to ensure a high level of protection and community outreach than Lame-Burra Game Reserve and Sumu Wildlife Park. Interestingly, the findings of the study relate to the findings of Watson *et al.* (2014) where the authors identified the need for adequate staffing to perform management activities.

Yankari Game Reserve has adopted the approach of engaging members of local communities surrounding them in boundary demarcation. This is more of a technique of showing them the boundary. Relating the size of Lame-Burra Game Reserve to its staff strength, one can easily understand that it is difficult for the managers to adopt the approach of Yankari. This implies that communities around Lame Burra can be left out in terms of outreach, which can further limit their understanding of conservation area boundaries.

The differences in understanding conservation area rules and regulations among the communities as revealed by the quantitative results may be due to the level of communication between conservation area managers and members of the local communities surrounding them. Interestingly, communities that indicated adequate communication between them and the managers of their respective conservation areas tend to understand the conservation area rules and regulations well, while those that indicated less communication between them and the management of their respective conservation areas indicated less understanding of the conservation area rules and regulations. Therefore, frequent communication between conservation area managers and local communities is highly needed for a better understanding of conservation area rules and regulations. It is also significant in achieving conservation policies.

The communities have not been involved in decision-making about the conservation areas. This further proved that management of the conservation areas are top-down approach, where managers and respective institutions/ authorities decide on the conservation areas. In this situation, local communities are completely neglected, thereby neglecting local knowledge that may have regional and global impacts. The level at which community members were neglected when it comes to deciding on the conservation area is almost the same across all the communities studied. This may serve as a stumbling block to achieving effective

management of the conservation areas because, when the management of any conservation area takes a decision that may affect the local communities, they may in one way or another other reacts and their reaction may directly or indirectly threaten the well-being of the conservation areas. Based on the findings of the study, communities that are in good relationships with the management of conservation areas near them tend to strengthen their relationship and have more interest in the well-being of the conservation areas.

The findings of this study corroborate with the findings of Ribot *et al.* (2006) and Lockwood (2010) who revealed that public, indigenous, and local communities in the developing world are neglected in both the planning and management process of conservation areas; thereby resulting to encroachment and unsustainable practices in the conservation areas (Carey, Dudley and Stolton, 2000). The contribution of this study is that it revealed that the Top-Down approach used by the colonial masters is still in practice. This is despite previous studies reporting its failure to achieve the primary objective of protection and conservation (Ite, 1998; Ite and Adams, 1998; Poffenberger, 1990). This is a threat to the conservation areas and can have negative implication on their performance because local knowledge that can promote conservation and enhance their performance are not allowed to be contributed. The contribution of local knowledge and strategies have been identified to have protected conservation areas and sustainable use in the past (Berkes, *et al.* 1989). This implies that local knowledge and strategies are vital in improving the performance of the conservation areas. Theoretically, the participation of the public in conservation planning and management is institutionalized and recognized to build healthy environmental systems (Olalekan, 2019; Etemire, 2015; Odemene, 2015; Eneji, 2009; Aribigbola, 2008). Yet, it is neglected in practice.

Therefore, the contribution of this study is to develop a framework as in Figure 7 for integrating local communities and the public in the management and decision-making about conservation areas surrounding them for better relationships, health, and well-being of the conservation areas. This is vital particularly because previous researchers revealed that, community members neighboring conservation areas have an interest in the management of conservation areas, and that most of them are willing to accept management responsibilities if assigned (Hassan, 2019). This is also an opportunity for the management to extend the hands of collaboration to the local communities around their conservation areas for a better and sustainable planning and management output. Despite the communities' interest and their willingness to accept management responsibilities, there is a need for continuous awareness of the importance of the conservation areas. This can go a long way in mitigating the negative impacts of human activities on the conservation areas, particularly since, most of the negative impacts are human-related (Hassan, 2019).

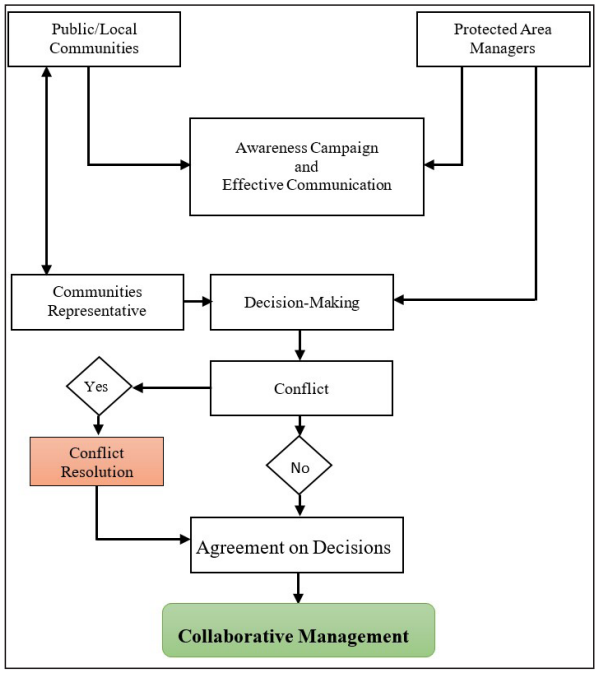

Figure 7. Framework for integrating local communities in conservation area management.

6. Conclusion

Effective environmental conservation needs to involve environmental managers as well as the public, stakeholders, and local communities surrounding conservation areas. Involvement of the public, specifically, local communities in the planning and management processes of conservation areas plays a significant role in achieving conservation goals. The study has demonstrated the role of communication in understanding conservation area boundaries as well as rules and regulations governing the conservation areas, particularly in Yankari Game Reserve. However, Yankari needs to double its efforts and increase awareness of boundaries, rules, and regulations among the communities surrounding it. Especially as the conservation area has more opportunities when it comes to staff strength, achievement of conservation goals and objectives, and implementation of the management plan. Communication between managers and local communities leads to understanding between the two parties and can build trust and confidence. This alone can facilitate protection. However, the non-involvement of local communities in the decision-making process and their inability to influence management decisions indicate a lack of collaboration between conservation managers and their host communities. This also indicates a Top-Down approach to managing the conservation areas. Therefore, the conservation managers and agencies involved in planning and managing the conservation areas should accommodate the public, particularly the local communities surrounding the conservation areas in the decision-making process and allow them to influence decisions where necessary. This is because local knowledge can have a global impact on environmental protection and management.

Recommendations

The study made the following recommendations:

i. Policy and decision-makers should re-strategize and ensure full inclusion of public/local communities/ indigenous people in the planning and management processes of conservation areas

ii. Traditional and local knowledge/practices should be integrated with modern conservation techniques for the sustainability of the conservation areas.

iii. The management of the conservation areas needs to collaborate with the local communities around them

iv. The management of the conservation areas needs to encourage the formation of Community-Based organizations and ensure the representation of each of the CBOs in the decision-making process. This is to allow the wider representation of community members in the decision-making process

v. Future research should focus on assessing the planning and management processes of the conservation areas and determining other factors that may contribute to effective planning and management of the conservation areas.

References

Afridi, M.A., Kehelwalatenna, S., Naseem, I., Tahir, M., (2019). Per capita Income, Trade Openness, Urbanization, Energy Consumption, and CO2 Emissions: An Empirical Study on the SAARC Region. Environ. Sci. Pollut. Control Ser. 26 (29), 29978–29990.

Aribigbola, A. (2008). Public participation in planning in developing countries: the example of Akure, Ondo State, Nigeria. In GBEN 2006 International Conference on Global Built Environment: Towards an Integrated Approach for Sustainability (p. 70). Lulu. Com.

Berkes, F. (2009). Evolution of Co-Management: Role of Knowledge Generation, Bridging Organizations and Social Learning. Journal of Environmental Management, 90: 1692-1702.

Berkes, F. (2010). Devolution of Environment and Resources Governance: Trends and Future. Environmental Conservation, 37(4); 489-500.

Berkes, F., Feeny, D., McCay, B. J. and Acheson, J. M. (1989). The Benefits of the Commons: Commentary. Nature, 340; 91-93.

Berkes, F., George, P. J. and Preston, R. J. (1991). The Evolution of Theory and Practice of the Joint Administration of Living Resources. Alternatives, 18: 12-18.

Bernard, H.R. (2006). Research Methods in Anthropology: Qualitative and Quantitative Approaches. Fourth Edition. Lanham: AltaMira Press.

Blaikie (2000). Designing Social Research. Cambridge: Polity Press.

Bockstael, E., Bahia, N. C., Seixas, C. S., and Berkes, F. (2016). Participation in Protected Area Management Planning in Coastal Brazil. Environmental Science and Policy, 60, 1-10.

Briassoulis, H. (1989). Theoretical Orientations in Environmental Planning: An Inquiry into Alternative Approaches. Environmental Management, 13(4), 381-392.

Brockington, D., and Igoe, J. (2006). Eviction for conservation: A Global Overview. Conservation and Society, 4(3), 424.

Brooks, Brooks, J., Waylen, K. A., and Mulder, M. B. (2013). Assessing Community-Based Conservation Projects: A Systematic Review and Multilevel Analysis of Attitudinal, Behavioral, Ecological, and Economic Outcomes. Environmental Evidence, 2(1), 2.

Burki, M. A. K., Burki, U., & Najam, U. (2021). Environmental Degradation and Poverty: A Bibliometric Review. Regional Sustainability, 2(4), 324-336.

Carey, C., Dudley, N. and Stolton, S. (2000). Squandering Paradise? The Importance and Vulnerability of the World's Protected Areas. Gland, Switzerland: WWF.

Chakravarty, D., Mandal, S.K., (2020). Is Economic Growth a Cause or Cure for Environmental Degradation? Empirical Evidences from Selected Developing Economies. Environ. Sustain. Indic. 7, 100045.

del Pilar Moreno-Sánchez, R., and Maldonado, J. H. (2010). Evaluating the Role of co-Management in Improving Governance of Marine Protected Areas: An Experimental Approach in the Colombian Caribbean. Ecological Economics, 69(12), 2557-2567.

Dixon, M., and Dougherty, D. (2010). Managing the Multiple Meanings of Organizational Culture in Interdisciplinary Collaboration and Consulting. Journal of Business Communication, 47, 3–19.

Eneji, V. C. O., Gubo, Q., Okpiliya, F. I., Aniah, E. J., Eni, D. D., & Afangide, D. (2009). Problems of public participation in biodiversity conservation: the Nigerian scenario. Impact Assessment and Project Appraisal, 27(4), 301-307.

Etemire, U. (2015). Law and practice on public participation in environmental matters: the Nigerian example in transnational comparative perspective. Routledge.

Ezebilo, E.E. and Mattsson, L. (2010). Socio-Economic Benefits of Protected Areas as Perceived by Local People Around Cross River National Park: Nigeria. Forest Policy and Economics. 12(3), 189-193.

FAO (2010). Global Forest Resources Assessment: Main Report. Food and Agriculture Organization of the United Nations of the United Nations: Rome.

Federal Government of Nigeria (2012). Nigeria's Path to Sustainable Development Through Green Economy. Country Report to the Rio + 20 Summit. June 2012.

Fourth National Biodiversity Report (2010). Abuja, Federal Republic of Nigeria.

Gbadegesin, A. and Ayileka, O. (2000). Avoiding the Mistakes of the Past: Towards a Community Oriented Management Strategy for the Proposed National Park in Abuja-Nigeria. Land Use Policy: 17(2), 89-100.

Gray, B. (1989). Collaborating: Finding Common Ground for Multiparty Problems. San Francisco: Jossey-Bass.

Hassan, A. (2019). Human-Nature Relationship: A Case of Selected Conservation Areas in Nigeria. Adamawa State University Journal of Scientific Research, 7(1), 77-86.

Hassan, A., Johar, F., Rafee, M. and Idris, N. M. (2015). Protected Area Management in Nigeria: A Review. Jurnal Teknologi, 77:15; 31-40.

https://doi.org/10.1007/s11356-019-06154-2.

https://www.nationsonline.orgmapsnigeria-administrative-map.jpg

Hyakumura, K. (2010). 'Slippage' in the Implementation of Forest Policy by Local Officials: A Case Study of a Protected Area Management in Lao PDR. Small-Scale Forestry. 9(3), 349-367.

Ite, U. E. (1996). Community Perceptions of the Cross River National Park, Nigeria. Environmental Conservation, 23(4), 351-357.

Ite, U. E. (1998). New Wine in an Old Skin: The Reality of Tropical Moist Forest Conservation in Nigeria. Land Use Policy, 15(2), 135-147.

Ite, U.E. and Adams, W.M. (1998). Forest Conservation, Conservation and Forestry in Cross River State, Nigeria. Applied Geography: 18(4), 301-314.

Koontz, T. M. (2006). Collaboration for Sustainability? A Framework for Analyzing Government Impacts in Collaborative Environmental Management. Sustainability: Science, Practice and Policy. 2(1); 15-24.

Kurdoglu, O. and Cokcaliskan, BB.A. (2011). Assessing the Effectiveness of Protected Area Management in the Turkish Caucasus. African Journal of Biotechnology. 10(75), 17208-17222.

Lockwood, M. (2010). Good Governance for Terrestrial Protected Areas: A Framework, Principles and Performance Outcomes. Journal of Environmental Management, 91(3), 754-766.

Mohammed, I., Shehu, A.I., Adamu, M.B. and Saleh, U.F. (2010). Comparative Analysis of Fauna Numerical Characteristics of Yankari Game Reserve from 1980-2008. Environmental Research Journal. 4(2), 177-181.

Mulongoy, J.K. and Chape, S.P. [Eds] (2004). Protected Areas and Biodiversity: An Overview of Key Issues. CBD Secretariat, Montreal, Canada and UNEP-WCMC, Cambridge, UK.

Nakakaawa, C., Moll, R., Vedeld, P., Sjaastad, E., and Cavanagh, J. (2015). Collaborative Resource Management and Rural Livelihoods Around Protected Areas: A Case Study of Mount Elgon National Park, Uganda. Forest Policy and Economics, 57, 1-11.

Neuman, L. W. (2007). Basics of Social Research: Qualitative and Quantitative Approaches. Prentice Hall:

Newing, H. (2011). Conducting Research in Conservation: Social Science Methods and Practice. Routledge, Taylor and Francis Group: London and New York

Nielsen, G. (2012). Capacity Development in Protected Area Management. International Journal of Sustainable Development and World Ecology. 19(4), 297-310.

Nursey-Bray, M. and Rist, P. (2009). Co-Management and Protected Area Management: Achieving Effective Management of a Contested Site, Lessons from the Great Barrier Reef World Heritage Area (GBRWHA). Marine Policy. 33: 118-127.

O'Riordan, T. (1989). The Challenge of Environmentalism. In R. Peet & N. Thrift (Eds.), New Models in Geography (pp. 77–102). London, England: Unwin Hyman.

Odemene, S. (2015). Optimizing Public Participation in Environmental Decision Making in Nigeria. Available at SSRN 2698484.

Ogunjinmi, A.A., Ojo, L.O., Onadeko, S.A. and Oguntoke, O. (2009). An Appraisal of Environmental Interpretive Policies and Strategies of Nigeria National Parks. Tropical Agricultural Research and Extension: 12(1), 7-12.

Olalekan, R. M., Omidiji, A. O., Williams, E. A., Christianah, M. B., & Modupe, O. (2019). The roles of all tiers of government and development partners in environmental conservation of natural resource: a case study in Nigeria. MOJ Ecology & Environmental Sciences, 4(3), 114-121.

Osemeobo, G.J. (1990). Land Use Policies and Biotic Conservation: Problems and Prospects for Forestry

Osemeobo, G.J. (2001). Is Traditional Ecological Knowledge Relevant in Environmental Conservation in Nigeria? International Journal of Sustainable Development and World Ecology. 8(3), 203-210

Parks and Wildlife Commission (2002). Public Participation in Protected Area Management Best Practice. Prepared for: The Committee on National Parks and Protected Area Management Benchmarking and Best Practice Program August 2002, by Parks and Wildlife Commission of the Northern Territory.

Parr J. W. K., Jitvijak, S., Saranet, S. and Buathong, S. (2008). Exploratory Co-Management Interventions in Kuiburi National Park, Central Thailand, Including Human-Elephant Conflict Mitigation. International Journal of Environment and Sustainable Development. 17(3); 293-310.

Participatory Management Plan of Lame-Burra Game Reserve (2007). Environ-Consult.

Participatory Management Plan of Yankari Game Reserve (2007). Environ-Consult.

Pfahl, M., Casper, J., Trendafilova, S., McCullough, B. P., and Nguyen, S. N. (2015). Crossing Boundaries: An Examination of Sustainability Department and Athletics Department Collaboration Regarding Environmental Issues. Communication & Sport, 3(1), 27-56.

Poffenberger, M. (1990). Keepers of the Forest: Land Management Alternatives in Southeast Asia.

Ramirez, B. (2014). Improving Sustainable Development Outcomes Through Best Management Practices. 12, 25–45.

Ribot, J. C., Agrawal, A., and Larson, A. M. (2006). Recentralizing while Decentralizing: How National Governments Reappropriate Forest Resources. World Development, 34(11), 1864-1886.

Selin S. and Chavez, D. 1995. Developing a Collaborative Model for Environmental Planning and Management. Environmental Management, 19(2): 189-195.

Stolton, S. (2004). Issues that Arise for the Categories in a Changing World. Parks: 14(3), 63-71.

The World Bank (1999). Report from the International CBNRM Workshop, Washington D.C., 10-14 May 1998. URL: http://www.worldbank.org/wbi/conatrem/

Thomas, L. and Middleton, J. (2003). Guidelines for Management Planning of Protected Areas. IUCN Gland, Switzerland and Cambridge, UK. Ix + 79pp.

United Nations Environment Programme (2007). Global Environmental Outlook: Environment for Development. UNEP, Nairobi, Kenya

United States Agency for International Development (USAID). 2008. Nigeria Biodiversity and Tropical Forestry Assessment: Maximizing Agricultural Revenue in Key Enterprises for Targeted Sites (Markets). Chemonics International Inc.

Vodouhe, F.G., Coulibaly, O., Adegbidi, A. and Sinsin, B. (2010). Community Perception of Biodiversity Conservation within Protected Areas in Benin. Forest Policy and Economics. Volume 12; 505-512

Watson, J. E., Dudley, N., Segan, D. B., and Hockings, M. (2014). The Performance and Potential of Protected Areas. Nature, 515(7525), 67-73.

Wildlife Conservation Society (2012-2016). Nigeria Program Conservation Strategy.

Woodland, R. H., and Hutton, M. S. (2012). Evaluating organizational Collaborations Suggested Entry Points and Development in Nigeria. Land Use Policy: 7(14), 314-322.

Strategies. American Journal of Evaluation, 33(3), 366-383.

JJEES

JJEES (2023) 14 (2): 113-125
ISSN 1995-6681

Jordan Journal of Earth and Environmental Sciences

Hydrogeological Modeling of the Sandstone Aquifer of Mostaganem Plateau (North-West Algerian) and Perspectives on the Evolution of Withdrawals

Bentahar Fatiha[1], Mesbah Mohamed[1], Ribstein Pierre[2]

[1]Department of Geology, Faculty of Earth Sciences, Geography and Spatial Planning (FSTGAT), University of Science and Technology Houari Boumediene, B.P.32 El Alia, Bab Ezzouar, Algiers, Algeria.
[2]UMR.7619 Sisyphe, University Pierre and Marie Curie (Paris IV). Case 123, Tour 564 55-th floor, 4 place Jussieu, 75252 Paris Cedex 05, France.

Received 3rd June 2022; Accepted 26th October 2022

Abstract

overexploitation of the Mostaganem aquifer has considerably reduced its groundwater resources. Based on this fact, the objective of our work is to study the modifications, the evolution, and the impact of the withdrawals of the aquifer in two aspects: magnitude and causes; by modeling groundwater with the Visual Modflow program. The setting was carried out in a steady state, which was calibrated and validated on Gauchez's piezometric maps, then in a transient state.

To predict the possible drop in groundwater levels for the upcoming years, three prospective scenarios were considered. In scenario 1, operating flows of drinking water supply and irrigation will remain constant from 2010 to 2035, the only variable is time, We notice that over 25 years the groundwater level of the slick for scenario-1 will continue to decline, especially in the central part where we note a fall of 5m and 7.5m. In scenario 2, half of the boreholes intended for the supply of drinking water on the Mostaganem plateau are at a standstill as of 2014, the launch of the Mostaganem, Arzew, Oran (MAO) project commissioning of the Chelif Dam is launched and the flow rates for irrigation are kept constant, after simulation, in the central part of the Mostaganem Plateau, we note a marked improvement in the drawdowns, which pass from 2.5 meters and 5 meters has drawdowns from 1 meter to 2.5 meters As, for scenario 3, an increase in the population of 2.51% is observed each year. In addition, the flows of drinking water supply and irrigation will be multiplied by 2.51% from 2010 to 2035, The drawdowns for scenario-3 (Figure 20), give worrying values, especially in the south of the Mostaganem plateau.

In the three scenarios, there is a continuous depletion of the groundwater resource due to significant withdrawals compared to the recharge of the aquifer. These simulations suggest that current sampling rates cannot be sustained over the long term.

Keywords: *Mostaganem aquifer, Over-exploitation, Groundwater levels, Hydrogeological modeling, Visual Modflow, Simulation scenarios.*

1. Introduction

Water is a key component of global socioeconomic development (Soular et. al., 2020). Groundwater, the world's largest freshwater reservoir, supports the survival and sustainability of human life worldwide. It is the main source of drinking water supply (DWS) at 50%, and irrigation at 70% (Seibert et al., 2010; Smith et al., 2016; Gleeson et al., 2016; Dieter et. al., 2018). The dependence of human activities on the availability of groundwater has increased with time and development. (Thakur Praveen, 2020). Moreover, it accounts for almost half of the world's drinking water (Unesco, 2009). Its unique characteristics, such as its subterranean nature, make it a difficult resource to manage, thus contributing to the increase of pressure on this resource. (Les Landes, 2015).

The Mostaganem Plateau is characterized by scarcity or even the absence of surface water. The main source of drinking water supply for human, agricultural, and industrial consumption is groundwater. This resource is limited and has experienced qualitative and quantitative degradation in recent decades due to anthropogenic (over-exploitation and pollution) and natural constraints (type of climate and global warming) (Bahir and Ouhamdouch, 2020; Boufekane and Saighi, 2019).

For several years, the Plateau aquifer has experienced a significant decline in the groundwater level of its main aquifer, consisting of Calabrian sandstones. This is due to a large demographic increase and an extension of irrigated perimeters leading to strong demand for water (Bentahar and Mesbah, 2007).

The water level decline of the aquifer implies the digging of even deeper boreholes. (ANRH, Sogreah consultants, 2006). In this context, hydrogeological studies have been carried out on the Mostaganem Plateau: (Perrodon, 1957), (Bonnet, 1967), (CGG, 1968), (Gauchez, 1981), the explanatory notice of the hydrogeological map of the Mostaganem Plateau at scale 1/10 000th (1978), (Gauchez.1981), (Baiche, 1994), (Saibi, 2000), (Sogreah, 2006), (Bentahar, 2007).

Several new approaches that were established to address groundwater depletion worldwide to enrich the future

* Corresponding author e-mail: fatiha.bentahar@yahoo.fr

trajectory have been adopted (Bhat & al., 2019; Kaur & al., 2020). In the early 2000s, faced with the challenges of water management marked by water stress, the Algerian public authorities, initiated a series of major hydraulic infrastructure construction projects. In Algeria, 50% of the drinking water supply comes from underground resources and 33% comes from surface water. The average supply of a citizen is 180 liters/day (Algerian water supply, ADE, 2019). Among these new approaches, Algeria has opted for the desalination of seawater. The country has 21 desalination stations according to the Ministry of Water Resources (MRE, 2019), which allows supplying 6 million inhabitants with drinking water, with a volume of 1.34 million m^3/day (ADE, 2019). The only and best solution to guarantee the supply of drinking water in the long term is to move towards the use of unconventional waters, including seawater desalination since most of the population lives near and along the coastline. (Berraki, 2021).

To decrease the exploitation of the Plateau aquifer, two measures were opted for by the Ministry of Water Resources. The construction of a desalination station was commissioned in 2010, providing 200,000m^3/day of drinking water (ADE, 2019). The large MAO project consists of a water-dam-transfer structuring project from the Chelif dam (50 million meters cubic of retention) and a treatment station with a capacity of 600,000 m^3/day, and a pumping station, which supplies Mostaganem, Arzew, and Oran with drinking water. It allows the transfer of 45 million m^3/year for the benefit of the wilaya of Mostaganem. (ANBT, 2010).

Following this program, half of the boreholes intended for the supply of drinking water on the Mostaganem plateau are at a standstill as of 2014, according to the Mostaganem water supply department (DHW, 2015). Even with these important decisions, the level of the aquifer remains at risk; this is due to the large number of boreholes intended for irrigation that was not deemed useful to stop or reduce pumping, and the very large number of illegal boreholes for personal use. Despite the construction of new dams and the use of desalination, Algeria will record a water deficit of 1 billion m^3 by the year 2025 (Remini, 2010.)

Therefore, to better understand the role of current and future water use in different sectors (irrigation, drinking, and industry), the impact of climate change (Döll, 2009), population growth, and the policy interventions on groundwater availability in a quantitative manner, it is necessary to use advanced methods, such as geospatial technology and three-dimensional numerical modeling of groundwater.

The objective of this work is to study the functioning and evolution of groundwater, and the impact of abstractions on the sandstone aquifer of Calabrian, by implementing a management model using the Visual Modflow program.

This modeling will make it possible to advance the understanding of the modeled system operation and to predict future situations of the system according to different solicitations (predictive mode; changing input variables) or even to evaluate the system response to different usage scenarios (management mode; variations in boundary parameters and conditions). (Villeneuve and al., 1998).

The proposed conceptual model for the Mostaganem Plateau Aquifer System takes into account precipitation infiltration, saturated zone flows, drinking water abstraction (DWA), irrigation, and industry needs.

To characterize and understand the structure of the Plateau Calabrian aquifer, we used multi-source data (geological, topographical, geophysical, hydrodynamic), and we created a GIS database built under ArcGIS, which will be used for the implementation of the model.

2. Study area

The Plateau of Mostaganem is in northwest Algeria, in the Wilaya of Mostaganem, 363 km west of the capital Algiers. Bounded in the north by the lower Chelif Plain and the Dahra mountains, in the west by the Mediterranean Sea, in the south by the Bordjias Plain, and in the west by the Mina Plain (Figure 1). The study region is located between coordinates the coordinates are X1= 246 000 m, X2= 304 000 m, and Y1= 274 00 m Y2= 304 000 m (Projected Coordinate System: North_Algeria

Projection: Lambert_Conformal_Conic).

To determine the elevation of our study area, Four Shuttle Radar Topography images with a 30-meter resolution are obtained from the SRTM (2011). Its satellite images are downloaded from the UGSS (2014) in Geotif format.

The study area consists of 11 municipalities: Mostaganem (main city), Ain Tedles, Bouguirat, Sirat, Souaflia, Mesra, Ain Sidi Sheriff, Mansourah, Touahria, and Sayada. And represents 0.029% of the total area of Algeria. (National Statistics Office, NSO, 2008).

During the French colonization, vine cultivation was introduced on the Plateau. After the independence of the country, it was replaced by irrigated markets for gardening, citrus fruit, and cereal crops (Marc Cote, 1996).

The Plateau of Mostaganem is a first-rate agricultural and tourist area, it is tabular with an area of 700 km^2. This plateau drops steadily towards the west towards the plain of Habra and the Gulf of Arzew. (Gauchez, 1981). It has a series of parallel wrinkles and depressions-oriented southwest and northeast. (Baiche, 1994).

The altitude of the Plateau is situated between 110 m (in the west) and 470 m (in the east) with an average of 200 m which decreases gradually to 100 m at the level of the Macta. (Bentahar, 2007).

In the north, the plateau regularly overlooks the lower Chelif Valley, showing a series of cliffs whose heights vary from 150 m to 200 m. To the northeast, it comes up against the Cretaceous spur of the Djebel Diss (Dahra) which culminates at an altitude of 400 m. To the South-East, it is bordered by a line of relief materialized by the strong buttresses of Akboube and Ennaro which separates it from the plain of Relizane. (Bellal S, & al., 2019).

The hydrography of the Mostaganem plateau is very modest. It is limited to two small permanent rivers (wadis).

The first, the Sefra wadi, 11 km long, originates in the region of the "seven wells", and becomes perennial at the entrance of the town of Mostaganem where it receives the overflow of sources captured from Kheir eddine (ex Pélissier), before flowing into the sea. The second, the Kheire Wadi 6 km long, is a tributary of the Chelif. It is fed by the sources of Ain Soltane and Ain Hallouf (Gauchez,1981).

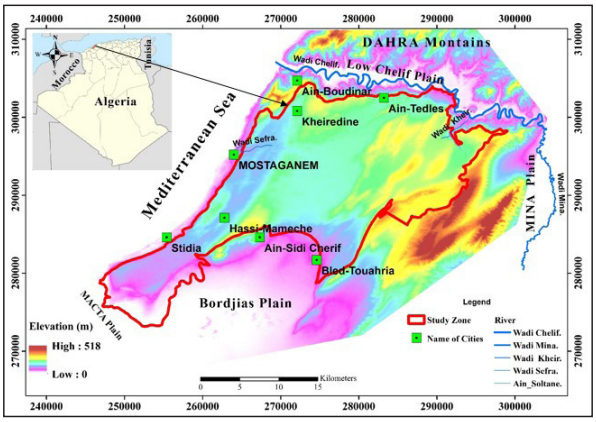

Figure 1. The geographical location of the Mostaganem Plateau.

2.1 Geological and Hydrogeological Characteristics

At the level of the Mostaganem plateau (Figure 2), there are two types of formations:

- Allochthonous formations are the oldest, we can define the Trias which consists of white gypsum located South of the Mostaganem plateau. The tablecloths are in the north of Mostaganem (Karouba, Djebel Diss), where appears a whole set of land belonging to the tablecloths of the Numidian age, extends into the region of Mina. diapirism occurs east of Ain Nouissy.

- Indigenous formations are predominant, they include: the Lower Miocene corresponds to a blue marl level; the upper Miocene is characterized by blue marl interposed by levels of sandstone with calcareous-clay cement, cinerites 0.20 m thick, (Perrodon, 1957). These blue marls are very well exposed at the level of the Akboube State Forest, where they extend widely on the axis of this anticline under quaternary deposits. The Pliocene is almost everywhere on the borders of the Mostaganem plateau. It consists of ancient marl or sandy horizon of 200 to 500 m thick, and the Astian formed of limestone sandstone with a maximum thickness of 100 m. The Quaternary is represented by the transgressive and discordant Calabrian on the deposits of the Mio-Pliocene. It is formed by limestone sandstones. The Calabrian covers the whole plateau of Mostaganem.

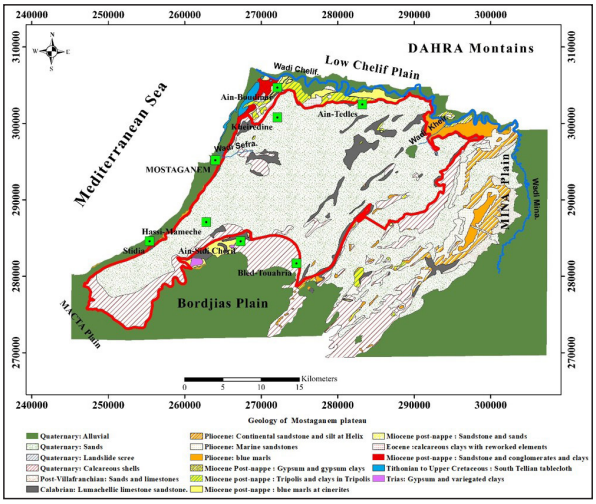

Figure 2. Geological map of the Mostaganem Plateau.

2.2 Climatology characteristics

The Mostaganem plateau is characterized by a semi-arid to temperate winter climate and rainfall ranging between 350 mm and 600mm (1962-2017). Eight metrological stations were selected for this study. Rainfall data were provided by the National Water Resources Agency (ANRH) of Algiers. Temperature data are obtained from the National Meteorological Office (ONM), Dar El Beida, Algiers. A meteorological station is located near the Mostaganem city, and seven rainfall stations (cultivated dunes, Ain Tadles, Hassi-Mameche, Khierdine, Ferme Assorain, Oued-Keir, Fornaka), are distributed through the entire Plateau (Figure 3). The Mostaganem station (04-06-12) and the Ferme Assorain station (11-16-17) present the longest and most complete series of monthly rains (1968-2017). The duration of observations varies from 49 years for the Mostaganem station (04-06-12) to 33 years for the Hassi Mameche station (04-06-03). The data contains gaps in observations, which required their filling by the method of least squares (Table 1).

Table 1. Climate data available at Mostaganem Plateau.

Station Name	Code	X	Y	Data type	Frequency	Period	Deficiency rate (%)	Annual average[1]	Standard deviation
Mostaganem	04-06-12	264800	296250	Evapotranspiration	Monthly	1968-2017.		422	
				Temperature	Monthly	1962-2010	0	18	0.68
				Rain	Monthly	1906-1926 1935-1938 1942-1961 1968-2017	0 0 0 0.5	388	
Cultivated dunes	04 06 11	274000	288300	Rain	Monthly	1970-2010	3.12	336	
Ain Tadles	04 06 06	283100	302600	Rain	Monthly	1942-1961 1968-2009	3.04		
Hassi-Mameche	04 06 03	263050	287600	Rain	Monthly	1928-1961	8.83		
Khierdine	04 06 02	272100	300750	Rain	Monthly	1969-2009	1.66	358	
Assorain Farm	11 16 17	281250	291850	Rain	Monthly	1968-2009	1.82	337	
Oued-Keir	01-36-06	291500	297600	Rain	Monthly	1970-2009	2.99	346	
Fornara	11 16 06	250800	278500	Rain	Monthly	1967-2009	1.59	268	

Units: Rain and Evapotranspiration in mm; Temperature in °C.

Precipitation on the Mostaganem plateau varies in time and space; we note an irregularity of rainfall from one year to another and from one station to another (Figure. 3). Thus, the height of precipitation is greater in the northern part of the plateau (04-06-12 = 592 mm for 1971, 04-06-02 = 556 mm for 1979, 04-06-06 = 575 mm for 1971) than in the southern part (11-16-06 = 486 mm for 1969, 04-06-11 = 402 mm for the year 1971,11-16-17 = 494mm for 1971). Over 49 years, the rainy months extend from September to April, and the driest months from July to August.

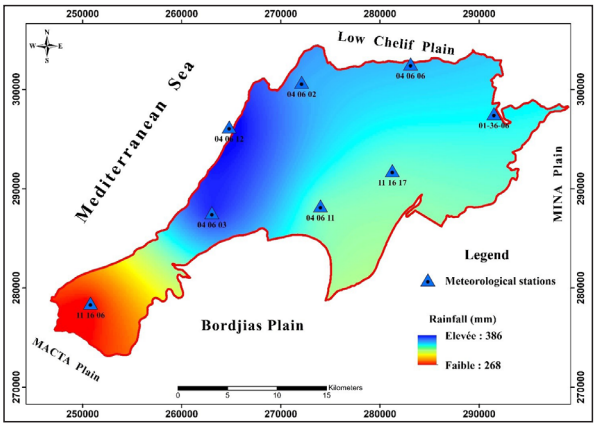

Figure 3. Annual rainfall distribution through rainfall stations on the Mostaganem Plateau over the period 1968-2017.

The year 1981 is the driest in the entire Mostaganem Plateau with minimum precipitation of 85 mm at station 11-06-06 located in the south of the study area.

Evapotranspiration (ET) is the amount of water transferred to the atmosphere by evaporation at ground level and the level of precipitation interception and by transpiration of plants. Potential evapotranspiration (ETP) is the amount of water that would evaporate or transpire from a watershed if the water available for evapotranspiration was not a limiting factor (Laborde, 2003). Evapotranspiration is measured by the Thornthwaite method:

$$\mathbf{ETP = 1.6\ (10T/I)^a} \quad (1)$$

With:

ETP: potential evapotranspiration in mm

T: average monthly temperature of the month in °C

$\boldsymbol{I = \sum_{i=1}^{12} i}$: The annual heat indexes

a= 0.492+1.79×10^{-2}×I-7.71×10^{-5}×I^2+6.75×10^{-7}×I^3

Were

i = (T/5)$^{1.514}$ monthly heat index

The mean ETP values (Figure 4) range from 23.18mm in January to 152.25mm in July.

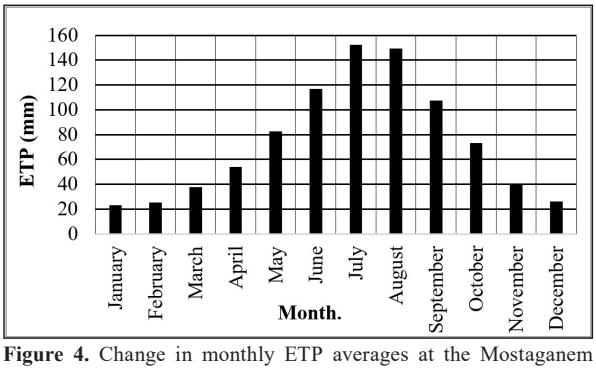

Figure 4. Change in monthly ETP averages at the Mostaganem plateau (1968-2017).

Real Evapotranspiration (ETR) is the amount of water evaporated or transpired by soil, plants, and open water in a watershed (Laborde, 2003). The ETR is calculated by the empirical formula based on the Turc method.

$$\boldsymbol{ETR = \frac{P}{0.9} + \frac{P^2}{L^2}} \quad (2)$$

ETR = actual annual evapotranspiration in mm

P = annual precipitation in mm

L = the evaporating power.

L^2 = (300+25T+ 0.05T^3)^2.

T = average annual temperature in °C.

Precipitation and Temperatures (Figure 5), used in our calculation will be those relating to the Mostaganem 04-06-12 station (period 1969-2017).

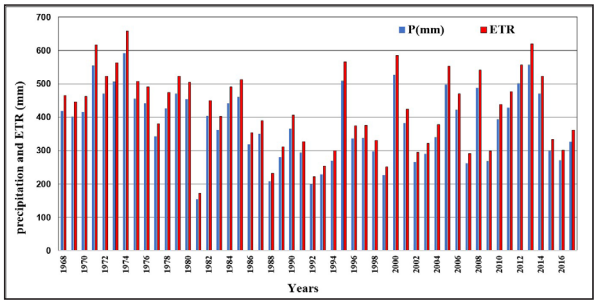

Figure 5. Interannual variation of the ETR at the level of the Mostaganem Plateau.
(Period 1968-2017)

At the station of Mostaganem (Figure 5) period 1968-2017, the maximums rainfall, recorded during the year 1974 with 657mm. The minimum is observed during 1981 with 171mm.

The **Thornthwaite** method was adopted to estimate the different terms of the hydrological balance equation that was established over 49 years (1968-2017), whose formula is written as follows:g

$$\boldsymbol{P = ETR + R + I} \quad (3)$$

With:

P: average annual precipitation (mm)

ETR: actual annual evapotranspiration (mm)

A: average annual runoff (mm)

I: average annual infiltration (m)

The study of the flow deficit at the scale of the study area resulted in an evaluation of the real evapotranspiration (ETR) estimated by the Turk method at 422 mm. The infiltrated water layer determined by the Sogeta-Sogreah method was estimated at 19 mm. Runoff reaches 23mm (1968-2017).

2.3 Hydrogeological characteristics

The Mostaganem Plateau has an impermeable marly substrate, topped with sandy-past sandstone or sandy-clay sandstone that contains the main aquifer (Figure 6). The sand overcomes all this, with facies and thickness varying according to their location, where it is possible to show the presence of a sandy limestone crust associated or not with red soil. Calabrian is the main aquifer with varying thicknesses. Thus, it can reach a power of 100 to 120 m in topographical depressions while on the bulges of the base, the formation will be 20 to 30 m. In general, the thickness of this series decreases from ENE to WSW. The Miocene and Lower

Pliocene formations constitute the impermeable substratum of the main aquifer. The Miocene is essentially represented by blue marl, sometimes including gypsum levels. The Quaternary is transgressive and discordant in earlier series.

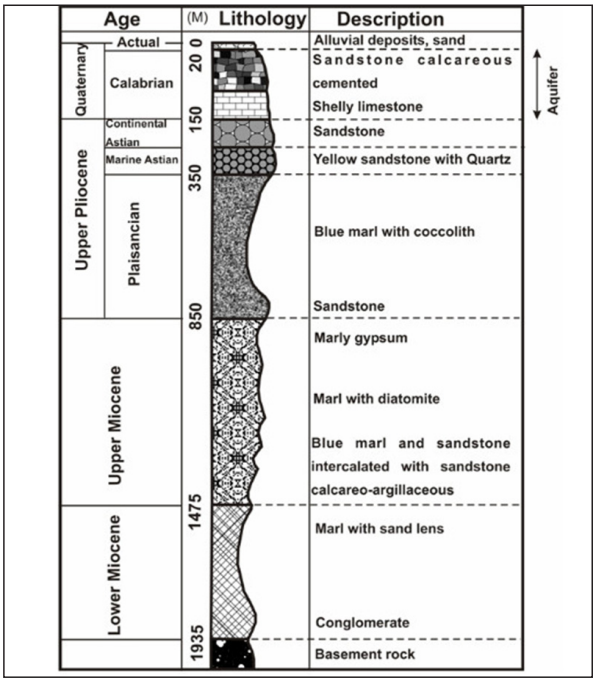

Figure 6. Well log stratigraphy at Mostaganem plateau (Saibi, 2008).

The sandstone aquifer of Calabrian has been the subject of several piezometric companies: during the year 1970 by the Office of Hydraulic Inventory and Research of the ANRH of Algiers, and a piezometric campaign of June 1990 by (Baiche, 1994) in the framework of a Magister supported at the University of Oran. The ANRH of ORAN carried out the last piezometric surveys, on one hand, during the years 1995 and 1996-1997, which covered 12 piezometers, and on the other hand, during the hydrological years 1998-1999, 1999-2000, 2010, 2011, 2012 and which covered 17 piezometers and whose main role is to control the Mostaganem Plateau aquifer.

The variations in the groundwater level during periods of high and low water are small (Figure 7). They are 1 to 2m in areas where the aquifer is less than 10m deep and 0.5m on the rest of the Plateau. The aquifer is fed exclusively by the infiltration of precipitation water. Sources account for 85% of the flow of natural outfalls. They are located on the periphery of the Plateau where the impermeable substrate collapses. The piezometric surface emphasizes the general conformity of the layer with the surface of the ground. (DEMRH, 1971).

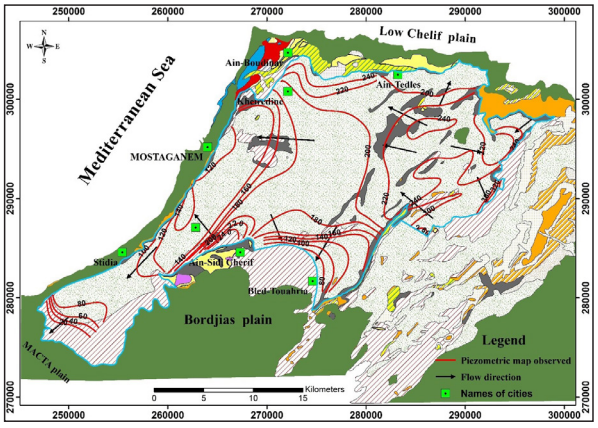

Figure 7. Piezometric map of the Mostaganem Plateau 1970.

3. Materials and Methods

3.1 Model implementation

For modeling an aquifer system, the first step is to assign boundary conditions and calculation parameters (EL Arbi Toto et. al., 2009). This phase was accomplished through the literature review of available data.

The software used is Visual Modflow 2011.1, which simulates groundwater flows and contaminant transport in both steady and transient conditions. The Visual Modflow includes several modules: Modflow-2000: developed by USGS (Pallok, 1989) to simulate underground flows. Modpath: a program used to simulate particle flow lines downstream or upstream of a reference point. MT3D: program modeling the transport of solutions or contaminants in the aquifer.

Conceptual modeling using the Modflow 2000 code, which resolves the partial derivative diffusivity equation of groundwater flow in a porous media by the finite difference method,

$$\frac{\partial}{\partial_x}\left(k_{xx}\frac{\partial h}{\partial_x}\right)+\frac{\partial}{\partial_y}\left(k_{yy}\frac{\partial h}{\partial_y}\right)+\frac{\partial}{\partial_z}\left(k_{zz}\frac{\partial h}{\partial_z}\right) div(k\ grad\ h)-w=s_s\frac{\partial h}{\partial t} \quad (4)$$

With k the hydraulic conductivity (L/T), h the hydraulic load (L), $_{Ss}$ the specific storage coefficient (L^{-1}), W the volumetric flow per unit volume representing the term well or source (T^{-1}), and the time (T).

Modeling is initiated by trial and error to obtain the best set of calculated piezometric concerning the observed values.

3.2 Delimitation of the study area extension

The modeled study area corresponds to the Calabrian sandstone aquifer of the Mostaganem Plateau, with an area of 700 km^2, and the coordinates are X1= 246 000 m, X2= 304 000 m, and Y1= 274 00 m Y2= 304 000 m. The first step in building the model consists of defining the number of layers and defining the mesh of the study area (Figure 8).

The discretization of the space in regular square meshes presents a great facility both in the use and in the implementation of the models. (Ledoux E, 2003). The study area was discretized in a single layer regularly in a square mesh of 500×500m aside, for a total of 2520 active meshes.

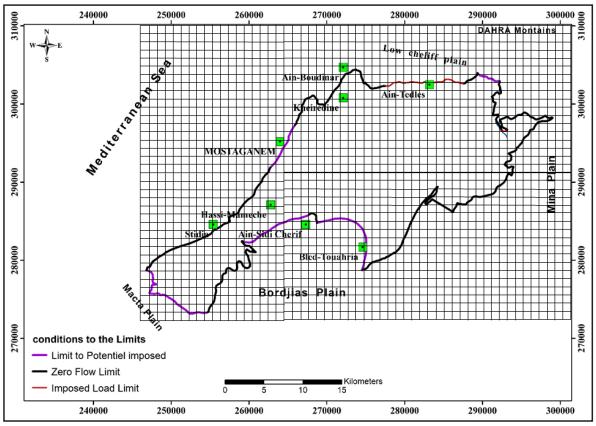

Figure 8. Discretization of the Calabrian aquifer of the Mostaganem Plateau.

3.3 Boundary conditions

The relationship between the modeled domain and the external environment is described through three types of boundary conditions. The first is the imposed load condition (Dirichlet condition): the piezometric height is known along the boundary. The second is the Required flow condition (Neumann condition): when the exchanged flow rates are known. the tightness limits (tight limits) or limits through which the flow rate is negligible are considered zero flow limits. The third concerns the Mixed load and flow condition (Fourier or Cauchy condition): the flows are dependent on the piezometric height. This is the case for rivers draining or feeding the aquifer. These types of boundary conditions can simulate flows between the groundwater and surface waters (Dassargues, 1995).

The boundary conditions concern the rules for the exchange of flows between the modeled domain and the external environment (Ledoux, 2003):

- in the North limit with no flux, (Figure 9) constituted by the marls and clays of the Miocene of Djebel Bel Hacel.
- in the North-East, an imposed load limit.
- in the East and South-East, zero-flow limits.
- in the South, a limit to be imposed is the exit of the piezometry towards the plain of the Bordjias;
- in the South-West, there is also an imposed load limit, which is the exit of the aquifer towards the plain of the Bordjias.

-The western limits are a zero-flow limit except for the area of the city of Mostaganem, where an imposed charge flow was been imposed.

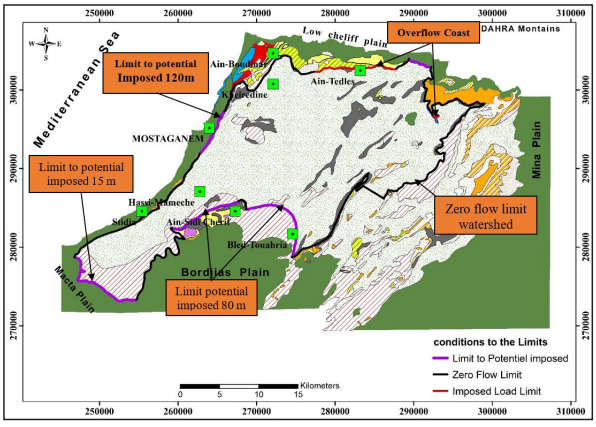

Figure 9. Map representing the boundary conditions of the Calabrian aquifer of the Mostaganem Plateau.

3.4 Results and discussion

3.4.1 Simulation and calibration in steady-state

A steady state is a condition that characterizes an aquifer before a variation is introduced. (Bandani E & al., 2011). The steady-state piezometry of the Mostaganem Plateau aquifer is established using data from the 1970 piezometric campaign (Gauchez, 1971), minimizing the gap between calculated and observed piezometry. The parameters used are the permeability, the recharge, and the thickness of the aquifer.

Adjustments were made to the permeability to best match the simulated piezometric map to that observed one (Table 2).

Table 2. Permeability Adjusting in steady state.

Borehole N°	Initial K (m/s)	K modified (m/s)
F111	0.125×10^{-4}	1×10^{-4}
F56	0.125×10^{-4}	1×10^{-4}
F41	0.125×10^{-4}	6×10^{-4}
F42	1.5×10^{-4}	6×10^{-4}
F43	0.125×10^{-4}	6×10^{-4}
F85	3×10^{-4}	6×10^{-4}
F92	3×10^{-4}	4.5×10^{-4}
F20	3×10^{-4}	6×10^{-4}
F21	4×10^{-4}	4.5×10^{-4}
F65	6×10^{-4}	6×10^{-4}

At the end of the calibration, a map of the spatial distribution of the permeabilities was drawn up across the Calabrian aquifer (Figure 10). Five zones of permeability are shown, the values are between 1×10^{-4} and 1.5×10^{-4} on most of the central part of the Plateau and the extreme southwest of the Plateau. South of Ain Tedles is a V-shaped zone (boreholes F41, F42, F43) whose tip points towards the center of the Plateau and whose permeability value is the highest of the order of 6×10^{-4} to 7.5×10^{-4}, another zone lying to the east of the city of Mostaganem (boreholes F66, F67), and at the eastern end (borehole F85) of the Plateau. These values are explained by the presence of lumachellic sandstones and limestones. These zones of low permeability values are progressively surrounded by ranges of intermediate permeability values in the range of 4.5×10^{-4} to 6×10^{-4} and then values in the range of 3×10^{-4} to 4.5×10^{-4}.

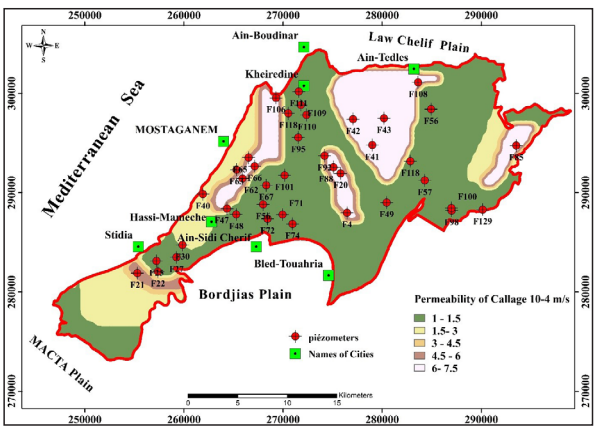

Figure 10. Spatial distribution of the permeability of callage after calibration in steady-state 1970.

The recharge of the aquifer is constituted by the flow calculated in the form of effective rainfall infiltration rates determined by the hydrological balance sheets and by the flows imposed on the lateral limits of the modeled domain (Kessasra, 2015). The average infiltration is calculated from the rain and temperature archives recorded in the stations distributed on the Mostaganem Plateau.

The thickness of the aquifer is calculated using the drilling logs over the Mostaganem Plateau. The study is complemented by geophysical analysis and geological sections. A thickness distribution map was made using all of its data (Figure 11). The maximum thickness of the aquifer is 125 m in the eastern part of the plateau, while the entire central part is between 50 and 75 meters thick, up to 100 meters thick, and it is in this part of the Plateau where most of the drilling is concentrated, especially those intended for the supply of drinking water.

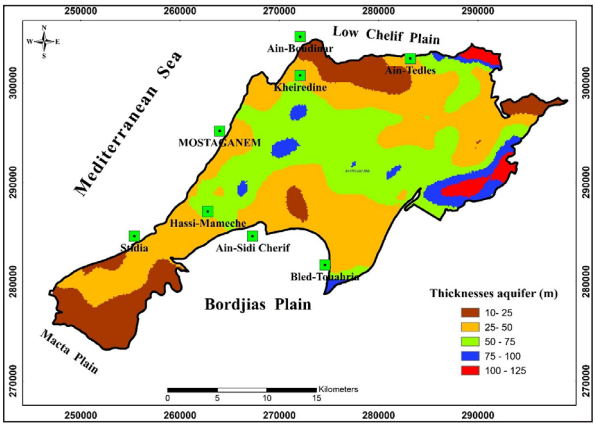

Figure 11. Spatial distribution of the thicknesses of the Mostaganem Plateau aquifer.

The simulated head is well correlated with the observed head (Figure 12), with a correlation coefficient of 0.99. Statistical analysis of the calibration results of the model mentioned in Table 3 gives acceptable values. The residue is between 0.56 m and 18.85 m. The average absolute value of the residues is 0.978 m for a groundwater level between 84.3 m and 285 m. The square root of the quadratic mean error (RMS) is 6,264 m.

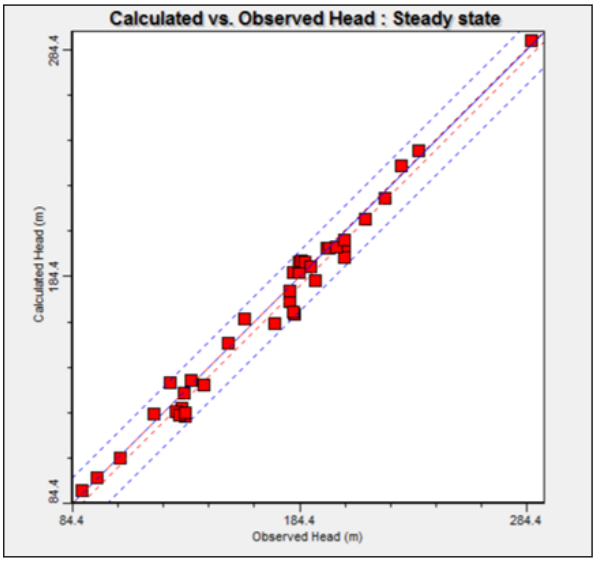

Figure 12. Comparison of calculated and observed heads in steady state.

Table 3. Statistical indices of the results of the model calibration.

Number of points	38
Minimum residue	-0.338
Maximum Residue	-14.105
Average absolute error (m)	0 978
RMS (m)	6 264
Standard RMS %	3 163
Correlation coefficient	0.99

The setting in steady-state, as shown in (Figure 13), is considered optimal. It is satisfactory because the calculated hydraulic loads correspond overall to the piezometric measurements made in the Calabrian sandstone aquifer of the Plateau de Mostaganem. The shape of the isopiezes appears to be like the measured isopiezes, the same piezometric tendencies have been largely reproduced throughout the Plateau. However, isopiezes seem to be shifted in the South-West probably due to a poor estimation of the permeability set due to the lack of measurements in this Plateau area and the lack of pumping tests carried out.

On the Mostaganem plateau, the simulated piezometry has a flow direction identical to that observed, it is done from the central part towards the south, the east, and the west. In the east part, the flow has a divergent aspect, it is done towards the east and the west. In the southern part of the plateau, the groundwater level passes from 180m to 100m and the flow goes south, towards the plain of the Bordjias. In the southwest, the groundwater level goes from 80m to 20m, and the flow is towards the plain of the Macta. In the western part of the plateau, the general flow direction goes from the city of Mostaganem where the groundwater level passes from 180m to 120m.

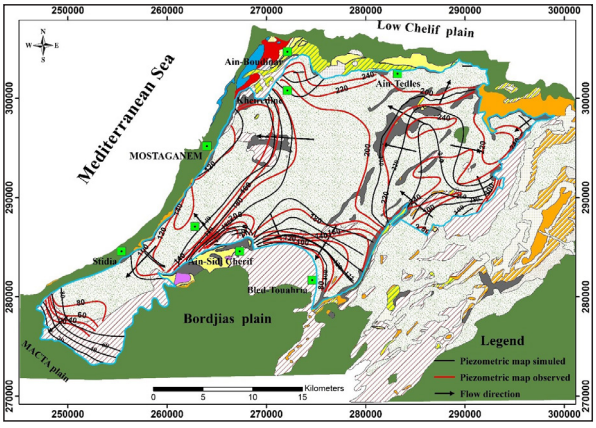

Figure 13. Simulated and observed groundwater head maps of the Calabrian aquifer of Mostaganem Plateau for the steady state of 1970.

3.4.2 Transient state

The calibration of the model in a transient state was developed considering the arrangement of piezometric chronicles and samples in the aquifer. The transient state extends from 1st September 2010 to 31 December 2010. The simulated piezometry in 2010 is presented in (Figure 14), it is calculated from the piezometry observed by the ANRH (National Water Resources Agency). A new parameter is included in the setting, namely the storage coefficient.

3.5 Results and Discussion

The general appearance of the simulated piezometry between 1970 and 2010 is similar, especially in its western part towards the city of Mostaganem. Piezometry is also similar between the two simulation periods in the southwestern part of the Mostaganem Plateau south of the town of Stidia, where the flow goes south towards the Macta Plain, and near the towns of Blad Touahria and Ain Sidi sheriff. The general shape of the piezometry is also similar between the two simulation periods. The flow is towards the plain of the Bordjias. The difference between these two maps (1970 and 2010) is observed in the eastern part of the Mostaganem Plateau where the 240m isopieze curve becomes concentric on the 2010 map.

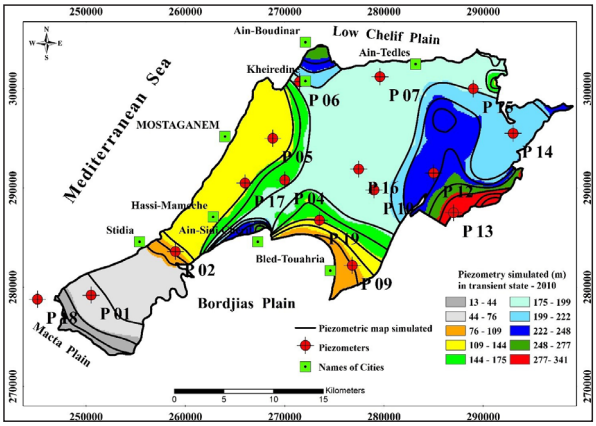

Figure 14. Simulated groundwater head of Calabrian aquifer for transient state period 2010.

The general flow direction observed on the piezometric maps is identical for both simulation periods. We have also monitored the drawdowns of the aquifer by way of drilling (Table 4). We find that over 10 years, the groundwater level has dropped considerably. The largest drop is observed at the P19 borehole in the Blad Touahria region south of the Mostaganem Plateau, at 9m. The other major drawdown is at the level of the P06 piezometer in the Kheir-Eddine region, which is 1.22m. We note that the major drawbacks are in the edge areas of the Mostaganem Plateau where the depth of the aquifer is shallow and where exploitation is intense, especially in the central part of the Plateau.

3.5.1 Aquifer Water Balance

Modflow allows the calculation of detailed water balances in system inputs and outputs of the system on all model elements or by area. These balance aquifers, in the form of scales, make it possible to determine the storage capacity of the aquifer and the share of recharge by the rains and the external borders (Kessasra, 2015).

The transient water balance is shown in Table 5, it highlights the supply and output terms following the hydrogeological functioning of the Mostaganem Plateau aquifer. In terms of inputs, the aquifer is fed by direct infiltration of precipitation, which represents 24% of the groundwater input. The rest of the inflows come from the external and lateral limits of the systems called boundary zone inflows, which represent 28.37%.

The main exit points of the model are represented by the water withdrawals by DWS (drinking water supply), agricultural and industrial catchments that represent 57.6%, and the exits in the southern parts towards the plain of the Borgias and the Macta plain 38%, the sources 3.44%. The storage capacity of the Mostaganem plateau aquifer is an important term, it is 34 570 m^3/day, and the destocking of the aquifer represents 0.82%.

Table 4. Changes in the piezometric levels of the Mostaganem Plateau aquifer (ANRH Relizane-2010)

Piezometer N°	Name	1998	1999	2000	2010
P 07	Mostaganem	237 80	237 80	237 80	235.89
P 19	Blad touahria	157.41	156 97	156 98	147.14
P 01	Douar louiza	73.88	73.65	73.65	73.28
P 04	Douar benattia	172 80	172 80	172-01	170.85
P 05	Sidi fellag	131.83	131.83	131.55	131 95
P 06	Kheir - eddine	160 78	160 78	160.79	162.17
P 12	Ennaro	223.62	223.61	223.61	220.25
P 13	Bled fernaka	273 83	273 83	272.39	270.12
P 14	Ain soltane	198.11	198.11	197.61	194.81
P 15	Sour kelmitou	201.72	201.72	201-08	199.58
P 16	Douar medjahri	171.24	170.36	170.35	169 96
KD2	Kheir-eddine 2	145.03	145 59	145 59	154 53
P2		251.38	251.24	251.24	264 57
BT1	Blad touahria	107.07	107.15	106 92	/

Table 5. Water balance of the Mostaganem Plateau aquifer in the transient state.

Mostaganem Plateau	Inbound (m^3/day)	Outflow (m^3/day)
Storage	34570	737.85
Border contribution	25558	34321
Pumping	0	51867
Drains	0	3105.2
Refill	29934	0
Total	90062	90031

To predict the possible decrease in the groundwater level for the following years on the Calabrian aquifer of the Mostaganem Plateau, the schematic conceptual model revealed a consistent behavior of the flows to predict the possible decrease in the groundwater level for the following years of the Calabrian aquifer of the Mostaganem Plateau. The schematic conceptual model revealed a coherent behavior of the underground flows. During the summer, the decrease in the recharge of precipitation and the increase in the withdrawals cause a lowering of the piezometric surface over the entire Mostaganem Plateau.

Three scenarios have been constructed to assess the impact of the changes, which would be due to the exploitation of groundwater at the drilling level, to consider rational management of the groundwater.

3.5.2 Description of Scenarios

Scenario 1: the operating flows for DWS and irrigation will be constant from 2010 until 2035. The only variable is time.

Scenario 2: half of the boreholes intended for the supply of drinking water on the Mostaganem plateau are at a standstill as of 2014, the launch of the MAO project, which supplies some municipalities of the Plateau de Mostaganem by the transfer of water from the Chelif Dam. Irrigation flow rates are kept constant from 2010 to 2035.

Scenario 3: An increase in the population of 2.51% is observed each year (according to the National Statistics Office), the flows of drinking water supply and irrigation will be multiplied by 2.51% from 2010 to 2035.

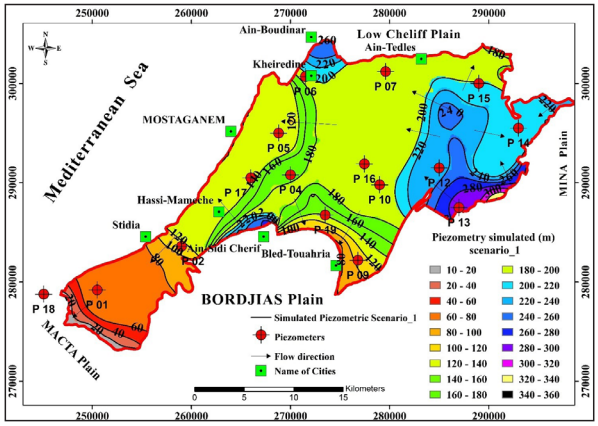

Figure 15. Simulated Piezometric map of Calabrian Aquifer scenario-1.

We notice that over 25 years the groundwater level of the slick for scenario-1 will continue to decline, especially in the central part where we note a fall of 5m and 7.5m. South of the town of Stidia in the southwest part of the Plateau, the lowering of the aquifer is 12.5 m. The maximum value of the blowdown recorded is between 17.5 m and 20 m, and it is mainly at the level of the boreholes which overexploit the aquifer (Figure 15).

The drawdown for scenario-1 is very important: at borehole P01 with 10.25 m in 2035, borehole P15 with a 5.75 m drop, borehole P16 in the central part of the Plateau shows a 2.81 m drop, and borehole P05 with a 1.01 m drop (Figure 16).

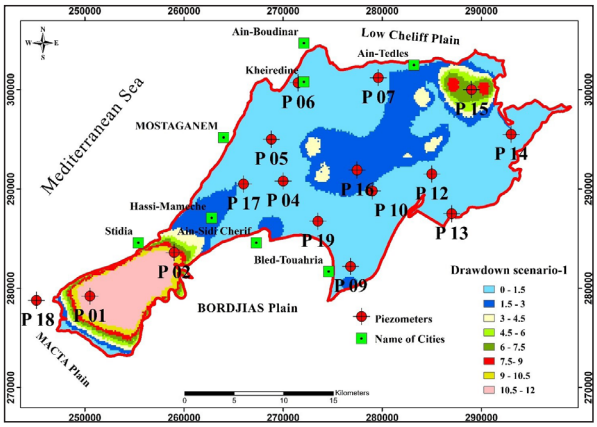

Figure 16. Drawdown map of Calabrian Aquifer Scenario-1.

Nine municipalities in the Mostaganem Plateau were connected in 2014 to the drinking water supply network from the Mostaganem-Arzew-Oran water transfer complex (MAO) and the Sonactel seawater desalination station (DHW Mostaganem). This operation affected the douars belonging to the municipalities: Mostaganem, Ain Tedèlès, Sidi Belattar, Oued El Kheir, Bouguirat, Hassi Mameche, Stidia, and Mesra, with a total population of 37 338.

The project will provide 24/7 drinking water to populations to meet a quota of 150 l/day per capita, whereas previously these populations were supplied by tanks from wells. The annual volume of the MAO transfer is 155 Hm^3 of which 45 Hm^3 for the northern part of the Mostaganem plateau. After the MAO transfer has been put into operation, the 60 AEP boreholes that fed the town of Mostaganem and some neighboring municipalities will be shut down, leaving the plateau aquifer at rest. It is from this state that the 2nd scenario was envisaged.

Scenario-2 simulation results showed a marked improvement in the downturn compared to scenario-1. East of the town of Ain Tedles, which lies northeast of the Mostaganem Plateau, the drawdown varies between 5 and 7.5m and is up to about 12.5m to 15m for Scenario-1. However, we note a clear improvement for Scenario-2, where significant drawdown values have improved to arrive at drawdowns ranging from 2.5m to 5m.

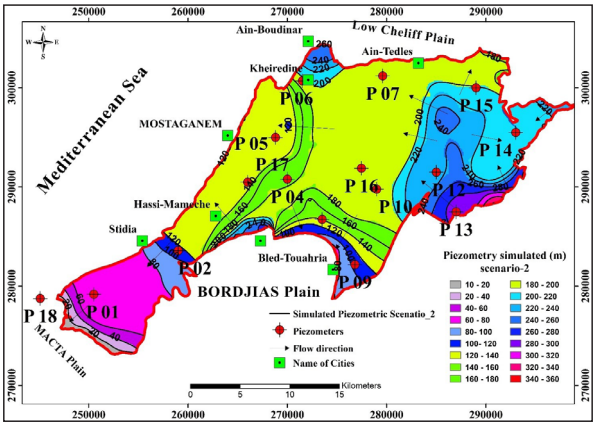

Figure 17. Simulated Piezometric map of Calabrian aquifer scenario-2.

In the central part of the Mostaganem Plateau, we note a marked improvement in the drawdowns, which pass from 2.5 meters and 5 meters have drawdowns from 1 meter to 2.5 meters (Figure 17).

For Scenario-2 (Figure 18), there is a clear improvement compared to Scenario-1, for drilling P3 where there is a stabilization of the groundwater level throughout the simulation period, with a clear improvement in the lowering, the same is true for drilling P16. On the other hand, the lowering of the aquifer is significant in the southern part of the Plateau at drilling P01 with a value of 16.31m and at drilling P06 (Kheireddine-2) with 2.9m.

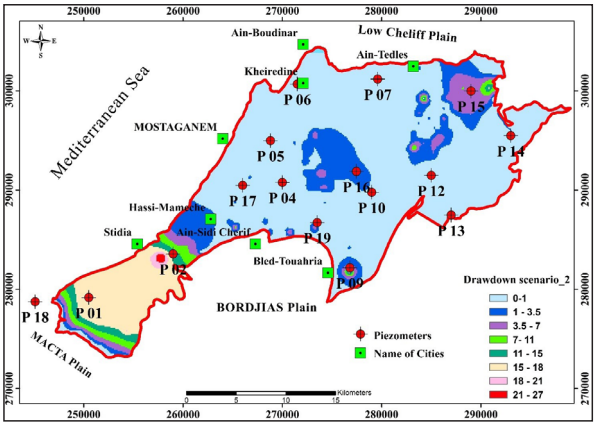

Figure 18. Drawdown map of Calabrian aquifer Scenario-2.

Table 6. Water balance of the Mostaganem Plateau aquifer resulting from scenario-2, (Period 2010-2035).

Mostaganem Plateau	Inbound (m^3/day)	Outflow (m^3/day)
Storage	23651	1190.2
Border contribution	25137	35653
Pumping	0	38723
Drains	0	3110.5
Refill	29934	0
Total	78723	78677

49.20% represents the abstraction at the level of the Plateau aquifer after half of the drilling for DWF has stopped, so we note an improvement in the volume taken (Table 6).

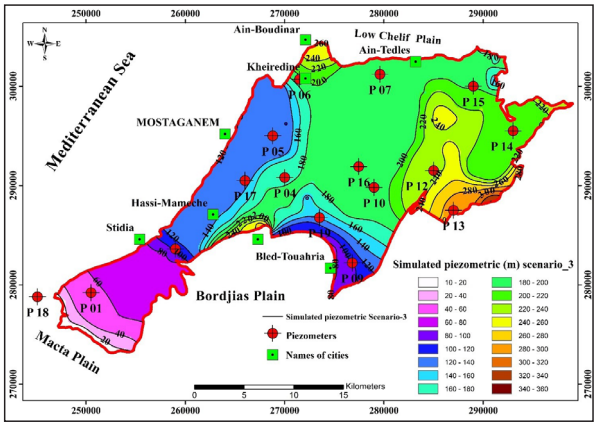

Figure 19. Simulated piezometric map of Calabrian aquifer scenario-3.

The general shape of the piezometry during scenario-3 (Figure 19) is modified in the northeastern part of the Mostaganem Plateau, east of the city Ain-Tedles. The piezometric curves become concentric with the 2010 simulated map where the curves were parallel at this location. On the rest of the Plateau, the general appearance of the piezometry is like the simulated map of 2010 with some less marked deformations.

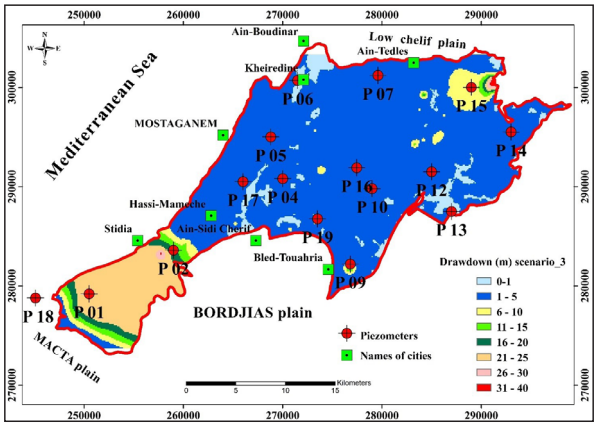

Figure 20. Drawdown map of Calabrian aquifer Scenario-3.

The drawdowns for scenario-3 (Figure 20), give worrying values, especially in the south of the town of Stidia which are of the order between, 21 m to 25 m especially the boreholes P02 and P01. On the rest of the Plateau, the drawdowns reach 5 meters. On the other hand, in the northeast part of the Plateau, the drawbacks vary between 6 and 25 m.

Table 7. Water balance of the Mostaganem Plateau aquifer resulting from scenario-3. (Period 2010-2035)

Mostaganem Plateau	Inbound (m^3/day)	Outflow (m^3/day)
Storage	43293	1126.1
Border contribution	25670	32928
Pumping	0	61773
Drains	0	3040.6
Refill	29934	0
Total	98897	98868

62.50% is the withdrawal from the Plateau aquifer for scenario-3, which indicates a strong increase in the volume was withdrawn (Table 7).

3.5.3 Comparison of the three Scenarios

Figure 21. Comparison with the three scenarios on the Mostaganem plateau.

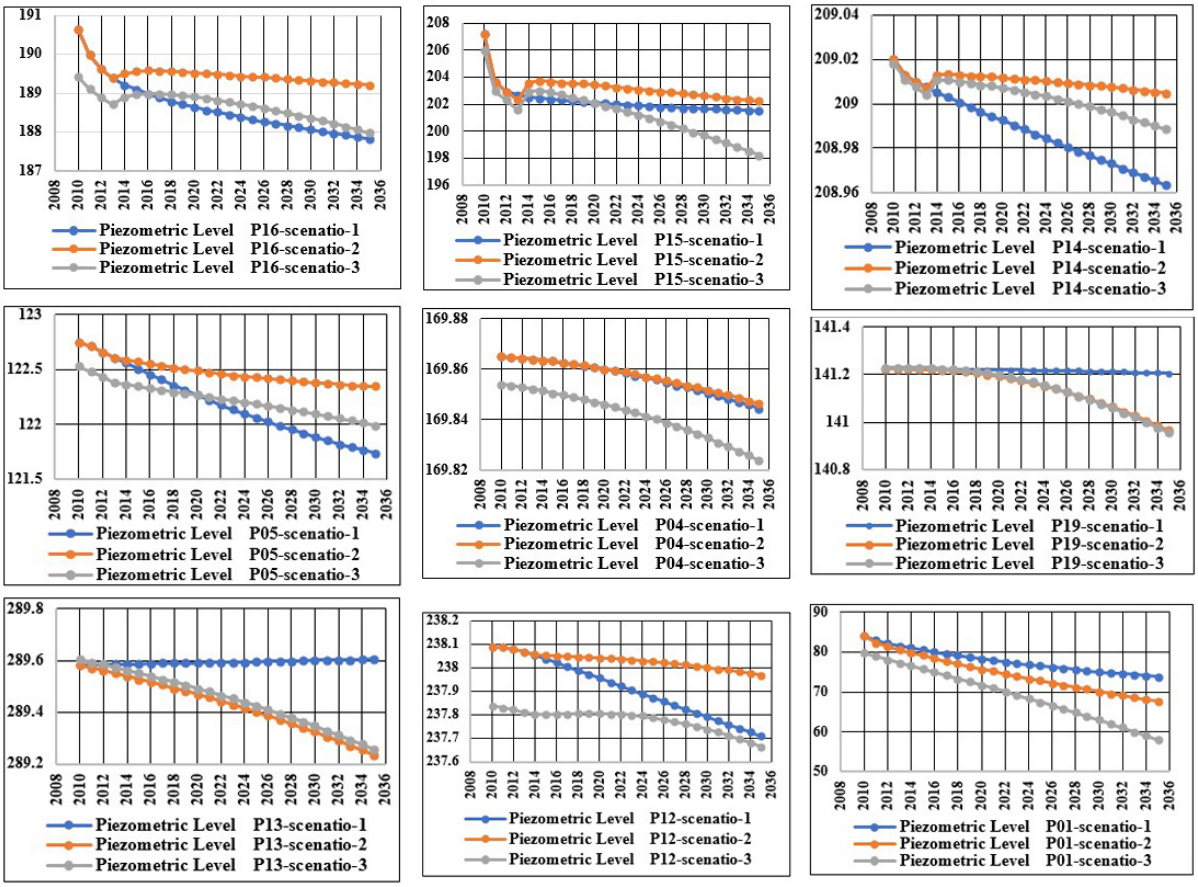

The three scenarios were combined in a single graph (Figure 21 and Table 8) for each of the boreholes to compare them. We see the first group of boreholes with the same pattern, P16, P15, and P14, the groundwater level of these three boreholes drops during the period 2010 to 2013. In 2014 we notice an improvement in the groundwater level for scenario-2 and 3, while for scenario-1 the groundwater level continues to drop until the end of the simulation. These three boreholes are in the central and eastern parts of the plateau, where the thickness of the aquifer is significant.

The P05 and P04 boreholes are in the western part. After a drop in the groundwater level, drilling P05 shows stabilization of the groundwater level for scenarios-2, while the continuous level decreases for scenarios-1 and 2. The groundwater level curves of scenarios-1 and 2 overlap for P04 and show a slight drop from the beginning to the end of the simulation.

P01 is located southwest of the plateau where the aquifer thickness is small. We notice a decrease in its groundwater level for all three scenarios. The P19 and P13 boreholes have identical graphs with a stable groundwater level during the simulation for scenario-1, while a decrease in piezometric levels is observed for scenarios-2 and 3. The P12 borehole reacts well to scenario-2, whereas we note a decrease in the level during scenarios-1 and 3.

Table 8. Drilling down to the level of the Mostaganem Plateau boreholes for the three scenarios

	P3	P19	P16	P15	P14	P13	P12	P05	P04	P01	KD2	BT1
Scenario-1	0.01	0.02	2.81	5.75	0.06	-0.02	0.37	1.01	0.02	10.25	1.05	0.69
Scenario-2	0,003	260 0	414 1	5,033	0,016	347 0	117 0	408 0	0,018	16,312	2,085	
Scenario-3	0,006	274 0	440 1	695 7	0,030	347 0	173 0	538 0	0,030	840 21	326 1	188 2
	-0.003	255 0	369 -1	945 1	-0.027	370 0	-0.202	-0.471	0,010	11,588	280 0	498 1

(Table 9) shows the results from the transient scenarios through the variations in the groundwater level on the Plateau: at borehole P01 in the south-west, borehole P15 in the far north-east and south of the town of Ain Tedles, and borehole BT1 in the south of the Plateau. Figures.6 and 7 illustrate the piezometric mapping of the different scenarios chosen in this study.

(Figures 19, 20, and 21) show the different drawdowns observed during the three scenarios envisaged for the Mostaganem Plateau aquifer.

Table 9. Variations in simulated groundwater levels of the Calabrian Tablecloth of the Mostaganem Plateau

	P3	F19	F16	P15	P14	F13	P12	P05	P04	P01	BT1
Scenario-1	214.78	141.20	187.82	201.49	208.96	289.60	237.71	121.74	169.84	73.84	108.90
Scenario-2	214.79	140.96	189.21	202.21	209.00	289.23	237.97	122.34	169.85	67.68	107.50
Scenario-3	214.78	140 .6	187.98	198.23	208 99	289.26	237.67	121.99	169.82	57.99	107.38

4. Conclusion

In these difficult water conditions (lowering of the groundwater level, overexploitation of the aquifer), all economic and environmental activities of the Plateau are affected. Drinking water supply (DWF) is disrupted and agricultural production is reduced.

Modeling in hydrogeology advances the understanding of the functioning of the modeled system and predicts future the state of the aquifer according to different solicitations (predictive mode, modification of variations of input variables) or to evaluate the response of the system to different scenarios of use of the system (management mode; variations in boundary parameters and conditions) (Villeneuve & al., 1998).

Transient state modeling may be useful in determining the location of operational boreholes and piezometers for groundwater monitoring. The transient state simulations are used to model time-dependent problems where large volumes of water are released from the aquifer.

The Mostaganem Plateau has discontinuous data over time and a piezometric monitoring network that is well distributed over the entire plateau, but certainly with an insufficient number, which can lead to gaps and uncertainties in forecasts.

For all scenarios, there is a sharp piezometric decline over the whole of the Plateau de Mostaganem, until 2035. The Calabrian aquifer is continuously overexploited, and this has been for many years. This continuous depletion of the underground resource is due to greater withdrawals compared to the total recharge of the aquifer, and consequently, the volume stored continues to decrease. These simulations, therefore, suggest that current sampling rates cannot be maintained in the long term, especially with the current drought that the country and North Africa in general, are experiencing.

Based on the results of these scenarios, it is so important for sustainable management of the Mostaganem Plateau aquifer to set up a follow-up of the withdrawals (DWS, AEA, and AEI), to limit as far as possible the carrying out of new catchments in this aquifer and above all to control and sometimes penalize illegal drilling.

Acknowledgments

We recognize the support, and encouragement received from the Directorate General of Scientific Research and Technological Development (DGRST) Algeria, University Amar Telidji Laghouat, and The Sisyphe laboratory Paris V. The authors thank all organizations for the observed data, which was obtained by the first author: The Directorate-General for Water Resources (ANRH: Algiers, Oran, Relizane). The Directions Wilayas Hydraulic (DHW: Mostaganem, Relizane, Mascara, Chlef), the National Meteorological Office Algiers (ONM).

Ethics declarations

Competing interests

The authors declare that they have no competing interests.

Abbreviations

ADE: Algerian Water
AEA: Agricultural water supply
AEI: Industrial water supply
ANRH: Directorate-General for Water Resources
CGG: General Company of Geophysics
DGRST: Directorate General of Scientific Research and Technological Development
DHW: Direction Wilaya Hydraulic
DWS: Drinking water supply
DWA: Drinking water abstraction
Hm3 : cubic hectometres
ONM: National Meteorological Office Algiers
MAO: Mostaganem, Arzew, Oran.

References

Algerian Water (ADE).(2019) - https://www.aps.dz/economie/85461-ade-pres-de-17-de-l-eau-distribuee-provient-desalination station

Baiche. A (1994). Hydrogeology of the region of Mostaganem, Thesis of Magister University of Oran.

Baiche. A, Sidi Mohamed. H, Abdelaoui H. (2015) Overexploitation of the water resources of the Plateau aquifer Mostaganem. Larhyss Journal, ISSN1112-3680, No. 22, June 2015, pp.153-165 ©All rights reserved, Legal Deposit 1266-2002. pp.154-165

Bahir M, Ouhamadouche. S, Driss Ouazar Nabil El Moçayd (2020) Effect of climate change on Characteristics of groundwater in semi-arid areas of western Morocco https://doi.org/10.1016/j.gsd.2020.100380

Bandani, E. Moghadam, M. (2011) - Application of groundwater mathematical model for assessing the effects of Galoogah dam on the shooro aquifer Iran. European Journal of Scientific Research; ISSN 1450-216X Vol.54 No. 4 (2011, pp. 499-511)

Bentahar. F, and Mesbah M (2007). Hydrogeological mapping of the Mostaganem Plateau and Lower Chelif (Wadi section Djidiouia-Oued Myna) North-West Algeria. Thesis magister, University of Science and Technology HOUARI Boumediene, USTHB, Algiers.

Bellal Sid-Ahmed (2019): Drought and fluctuations in groundwater resources: The case of the Plateau de Mostaganem (West Algerian). Western Geographical Notebooks.

Bhat Sultan. M, Akhtar Alam, Bachir Ahmad, Bahadur S Kotlia, Hakim Farooq, Ajay K. Taloor, Shabir Ahmad. (2019). Flood frequency analysis of river Jhelum in Kashmir basin. Quaternary International, Volume 507, pages 288-294. http://doi.org/10.1016/j.quaint.2018.09.039

Berraki. Arezki. (2021) Minister of Water Resources. Algeria. https://www.aps.dz/economie/115942-le-desalination-seawater-single-solution-to-ensure-drinking-water-supply

Bonnet. M. (1967): Hydrogeology of the Mostaganem Plateau and the Bordjias Plain, S.E.S. No. 12/16/ DH1. (ANRH).

Boufekane. A. Saighi. O (2019). Assessing groundwater quality for irrigation using geostatistical method - Case of Wadi Nil Plain (North-East Algeria). Groundwater for Sustainable Development Pages 179 186 .https://doi.org/10.1016/j.gsd.2018.11.003

Castany. G: Hydrogeology Principles and methods. CGG. (1968). Hydrogeological study by electrical prospecting in the Mostaganem region, H.E.S Bir Mourad Rais, Algiers. Algeria

Cote Mark. (1996). Guide to Algeria: landscapes and Heritage. Algeria Media-plus. 319 pages. ISBN 9961-922-00-X, p. 63

Dassargues A. (1995). Mathematical models in hydrogeology and parameterization. Tempus program: Water and Environmental Sciences,125p.

Dieter. Cheryl A. et al (2018) Estimated use of water in the United States in 2015. U.S. Geological Survey Circular 1441, 65 p., https://doi.org/10.3133/cir1441. [USGS Open-File Report 2017-1131.]

Direction Wilaya Hydraulics Mostaganem, (DHW.2015). Algeria.

El Arbi Toto, Lahcen Zouhir and Jgounni, Abdellatif (2009) Direct and inverse modeling of Underground flow in porous media, Hydrological Sciences Journal,54:2,327-337, DOI:10.1623/hysj.54.2.327

Gauchez J. (1981): Hydrogeological study of the region of Mostaganem, Thesis 3rd cycle: Science, Geology of Sedimentary ensembles, Universitaté Claude Bernard, Lyon.250 pages.

General Company of Geophysics CGG (1968): hydrogeological survey by electric prospecting in the region of Mostaganem, S.E.S Bir Mourad Rais, (ANRH), Algiers.

Gleeson, T., Befus, K., Jasechko, S. et al. (2016). The global volume and distribution of modern groundwater. Nature Geosci 9, 161-167 (2016). https://doi.org/10.1038/ngeo2590

Hydrogeological map of the Mostaganem Plateau at 1:100,000. (1978). National Water Resources Agency (A.N.R.H). Bir-mourd Rais Alger.

Kessasra Farès. 2015.Hydrogeological modeling of underground and surface flows of the aquifer Soummam Valley Alluvids (Northeastern Algeria) - Impact on the environment and ecosystems. Doctoral thesis. University of Science and Technology Houari Boumediene, USTHB, Algiers.452p

Krause Stefan, Bronsterb Axel, Zehe Erwin 2007 Groundwater-surface interactions in North German lowland floodplain-involvement for the river discharge dynamics and rispain water balance. Journal of Hydrology, Volume 347, Issues 3-4, pages 404-417.

Ledoux. E 2003 Mathematical models in hydrogeology Center d'Informatique Géologique Ecole Nationale Superior des Mines de Paris.133p

Laborde. J.P. 2003. Surface hydrology. National Water Resources Agency (A.N.R.H). Bir-mourd Rais Algiers.

Les Landes Antoine Armandine (2014). Impact of climatic variations on hydrogeological resources. Hydrology. Rennes University 1, 2014. French. NNT: 2014REN1S101ff.

Ministry of the Water Resources (2021) http://www.mre.gov.dz/ https://www.aps.dz/economie/115942-le-dessalement-single-solution-to-ensure-drinking-water-supply

National Agency for Dams and Transfers (ANBT) (2011). https://www.suezwaterhandbook.fr/etudes-de-case/drinking-water-production/drinking-water-production-plant-Mostaganem-Arzew-Oran-Algerie

National Water Resources Agency, ANRH, Algiers. Rainfall data.

National Meteorological Office (ONM,2014-2019), NAME. Temperature data. Dar El Beida, Algiers.

Nechifor. V, Winning. 2017 Projecting irrigation water requirements across multiple socio-economic development futures-A global CGE assessment. Water Resources and Economics http://doi.org/10.1016/j.wre.2017.09.003

Perrodon. A. (1957). Geological Survey of sub-coastal neogenous basins in western Algeria. Publications of the Algerian Geological Map Service (New series) Bulletin No. 12. Algiers.

Remini. B (2010). The water problem in Northern Algeria. Larhyss Journal, ISSN 1112-3680, No. 08, June 2010, pp. 27-46

Saibi. H (2000). Contribution to the hydrogeological study of the Plateau de Mostaganem (North-West Algeria), approach to groundwater vulnerability to pollution by the Drastic method.

Saibi. H (2000). Contribution to the hydrogeological study of the Mostaganem Plateau (North-West Algeria), approach of groundwater vulnerability to pollution by the Drastic method: Bachelor Thesis, Faculty of Earth Sciences, University of Science and Technology Houari Boumediène, Algiers, Algeria, 158 p.

Saibi. H (2008). Hydrogeology and vulnerability assessment of groundwater resources in the Mostaganem plateau, Northwestern Algeria. Journal of Environmental Hydrology. http://www.hydroweb.com

Sogreah consultants. (2006). Great Aquifer Modeling: Operation ND5.312.6.261.375.02. Modeling of 4 Aquifer Systems, Mostaganem Plateau. Mission Report 1.

Sogreah consultants. (2007). Great Aquifers Modeling: Operation ND5.312.6.261.375.02. Modeling of 4 Aquifer Systems, Mostaganem Plateau. Mission Report 2.

Sula. Rania. Chebli. Ali, MCcann. Laura, Mahdjoub. Rajouene. (2020). Water scarcity in the Mahdia region of Tunisia: Are improved water policies needed? Groundwater For Sustainable Development. https://doi.org/10.1016/j.gsd.2020.100510

Thakur. Praveen K. et al (2020). Groundwater modeling with inputs from geospatial technology for assessing the sustainability of water uses in the Solani watershed, Ganga River basin (India). Groundwater for Sustainable Development. https://doi.org/10.1016/j.gsd.2020.100511 Unesco, 2009. Water in a changing world.

USGS (United States Geological Survey) (2014) https://earthexplorer.usgs.gov.

Villeneuve, J. P., Hubert, P., Mailhot, A. & Rousseau, A. N. (1998). Hydrological modeling and water management. Journal of Water Science, 11, 19-39. https://doi.org/10.7202/705327ar

Yofe tirogo Justine. (2016): Study of the Hydrodynamic Functioning of the Sedimentary Aquifer of the Kou in Southwest Burkina Faso. Doctoral thesis Hydrogeology, Pierre and Marie Curie University (UPMC) Paris.260p.

JJEES

JJEES (2023) 14 (2): 126-134
ISSN 1995-6681

Jordan Journal of Earth and Environmental Sciences

Geochemistry of Detrital Chromite from Gercus Formation (M. Eocene), Northern Iraq: Implications for the Provenance and Paleotectonic

Zahraa J. Al-Jubory[1], Falah A. Al-Miamary[1], Safwan F. Al-Lhaebi[1], Harvey E. Belkin[2]

[1] Department of Geology, College of Science, Mosul University, Iraq.
[2] U.S. Geological Survey, 11142 Forest Edge Drive, Reston, VA 201904026-, USA

Received 16th June 2022; Accepted 26th October 2022

Abstract

The current research dealt with the mineralogical and geochemical characteristics of the detrital chromite mineral in the sandstone from the Gercus Formation (Middle Eocene). Three sections of the north of Iraq were selected to identify the nature and type of the source rocks and the tectonic setting. Detrital chromite is found in high concentrations in fine sandstone with glossy black color. Based on the geochemical analysis, it is evident that the mineral contains 33.35% - 6.534% Al_2O_3, 65.36% - 33.27% Cr_2O_3, 16.44% - 6.49% MgO, 22.37% - 10.806% FeO, 0.0 - 9.012% Fe_2O_3, and 0.014% - 0.9% TiO_2, therefore, it can be classified as Al-chromite. Additionally and according to the ternary plot of Cr^{3+}, $Al^{3+,}$ and Fe^{3+}, it is concluded that the origin of the chromite in question is compatible with Alpine-type peridotites chromite (which contains harzburgitic mantle peridotites) and it was developed primarily in a supra-subduction zone environment.

Keywords: *Detrital chromite, the Gercus Formation, Provenance, Tectonic setting.*

1. Introduction

The use of heavy mineral assemblages to identify and describe sediment source areas has become familiar. In provenance studies, the variation of the chemical composition of a single mineral species is a very important technique (Morton, 1985), because the weathering, diagenesis, and sedimentation do not affect these minerals (Morton and Hallsworth, 1999).

The data of heavy minerals (especially chromite) in sedimentary rocks are commonly used as indicators of the petrological characteristics of the parent rocks. Many petrological studies point out the relations between the chromite spinel group (that includes chromite, chromit-spinel, and spinel) chemistry, rock type, and provenance (Lee, 1999).

Chromite is used as a guide in petrological studies. Some chemical ratios of oxides in chromite are considered important parameters, such as Mg# ($Mg/Mg + Fe^{2+}$), Cr# ($Cr/Cr + Al$), and TiO_2.

The chemistry of chromite is important for classifying mantle-derived peridotites in terms of the origin and the tectonic setting. Chromite from stratiform deposits has (Cr#: 0.6 to 0.8), (Mg# 0.2 to 0.8). On the other hand, chromite from podiform deposits may have (Cr#: 0.15-0.85; Mg# (0.4-0.8) (Steele et al., 1977; Al-Juboury et al. 2009).

The present research deals with the geochemistry of chromite from the Gercus Formation (Middle Eocene) in the north of Iraq (Fig. 1) and it discusses the use of chromite mineral chemistry to make inferences regarding provenance and tectonic setting.

2. Material and Methods

Nine samples were collected from Gercus Formation from three sections: three samples from the Dohuk section, four samples from the Badi section, and two samples from the Shaqlawa section. The mineralogy of the samples has been revealed optically and by electron probe microanalysis (EPMA) and back-scattered electron imaging.

The analysis was conducted in the labs of the US Geological Survey. To diagnose and describe the chromite grains, A binocular microscope was used, with a fully automated JEOL JXA-8900 five-spectrometer electron microprobe that uses wavelength-dispersive X-ray spectroscopy and quantitative electron microprobe to determine the main and minor elements. The points of analysis were defined using optical and back-scattered electron imaging. Analyses were performed using a 1 to 20-micrometer diameter probe spot and a 15 keV (silicates and carbonates) or 20 keV (oxides) accelerating voltage, 10, 20, or 30 nA probe current and the counting times were 10 to 120 seconds.

Standard reference materials, both natural and synthetic were used. The analyses were corrected for electron beam/matrix effects, experimental drift, and dead time using the JEOL JXA-8900 electron microprobe's Phi-Rho-Z (CITZAF; (Armstrong, 1995) method. Based on a comparison of measured and published compositions of standard reference materials, the relative accuracy of the analyses was 1-2% for major oxides and 5-10% for minor oxides concentrations.

* Corresponding author e-mail: zahraa1981@uomosul.edu.iq

3. Geological Setting

The Gercus Formation is made up of clastic, carbonate, and evaporate sequences. It consists of sandstone, mudstones, conglomerates, siltstone, and marls with a gypsum lens and little thin micritic carbonate beds. These beds were deposited in a range of sedimentary environments, such as arid to semiarid (dry) alluvial fans, ephemeral streams, interdunes, and lakes, aeolian dunes (Hussain and Aghwan, 2015; Awad and Ahmed Alsultan, 2020) Dohuk Dam, Brifca, and Shaqlawa. Moreover, this Formation can be regarded as part of Megasequence AP 10 (Arabian Plate10) (Sharland. et al., 2001) and it is regarded as a Middle-Late Eocene sequence, which is part of the Megasequence Middle Paleocene–Eocene (Jassim and Goff, 2006).

The deposition of the Gercus Formation during the period of renewed uplift of the eastern margin (Zagros margin) of the Arabian Plate at the end of the Early Eocene (Aqrawi et al., 2010). As it was deposited in the period of the final phase of the subduction and the closing of the remains of the New Tethys Ocean, it was deposited in a basin located to the southwest of the Balambo-Tanjero zone (Jassim and Goff, 2006).

The area studied is located in the northern part of Iraq, in high folded zones according to tectonic divisions of Iraq (Fouad, 2015) (Fig.1). Three sections were chosen and these sections are represented by Dohuk (near Dohuk dam), Badi and Shaqlawa.

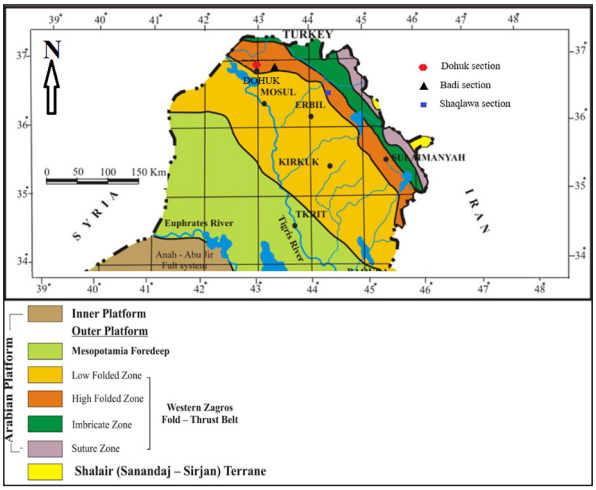

Figure 1. Tectonic map of Iraq (Fouad, 2015) and location of the studied sections.

4. Result and Discussions

4.1 Petrography and Field Description

According to previous petrological and chemical research (AL-Rawi, 1982; Dhannoun et al. 1988), dolomite and serpentinite were the primary sources of the Gercus sediments. The chromite grains are glossy black under the reflected light, with sharp edges and conchoidal fracture (plate 1-A). Scanning electron microscope (SEM) and back-scattered electron (BSE) images show the typical millimeter-scale oxide (chromite, magnetite, and ilmenite) detrital layers separated by detrital silicate and carbonate grains (plate1-B), while the enlargement of a typical oxide layer demonstrates the predominance of angularity in both the oxide and silicate-carbonate grains in the sample.

Most chromite grains exhibit weak deformations such as polygonal or angular crystal appearances and ductile deformations (such as elongated worm-like shapes) and cluster to form chromite bands or disseminated varieties (plate1-B and C). In the Dohuk section, sandstone beds (0.2 to 6.0 m thick) are often moderately to well sorted, with sedimentary structures such as wind lamination, massive bedding, and cross-bedded strata with high-angle inclination. Sometimes the sandstones are badly sorted and pebbly. The mineral assemblage mainly comprises dolomite, quartz, serpentine, and altered Fe-oxides. EPMA- revealed amphibole, chlorite, chromite, and feldspar. In the Badi section, reddish brown, red-orange, pale yellow, and dark grey sandstones (0.2-1.0 m thick) with peat were distinguished. Good bedded or lenticular beds can be observed in the sandstones, especially where they are interbedded with conglomerates and can be followed laterally several hundred meters. Some of the sand sheets are made up of fine -to medium-grained, well-sorted sandstones with a parallel lamination and low-angle tabular cross-bedding. Both types of bedded sandstone have local burrows and pebble lineation with ventifacts. The sand sheet consists of medium to coarse-grained sandstones that have been inadequately sorted in other circumstances. These sandstones can be found as thick beds with scattered mud pebbles and wind-worn clast (gravels) or as tabular cross-bedding that is laterally persistent.

The mineral assemblage of the Badi section consists mainly of dolomite, quartz, serpentine, altered Fe oxides, and rare titanite -EPMA- documented the presence of chlorite, chromite, and feldspar. In the Shaqlawa section, the sandstone thickness ranges from 0.2 to 4.0 m. Moreover, the fresh surfaces are normally pink to light reddish brown, and even dark brown peat. However, weathered surfaces are often pale. These sandstone beds are usually fine- to medium-grained, well-sorted, massive, laminated, and commonly cross-bedded. Some sandstone beds are massive and structureless rock, sheet-like beds with parallel laminations and are typical in laminated sandstone in addition to that low-angle cross-bedding is occasionally observed. The mineral assemblage consists of Calcite, calcite cement, dolomite, quartz, altered serpentine EPMA: amphibole, chlorite, chromite, and feldspar.

4.2 Mineral chemistry of Chromites

The structural formula for representative analyses was recalculated based on 32 oxygen and determined in atoms per formula unit (a.p.f.u.) as shown in Tables 1, 2, and 3. Excel spreadsheets from GabbroSoft (http://www.gabbrosoft.org/spreadsheets) were used to calculate mineral formulas. Fe^{+2} and Fe^{+3} were determined stoichiometrically. The analysis indicates that the chromite contains 33.35% - 6.534% Al_2O_3, 65.36% - 33.27% Cr_2O_3, 16.44% - 6.49% MgO, 22.37% - 10.806% FeO, 0.0 - 9.012% Fe_2O_3 and 0.014% - 0.9% TiO_2. MnO and ZnO are typically present in only minor abundance, generally < 0.5%. Titanium (Ti^{4+}), which occurs in magma, can enter the spinel structure by coupling with Fe^{2+} and replacing two Fe^{3+} in the octahedral site (Ghosh and Konar, 2011). According to the nomenclature of Stevens (1944), the

studied chromite is classified as Al-chromite (Fig.2). Basaltic melts or metasomatic processes are the primary sources of Al-rich chromite (Franz and Wirth, 2000; Daczko et al., 2012). Zoning has not been observed, except the analysis of one grain of the sample (GD3) that shows compositional zonation were chromite (Chr) illustrating alteration along a crack and on the edges. EPMA analysis of Rim wt% (Al_2O_3 = 16.2, Cr_2O_3 = 53.1, FeO total = 20.5) and Core wt% (Al_2O_3 = 0.67, Cr_2O_3 = 47.2, FeO total = 44.5) shows that the alteration fluids were iron-rich and preferentially removed Al, dolomite (Dol) grains surrounding the chromite show evidence of pressure dissolution (plate1-D).

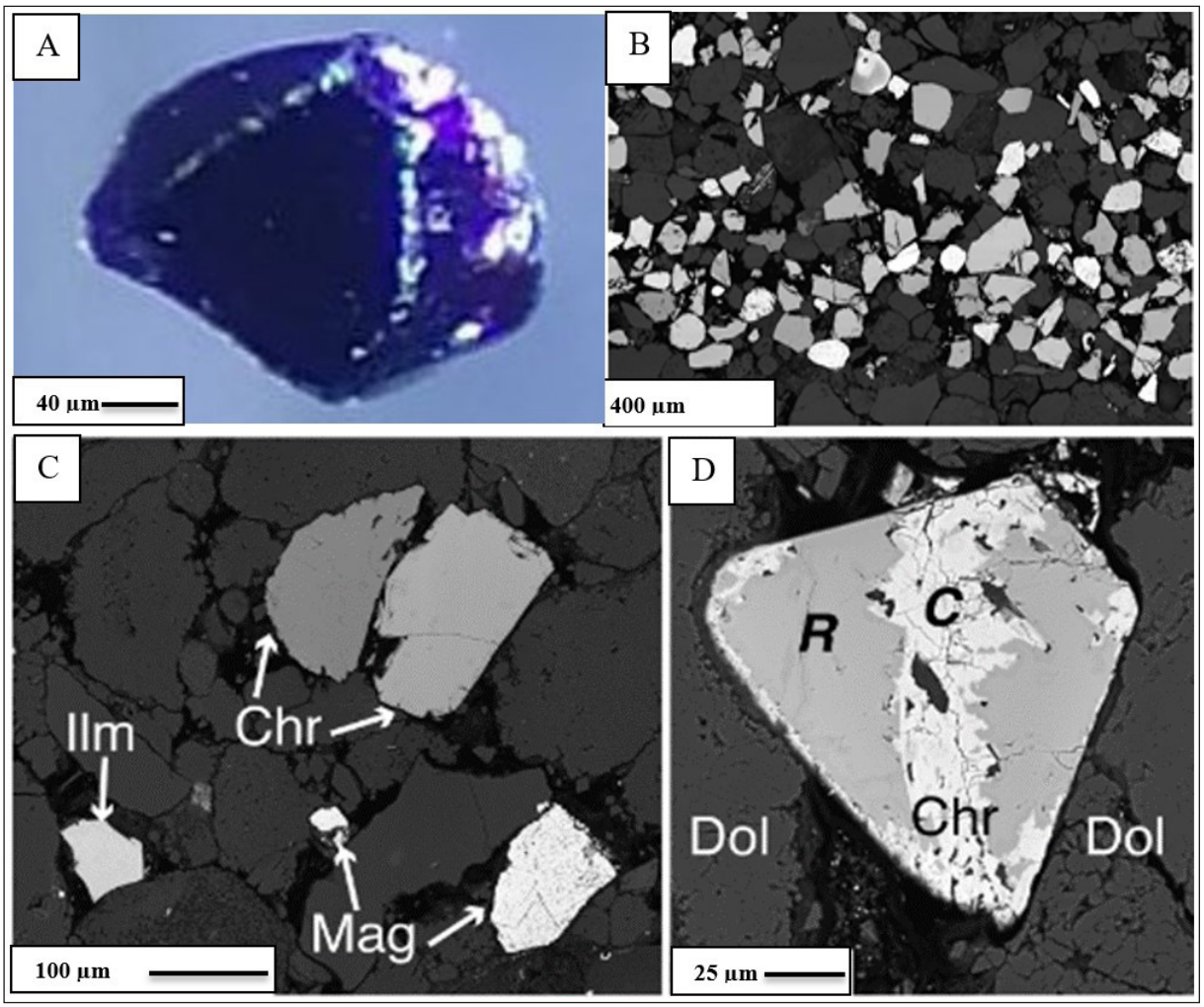

Plate 1. A- Magnified photomicrograph of chromite grain with shiny black under reflected light; B- Scanning electron microscope (SEM) of enlargement of a typical oxide layer (sample GD4); C- SEM-BSE images of typical habits of the oxides; chromite (Chr), magnetite (Mag) and ilmenite (Ilm); sample GD3. D- SEM-BSE images for Chromite (Chr) illustrating alteration along a crack and on the edges, dolomite (Dol), rim (R), and core (C).

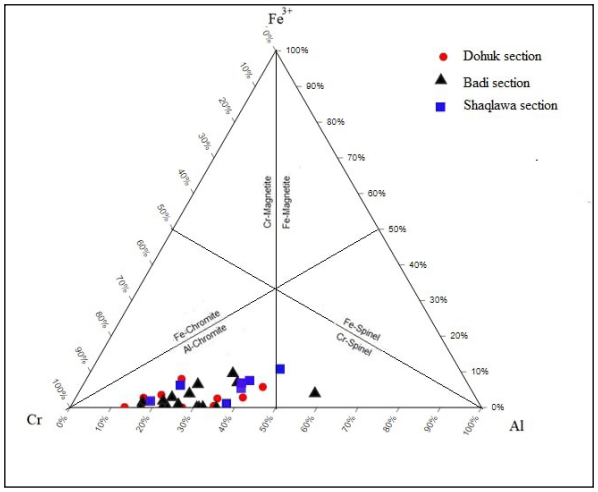

Figure 2. (Fe^{3+}, Al, Cr) diagram shows a type of detrital chromite from the Gercus Formation, The fields from (Stevens, 1944).

Table 1. Chemical composition of detrital chromite from Dohuk section, Gercus Formation.

Section	Dohuk section									
Sample no	GD1				GD3				GD4	
Spots	1	2	3	4	1	2	3	4	1	2
SiO_2%	0.01	0.01	0.00	0.00	0.00	0.00	0.00	0.00	0.00	0.00
TiO_2%	0.04	0.31	0.06	0.01	0.05	0.04	0.07	0.04	0.06	0.04
Al_2O_3%	24.87	11.87	22.42	8.48	6.53	9.17	18.79	10.50	18.47	14.44
Cr_2O_3%	42.39	52.75	46.57	61.79	63.91	65.36	52.33	58.18	50.15	57.45
Fe_2O_3%	5.10	6.44	2.43	2.20	0.07	0.00	0.35	2.84	2.11	0.00
%FeO	14.87	18.72	16.80	18.04	15.59	14.09	17.00	18.16	15.77	14.97
%MnO	0.27	0.42	0.32	0.45	5.45	0.72	0.33	0.66	0.37	0.56
%MgO	13.85	9.78	12.12	9.83	7.08	9.66	11.65	9.62	12.06	11.51
%CaO	0.02	0.05	0.06	0.06	0.05	0.07	0.02	0.08	0.01	0.01
%ZnO	0.12	0.14	0.21	0.13	1.29	0.40	0.15	0.20	0.14	0.19
TOTAL	101.54	100.49	100.99	100.98	100.03	99.50	100.70	100.27	99.13	99.22
apfu										
Si	0.00	0.00	0.00	0.00	0.00	0.00	0.00	0.00	0.00	0.00
Ti	0.01	0.06	0.01	0.00	0.01	0.01	0.01	0.01	0.01	0.01
Al	7.03	3.67	6.49	2.64	2.11	2.89	5.55	3.27	5.52	4.40
Cr	8.03	10.94	9.04	12.92	13.85	13.83	10.36	12.15	10.06	11.75
V	0.00	0.00	0.00	0.00	0.00	0.00	0.00	0.00	0.00	0.00
Fe^{+3}	0.92	1.27	0.45	0.44	0.02	0.00	0.07	0.56	0.40	0.00
Fe^{+2}	2.98	4.10	3.45	3.99	3.57	3.15	3.56	4.01	3.34	3.24
Mn	0.05	0.09	0.07	0.10	1.27	0.16	0.07	0.15	0.08	0.12
Mg	4.95	3.82	4.44	3.87	2.90	3.85	4.35	3.79	4.56	4.44
Ca	0.01	0.01	0.02	0.02	0.01	0.02	0.01	0.02	0.00	0.00
Zn	0.02	0.03	0.04	0.02	0.26	0.08	0.03	0.04	0.03	0.04
TOTAL	24.00	24.00	24.00	24.00	24.00	24.00	24.00	24.00	24.00	24.00
#Mg	0.62	0.48	0.56	0.49	0.45	0.55	0.55	0.49	0.58	0.58
Fe3+#	0.06	0.08	0.03	0.03	0.00	-	0.00	0.04	0.03	0.00
#Cr	0.53	0.75	0.58	0.83	0.87	0.83	0.65	0.79	0.65	0.73

Table 2. Chemical composition of detrital chromite from Badi section, Gercus Formation.

Section	Badi section															
Sample no.	GB2				GB3				GB4				GB5			
Spots	1	2	3	4	1	2	3	4	1	2	3	4	1	2	3	4
SiO_2%	0.00	0.00	0.00	0.00	0.00	0.00	0.01	0.00	0.00	0.00	0.00	0.00	0.00	0.00	0.00	0.00
TiO_2%	0.24	0.24	0.24	0.24	0.24	0.24	0.24	0.24	0.04	0.30	0.14	0.05	0.04	0.05	0.08	0.29
Al_2O_3%	11.08	14.56	14.28	8.30	18.41	12.00	20.01	33.35	12.68	13.03	11.23	19.18	16.79	8.90	16.96	17.08
Cr_2O_3%	58.15	51.23	54.28	59.69	43.88	56.51	44.73	33.27	61.00	54.96	57.96	51.82	56.23	64.13	55.41	53.48
Fe_2O_3%	1.50	5.33	3.20	1.17	7.92	2.29	5.92	3.58	0.00	0.67	0.00	0.00	0.00	0.00	0.00	0.09
FeO%	19.34	17.65	15.78	22.37	17.05	18.08	15.75	11.19	16.91	21.30	22.10	18.54	15.36	17.75	16.67	17.33
MnO%	0.40	0.42	0.38	0.55	0.35	0.53	0.35	0.21	0.39	0.36	0.36	0.32	0.32	0.46	0.39	0.30
MgO%	9.16	10.86	11.77	6.49	11.07	9.74	12.39	16.44	8.85	7.98	7.15	8.66	10.87	7.94	10.20	11.31
CaO%	0.02	0.09	0.05	0.02	0.33	0.10	0.03	0.06	0.00	0.02	0.02	0.04	0.05	0.02	0.01	0.01
ZnO%	0.14	0.13	0.12	0.24	0.17	0.21	0.11	0.18	0.19	0.09	0.10	0.18	0.12	0.26	0.16	0.08
TOTAL	100.03	100.51	100.10	99.07	99.41	99.70	99.53	98.52	100.05	98.71	99.05	98.78	99.78	99.51	99.88	99.95
Apfu																
Si	0.00	0.00	0.00	0.00	0.00	0.00	0.00	0.00	0.00	0.00	0.00	0.00	0.00	0.00	0.00	0.00
Ti	0.03	0.08	0.02	0.02	0.05	0.01	0.04	0.01	0.01	0.06	0.03	0.01	0.01	0.01	0.01	0.06
Al	3.46	4.40	4.32	2.70	5.54	3.73	5.92	9.20	3.94	4.11	3.58	5.87	5.07	2.84	5.13	5.12
Cr	12.18	10.40	11.02	13.02	8.85	11.79	8.88	6.15	12.72	11.63	12.40	10.63	11.38	13.75	11.25	10.75
V	0.00	0.00	0.00	0.00	0.00	0.00	0.00	0.00	0.00	0.00	0.00	0.00	0.00	0.00	0.00	0.00
Fe^{+3}	0.30	1.03	0.62	0.24	1.52	0.46	1.12	0.63	0.00	0.14	0.00	0.00	0.00	0.00	0.00	0.02
Fe^{+2}	4.29	3.79	3.39	5.16	3.64	3.99	3.30	2.19	3.73	4.77	5.00	4.02	3.29	4.02	3.58	3.69
Mn	0.09	0.09	0.08	0.13	0.08	0.12	0.07	0.04	0.09	0.08	0.08	0.07	0.07	0.11	0.08	0.06
Mg	3.62	4.16	4.51	2.67	4.21	3.83	4.64	5.73	3.48	3.19	2.88	3.35	4.15	3.21	3.90	4.29
Ca	0.01	0.02	0.01	0.01	0.09	0.03	0.01	0.02	0.00	0.01	0.01	0.01	0.01	0.01	0.00	0.00
Zn	0.03	0.02	0.02	0.05	0.03	0.04	0.02	0.03	0.04	0.02	0.02	0.03	0.02	0.05	0.03	0.01
TOTAL	24.00	24.00	24.00	24.00	24.00	24.00	24.00	24.00	24.00	24.00	24.00	24.00	24.00	24.00	24.00	24.00
Mg#	0.46	0.52	0.57	0.34	0.54	0.49	0.58	0.72	0.48	0.40	0.37	0.45	0.56	0.44	0.52	0.54
Fe3+#	0.02	0.07	0.04	0.02	0.10	0.03	0.07	0.04	-	0.01	-	-	-	-	-	0.00
Cr#	0.78	0.70	0.72	0.83	0.62	0.76	0.60	0.40	0.76	0.74	0.78	0.64	0.69	0.83	0.69	0.68

Table 3. Chemical composition of detrital chromite from Shaqlawa section, Gercus Formation.

Section.	Shaqlawa section						
Sample no	GS3				GS4		
Spots	1	2	3	4	1	2	3
SiO_2%	0.00	0.00	0.00	0.00	0.00	0.00	0.00
TiO_2%	0.15	0.90	0.05	0.15	0.75	0.15	0.10
Al_2O_3%	9.56	20.96	20.60	12.38	24.34	21.74	20.96
Cr_2O_3%	60.84	44.77	50.36	54.58	34.62	42.76	44.86
Fe_2O_3%	1.48	4.56	0.96	5.11	9.01	6.47	5.91
FeO%	15.66	14.94	10.81	15.94	19.23	14.42	14.19
MnO%	0.33	0.31	0.20	0.34	0.33	0.32	0.31
MgO%	11.41	13.58	15.56	11.55	10.68	13.31	13.57
CaO%	0.05	0.03	0.04	0.11	0.15	0.10	0.02
ZnO%	0.04	0.12	0.05	0.08	0.14	0.13	0.10
TOTAL	99.52	100.17	98.63	100.24	99.25	99.40	100.02
apfu							
Si	0.00	0.00	0.00	0.00	0.00	0.00	0.00
Ti	0.03	0.17	0.01	0.03	0.14	0.03	0.02
Al	2.97	6.09	5.99	3.78	7.18	6.35	6.10
Cr	12.68	8.73	9.82	11.17	6.85	8.38	8.76
V	0.00	0.00	0.00	0.00	0.00	0.00	0.00
Fe^{+3}	0.29	0.85	0.18	0.99	1.70	1.21	1.10
Fe^{+2}	3.45	3.08	2.23	3.45	4.02	2.99	2.93
Mn	0.07	0.06	0.04	0.07	0.07	0.07	0.06
Mg	4.48	4.99	5.72	4.46	3.98	4.92	5.00
Ca	0.01	0.01	0.01	0.03	0.04	0.03	0.01
Zn	0.01	0.02	0.01	0.02	0.03	0.02	0.02
TOTAL	24.00	24.00	24.00	24.00	24.00	24.00	24.00
Mg#	0.57	0.62	0.72	0.56	0.50	0.62	0.63
Fe3+#	0.02	0.05	0.01	0.06	0.11	0.08	0.07
Cr#	0.81	0.59	0.62	0.75	0.49	0.57	0.59

4.3 Chromite provenance and paleotectonic setting

The chemical composition of chromite gives information on the types of source rocks in various tectonic settings (Lee, 1999). Chromite spinels form under a variety of settings, either from partial melting of upper-mantle peridotite or from mafic and ultramafic magmas. As a result, they are significant indicators of the host rock's original composition (Roeder, 1994). The geochemistry of chromite in mantle peridotites provides information about the residual mantle like its melting degree and melting condition, as well as the nature and the extent of melt/rock interaction, thus this information can be used to determine whether the mantle sequence was formed at Mid-Ocean Ridge (MOR) setting, at a Supra-Subduction Zone (SSZ), or those that were formed due to multiple tectonic settings. The important chemical parameters, which are used to determine the provenance of chromite are Cr #, Mg#, Fe^{3+}#, and Ti content (Al-Juboury et al., 2009). Cr # [Cr/(Cr + Al)] ranges between 0.4 and 0.87; Mg# [Mg/(Mg + Fe^{2+})] ranges from 0.34 to 0.72; Fe^{3+}# [Fe^{3+}/(Cr + Al + Fe^{3+})] ranging from 0.00 - 0.11 and Ti content ranging from 0.00 - 0.17. The TiO_2 content of chromite is also a very useful tool to elucidate the paleotectonic setting, low Ti, and Fe^{3+} of chromite point to peridotites origin. This issue can be supported by using the ternary plot of Cr^{3+}, Al^{3+}, and Fe^{3+} (Fig. 3), which indicates that all samples are compatible with Alpine-type peridotites chromite.

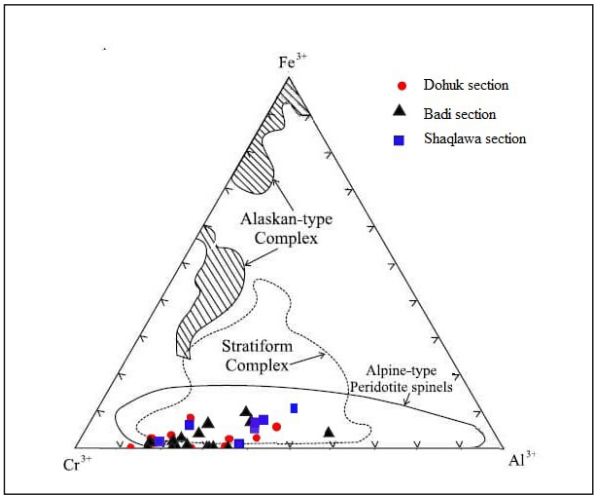

Figure 3. Ternary diagram of Cr^{3+}, Al^{3+}, and Fe^{3+} for detrital chromite of Gercus samples. The fields of Alpine-type peridotite, stratiform and Alaskan-type complexes are from (Cookenboo et al. 1997).

The high refractory nature of chromite (Cr # = 0.4 - 0.87) is more typical of supra-subduction zone chromite than chromite generated during the petrogenesis of mid-ocean ridge basalts (Dick and Bullen, 1984; Batanova and Sobolev, 2000). This conforms with the plotting of TiO_2 vs. Al_2O_3, which shows that the majority of samples fall in the field of supra-subduction zone peridotite (SSZ peridotite) (Fig. 4). Through using the discrimination plot of (Pober and Faupl, 1988) (Fig. 5), it is evident that the samples fall within the range of harzburgite, which is more common than lherzolite.

The Cr# of chromite from on-land Alpine-type peridotites ranges between 0.08 - 0.95. Peridotites that are predominate around the harzburgite-lherzolite boundary have Cr# = 0.5 (Values greater than 0.5 are harzburgites).

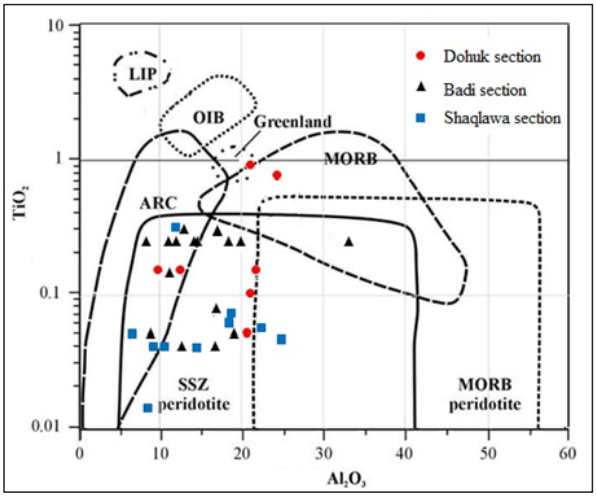

Figure 4. TiO_2 vs. Al_2O_3 relationship showing the tectonic setting for detrital chromite of the Gercus Formation (after Kamenetsky et al., 2001).

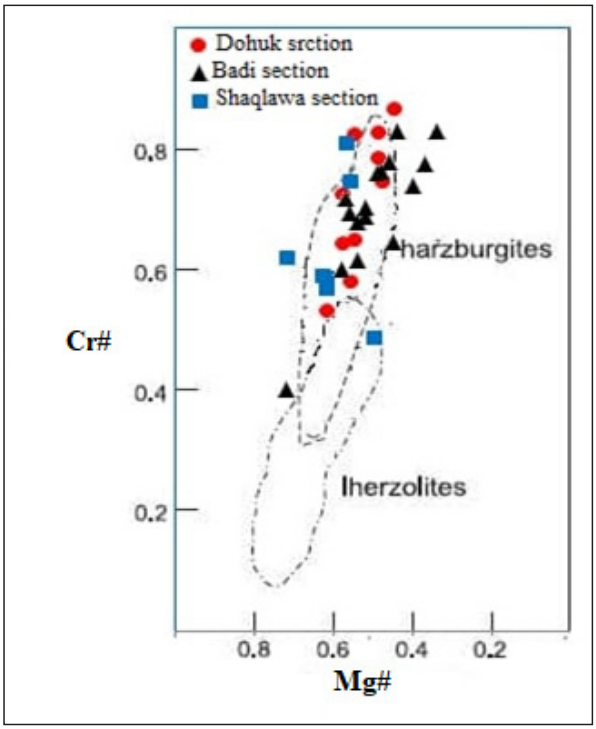

Figure 5. Cr# - Mg# diagram showing the discrimination fields of chromite derived from the two major peridotite subtypes (Pober and Faupl, 1988).

Ophiolitic harzburgites have similar characteristics to fore-arc peridotites, which belong to ocean-floor peridotites (Arai, 1994). When using Cr# - Mg# diagram (Fig. 6), the samples plot within the forearc peridotite field with a minor boninite signature. We primarily describe chromite chemistry to Tethyan ophiolites as chromites are Al-chromite (with intermediate Cr# 0.4 to 0.9) more related to the podiform Alpine-type and they can be compared to other chromites from Iraqi and Turkish ophiolitic complexes, (chromites from Iraq's Zagros ophiolitic complexes (Buda and Al-Hashimi, 1977), as well as those from Turkey's Ortakale region (Tiiysiiz, 1993). The Zagros ophiolite peridotites have high Cr# spinel compositions, which mostly plot in the fore-arc field (Moghadam and Stern, 2011). The serpentinized peridotites and related chromites from north of Iraq according to (Al-Jawadi, 1980) are chemically, mineralogically, and texturally closer to Alpine-type peridotites. They are rich with Al in general and more similar to those of podiform alpine-type. This supports the interpretation of the current research findings. The subduction of the Neo-Tethyan oceanic crust beneath the Iranian and Turkish microcontinents is part of the history of the Alpine Orogeny in the north of Iraq. Subduction in this area lasted for most of the Cretaceous and Tertiary periods and the continental plate collision between the Arabian passive margin and the active edges of Turkey and Iran consumed the Neo-Tethyan oceanic crust completely (Buday and Jassim, 1987).

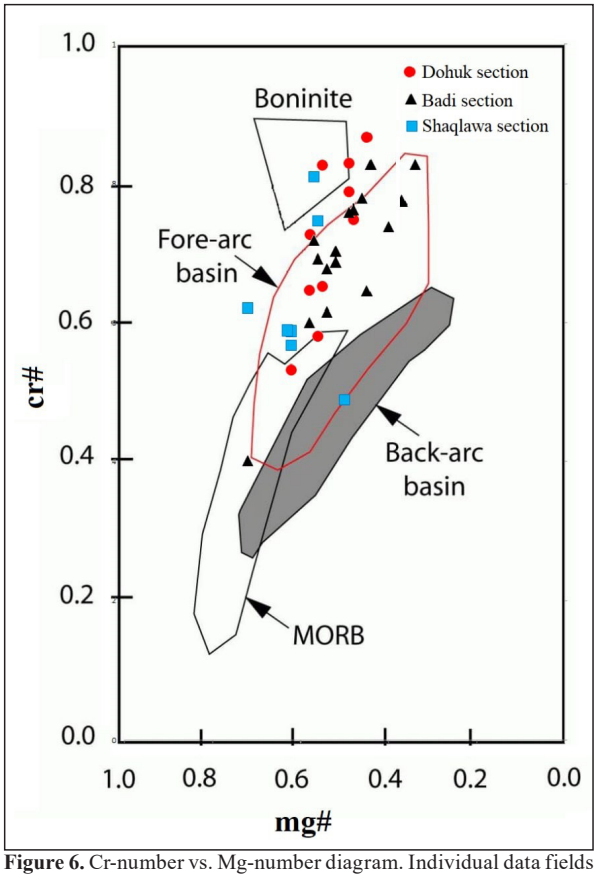

Figure 6. Cr-number vs. Mg-number diagram. Individual data fields are the composition of chromites from back-arc and fore-arc basin peridotites (Dick and Bullen, 1984).

5. Conclusion

Chromite is a sensitive mineral that indicates the source and tectonic setting of the rocks, which host the mineral. In the current study, a mineralogical and geochemical study of the detrital chromite mineral was conducted in the sandstone of the Gercus Formation (middle Eocene). Chromite exists in fine sandstone and is characterized as grains with shiny black color. Based on the geochemistry of detrital chromite from the Gercus Formation, it can be concluded that detrital chromite grains are almost classified as Al-chromite. The comparison of the chromite displays relatively high Cr# (0.4 to 0.87) and low TiO_2 content (0.014% - 0.9%) suggesting that clastics of the formation were derived from ophiolite source rocks that contain harzburgitic mantle peridotites and developed primarily in a supra-subduction zone environment. The Al- chromite is more related to the podiform Alpine type and they are equal to other chromite from Iraqi and Turkish ophiolitic complexes (chromites from Iraq's Zagros ophiolitic complexes and Turkey's Ortakale region).

Acknowledgments:

We would like to extend our great thanks to the Department of Geology staff at the College of Sciences, Mosul University for providing access to their facilities and for the kind assistance, they offered. Furthermore, we would like to thank Dr. Salim Hamed Husain, Department of Geology staff at the College of Sciences for the help and support he offered that facilitated the collection of samples from the fields.

References

Al-Jawadi, M.R. (1980) 'Petrology and geochemistry of the Band-i-Zard serpentinite and associated chromites occurring around Rayat, Northeastern Iraq'. M. Sc. thesis, Mosul University (Unpublished), 166p.

Al-Juboury, A.I., Ghazal, M.M. and McCann, T. (2009) 'Detrital chromian spinels from Miocene and Holocene sediments of northern Iraq: provenance implications', Journal of Geosciences, 54(3), pp. 289–300.

AL-Rawi, Y. (1982) 'Carbonate-rich sandstones: occurrence, classification and significance', Iraqi Journal of Science, 23(3), pp. 371–419.

Aqrawi, A.A.M., et al. (2010) The petroleum geology of Iraq. Scientific Press.

Arai, S. (1994) 'Characterization of spinel peridotites by olivine-spinel compositional relationships: review and interpretation', Chemical Geology, 113(3–4), pp. 191–204.

Armstrong, J.T. (1995) 'Citzaf-a package of correction programs for the quantitative Electron Microbeam X-Ray-Analysis of thick polished materials, thin-films, and particles', Microbeam Analysis, 4(3), pp. 177–200.

Awad, K.H. and Ahmed Alsultan, H.A. (2020) 'Stratigraphic analysis of Gercus Formation in Dohuk Area, Northern Iraq', Iraqi Journal of Science, 61(9), pp. 2293–2302. doi:10.24996/ijs.2020.61.9.16.

Batanova, V.G. and Sobolev, A. V (2000) 'Compositional heterogeneity in subduction-related mantle peridotites, Troodos massif, Cyprus', Geology, 28(1), pp. 55–58.

Buda, G.Y. and Al-Hashimi, W.S. (1977) 'Petrology of Mawat ophiolitic complex', Jour. Geol. Soc. Iraq, X, pp. 69–98.

Buday, T. and Jassim, S.Z. (1987) 'The regional geology of Iraq, vol. 2: tectonism, magmatism and metamorphism', GEOSURV, Baghdad, 352pp [Preprint].

Cookenboo, H.O., Bustin, R.M. and Wilks, K.R. (1997) 'Detrital chromian spinel compositions used to reconstruct the tectonic setting of provenance; implications for orogeny in the Canadian Cordillera', Journal of Sedimentary Research, 67(1), pp. 116–123.

Daczko, N.R. et al. (2012) 'Petrogenesis and geochemical characterisation of ultramafic cumulate rocks from Hawes Head, Fiordland, New Zealand', New Zealand Journal of Geology and Geophysics, 55(4), pp. 361–374.

Dhannoun, H.Y., Al-Dabbagh, S.M.A. and Hasso, A.A. (1988) 'The geochemistry of the Gercus red bed formation of northeast Iraq', Chemical Geology, 69(1–2), pp. 87–93.

Dick, H.J.B. and Bullen, T. (1984) 'Chromian spinel as a petrogenetic indicator in abyssal and alpine-type peridotites and spatially associated lavas', Contributions to mineralogy and petrology, 86(1), pp. 54–76.

Fouad, S.F.A. (2015) 'Tectonic map of Iraq, scale 1: 1000 000, 2012', Iraqi Bulletin of Geology and Mining, 11(1), pp. 1–7.

Franz, L. and Wirth, R. (2000) 'Spinel inclusions in olivine of peridotite xenoliths from TUBAF seamount (Bismarck Archipelago/Papua New Guinea): evidence for the thermal and tectonic evolution of the oceanic lithosphere', Contributions to Mineralogy and Petrology, 140(3), pp. 283–295.

Ghosh, B. and Konar, R. (2011) 'Chromites from meta-anorthosites, Sittampundi layered igneous complex, Tamil Nadu, southern India', Journal of Asian Earth Sciences, 42(6), pp. 1394–1402.

Hussain, S.H. and Aghwan, T.A. (2015) 'Sedimentology and evolution of a foreland desert basin, Middle Eocene Gercus Formation (North and Northeastern Iraq)', Arabian Journal of Geosciences, 8(5), pp. 2799–2830. doi:10.1007/s12517-014-1352-8.

Jassim, S.Z. and Goff, J.C. (2006) Geology of Iraq. DOLIN, sro, distributed by Geological Society of London.

Kamenetsky, V.S., Crawford, A.J. and Meffre, S. (2001) 'Factors controlling chemistry of magmatic spinel: an empirical study of associated olivine, Cr-spinel and melt inclusions from primitive rocks', Journal of Petrology, 42(4), pp. 655–671.

Lee, Y. Il (1999) 'Geotectonic significance of detrital chromian spinel: a review', Geosciences Journal, 3(1), pp. 23–29. doi:10.1007/bf02910231.

Moghadam, H.S. and Stern, R.J. (2011) 'Late Cretaceous forearc ophiolites of Iran', Island Arc, 20(1), pp. 1–4.

Morton, A.C. (1985) 'Heavy Minerals in Provenance Studies in Zuffa, G.G. ed., provenance of arenites', D. Reidel Publishing Company, 148, pp. 249–277.

Morton, A.C. and Hallsworth, C.R. (1999) 'Processes controlling the composition of heavy mineral assemblages in sandstones', Sedimentary Geology, 124(1–4), pp. 3–29. doi:10.1016/S0037-0738(98)00118-3.

Pober, E. and Faupl, P. (1988) 'The chemistry of detrital chromian spinels and its implications for the geodynamic evolution of the Eastern Alps', Geologische Rundschau, 77(3), pp. 641–670.

Roeder, P.L. (1994) 'Chromite; from the fiery rain of chondrules to the Kilauea Iki lava lake', The Canadian Mineralogist, 32(4), pp. 729–746.

Sharland. R, P. et al. (2001) 'Arabian Plate Sequence Stratigraphy (Paleo.blogfa.com).pdf', (January), pp. 2–8.

Steele, I.M. et al. (1977) 'The Fiskenæsset complex, West Greenland, part III', Chemistry of silicates and oxide minerals

from oxide bearing rocks, mostly from Qeqertarssuatsiaq. Grønl Geol Unders Bull, 124, p. 38.

Stevens, R.E. (1944) 'Composition of some chromites of the western hemisphere', American Mineralogist: Journal of Earth and Planetary Materials, 29(1–2), pp. 1–34.

Tiiysiiz, N. (1993) 'Characteristics and origin of chromite occurrences in Ortakale (Sarikamis-Kars) region, E-Turkey. Geol', Bull. Turkey, 36, pp. 151–159.

JJEES

JJEES (2023) 14 (2): 135-145
ISSN 1995-6681

Jordan Journal of Earth and Environmental Sciences

Effect of Irrigation with Treated Wastewater on Potatoes' Yields, Soil Chemical, Physical and Microbial properties

Hasan Alkhaza'leh[1*], Ahmad Abu-Awwad[2], Mohammed Alqinna[3]

[1] Ph.D. Student in Land, Water, and Environment, Department of Lands, Water, and Environment, University of Jordan, Amman, Jordan.
[2] Professor of Agriculture Engineering and Irrigation, Department of Lands, Water, and Environment, University of Jordan, Amman, Jordan.
[3] Associate Professor of Environmental Soil Physics, Department of Land Management and Environment, The Hashemite University, Zarqa, Jordan.

Received 20th July 2022; Accepted 26th October 2022

Abstract

In this study, the effects of irrigation with treated wastewater (TWW) on the physical, chemical, microbiological, and yield of potatoes were investigated. Potatoes (*Solanum tuberosum*) were irrigated by drip irrigation system using conventional irrigation water (CIW), TWW, and blended irrigation water (BIW). The concentration of all chemical and microbial characteristics of irrigation water was falling within the limits of Jordanian standards (JS893/2021), except for turbidity and boron. Pathogen indicators, *Salmonella*, and *Helminth* eggs were not found in TWW. The TWW-irrigated plots were significantly higher than BIW and CIW in electrical conductivity, organic carbon, total nitrogen, and sodium adsorption ratio (SAR). Soil iron, total *Coliform*, and *Escherichia coli* (*E,coli*) contents increased significantly within TWW-irrigated plots. Potatoes' fresh yield weight irrigated with TWW was significantly higher compared to the CIW. Treated wastewater and BIW treatments tended to have more considerable fruit weight and size than CIW. The *E. coli* was not significantly different on the surface of potato fruits, while total *Coliform* increased significantly for fruits within the TWW-irrigated plots.

Keywords: *Treated wastewater, Blended water, Escherichia coli, Pathogens, Salinization, Potatoes, Jordan.*

1. Introduction

Jordan has one of the lowest water availability rates in the world. Since 1964, the Jordanian individual's share of annual water use has decreased from 3,600 to less than 100 m^3/capita, which is less than 10% of the estimated worldwide water poverty level of 1,000 m^3/capita (MWI, 2019). Jordan's Ministry of Water and Irrigation adopted National Strategic Plan (2016-2025) that incorporates blended irrigation water (BIW) with treated wastewater (TWW) a water source added to the water budget for unrestricted reuse utilization for agricultural irrigation. Agriculture uses 52% of the total conventional water in the country; 29% of the irrigation water comes from TWW (MWI, 2020).

Using TWW for agriculture irrigation could be associated with potential problems such as health hazards, salinity build-up, and toxicity hazards (Hashem and Qi, 2021; Qiu et al., 2015). To safeguard public health and make TWW use in agriculture safe, the Jordan Standards and Metrology Organization (JSMO) developed and issued the Jordanian Standards 893/2021 (JSMO, 2021), based on WHO guidelines (WHO, 2006). These standards prohibit the use of TWW for irrigating vegetables that are eaten raw (uncooked).

Although wastewater contains nutrients important for soil productivity, it may contain toxic materials that may influence soil health and crop yield, besides pathogens (Ahmad et al., 2016). Several studies evaluated the positive and negative impact of TWW-irrigation on soil quality and yield, (Chaganti et al., 2021; Jahany and Rezapour, 2020; Paudel et al., 2018; Urbano et al., 2017; Akhtar et al., 2012; Gharaibeh et al., 2016; Cirelli et al, 2012). Furthermore, some studies show that there is a possibility for the transport of pathogens through the leaf, stem, cracks, or flaws in the skin (Serrano et al., 2014; Tournas, 2005). Soil salinization related to irrigation with wastewater is still a concern (Bedbabis et al., 2014). In arid and semiarid areas, salinization is a common problem. Around the world, 0.3–1.5 million hectares of arable land are abandoned each year as a result of salinization (Harper et al., 2021). Therefore, scientific researchers suggested measures to mitigate problems related to TWW irrigation (Nogueira et al., 2013; Cirelli et al, 2012)

The entire world cultivates and consumes potatoes and their production exceeded 370 million tons per year (FAO, 2019). In Jordan, potatoes were the second area planted vegetable after tomatoes in 2019 with a total production of 379 thousand tons (Suleiman, 2022). Potatoes production is concentrated in Jordan Valley, where the irrigation water is from King Talal Dam (KTD). Some potential sources of contaminants affecting the water quality of KTD, contaminants include discharges from the Samra wastewater treatment plant (WWTP) and Wadi Rmemeen (Al-Taani et al., 2018). Although the fact that potatoes are eaten cooked, and subsequently safe, high microbiological irrigation water quality is required because the high and constant humidity beneath the potato crop canopy is conducive to pathogen growth (Adams and Stevenson, 1990). Jordan standard (893/2021) for TWW use for irrigation includes root and tuber crops under the same category as other vegetables that are eaten cooked.

* Corresponding author e-mail: hasan-khazaleh@aabu.edu.jo

This study aimed to investigate the effects of TWW used for agriculture irrigation on soil chemical, physical, and microbial properties, and potatoes' yield.

2. Materials and Methods

2.1. Study area and experimental conditions

The experiment was conducted on a farm located in Deir Alla (32.233615°N, 35.603982°E) at an elevation of -224 m below sea level. Summers in Deir-Alla are hot and dry, and winters are mild and wet (Kool, 2016), with an annual mean temperature of 23.6°C. The temperature in summer is around 40°C and rarely drops below 20°C in winter. The average total annual rainfall is 285 mm (Kool, 2016; Tarawneh and Kadıo˘glu, 2003).

A randomized complete block design (RCBD) with three replicates, was used to examine treatments: (i) CIW; (ii) BIW (50% CIW blended with 50% TWW); (iii) TWW. Three separate tanks and three irrigation pumps were used. Each block was distributed in a random order so that they would not be next to each other. Potato tubers (*Solanum tuberosum*) cv. (Florice) was planted in clay loam soil, in January 2021. Every row was irrigated using drip irrigation covered with plastic mulch.

Temporary plastic tunnels were used, at the time of rainfall, to prevent rainwater from entering the treatment plots. Each plot contained three rows, each 7 m long. The plants were spaced 40 cm apart and rows were separated by 130 cm. Each row had an irrigation line, and 6 liters hr^{-1} discharge emitters. Potatoes were harvested in April 2021. TWW was sourced from the secondary stage of the Kufranjah-wastewater treatment plant (KWWTP). The KWWTP plant comprises preliminary treatment (screening, grit removal), activated sludge, tertiary treatment, and sludge treatment.

In this study, the fertilizer requirement for potatoes was divided into three applications throughout the growing season. In the first growth stage, nitrogen-phosphorus-potassium granular (NPK 18-18-5) was applied at the planting date. In the second stage, phosphorus is required at higher levels, so fertilizer (NPK, 12-61-0) is applied while supplying low nitrogen levels to sustain vegetative growth. In the maturity stage, NPK 13-0-46 was applied. The fungicide (Ultimatrix 52.5%WG) was used to control the early blight of potatoes.

For each irrigation event, the irrigation depth was applied and recorded. Farmer's experience was the decisive factor in the timing and amount of irrigation to meet crop water requirements.

2.2. Water analyses

During the experiment (January, February, and March 2021), water samples were collected from the holding tank in clean plastic bottles. Water sampling was conducted whenever the tanks are filled. According to the American Public Health Organization's standards (APHA, 2005), electrical conductivity (EC) was immediately measured using a conductivity meter (Jenway Conductivity Meters); pH using a pH-meter (Mettler Toledo, model FP20 Meter); dissolved oxygen (DO) was measured using a dissolved oxygen meter (Lovibond SD 400 Optical); A turbidity (TUR) meter (Mettler Toledo FSC402) was used to measure TUR (Mettler Toledo FSC402).

Total suspended solids (TSS) were measured using the filtration method, then drying the filtered sample at 105°C. Total nitrogen (TN as N) was measured using the Kje1dahl method. Ion chromatography (Dionex DX-120) was used to analyze chloride, nitrate, phosphate, and sulfate. Potassium and sodium were determined by a flame photometer (Jenway Clinical PFP7). Calcium was measured by ethylenediaminetetraacetic acid (EDTA) titrimetric method, and magnesium was measured by the difference between calcium and hardness (APHA, 2005).

HCO_3 was determined using the titration method. Equation (1) was used to calculate the sodium adsorption ratio (SAR), as described by Lesch and Suarez (2009); Inductively Coupled Plasma (ICP-OES - Perkin Elmer, Model 2000 DV) was used to measure heavy metals.

$$SAR = \frac{[Na^+]}{\sqrt{\frac{[Ca^{2+}]+[Mg^{2+}]}{2}}} \quad (1)$$

The BOD-5Day method was used to determine biological oxygen demand (BOD5), and the Closed Reflux, Titrimetric Method was used to measure chemical oxygen demand (COD) (APHA, 2005).

For microbiological analysis, water samples were collected in sterilized glass bottles with sodium thiosulphate. The samples were kept cold in an icebox below (10°C) during the transport period. The multiple tube fermentation method (MTF) was used to count *E. coli* and total *Coliforms* (APHA, 2005). The modified-Bailenger method was used to count *Helminth* eggs (Ayres et al., 1996). *Salmonellae* were measured as described by APHA (2005) and (Collee et al., 1989).

2.3. Soil analyses

Potatoes were harvested in April 2021, after 104 days of planting. Soil samples were collected from each plot, between the plants (emitters) for each depth of 0-20 cm, 21-40 cm, and 41-60 cm. Three soil samples were homogenized as composite samples from each plot for each depth. The air-dried soil samples were crushed and sieved using a 2-mm screen.

The soil texture was determined using the pipette method (Gee and Bauder, 1986); The oven-dry reference mass was used to calculate field capacity using the gravimetric method; the bulk density of the soil was determined using the core technique (Blake and Hartge, 1986). Equation(2) was used to calculate porosity. According to Richards (1954), the saturation paste extract and soil suspension was prepared.

$$Porosity = 1 - \left(\frac{BulkDensity}{ParticleDensity}\right) \quad (2)$$

ECe (dS m^{-1}) and pH were measured (1 soil: 1 water) as described by Richards (1954) and Jackson (1958), respectively. Sodium was measured directly by flame photometer according to Richard (1954). The sodium adsorption ratio (SAR) was calculated according to equation (1); Kjeldahl digestion was used to measure total nitrogen, then by distillation of steam (Jackson, 1958); the hot water technique was used to measure

boron (B) (Gupta, 1993).

The Walkley-Black method was used to determine organic carbon (Walkley and Black, 1934). Organic matter (OM) % =Total Organic Carbon (TOC) % × 1.729. The DTPA method (Lindsey and Norvell, 1978) was used to determine micronutrients such as manganese (Mn), iron (Fe), copper (Cu), and zinc (Zn), using atomic absorption spectrophotometer (AAS) (Perkin Elmer, model AA 300). *E. coli* and total *Coliforms* were analyzed by the multiple tube method according to Turco (1994). The MPN table was used to calculate the most probable number (MPN) according to Cochran (1950). The results were expressed in MPN/g.

2.4. Yield and microbiological characteristics

Potatoes were harvested after four days of the last irrigation event, from the middle rows of each treatment. Potatoes were collected, weighed, and enumerated for every plant.

For microbial analysis, composite samples (six medium-sized fruits, around 500 g) were collected from the middle rows of each treatment. Gloves were changed to prevent contamination between plots. To detect *E.coli*/total *Coliform*, 500 ml sterile of 0.1% buffered peptone water (BPW) aliquots were added to a nylon bag containing the vegetable sample, as described by Seow et al. (2012). To suspend the microorganisms from the surface of the fruits, the sample was rubbed and shaken for 2 minutes in a nylon bag to catch the microorganisms present on the surface of the fruit. For each appropriate dilution (1: 10 of the rinse fluid was prepared using BPW), the sample (0.1 ml) was spread on chromogenic agar (Brilliance *E. coli*/*Coliform*; Oxoid), following a 24-hour incubation time at 37°C. Pink and violet colonies have been counted. Results were reported as colony-forming units per gram (cfu/g).

Salmonellae were measured by suspending the microorganisms from the surface of the fruits as described above (Seow et al., 2012). Then, filtering the sample through a 47 mm and 0.45 um (HA membrane filter, Millipore Corp), as described by APHA (2005). The filter membrane was then thoroughly blended with 100 ml of sterilized BPW (0.1 %), and then the sample was selectively enriched. The 0.1 ml of samples were streaked after enrichment and Biochemical and serological tests were used to confirm the isolates (colonies), according to Collee et al. (1989). The results were reported as colony-forming units per gram (cfu/g).

Helminth eggs were detected by preparing homogenate BPW as described above, then, the modified-Bailenger method was used to count *Helminth* eggs (Ayres et al., 1996).

2.5. Statistical analyses

Treatment effects were determined using analysis of variance (ANOVA). When the F ratio was significant, the Tukey-Kramer HSD was used to compare the mean values of all parameters at a 0.05 probability level. Statistical analyses were performed with the program JMP software (Version 12, 2015, SAS Institute Cary, NC, USA) (SAS, 2015). Deviation from the mean is presented in the tables of water quality as standard deviation. The relationship between potatoes number and their weight in each treatment was estimated using the Linear Regression JMP model (SAS, 2015)

3. Results and discussion

3.1. Irrigation water characteristics

Chemical and biological analyses were done to assess CIW and TWW (Table 1). Most of the average characteristics of TWW and CIW used for irrigation (in mg L^{-1}) were within the limits of FAO recommended concentrations (Pescod, 1992), and the technical regulation of reclaimed domestic wastewater use, number 893/2021 in Jordan (JSMO, 2021). The turbidity of TWW (25 NTU) was higher than the maximum limits for irrigation (10 NTU). High TUR and TSS in TWW could cause emitter clogging, particularly if micro-irrigation is used (Li et al., 2013; Pescod, 1992). The electrical conductivity (EC) of TWW (2.06 dSm^{-1}) was 3.27 times higher than CIW electrical conductivity (0.63 dSm^{-1}). In general, TWW salinity is 1.5 – 2 times higher than freshwater salinity, according to Chen et al. (2013).

Boron (B) content of CIW (2.08 mg L^{-1}) was 4.73 times higher than TWW (0.44 mg L^{-1}) and exceeded the maximum limits for irrigation in JS893/2021(JSMO, 2021) (1.0 mg L^{-1}) and FAO (Ayers and Westcot, 1985) (2 mg L^{-1}). Boron (B) is often found in high concentrations in association with saline soils and saline well water (Hilal et al., 2011). Higher B concentration can be interpreted as caused by distillation units of groundwater wells for CIW. The reverse osmosis (RO) membrane desalination process is an efficient and reliable technology for the production of drinking water from brackish water. However, RO membranes reject the B (Jung et al., 2020).

Potatoes are moderately sensitive to B (1.0 to 2.0 mg L^{-1}) (Pescod, 1992). The B is significant for improving potato tuber yield and quality by increasing the immunity of potato plants to early blight and thus reducing the usage of fungicides in crop production (Marschner, 2011).

Table (1) indicates that TWW contains higher amounts of total nitrogen (T-N), phosphorous (P-PO_4), and potassium (K), as compared with the CIW, which are necessary for plant growth and development. In Jordan, wastewater can supply about 75% of the fertilizer needs of typical farms (Carr et al., 2011). Heavy metals including micronutrients (Fe, Mn, Cu, and Zn), nickel (Ni), chromium (Cr), cadmium (Cd), and lead (Pb) were measured in irrigation water and were within acceptable values.

On the other hand, microbial pollution is one of the significant issues, which is directly related to the health risks of using TWW for agricultural irrigation. In terms of total *Coliforms*, *E. coli*, *Salmonella*, and *Helminth* eggs, the microbiology quality of water was assessed. No microorganisms were detected in the CIW, while the mean concentrations of *E. coli* in TWW (5.7×10^4 MPN 100 ml^{-1}) were greater than the limit (100 MPN 100 ml^{-1}) required for irrigating vegetables according to JS 893/2021. *Salmonella* and *Helminth* eggs were absent in TWW (Table 1). These findings agreed with several studies that found no *Salmonella* in municipal TWW (Lonigro et al., 2016; Cirelli et al., 2012). The presence and/or concentrations of the most important pathogens in water cannot be accurately predicted by only

coliform indicators (Pachepsky et al., 2016).

The absence of *Salmonella* could indicate that the treated water eco-environment is harsher, more complex, and more dynamic. Numerous environmental conditions influence Salmonella's ability to survive and persist in water (Wanjugi and Harwood, 2013). In addition, the removal of suspended solids in WWTP aids in the control of pathogenic organisms and viruses and makes disinfection more effective. Because disinfectants such as chlorine and ozone react with organic compounds, thus pathogens become protected from disinfectants (Winward et al., 2008). These results reflect the treatment effectiveness of Kufranja WWTP or the low prevalence of Salmonella infections in the community. These results agreed with the findings reported by Karpiscak et al. (2001), which indicated that the much higher turbidity of wastewater the lesser effectiveness of treatment systems to remove some microbial indicators and pathogens.

Table 1. Characteristics of irrigation water in the study.

Parameters	Conventional irrigation water (CIW)		Treated wastewater (TWW)		Jordanian Standards (JS 893/2021/Class 1)
ECw (dSm^{-1})	0.63	±0.05	2.06	±0.53	2.3
pH	7.69	±0.12	7.60	±0.16	6-9
Cl^{-}(mg L^{-1})	97.82	±2.67	202.91	±88.76	400
SO_4^{-2} (mg L^{-1})	58.62	±4.87	79.89	±16.88	500
HCO^{-}_3(mg L^{-1})	57.96	±4.76	351.89	±134.89	400
P-PO_4^{-3} (mg L^{-1})	0.00	±0.01	18.69	±11.40	30
N-NO_3^{-}(mg L^{-1})	3.52	±2.60	12.02	±3.18	30
K^{+} (mg L^{-1})	6.11	±1.26	47.44	±10.52	N/A
B-H_3BO_3(mg L^{-1})	2.08	±0.15	0.44	±0.07	1.0
Ca (mg L^{-1})	20.57	±1.72	91.67	±19.52	230
Mg^{+2} (mg L^{-1})	23.97	±3.49	37.57	±8.57	100
Na^{+} (mg L^{-1})	74.22	±10.87	200.56	±27.02	230
SAR	2.39	±0.78	4.46	±0.29	9.0
T-N (mg L^{-1})	-	-	9.92	±1.60	N/A
TSS (mg L^{-1})	-	-	41.70	±12.80	50
TUR (NTU)	-	-	25	±27.00	10
BOD5 (mg L^{-1})	-	-	25.44	±4.44	30
COD (mg L^{-1})	-	-	59.92	±9.01	100
DO (mg L^{-1})	-	-	4.09	±3.58	>2
Cu^{+2} (ppm)	< 0.008	-	< 0.008		0.2
Fe^{+3} (ppm)	< 0.013	-	0.06	±0.00	5.0
Zn^{+2} (ppm)	< 0.017	-	< 0.017	-	5.0
Mn^{+2} (ppm)	< 0.017	-	< 0.017	-	0.2
Cd^{+2} (ppm)	< 0.009	-	< 0.009	-	0.01
Cr^{+2} (ppm)	< 0.005	-	< 0.005	-	0.1
Ni^{+2} (ppm)	< 0.01	-	< 0.01	-	0.2
Pb^{+2} (ppm)	< 0.008	-	< 0.008	-	0.2
TC (MPN100mL^{-1})	< 1.1	-	>1600000	-	N/A
E. coli (MPN 100mL^{-1})	< 1.1	-	57333	±38911	100
Salmonella (MPN L^{-1})	ND	-	ND	-	N/A
Nematode Eggs	ND		ND	-	≤ 1

ECw: electrical conductivity water; SAR: sodium adsorption ratio; BOD5: biochemical oxygen demand at 5 days; COD: chemical oxygen demand; TSS: total solid suspended; TIN: total inorganic nitrogen; DO: dissolved oxygen; NTU: N nephelometric turbidity units; TUR: turbidity; MPN: most probable number; CFU: colony-forming unit; ND: not detected.

3.2. Soil characteristics

3.2.1. Soil physical characteristics

The soil texture is primarily clay loam, silty loam, and clay loam at 0-20, 20-40, and 40-60 cm depths, respectively (Table 2). The clay loam soil has high field capacity, medium till ability, fair internal drainage, and low wind erodibility (Finkel, 2019). Deep, well-drained sandy loam soils to loam soils have the best characteristics for high-quality potato farming (Martins et al., 2018; Lambeth, 1953).

The results of soil porosity and bulk density after harvesting the crop are presented in Table (3). As expected, for a short period of TWW application, both soil porosity and bulk density were much more resistant to soil alteration by treated wastewater irrigation.

3.2.2. Soil chemical characteristics.

The impact of TWW irrigation on the soil's chemical properties is mainly reflected by the electrical conductivity (ECe) (Table 4). Soil salinity is undoubtedly a fundamental factor for soil suitability for crop production. Soil contains both organic and inorganic chemicals that contribute to salinity stress, such as $CaSO_4$, $MgCl_2$, NaCl, Na_2SO_4, $MgSO_4$, Na_2CO_3, and KCl (Strawn et al., 2020; Munns and Tester, 2008).

Table 2. Soil texture characteristics.

Soil separates	Soil depth (cm)		
	0 -20	21-40	41-60
Sand (%)	22.0	22.9	33.9
Silt (%)	42.3	53.2	35.2
Clay (%)	35.7	24.0	30.9
Texture	Clay loam	Silty loam	Clay loam

Table 3. Soil's porosity and bulk density characteristics after harvesting. (*).

Treatments	Porosity (%)	Bulk density (mg m^{3-1})
TWW	52.6 a	1.23 a
BIW	51.7 a	1.28 a
CIW	51.7 a	1.30 a

(*) Means with the same letters in the same column are not significantly different at the 0.05 probability level according to the Tukey-Kramer HSD test.

The results showed that soil ECe was significantly higher for treatment irrigated with TWW compared to treatments irrigated with BIW and CIW by 27% and 69%, respectively (Table 4). In addition, ECe for treatment irrigated using BIW was significantly higher than that for treatments irrigated using CIW by 33%. The significant increase in soil ECe in the TWW-irrigated plots (Table 4) resulted from the high concentration of salts in the TWW (2.06 dS m^{-1}) compared with CIW (0.63 dS m^{-1}). These results agreed with the findings of Kaboosi (2017) and Qadir et al. (2000).

The pH of the soil samples ranged between 7.73 and 7.86 (Table 4). The results showed no significant differences between treatments. Urbano et al. (2015) reported the same finding for five cycles of lettuce fields irrigated using TWW. These findings could indicate that the soil has a buffering effect, thus, the pH value is steady, particularly in clay or organic-rich soil (Masto et al., 2009).

Organic matter (OM) constitutes a significant part of the soil, and its content is routinely used to assess soil fertility (Mugo et al., 2020; Giusquiani et al., 1995). The SOM improves soil fertility, increasing water-holding capacity, and improving soil structure, plant productivity, and microbial activity (Masmoudi et al., 2020; Marinari et al., 2000). Soil OM plays a key role in global warming. As a result, sewage irrigation became one source of soil organic carbon in cropland, contributing to global carbon circulation (Rattan et al., 2005).

The results showed that TOC was significantly higher for TWW-irrigated plots compared with treatments irrigated with CIW by 38% (Table 4). Organic matter of TWW resulted in a significant increase in TOC in the TWW-irrigated plots. These results agreed with the previous findings reported by Bedbabis et al. (2014) and Rattan et al. (2005). Trost et al. (2013) reported a rise of 11% to 35% in soil organic carbon in semiarid regions, regardless of irrigation water type. The results showed that soil TN (Table 4), at the top layer (0-20 cm) was significantly higher for treatment irrigated with TWW compared with treatments irrigated with BIW and CIW by 15.7% and 29.6%, respectively. Whereas no significant difference in TN for the deeper depths (20-60 cm) between treatments. These results agreed with the findings reported by Guo et al. (2017) and Becerra-Castro et al. (2015).

The SAR was significantly higher with TWW-irrigated plots compared with treatments irrigated with CIW by 61% (Table 4). However, the results were below the level for soil to be classified as sodic. These results agreed with the findings reported by Bedbabis et al. (2014), Hentati et al. (2014), Sou et al. (2013), and Al-Hamaiedeh and Bino (2010). Petousi et al. (2019) studied the impacts of secondary using TWW irrigation, and their results revealed no significant differences in soil properties compared with control, except for SAR and the EC, which were slightly higher in TWW soil samples. Most of these studies attributed the high SAR to the salinity of TWW, limited rainfall, high evaporation rates, and lack of drainage infrastructure all contributing factors.

Table 4. Some soil chemical characteristics (*).

Treatments	Soil depth(cm)	ECe (dSm^{-1})	pH	TOC (%)	T-N (%)	SAR
TWW	0-20	1.15 a	7.82 a	1.34 a	0.140 a	4.7 a
BIW		0.71 b	7.77 a	1.16 ab	0.121 b	4.5 a
CIW		0.51 c	7.86 a	0.98 b	0.108 c	3.2 b
TWW	20-40	1.37 a	7.82 a	1.86 a	0.33 a	9.49 a
BIW		1.11 b	7.81a	1.47 ab	0.12 a	7.15 b
CIW		0.82 c	7.80 a	1.34 b	0.075 a	6.38 b
TWW	40-60	1.85 a	7.74 a	1.24 a	0.18 a	15.45 a
BIW		1.61 b	7.73 a	0.80 a	0.101 a	10.25 b
CIW		1.25 c	7.79 a	0.80 a	0.06 a	8.78 b

(*) Means with the same letters in the same column (are not significantly different at the 0.05 probability level, according to the Tukey-Kramer HSD test.

Soil micronutrients are important to plant growth, plants need small amounts of them (Marschner, 2011). They are generally higher in the topsoil and decrease with soil depth. The most important soil micronutrients include boron (B), iron (Fe), copper (Cu), zinc (Zn), and manganese (Mn). Micronutrients can be a problem in case of their high concentration in the soil over time and phytotoxic bioaccumulation (Atafar et al., 2010).

Soil B was significantly higher for treatment irrigated with CIW compared with treatments irrigated with TWW and BIW by 54% and 35% (Table 5), respectively. The higher concentration of B in the CIW (2.08 mg L^{-1}) causes a significant increase in soil B compared to TWW (0.44 mg L^{-1}). Irrigation water is a key cause of excessive levels of soil B (Zaman et al., 2018), but some of the excess B could be leached by rainfall and/or irrigation. However, because B is adsorbed on soil particles, leaching could be problematic, and much higher water is needed. Soils in arid regions may have naturally toxic levels of B (García-Sánchez et al., 2020), making TWW use more difficult

The Fe concentrations were significantly higher with TWW-irrigated plots in the soil surface layer compared with treatments irrigated with CIW by 36.2% (Table 5). The higher concentration of Fe in the TWW (0.06 mg L^{-1}) caused a significant increase in Fe in the TWW-irrigated plots compared to CIW (<0.013 mg L^{-1}). The Mn concentrations were significantly higher with TWW-irrigated plots in the soil's deeper layer (40-6 cm) compared with treatments irrigated with CIW by 75%. (Table 5), while no significant differences were observed in the upper layers (Table 5). These results could be influenced by fertilizer applications made before the experiment. According to Wuana and Okieimen (2011), heavy metal traces could be found in N, P, and K fertilizer compounds.

The TWW irrigated soil (Zn and Cu) content was almost the same within all irrigation treatments. These results differ from other studies that showed soil heavy metal concentrations increased with TWW irrigation. Khaskhoussy et al. (2015) reported that TWW irrigation increased copper concentration in the soil. In another study, Fe and Zn increased a two-to eight-fold accumulation in the soil surface after two years of irrigation using TWW (Salgado-Méndez et al., 2019). On the other hand, several studies showed significantly increased heavy metals concentration in clayey soil irrigated with TWW compared with sandy soils (Alnaimy et al., 2021; Kinuthia et al., 2020; Hidri et al., 2014; Klay et al., 2010). Diverging findings can be interpreted, that heavy metal levels in domestic wastewater in Jordan that are used for irrigation of crops were within the recommended levels by the world standards as reported by Othman et al., (2021), as well as Jordan is not an industrial country, and industrial wastewater is treated separately. Furthermore, the low loading rate during irrigation with such water contributes to the slow accumulation of heavy metals (Abdelrahman et al., 2011; Mohammad and Mazahreh, 2003). Nevertheless, the long-term use of this reused water could increase the risk of contaminating soil and crops with several toxic heavy metals.

3.2.3. Soil microbial characteristics.

Pathogens are the main health concern and the most common threat to wastewater reuse in agriculture, both for workers and consumers. However, other sources of contamination, such as stray animals and birds, have the potential to contaminate the irrigated soil with *E. coli*, as reported by Fonseca et al., (2020) and Venglovsky et al. (2006). The most microbial reliable indicator for water reuse in irrigation, is the *E. coli* count, and the most important indicator that shows the potential presence of harmful bacteria causing diseases (Price and Wildeboer, 2017; Pescod, 1992).

The *E. coli* was not detected, while the total *Coliform* was 7 MPN g^{-1} in the soil before the beginning of the experiment. García-Orenes et al. (2007) reported that the decrease in soil water content under semiarid conditions could be the main factor in the decrease of *Coliform*. After harvesting, total *Coliform* and *E. coli* were significantly higher in TWW irrigated plots compared to CIW plots, where total *Coliform* and *E. coli* increased from 16 to 803 and from 1.8 to 120 (MPN g^{-1}) (Table 6), respectively. These results agreed with the findings reported by Petousi et al. (2019), Farhadkhani et al. (2018), Al-Rashidi et al. (2013), and Gerba and Smith (2005).

3.2.4. Yield and microbiological characteristics.

(1) Yield: Several crops have been successfully irrigated with TWW (Maaß and Grundmann, 2018; Hanjra et al., 2012), with crop yields increasing from 10% to 30% (Lazarova and Bahri, 2004). The marketable yield of tomatoes in the TWW application was 1.21 times greater than the value of the FW application, according to Demir and Sahin (2017).

Table 5. Soil chemical characteristics after harvesting (*).

Treatments	Soil depth (cm)	B (ppm)	Cu (ppm)	Fe (ppm)	Zn (ppm)	Mn (ppm)	Ni (ppm)
TWW	0-20	2.02 b	3.96 a	7.57 a	6.58 a	5.43 a	2.14 ab
BIW		2.2 b	3.39 a	6.61 a b	5.38 a	5.51 a	2.70 a
CIW		2.85 a	2.64 a	5.56 b	4.49 a	5.02 a	1.91b
TWW	20-40	1.51 b	1.75 a	5.85 a	4.0 a	4.33 a	3.17 a
BIW		1.80 b	1.39 a	6.40 a	2.9 a	4.40 a	2.91 a
CIW		2.4 a	1.54 a	5.80 a	3.2 a	2.80 a	2.25 a
TWW	40-60	0.62 b	1.22 a	5.75 a	4.13 a	4.65 a	2.70 a
BIW		0.75 b	1.10 a	6.65 a	2.70 a	5.00 a	1.65 a
CIW		1.14 a	0.67 a	6.25 a	3.65 a	2.65 b	2.13 a

(*)Means with the same letters in the same column (depth) are not significantly different at the 0.05 probability level, according to the Tukey-Kramer HSD test.

Table 6. Soil microbial characteristics after harvesting (*).

Treatments	Total coliform (MPNg^{-1})	E. coli (MPNg^{-1})
TWW	803 a	120 a
BIW	190 b	26 b
CIW	16 c	1.8 c

(*) Means with the same letters in the same column are not significantly different at the 0.05 probability level according to the Tukey-Kramer HSD test.

In this study, potato harvesting started after four days of stopping irrigation. The results showed that potato yield increased significantly for treatment irrigated with TWW (30.7 tons ha^{-1}) compared with treatments irrigated with CIW (25.7 tons ha^{-1}) by 19.5% (Table 7). Potatoes yield in TWW irrigated plots was higher than that in BIW irrigated plots by 6%, even though it was not significantly different. In addition, potatoes yield in BIW-irrigated plots was higher than that in CIW - irrigated plots by 12.7%. These results agreed with the findings of potatoes experiments reported by Abdul Mojid and Wyseure (2014), Marofi et al. (2013), and Zavadil (2009)

In this study, the results showed that the number of potatoes increased significantly for treatment irrigated with BIW compared with treatments irrigated with TWW and CIW by 6% and 21.9%, respectively (Table 7). The relationship between the increase in the number of potatoes for each treatment, and the increase in their total weight, was estimated using the Linear Regression JMP model. The results showed that the increase in total weight (kg) was significantly higher for treatment irrigated with TWW compared with treatments irrigated with BIW and CIW (Figure 1).

Table 7. Impact of irrigation water quality on potatoes yield (*)

Treatments	Yield (ton ha^{-1})	Yield (fruits ha^{-1})
TWW	30.70 a	117,600 ab
BIW	28.96 ab	124,800 a
CIW	25.70 b	102,400 b

(*) Means with the same letters in the same column are not significantly different at the 0.05 probability level, according to the Tukey-Kramer HSD test.

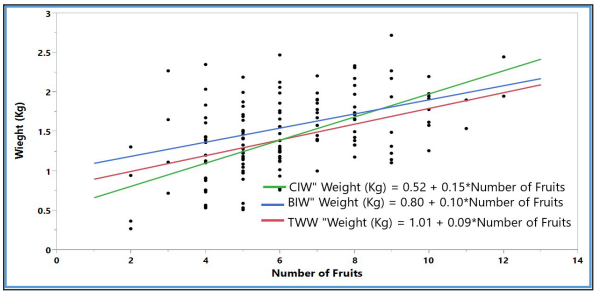

Figure 1. The relationship between the increase in the number of potatoes and the increase in their total weight for each treatment. Significant at a level of P<0.05.

On the other hand, it is natural that the lower the number of fruits per plant, the greater the weight per fruit. Figure 2 shows the relationship between the decrease in the number of potatoes per plant and the increase in weight per fruit for each treatment. The results showed the average increase in weight per fruit was significantly higher for treatment irrigated with TWW compared with treatments irrigated with BIW and CIW.

These results agreed with the findings reported by several authors (Pedrero et al., 2018; Nicolás et al., 2016; Pedrero et al., 2012). Pedrero et al. (2018) found that the size of nectarine fruit increased as the number of fruits per plant decreased, using TWW. In addition, the irrigation with TWW significantly reduced the number of nectarine fruits per tree compared to freshwater. However, the increase in the size of the fruits compensated for the reduction in the number of fruits.

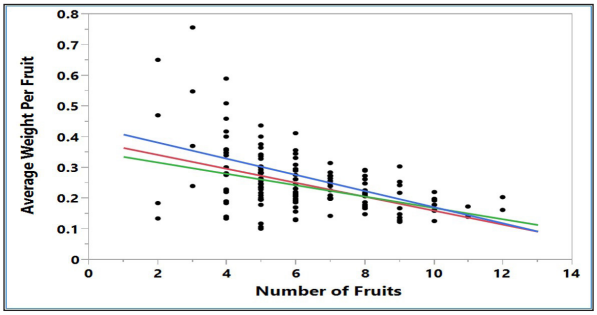

Figure 2. The relationship between the decrease in the number of potatoes per plant and the increase in weight per fruit for each treatment. Significant at a level of P< 0.05.

(2) Microbiological quality

Crops irrigated with TWW may carry pathogens such as parasitic, viral, and bacterial diseases to consumers (Domenech et al., 2018; Spanakos et al., 2015; WHO, 2006). Farhadkhani et al. (2018) reported that the irrigation method and plant type could be the most significant factors in crop microbial contamination.

Microbiologically, the harvested potatoes were analyzed. Total *Coliforms* were significantly higher on the surface of potato tubers in the TWW irrigated plots compared with BIW and CIW, (560, 70, and 30 cfu g^{-1}, respectively) (Table 8). No significant increase in *E. coli* was observed between treatments. These results agreed with those reported by Battilani et al. (2014); they observed no significant increase in *E. coli* for potatoes irrigated with TWW.

Pathogen indicators, such as *Salmonella* and *Helminth* eggs, were not found (Table 8). Lonigro et al. (2016) reported the same results. Chen et al. (2013) reported that there is limited evidence of the spread of the disease using TWW for agricultural irrigation. In contrast, *E. coli* recorded a significant increase for radishes under the drip and furrow system, but *Salmonella* was absent (Bastos and Mara, 1995). The presence of *E. coli* in the CIW irrigated plots could be attributed to different sources of contamination, such as roaming animals, and birds (Venglovsky et al., 2006). The contrast in the different studies' results could be because of the difference in the TWW quality, environment, or management method.

The successful measures reduce the potential microbial contaminations by reduction of the exposure of workers to wastewater. Some of the measures, such as drip irrigation and stopping irrigation before harvest, could play a significant role in the successful use of TWW for irrigation. A period without irrigation before harvest (1-2 weeks) can allow the die-off of bacteria and viruses to improve the quality of irrigated crops to levels seen in crops irrigated with fresh water, as reported by Vaz da Costa Vargas et al. (1996). However, this option is workable for some crops such as potatoes, and unworkable for

vegetables that need harvesting daily, because farmers will probably not wait or stop irrigation of leafy salad crops five days or more before harvest (Lamm, 2002; Aiello et al. 2007).

Table 8. Potatoes' microbiological characteristics.

Treatment	Total *coliform* (cfu g^{-1})	*E.coli* (cfu g^{-1})	*Salmonella* (cfu g^{-1})	*H.*eggs (egg g^{-1})
TWW	560 a	40 a	ND	ND
BIW	70 b	20 a	ND	ND
CIW	30 b	10 a	ND	ND

(*) Means with the same letters in the same column are not significantly different at the 0.05 probability level, according to the Tukey-Kramer HSD test

4. Conclusions

Water reuse is essential in Jordan. The TWW contributes significantly to the country's limited irrigation water supply, allowing agriculture to continue in some areas. The study showed the effects of irrigation with TWW on some physical and chemical properties of the soil. Physically, in the short term, no significant differences were observed. Chemically, in particular, TWW increased the organic matter and TN, specifically in the surface soil. Regarding the SAR and EC, TWW induced a significant accumulation in the soil layers. The higher B concentration in soil for CIW irrigated plots is due to the higher concentration of B in irrigation water. Microbially, total *Coliform* and *E. coli* were significantly higher in TWW irrigated plots compared with CIW plots. On the other hand, potatoes showed significant contamination by total *Coliform*. Therefore, although non-significant observed of *E.coli* and the absence of pathogens such as *Salmonella* and *Helminth* eggs, root and tuber crops may be exposed to microbial hazards. Thus, a period of stopping irrigation should be scheduled before harvest.

Finally, the results of this study indicated that the use of TWW with drip irrigation for potato production could be feasible with TWW. Another key fact is that TWW and BIW treatments tended more considerable fruit weight and size. However, more research is needed to show the positive impacts of TWW on potatoes' fruit quality measures.

Acknowledgments

The University of Jordan, Deanship for Scientific Research [Grant numbers 333/2021/19], supported this work. The authors thank the Directorate of Laboratories and Environment, the Jordan Valley Authority for helping to conduct the analyzes, and Ibrahim Al-Sharif Farms for their generous support in providing agricultural plots and agriculture expertise.

Disclosure statement

The authors reported no potential conflict of interest.

References

Ahmad, H. R., Aziz, T., Zia-ur-Rehman, M., Sabir, M., and Khalid, H. (2016). Sources and Composition of Wastewater: Threats to Plants and Soil Health, In Soil Science: Agricultural and Environmental Prospective .pp. 349-370

Abdelrahman, H. A., Alkhamisi, S. A., Ahmed, M., and Ali, H. (2011). Effects of Treated Wastewater Irrigation on Element Concentrations in Soil and Maize Plants. Communications in Soil Science and Plant Analysis 42(17): 2046-2063.

Abdul Mojid, M., and Wyseure, G. C. (2014). Fertility Response of Potato to Municipal Wastewater and Inorganic Fertilizers. Journal of Plant Nutrition 37(12): 1997-2016.

Adams, S. S., and Stevenson, W. R. (1990). Water Management, Disease Development, and Potato Production. American Potato Journal 67(1): 3-11.

Aiello, R., Cirelli, G. L., and Consoli, S. (2007). Effects of Reclaimed Wastewater Irrigation on Soil and Tomato Fruits: a Case Study in Sicily (Italy). Agricultural Water Management 93(1-2): 65-72.

Akhtar, N., Inam, A., Inam, A., and Khan, N. A. (2012). Effects of City Wastewater on the Characteristics of Wheat with Varying Doses of Nitrogen, Phosphorus, and Potassium. Recent Research in Science and Technology 4(5):18-29

Al-Hamaiedeh, H., and Bino, M. (2010). Effect of Treated Grey Water Reuse in Irrigation on Soil and Plants. Desalination 256(1-3): 115-119.

Alnaimy, M. A., Shahin, S. A., Vranayova, Z., Zelenakova, M., and Abdel-Hamed, E. M. W. (2021). Long-term Impact of Wastewater Irrigation on Soil Pollution and Degradation: a Case Study from Egypt. Water 13(16): 2245.

Al-Rashidi, R., Rusan, M., and Obaid, K. (2013). Changes in Plant Nutrients, and Microbial Biomass in Different Soil Depths after Long-term Surface Application of Secondary Treated Wastewater. Environmental and Climate Technologies 11(2013): 28-33.

Al-Taani, A. A., El-Radaideh, N. M., and Al Khateeb, W. M. (2018). Status of Water Quality in King Talal Reservoir Dam, Jordan. Water Resources 45(4): 603-614.

American Public Health Association (APHA) (2005). Standard Methods for the Examination of Water and Wastewater (23rd Edn.). Washington, DC: American Public Health Association. https://www.standardmethods.org

Atafar, Z., Mesdaghinia, A., Nouri, J., Homaee, M., Yunesian, M., Ahmadimoghaddam, M., and Mahvi, A. H. (2010). Effect of Fertilizer Application on Soil Heavy Metal Concentration. Environmental Monitoring and Assessment 160(1), 83-89.

Ayers, R. S., and Westcot, D. W. (1985). Water Quality for Agriculture 29: 174. Rome: Food and Agriculture Organization of the United Nations.

Ayres, R. M., and Mara, D. D. (1996). Analysis of Wastewater for Use in Agriculture: A Laboratory Manual of Parasitological and Bacteriological Techniques. World Health Organization. https://apps.who.int/iris/handle/10665/41832

Bastos, R. K. X., and Mara, D. D. (1995). The Bacterial Quality of Salad Crops Drip and Furrow Irrigated with Waste Stabilization Pond Effluent: An Evaluation of the WHO Guidelines. Water Science and Technology 31(12): 425-430.

Battilani, A., Plauborg, F., Andersen, M.N., Forslund, A., Ensink, J., Dalsgaard, A., Fletcher, T. and Solimando, D. (2014). Treated Wastewater Reuse on Potato (Solanum Tuberosum). Acta Hortic. 1038, 105-112

Becerra-Castro, C., Lopes, A. R., Vaz-Moreira, I., Silva, E. F., Manaia, C. M., and Nunes, O. C. (2015). Wastewater Reuse in Irrigation: a Microbiological Perspective on Implications in Soil Fertility and Human and Environmental Health. Environment International 75: 117-135.

Bedbabis, S., Rouina, B. B., Boukhris, M., and Ferrara, G. (2014). Effect of Irrigation with Treated Wastewater on Soil Chemical Properties and Infiltration Rate. Journal of Environmental Management 133: 45-50.

Blake, G.R., and Hartge, K.H. (1986). Bulk Density, In Methods of Soil Analysis, Klute, A. (Ed.). pp. 363-375.

Carr, G., Potter, R. B., and Nortcliff, S. (2011). Water Reuse for Irrigation in Jordan: Perceptions of Water Quality Among Farmers. Agricultural Water Management 98(5): 847-854.

Chaganti, V. N., Ganjegunte, G., Meki, M. N., Kiniry, J. R., and Niu, G. (2021). Switchgrass Biomass Yield and Composition and Soil Quality as Affected by Treated Wastewater Irrigation in An

arid Environment. Biomass and Bioenergy 151, 106160.

Chen, W., Lu, S., Jiao, W., Wang, M., and Chang, A. C. (2013). Reclaimed Water: A Safe Irrigation Water Source? Environmental Development 8: 74-83.

Cirelli, G. L., Consoli, S., Licciardello, F., Aiello, R., Giuffrida, F., and Leonardi, C. (2012). Treated Municipal Wastewater Reuse in Vegetable Production. Agricultural Water Management 104: 163-170.

Cochran, W. G. (1950). Estimation of Bacterial Densities by Means of the "Most Probable Number". Biometrics 6(2): 105-116.

Collee, J., Duguid, J., Fraser, A., and Marmion, B. (1989). Practical Medical Microbiology. Churchill Livingstone, London, New York, 2: 161-289.

Demir, A. D., and Sahin, U. (2017). Effects of Different Irrigation Practices Using Treated Wastewater on Tomato Yields, Quality, Water Productivity, and Soil and Fruit Mineral Contents. Environmental Science and Pollution Research 24(32), 24856-24879

Domenech, E., Amorós, I., Moreno, Y., and Alonso, J. L. (2018). Cryptosporidium and Giardia Safety Margin Increase in Leafy Green Vegetables Irrigated with Treated Wastewater. International Journal of Hygiene and Environmental Health 221(1): 112-119.

Farhadkhani, M., Nikaeen, M., Yadegarfar, G., Hatamzadeh, M., Pourmohammadbagher, H., Sahbaei, Z., and Rahmani, H. R. (2018). Effects of Irrigation with Secondary Treated Wastewater on Physicochemical and Microbial Properties of Soil and Produce Safety in a Semi-arid Area. Water Research 144: 356-364.

Finkel, H. J. (2019). Handbook of Irrigation Technology: Volume 1. CRC Press. p.14

Fonseca, J. M., Ravishankar, S., Sanchez, C. A., Park, E., and Nolte, K. D. (2020). Assessing the Food Safety Risk Posed by Birds Entering Leafy Greens Fields in the US Southwest. International Journal of Environmental Research and Public Health 17(23), 8711.

Food and Agriculture Organization (FAO), (2019) Food and Agriculture Organization Corporate Statistical Database (FAOSTAT). https://www.fao.org/faostat/en/

García-Orenes, F., Roldán, A., Guerrero, C., Mataix-Solera, J., Navarro-Pedreno, J., Gómez, I., and Mataix-Beneyto, J. (2007). Effect of Irrigation on the Survival of Total Coliforms in Three Semiarid Soils after Amendment with Sewage Sludge. Waste Management 27(12): 1815-1819.

García-Sánchez, F., Simón-Grao, S., Martínez-Nicolás, J. J., Alfosea-Simón, M., Liu, C., Chatzissavvidis, C., Pérez-Pérez, J. G., and Cámara-Zapata, J. M. (2020). Multiple Stresses Occurring with Boron Toxicity and Deficiency in Plants. Journal of Hazardous Materials 397, 122713.

Gee, G.W., and Bauder, J.W. (1986). Particle-size Analysis. In: Methods of Soil Analysis, Klute, A. (Ed.). pp. 383-411.

Gerba, C. P., and Smith, J. E. (2005). Sources of Pathogenic Microorganisms and their Fate during Land Application of Wastes. Journal of Environmental Quality 34(1): 42-48.

Gharaibeh, M. A., Ghezzehei, T. A., Albalasmeh, A. A., and Ma'in, Z. A. (2016). Alteration of Physical and Chemical Characteristics of Clayey Soils by Irrigation with Treated Waste Water. Geoderma 276, 33-40.

Giusquiani, P. L., Pagliai, M., Gigliotti, G., Businelli, D., and Benetti, A. (1995). Urban Waste Compost: Effects on Physical, Chemical, and Biochemical Soil Properties. American Society of Agronomy, Crop Science Society of America, and Soil Science Society of America 24(1): 175-182.

Guo, L., Li, J., Li, Y., and Xu, D. (2017). Nitrogen Utilization under Drip Irrigation with Sewage Effluent in the North China Plain. Irrigation and Drainage 66(5): 699-710.

Gupta, U. C. (1993). Boron and its Role in Crop Production. CRC press. pp.125-135

Hanjra, M. A., Blackwell, J., Carr, G., Zhang, F., and Jackson, T. M. (2012). Wastewater Irrigation and Environmental Health: Implications for Water Governance and Public Policy. International Journal of Hygiene and Environmental Health 215(3), 255-269.

Harper, R. J., Dell, B., Ruprecht, J. K., Sochacki, S. J., and Smettem, K. R. J. (2021). Salinity and the Reclamation of Salinized Lands. In Soils and Landscape Restoration. pp. 193-208. Academic Press.

Hashem, M. S., and Qi, X. (2021). Treated Wastewater Irrigation—A Review. Water 13(11), 1527

Hentati, O., Chaker, S., Wali, A., Ayoub, T., and Ksibi, M. (2014). Effects of Long-term Irrigation with Treated Wastewater on Soil Quality, Soil-borne Pathogens, and Living Organisms: a Case Study of the Vicinity of El Hajeb (Tunisia). Environmental Monitoring and Assessment 186(5): 2671-2683.

Hidri, Y., Fourti, O., Eturki, S., Jedidi, N., Charef, A., and Hassen, A. (2014). Effects of 15-year Application of Municipal Wastewater on Microbial Biomass, Fecal Pollution Indicators, and Heavy Metals in a Tunisian Calcareous Soil. Journal of Soils and Sediments 14(1): 155-163.

Hilal, N., Kim, G. J., and Somerfield, C. (2011). Boron Removal from Saline Water: A Comprehensive Review. Desalination 273(1), 23-35.

Jackson, M. L. (1958). Soil Chemical Analysis Prentice Hall. 498: 183-204. Inc., Englewood Cliffs, NJ.

Jahany, M., and Rezapour, S. (2020). Assessment of the Quality Indices of Soils Irrigated with Treated Wastewater in a Calcareous Semi-arid Environment. Ecological Indicators 109, 105800.

Jordan Standard Metrology Organization (JSMO). (2021). Standard Specification "Water- Reclaimed Domestic Wastewater" No. 893/2021tech. Rep. Amman, Jordan.

Jung, B., Kim, C. Y., Jiao, S., Rao, U., Dudchenko, A. V., Tester, J., and Jassby, D. (2020). Enhancing Boron Rejection on Electrically Conducting Reverse Osmosis Membranes through Local Electrochemical pH Modification. Desalination 476, 114212.

Kaboosi, K. (2017). The Assessment of Treated Wastewater Quality and the Effects of Mid-Term Irrigation on Soil Physical and Chemical Properties (a Case Study: Bandargaz-treated Wastewater). Applied Water Science 7(5): 2385-2396.

Karpiscak, M. M., Sanchez, L. R., Freitas, R. J., and Gerba, C. P. (2001). Removal of Bacterial Indicators and Pathogens from Dairy Wastewater by a Multi-component Treatment System. Water Science and Technology 44(11-12): 183-190.

Khaskhoussy, K., Kahlaoui, B., Messoudi Nefzi, B., Jozdan, O., Dakheel, A., and Hachicha, M. (2015). Effect of Treated Wastewater Irrigation on Heavy Metals Distribution in a Tunisian Soil. Engineering, Technology and Applied Science Research 5(3): 805-810.

Kinuthia, G. K., Ngure, V., Beti, D., Lugalia, R., Wangila, A., and Kamau, L. (2020). Levels of Heavy Metals in Wastewater and Soil Samples from Open Drainage Channels in Nairobi, Kenya: Community Health Implication. Scientific Reports 10(1): 1-13.

Klay, S., Charef, A., Ayed, L., Houman, B., and Rezgui, F. (2010). Effect of Irrigation with Treated Wastewater on Geochemical Properties (Saltiness, C, N, and Heavy Metals) of Isohumic Soils (Zaouit Sousse Perimeter, Oriental Tunisia). Desalination 253(1-3): 180-187.

Kool, J. (2016). The Jordan Valley, In Sustainable Development in the Jordan Valley. Springer, Cham. pp. 5-60.

Lambeth, V. N. (1953). Sweet Potato Production in Missouri, University of Missouri, College of Agriculture, Agricultural Experiment Station.

Lamm, F. R. (2002). Advantages and Disadvantages of Subsurface Drip Irrigation, In International Meeting on

Advances in Drip/Micro Irrigation, Puerto de La Cruz, Tenerife, Canary Islands. pp. 1-13.

Lazarova, V., and Bahri, A. (Eds.). (2004). Water Reuse for Irrigation: Agriculture, Landscapes, and Turf Grass. CRC press. pp. 6-7

Lesch, S. M., and Suarez, D. L. (2009). A Short Note on Calculating the Adjusted SAR Index. Transactions of the ASABE 52: 493-496.

Li, Y., Zhou, B., Liu, Y., Jiang, Y., Pei, Y., and Shi, Z. (2013). Preliminary Surface Topographical Characteristics of Biofilms Attached on Drip Irrigation Emitters Using Reclaimed Water. Irrigation Science 31(4): 557-574.

Lindsey, W. L., and Norvell, W. A. (1978). Development of DTPA Soil Test for Zinc, Iron, Manganese, and Copper. Soil Science Society of America Journal 42: 421-428.

Lonigro, A., Rubino, P., Lacasella, V., and Montemurro, N. (2016). Faecal Pollution on Vegetables and Soil Drip Irrigated with Treated Municipal Wastewaters. Agricultural Water Management 174: 66-73.

Maaß, O., and Grundmann, P. (2018). Governing Transactions and Interdependences between Linked Value Chains in a Circular Economy: The Case of Wastewater Reuse in Braunschweig (Germany). Sustainability 10(4), 1125.

Marinari, S., Masciandaro, G., Ceccanti, B., and Grego, S. (2000). Influence of Organic and Mineral Fertilisers on Soil Biological and Physical Properties. Bioresource Technology 72(1): 9-17.

Marofi, S., Parsafar, N., Rahim, G. H., Dashti, F., and Marofi, H. (2013). The Effects of Wastewater Reuse on Potato Growth Properties under Greenhouse Lysimeteric Condition. International Journal of Environmental Science and Technology 10(1): 133-140.

Marschner, H. (Ed.). (2011). Marschner's Mineral Nutrition of Higher Plants. Academic Press. pp. 3-4

Martins, J. D. L., Soratto, R. P., Fernandes, A., and Dias, P. H. (2018). Phosphorus Fertilization and Soil Texture Affect Potato Yield. Revista Caatinga 31, 541-550.

Masmoudi, S., Magdich, S., Rigane, H., Medhioub, K., Rebai, A., and Ammar, E. (2020). Effects of Compost and Manure Application Rate on the Soil Physico-chemical Layers Properties and Plant Productivity. Waste and Biomass Valorization 11(5), 1883-1894.

Masto, R. E., Chhonkar, P. K., Singh, D., and Patra, A. K. (2009). Changes in Soil Quality Indicators under Long-term Sewage Irrigation in A Sub-Tropical Environment. Environmental Geology 56(6): 1237-1243.

Ministry of Water and Irrigation (MWI). (2019). Facts and Figures of Jordanian Water Sectors for the Year 2019. Amman, Jordan. pp. 6. https://mwi.gov.jo

Ministry of Water and Irrigation (MWI). (2020). Facts and Figures of Jordanian Water Sectors for the Year 2020. Amman, Jordan. https://mwi.gov.jo. pp. 13-14

Mohammad, M. J., and Mazahreh, N. (2003). Changes in Soil Fertility Parameters in Response to Irrigation of Forage Crops with Secondary Treated Wastewater. Communications in Soil Science and Plant Analysis 34(9-10): 1281-1294.

Mugo, J., Karanja, N. N., Gachene, C. K., Dittert, K., Nyawade, S. O., and Schulte-Geldermann, E. (2020). Assessment of Soil Fertility and Potato Crop Nutrient Status in Central and Eastern Highlands of Kenya. Scientific Reports 10(1), 1-11.

Munns, R., and Tester, M. (2008). Mechanisms of Salinity Tolerance. Annual Review of Plant Biology 59: 651-681.

Nicolás, E., Alarcón, J., Mounzer, O., Pedrero, F., Nortes, P., Alcobendas, R., Romero-Trigueros, C., Bayona, J., and Maestre-Valero, J. (2016). Long-term Physiological and Agronomic Responses of Mandarin Trees to Irrigation with Saline Reclaimed Water. Agricultural Water Management 166, 1–8.

Nogueira, S. F., Pereira, B. F. F., Gomes, T. M., De Paula, A. M., Dos Santos, J. A., and Montes, C. R. (2013). Treated Sewage Effluent: Agronomical and Economical Aspects on Bermudagrass Production. Agricultural Water Management, 116: 151-159.

Othman, Y. A., Al-Assaf, A., Tadros, M. J., and Albalawneh, A. (2021). Heavy Metals and Microbes Accumulation in Soil and Food Crops Irrigated with Wastewater and the Potential Human Health Risk: a Metadata Analysis. Water 13(23), 3405.

Pachepsky, Y., Shelton, D., Dorner, S., and Whelan, G. (2016). Can E. coli or Thermotolerant Coliform Concentrations Predict Pathogen Presence or Prevalence in Irrigation Waters? Critical Reviews in Microbiology 42(3), 384-393.

Paudel, I., Bar-Tal, A., Levy, G. J., Rotbart, N., Ephrath, J. E., and Cohen, S. (2018). Treated Wastewater Irrigation: Soil Variables and Grapefruit Tree Performance. Agricultural Water Management 204, 126-137.

Pedrero, F., Allende, A., Gil, M. I., and Alarcón, J. J. (2012). Soil Chemical Properties, Leaf Mineral Status, and Crop Production in A Lemon Tree Orchard Irrigated with Two Types of Wastewater. Agricultural Water Management 109: 54-60.

Pedrero, F., Camposeo, S., Pace, B., Cefola, M., and Vivaldi, G. A. (2018). Use of Reclaimed Wastewater on Fruit Quality of Nectarine in Southern Italy. Agricultural Water Management 203: 186-192.

Pescod, M. B. (1992). Wastewater Treatment and Use in Agriculture-FAO Irrigation and Drainage Paper 47. Food and Agriculture Organization of the United Nations, Rome. http://www.fao.org/docrep/T0551E/T0551E00.htm

Petousi, I., Daskalakis, G., Fountoulakis, M. S., Lydakis, D., Fletcher, L., Stentiford, E. I., and Manios, T. (2019). Effects of Treated Wastewater Irrigation on the Establishment of Young Grapevines. Science of the Total Environment 658: 485-492.

Price, R. G., and Wildeboer, D. (2017). E. coli as an Indicator of Contamination and Health Risk in Environmental Waters. Escherichia coli-Recent Advances on Physiology, Pathogenesis, and Biotechnological Applications. p. 13.

Qadir, M., Ghafoor, A., and Murtaza, G. (2000). Amelioration Strategies for Saline Soils: a Review. Land Degradation and Development 11(6): 501-521.

Qiu, Y., Lee, B. E., Neumann, N., Ashbolt, N., Craik, S., Maal-Bared, R., and Pang, X. L. (2015). Assessment of Human Virus Removal during Municipal Wastewater Treatment in Edmonton, Canada. Journal of Applied Microbiology 119(6), 1729-1739.

Rattan, R. K., Datta, S. P., Chhonkar, P. K., Suribabu, K., and Singh, A. K. (2005). Long-term Impact of Irrigation with Sewage Effluents on Heavy Metal Content in Soils, Crops and Groundwater - a Case Study. Agriculture, Ecosystems and Environment 109(3-4): 310-322.

Richards, L. A. (1954). Diagnosis and Improvement of Saline and Alkali Soils. Soil Science 2, p. 154. LWW.

Salgado-Méndez, S., Gilabert-Alarcón, C., Daesslé, L. W., Mendoza-Espinosa, L., Avilés-Marín, S., and Stumpp, C. (2019). Short-term Effects on Agricultural Soils Irrigated with Reclaimed Water in Baja California, Mexico. Bulletin of Environmental Contamination and Toxicology 102(6): 829-835.

SAS Institute. (2015). JMP: Version 12: Design of Experiments Guide. Cary, NC: SAS Institute Inc

Seow, J., Ágoston, R., Phua, L., and Yuk, H. G. (2012). Microbiological Quality of Fresh Vegetables and Fruits Sold in Singapore. Food Control 25(1): 39-44.

Serrano, M., Coluccia, F., Torres, M., L'Haridon, F., and Métraux, J.P. (2014). The Cuticle and Plant Defense to Pathogens. Front. Plant Science 5: 1–8.

Sou, M. Y., Mermoud, A., Yacouba, H., and Boivin, P. (2013). Impacts of Irrigation with Industrial Treated Wastewater on Soil Properties. Geoderma 200: 31-39.

Spanakos, G., Biba, A., Mavridou, A., and Karanis, P. (2015).

Occurrence of Cryptosporidium and Giardia in Recycled Waters Used for Irrigation and First Description of Cryptosporidium Parvum and C. muris in Greece. Parasitology Research 114(5): 1803-1810.

Strawn, D. G., Bohn, H. L., and O'Connor, G. A. (2020). Soil Chemistry. John Wiley and Sons.pp 6-28

Suleiman, A. (2022). Modeling the Effect of Planting Dates and Nitrogen Application Rates on Potatoes Water Productivity in Jordan Valley. American Journal of Plant Sciences 13(1), 137-146.

Tarawneh, Q., and Kadıo˘glu, M. (2003). An Analysis of Precipitation Climatology in Jordan. Theoretical and Applied Climatology, 74(1): 123-136.

Tournas, V. H. (2005). Spoilage of Vegetable Crops by Bacteria and Fungi and Related Health Hazards. Critical Reviews in Microbiology 31(1), 33-44.

Trost, B., Prochnow, A., Drastig, K., Meyer-Aurich, A., Ellmer, F., and Baumecker, M. (2013). Irrigation, Soil Organic Carbon and N2O Emissions. A review. Agronomy for Sustainable Development 33(4): 733-749.

Turco, R. F. (1994). Coliform Bacteria. Methods of Soil Analysis: Part 2 Microbiological and Biochemical Properties 5: 145-158.

Urbano, V. R., Mendonça, T. G., Bastos, R. G., and Souza, C. F. (2015). Physical-chemical Effects of Irrigation with Treated Wastewater on Dusky Red Latosol Soil. Revista Ambiente and Água, 10: 737-747.

Urbano, V. R., Mendonça, T. G., Bastos, R. G., and Souza, C. F. (2017). Effects of Treated Wastewater Irrigation on Soil Properties and Lettuce Yield. Agricultural Water Management 181: 108-115.

Vaz da Costa Vargas, S., Bastos, R.K.X., and Mara, D.D. (1996). Bacteriological Aspects of Wastewater Irrigation. Tropical Public Health Engineering (TPHE) Research Monograph no.8, University of Leeds (Department of Civil Engineering) Leeds, UK. pp. 239,370. https://www.ircwash.org/resources/bacteriological-aspects-wastewater-irrigation

Venglovsky, J., Martinez, J., and Placha, I. (2006). Hygienic and Ecological Risks Connected with Utilization of Animal Manures and Biosolids in Agriculture. Livestock Science 102(3): 197-203.

Walkley, A., and Black, I. A. (1934). An examination of the Degtjareff Method for Determining Soil Organic matter, and a Proposed Modification of the Chromic Acid Titration Method. Soil Science 37(1): 29-38.

Wanjugi, P., and Harwood, V. J. (2013). The Influence of Predation and Competition on the Survival of Commensal and Pathogenic Fecal Bacteria in Aquatic Habitats. Environmental Microbiology 15(2): 517-526.

Winward, G. P., Avery, L. M., Stephenson, T., and Jefferson, B. (2008). Ultraviolet (UV) Disinfection of Grey Water: Particle Size Effects. Environmental Technology 29(2): 235-244.

World Health Organization (1996). Analysis of Wastewater for Use in Agriculture: AL Manual of Parasitological and Bacteriological Techniques. World Health Organization. pp.3-16. https://apps.who.int/iris/handle/10665/41832

World Health Organization (WHO). (2006). WHO Guidelines for the Safe Use of Wastewater Excreta and Greywater, vol. 1. World Health Organization. pp. 19-30 https://www.who.int/publications/i/item/9241546824

Wuana R. A., and Okieimen, F. E. (2011). Heavy Metals in Contaminated Soils: a Review of Sources, Chemistry, Risks and Best Available Strategies for Remediation. Communications in Soil Science and Plant Analysis 42, 111-122.

Zaman, M., Shahid, S. A., and Heng, L. (2018). Irrigation Water Quality. In Guideline for Salinity Assessment, Mitigation and Adaptation Using Nuclear and Related Techniques. Springer, Cham. pp. 113-131

Zavadil, J. (2009). The Effect of Municipal Wastewater Irrigation on the Yield and Quality of Vegetables and Crops. Soil and Water Research 4(3): 91-103.

JJEES

JJEES (2023) 14 (2): 146-157
ISSN 1995-6681

Jordan Journal of Earth and Environmental Sciences

Geochemistry and Tectonic Setting of the Metagabbros of Penjween Ophiolite Complex, Northeastern Iraq

Omar S. Al-Taweel [1], Flyah H. Al-Khatony [2],
Mohammed A. Al-Jboury [3], Shareef Th. Al-Hamed [4]

[1, 2, 3, 4] Department of Geology, College of Science, University of Mosul, Mosul, Iraq

Received 12th June 2022; Accepted 26th October 2022

Abstract

The Penjween Ophiolite Complex is part of the Zagros Suture Zone (ZSZ) and is located within the Penjween-Walash Subzone northeast of Iraq. It is an incomplete sequence that consists of two main igneous bodies: the ultramafic body and the gabbroic body. The Penjween layered metagabbros show wide variation in grain size and are composed of saussuritized plagioclase, and amphibole with relict pyroxene. The chondrite-normalized REE patterns in Penjween metagabbroic rocks exhibit LREE depletion and flat MREE and HREE patterns, with patterns that are nearly flat in general, and these patterns are similar to rocks generated in Island Arc Tholeiite (IAT) and subduction-related environments. The depletion in High Field Strength Elements (HFSEs) with enrichment in Large Ion Lithophile Elements (LILEs) and the strong negative Nb anomaly is typical of magmas formed in the supra subduction zone. The La/Nb and La/Ba ratios indicate that metagabbroic rocks originated in the asthenosphere mantle, while the La/Yb and Dy/Yb ratios imply shallow source partial melting of spinel-peridotite. The variable Sr/Nd and Ba/Th ratios with nearly constant Th/Yb and La/Sm ratios, indicate that fluids from slab dehydration modified the ancient mantle. Penjween ophiolite metagabbros are classified as Island Arc Tholeiite (IAT) because it contains very low to low-TiO_2 (0.11-0.69%). In conclusion, the low and very low Ti concentration strongly suggests that the metgabbroic rocks of the Penjween Ophiolite Complex are linked to Island Arc Tholeiite, which has a link to the supra subduction zone.

Keywords: *Metagabbro, Ophiolite, Penjween, Geochemistry, Tectonic Setting, Iraq.*

1. Introduction

Peridotites in the ophiolite complex generally involve serpentinized harzburgites, lherzolite, dunite, and existing pyroxenite (Snow and Dick, 1995). These peridotites represent the bottom category of the ophiolite; these comprise sub-continental or orogenic Alpine ultramafic rocks (Menzies and Dupuy, 1991) and slivers of ancient oceanic lithosphere obducted onto the continental or oceanic crust (Beccaluva et al., 1984; Nicolas and Boudier, 2003). Moreover, the oceanic origin represents mantle rocks that were extracted along normal and transform faults (Bonatti et al., 1981). Igneous oceanic crust is a second part of this complex formed at divergent plate boundaries and consists of gabbro rocks, pillow lava, and diabasic dykes (Klein, 2004; Jassim and Goff, 2006). Ophiolite complexes' classification normally depends on their geochemical features, interior structures, and regional tectonics (Pearce et al., 1984; Shervais, 2001; Pearce, 2008). A new classification of ophiolite complexes proposed by Dilek and Furnes (2011) implies subduction-related ophiolite complexes which involve volcanic arc and supra subduction zone, and subduction-unrelated ophiolite complexes which involve mid-oceanic ridge (MOR), plume (P-type), and continental margin (CM).

Zagros Suture Zone encompasses the Penjween-Walash Subzone that consists of volcano-sedimentary sequences created in the Cretaceous ocean spreading of the Neo-Tethys and is strongly affected by magmatism (Buday and Jassim, 1987). During Paleocene-Eocene, the final closure of Neo-Tethys, Paleocene arc volcanic and syn-tectonic essential intrusions created (Aswad, 1999), thus the area represents the residues of the Neo-Tethys which during Miocene-Pliocene thrust over the Arabian Plate, such as Pleistocene Al-Lajjoun Basaltic flows, central Jordan (El-Hasan and Al-Malabeh, 2008), and Precambrian Magmatic Rocks (Al-Malabeh et al., 2004) besides elsic dike swarms in Aqaba complex (Al-Fugha et al., 2013). The Penjween-Walash Subzone is divided into three thrust sheets, the upper Qandil, the middle Walash, and the lower Napurdan (Jassim and Goff, 2006; Aswad et al., 2011; Mohammad et al., 2014; Ali et al., 2016). This subzone forms an almost unbroken swath over the Iraqi-Iranian borders. Qandil thrust sheet includes basic igneous massifs consisting of Hasanbag, Pushtashan, Bulfat, Mawat, and Penjween (Ali et al., 2019), the study area is located within this thrust sheet. Penjween igneous complex is located to the south-west of Penjween town, about 50 kilometers to the east of Sulaimani city between latitudes (35° 36′ 16.4¨- 35° 37′ 15.6¨ N) and longitudes (45° 54′ 40.4¨- 45° 55′ 54¨ E), (Figure 1).

Gabbros are part of the crustal portion in an ophiolite complex and consist of (from bottom to top) layered gabbros, isotropic and then foliated gabbros formed by slow crystallized basaltic melt injection from the fundamental rising mantle (Kakar et al., 2013). According to Al-Hassan and Hubbard (1985); Al-Hassan (1987), the gabbroic rocks of

* Corresponding author e-mail: omarsaif@uomosul.edu.iq

the Penjween ophiolite formed as a result of partial melting of the upper mantle, leaving depleted dunite rocks. In Albian-Cenomanian, the gabbros of Penjween were intruded on during the ocean spreading process (Jassim and Goff, 2006). In this study, we discuss the petrogenesis and tectonic environment of the Penjween ophiolite meta gabbroic rocks based on their field observations, petrography, and chemical compositions.

2. General Geology

The Penjween Ophiolite Complex is situated to the south-west of Penjween town about 50 kilometers east of Sulaimani City northeast of Iraq (Figure 1a). The area is part of the Zagros Suture Zone (ZSZ) and the complex is located within Penjween-Walash Subzone (Jassim and Goff, 2006). The ZSZ is subdivided into two allochthonous thrust sheets; lower and upper allochthonous (Aswad, 1999). The Penjween-Walash Subzone (i.e. upper allochthonous) represents the ophiolitic complexes and Albian-Cenomenian Gemo-Qandil sequence (Aswad and Elias, 1988; Aziz, 2008; Aswad et al., 2011; Aziz et al., 2011). The Walash-Naopurdan sequence (Paleocene-Eocene) represents the lower allochthon which is separated from the upper allochthon by a thrust fault (Aswad, 1999).

The Penjween Ophiolite Complex is an elongated body that covers about 35 km^2 inside the Iraqi territories towards northwest-southeast parallel with the general tectonic trend of the ZSZ, while the large remnant parts of this complex are located within and adjacent to Iranian territories (Mahmood, 1978). The sequence of Penjween ophiolite is incomplete (Jassim and Goff, 2006). It consists of ultramafic rocks mainly peridotite with subordinate pyroxenites followed by gabbros and minor occurrences of diorites, granodiorites, and pegmatites (Mahmood, 1978), that is in contact with a volcano-sedimentary sequence (i.e. Gimo Group) (Jassim and Goff, 2006). The group is thrust over Merga Red Beds (Miocene molasse) in the west. The ultramafic body form about 70% of the complex and consists of relatively fresh dunite (Jassim and Al-Hassan, 1977). The gabbro body represents the second largest exposure in the area (18 km^2 in extent in Iraq) sharply overlies the ultrabasic body and is layered and laminated (Jassim and Al-Hassan, 1977).

3. Materials and Methods

Twenty-one samples from the meta gabbroic rocks were collected from two different locations within the Penjween Ophiolite Complex. The current study employed a variety of analytical techniques, starting with the use of a polarized microscope for petrographic study and ending with chemical analysis. Five samples among the least weathered were selected to represent the freshest rocks prepared for chemical analysis. Before that the samples were ground in a swing mill and then the Loss on Ignition (LOI) was determined in the laboratories of the University of Mosul, Department of Geology. The geochemistry of whole rocks (major, trace, and rare earth elements) was analyzed in the ACME Analytical Laboratories, Canada, Vancouver done by 6000 ELAN ICP-MS. To prepare the samples for analysis, 0.25 mg of rock powder is digested using a multi-acid digestion (H_2O_2-HF-$HClO_4$-HNO_3), then heated on a hot plate, cooled, and finally dissolved in 5% hydrochloric acid. The standards used in the analysis are OREAS 24P and OREAS 45P (For more information on analytical accuracy and precision, see Tables 1 and 2 .). Since this ICP-MS analysis measures iron as FeOt as it does not distinguish between ferric and ferrous oxides, it had to be measured and separated by ECIL CE 3021 Spectrophotometer at the Department of Geology, University of Mosul using the method of (Jeffery and Hutchison, 1981).

4. Results

4.1 Petrology and Petrography

Gabbro forms the second largest exposure in the area. It consists of a solid body extending to about 3 km of the upper and western edge of the mountain chain and southwest of Penjween village. These gabbros become a narrow sector in the northwest direction (Figure 1b). Gabbros are bordered by peridotite bodies as perpendicular and sharp contact and they are linked with the sandstones and conglomerates of the Merga Red Bed Group by a thrust fault near Kani Mangah village while they are in contact with Qandil metamorphic rock group in the southeastern direction. Depending on field observations and a previous study by Al-Hassan (1982) three types of gabbroic rocks are recognized in Penjween ophiolite; marginal gabbro, layered gabbro, and gabbro pegmatite (Figure 1b). Most gabbros in the field had suffered deformation in the form of fracturing and jointing (Figure 2b).

The metagabbros consist of saussuritized plagioclase, amphibole with relict pyroxene, chlorite, and opaque minerals. Some gabbros have been deformed, showing granular and porphyroclastic textures (Figure 2c, d). Also, these rocks show a schistosity texture (Figure 2e), those occurring along shear zones and western contact zone are severely crushed and foliated so much so that they impart schistosity to the rocks (Mahmood, 1978). The schistosity texture of Penjween metagabbros represents the thrusting movement and emplacement (Al-Hassan, 1982). Metagabbro also exhibits an ophitic and subophitic texture, with large crystals of amphibole completely or partially surrounding plagioclase (Figure 2f). The composition of plagioclase is An70-73 refers to the labradorite. Plagioclase shows wide variation in grain size due to granulation (Figure 2d). In sheared and schistose rocks, Williams et al. (1954) believed that many of the feldspars are granulated. The deformed plagioclase are characterized by fractured surface, wavy extinction, bent lamellae and well developed secondary twin (Figure 2e). The saussuritization process has partially changed the plagioclase grains into epidote (Figure 3a). A primary amphiboles have subhedral to anhedral grains, pleochroism that is primarily green to brown, and a cross-basal section that reveals two sets of cleavage (Figure 3b). Some amphibole grains have partially or completely altered to chlorite (Figure 3c). Primary amphibole shows kink bands due to deformation process along the shear zones (Figure 3d). The pyroxenes are mainly augite (extinction angle 42^o). The minerals and textures are typical of metagabbros, which can form during low grade metamorphism from gabbros (Koyi et al., 2010; Hassan and Ridha, 2018).

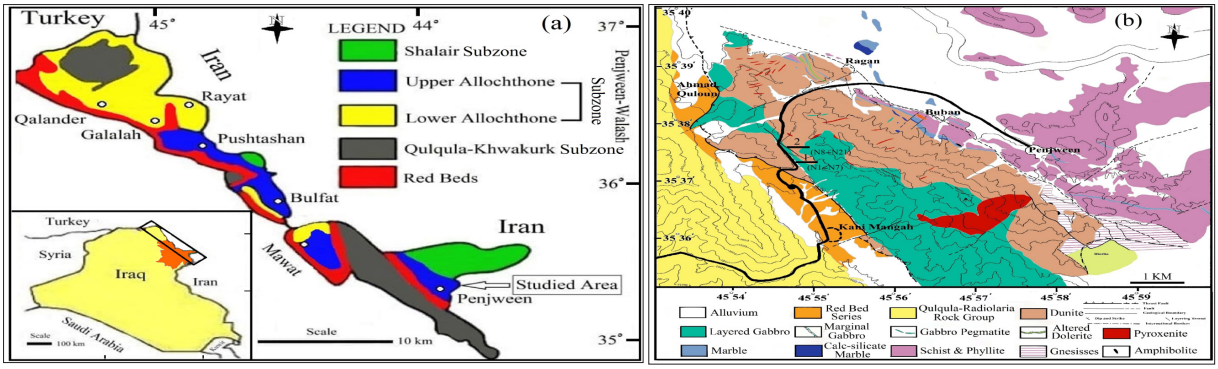

Figure 1. (a) Simplified geological map of the Zagros Suture Zone (ZSZ) showing the position of the study area; (b) Geological-topographic map of Penjween Ophiolite Complex, northeast Iraq, from (Al-Hassan, 1982) showing samples locations.

Table 1. Major and trace element composition for the Penjween ophiolite metagabbroic rocks, as well as accuracy, precision, and detection limits.

Elements	Sample No.						Analytical accuracy and precision				
	N31	N15	N14	N13	N12	R.N31	*45P	**45P	*24P	**24P	MDL
SiO_2	51.06	50.44	48.35	46.64	45.59	-	-	-	-	-	-
TiO_2	0.25	0.12	0.11	0.64	0.69	0.25	1.73	1.61	1.83	1.65	0.002
Al_2O_3	10.73	13.03	16.66	14.73	15.79	10.26	12.88	12.90	14.47	14.70	0.04
FeO	7.77	5.97	4.89	8.64	8.64	8.06	24.72	23.43	9.68	9.39	0.03
Fe_2O_3	0.32	0.75	1.20	4.13	5.24						
MnO	0.17	0.16	0.14	0.18	0.19	0.16	0.17	0.17	0.14	0.14	0.0003
MgO	13.53	13.31	11.99	9.42	8.03	13.23	0.32	0.32	6.85	6.73	0.03
CaO	12.24	12.86	13.81	12.61	12.63	12.13	0.42	0.42	8.16	8.09	0.03
Na_2O	1.38	0.52	0.52	0.49	0.69	1.35	0.11	0.11	3.15	3.36	0.003
K_2O	0.33	0.02	0.05	0.02	0.02	0.33	0.42	0.43	0.84	0.87	0.02
P_2O_5	0.02	0.002	0.002	0.002	0.002	0.02	0.11	0.10	0.31	0.32	0.002
LOI	2.20	2.80	2.30	2.50	2.50	-	-	-	-	-	-
Total	100.01	100.01	99.99	100.01	99.99	-	-	-	-	-	-
#Mg*	74.93	78.11	78.16	57.59	51.69	-	-	-	-	-	-
Ni	246.9	142.5	136.7	178.7	54.7	245	385	380.30	141.0	144.1	0.10
Cr	563	325	254	61.0	14.0	571	1089	1061	196	182	1.00
Sc	48.0	53.2	43.8	67.2	64.6	48.20	67.10	64.90	20.00	19.20	0.10
V	266	195	157	1229	1203	266.00	267.00	263.00	158.00	156.00	1.00
Ba	101	2.00	2.00	20.0	6.00	101.00	296.00	289.00	285.00	266.00	1.00
Rb	3.40	0.20	0.70	0.40	0.60	3.70	24.60	23.00	22.40	20.90	0.10
Sr	89.0	40.0	54.0	53.0	68.0	88.00	32.60	34.00	403.00	382.00	1.00
Cs	0.30	0.10>	0.10>	0.10>	0.10>	0.28	2.00	2.20	0.80	0.80	0.10
Zr	5.80	1.00	0.70	1.20	3.00	6.10	154.00	154.30	141.00	138.40	0.20
Y	7.40	2.50	2.50	3.70	3.10	7.30	13.00	12.90	21.30	20.50	0.10
Nb	0.44	0.06	0.07	0.06	0.09	0.43	21.60	20.27	21.00	19.47	0.04
Ga	8.65	8.03	9.68	13.61	14.67	8.53	22.50	22.05	19.43	19.39	0.02
Cu	14.41	57.42	85.03	854.5	349	14.13	749.00	703.30	52.00	48.69	0.02
Zn	53.0	38.3	43.7	75.4	71.5	51.70	141.00	140.50	119.00	116.40	0.20
Pb	1.03	0.69	2.52	1.17	0.92	0.95	22.00	23.14	2.90	2.80	0.02
Mo	0.46	0.09	0.18	0.12	0.13	0.45	2.10	2.04	1.50	1.47	0.05
Co	67.2	56.6	51.6	81.4	72.5	66.20	120.00	121.70	44.00	48.10	0.20
As	0.70	0.70	0.20>	0.60	0.90	0.50	12.00	12.80	1.20	2.00	0.20
Cd	0.07	0.08	0.07	0.09	0.15	0.05	0.20	0.21	0.15	0.16	0.02
Sb	0.18	0.05	0.07	0.03	0.05	0.20	0.82	0.81	0.09	0.09	0.02
W	95.6	34.8	41.0	39.7	53.9	95.30	1.10	1.00	0.50	0.40	0.10
Li	8.70	1.60	1.30	1.10	1.40	8.50	14.70	15.90	8.70	8.40	0.10
Hf	0.25	0.05	0.04	0.06	0.11	0.30	4.12	3.76	3.60	3.33	0.02
Th	0.10	0.09	0.09	0.09	0.09	0.10	9.80	10.00	2.85	2.80	0.10
Ta	0.30	0.10>	0.10>	0.10>	0.10	0.23	1.20	1.30	1.04	1.10	0.10

* Mg# =100 x Mg/(Mg+Fe^{+2}).
R. N31 : Repeated N31.
45P** : Calculated OREAS45P, 45P* : Published OREAS45P.
24P** : Calculated OREAS24P, 24P* : Published OREAS24P.
MDL: Method Detection Limit.

Table 2. REE elements composition (in ppm) of the Penjween ophiolite metagabbroic rocks, as well as accuracy, precision, and detection limits.

REEs	Sample No.					Analytical accuracy and precision					
	N31	N15	N14	N13	N12	R. N31	45P*	45P**	24P*	24P**	MDL
La	0.50	0.20	0.10	0.30	0.20	0.60	24.80	25.10	17.40	17.90	0.10
Ce	1.30	0.16	0.14	0.56	0.26	1.36	48.90	51.26	37.60	38.25	0.02
Pr	0.20	<0.10	<0.10	0.20	<0.10	0.14	6.00	5.80	4.70	4.80	0.10
Nd	1.10	0.20	0.20	0.60	0.30	1.20	23.2	23.20	22.00	21.00	0.10
Sm	0.40	0.10	0.10	0.20	0.10	0.40	4.24	4.00	4.70	4.60	0.10
Eu	0.20	<0.10	<0.10	0.10	0.10	0.20	1.10	1.10	1.60	1.50	0.10
Gd	0.80	0.30	0.30	0.50	0.30	0.90	3.80	3.40	5.30	5.30	0.10
Tb	0.20	<0.10	<0.10	0.10	<0.10	0.20	0.59	0.50	0.81	0.70	0.10
Dy	1.20	0.50	0.50	0.70	0.60	1.20	3.60	3.60	4.60	4.60	0.10
Ho	0.30	0.10	<0.10	0.10	0.10	0.26	0.65	0.60	0.80	0.80	0.10
Er	1.00	0.40	0.30	0.50	0.40	1.00	1.70	1.70	2.20	2.20	0.10
Tm	0.10	<0.10	<0.10	<0.10	<0.10	0.10	0.24	0.20	0.30	0.30	0.10
Yb	1.00	0.40	0.40	0.50	0.40	0.90	1.60	1.50	1.83	1.70	0.10
Lu	0.20	<0.10	<0.10	<0.10	<0.10	0.20	0.24	0.30	0.25	0.20	0.10
Ratios											
Samples	**N31**	**N15**	**N14**	**N13**	**N12**	**Samples**	**N31**	**N15**	**N14**	**N13**	**N12**
$(La/Yb)_N$	0.36	0.36	0.18	0.43	0.36	**Dy/Yb**	1.20	1.25	1.25	1.40	1.50
$(Gd/Yb)_N$	0.66	0.62	0.62	0.83	0.62	**Sr/Nd**	80.91	200	270	88.33	226.7
La/Nb	0.45	1.00	0.50	0.50	0.67	**Ba/Th**	1010	22.2	22.2	222.2	66.67
La/Ba	0.005	0.10	0.05	0.02	0.03	**Th/Yb**	0.10	0.23	0.23	0.18	0.23
La/Yb	0.50	0.50	0.25	0.60	0.50	**La/Sm**	1.25	2.00	1.00	1.50	2.00

R. N31 : Repeated N31.
45P** : Calculated OREAS45P, 45P* : Published OREAS45P.
24P** : Calculated OREAS24P, 24P* : Published OREAS24P.
MDL: Method Detection Limit

4.2 Major Oxides

The MgO-CaO-Al_2O_3 diagram (Colleman, 1977) has been used to differentiate between ultramafic and mafic cumulate rocks. Based on that the metagabbroic rocks of Penjween ophiolite are classified as mafic cumulate rocks (Figure 4a). The TAS diagram (Cox et al., 1979) shows that the Penjween ophiolite metagabbroic rocks are sub alkaline character (Figure 4b). On the AFM diagram, the Penjween ophiolite metagabbros exhibit the nature of tholeiitic igneous rocks (Figure 4c). The Penjween metagabbro rocks are classified largely as low-K rocks (Figure 4d). Generally, the Penjween metagabbros have a low content of TiO_2 (0.11 to 0.69 wt %), and P_2O_5 (0.002 to 0.02 wt %), K_2O (0.02 to 0.33 wt %) and Na_2O (0.49 to 1.38 wt %), with modest variations in SiO_2 (45.59 to 51.06 wt %), while the Al_2O_3, FeO, Fe_2O_3, MgO, and CaO have wide ranges and high concentrations, these ranges are 10.73 to 16.66 wt %, 4.89 to 8.64 wt %, 0.32 to 5.24 wt %, 8.03 to 13.53 wt %, and 12.24 to 13.81 wt % respectively (Table 1). Moreover, the metagabbros have very low total alkali concentrations, where Na_2O+K_2O values are between 0.51 to 1.7 wt% with the K_2O value much lower than Na_2O.

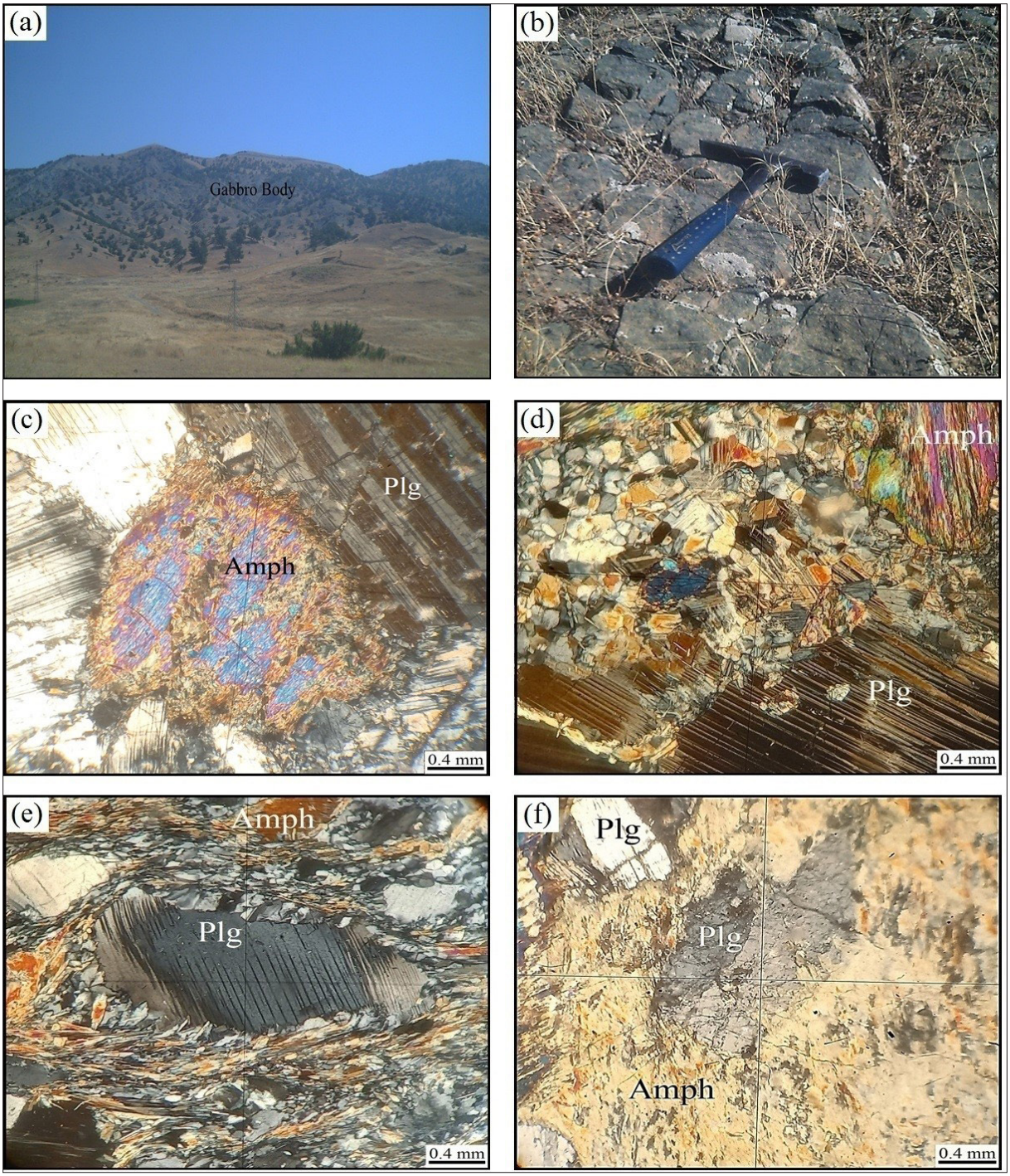

Figure 2. Field photos and photomicrographs showing: (a) Panoramic view of the studied gabbro; (b) Metagabbro fracturing and jointing, sample N11; (c) Granular textures in metagabbro , sample N10; (d) Porphyroclastic texture in metagabbro and the plagioclase show wide variation in grain size due to granulation, sample N14; (e) Metaga bbro show schistosity texture and secondary twin lamellae in plagioclase, sample N12; (f) Ophitic and subophitic texture, sample N10; [Plg: Plagioclase; Amph: Amphibole; Opq: Opaque].

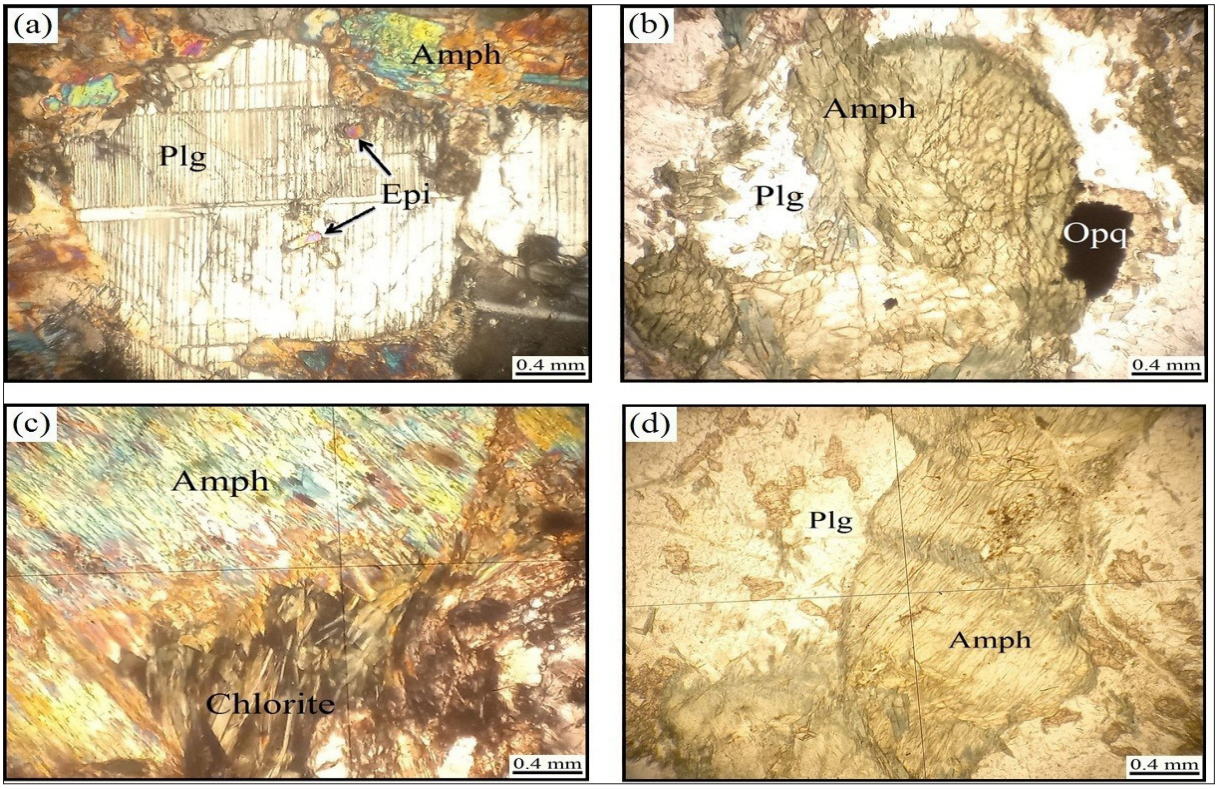

Figure 3. Photomicrographs showing: (a) Saussuritization process has partially changed the plagioclase grains into epidote, sample N5; (b) Amphibole has two sets of cleavage (56/124°), sample N6; (c) Alteration of amphibole into chlorite, sample N4; (d) Amphibole with kink bands, sample N4, [Plg: Plagioclase; Amph: Amphibole; Epi: Epidote; Opq: Opaque].

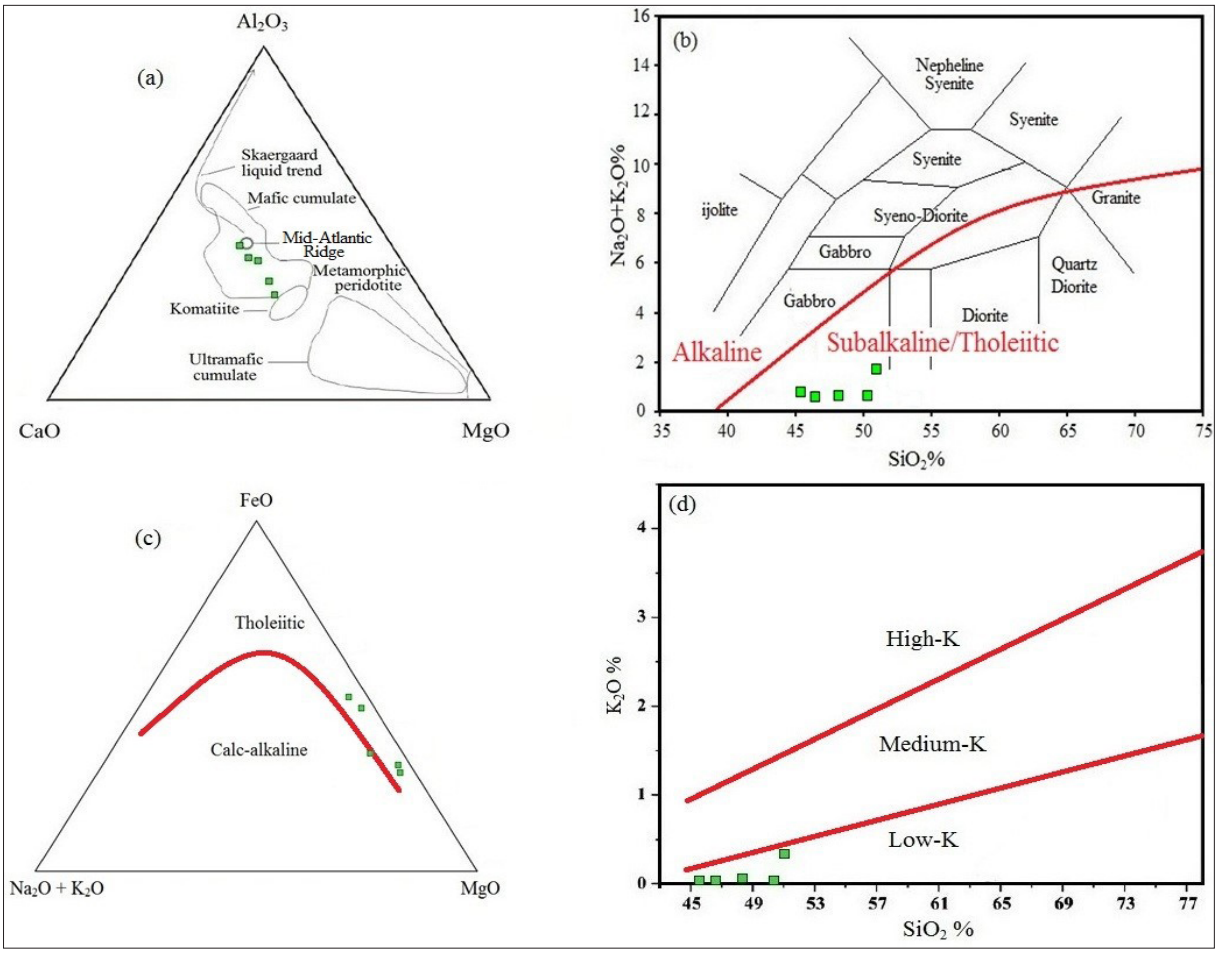

Figure 4. Geochemical classifications of the Penjween metagabbroic rocks: (a) CaO-Al_2O_3-MgO diagram for the Penjween ophiolite metagabbroic rocks (Colleman, 1977); (b) TAS plot of the gabbros (Cox et al., 1979); (c) AFM diagram (Irvin and Baragar, 1971) of metagabbros from Penjween Ophiolite Complex indicating their tholeiitic affinity; (d) SiO_2 vs. K_2O diagram (Le Maitre, 2002).

4.3 Trace and Rare Earth Elements (REEs)

Both Large Ion Lithophile Elements (LILE) and the High Field Strength Elements (HFSE) have variable amounts in the Penjween metagabbros, like Ba (2-101 ppm), Sr (40-89 ppm), Rb (0.2-3.4 ppm), Pb (0.69-2.52 ppm), Zr (0.7-5.8 ppm), Nb (0.06-0.4 ppm), and Y (2.5-7.4 ppm) (Table 1). LIL elements (Ba, Rb, Sr, and K) are thus probable to have been remobilized during alteration and metamorphism to greenschist facies (Staudigel, 2003).

The REEs in the Penjween metagabbro rocks are generally characterized by relatively parallel REE patterns with enrichment of HREE and depletion in light rare earth elements (LREE) [(La/Yb)N= 0.36-0.43]. These ratios indicate the enrichment of these rocks in HREE and MREE compared to LREE (Figure 5a). The spider diagram (multi elements) exhibits depletion in HFSEs like Zr, Nb, Y, and Hf with enrichment in LILEs like Sr, Ba, Rb, and Pb (Figure 5b). The depletion in Nb and LREE refers to a source originating from the lower crust (Taylor and McLennan, 1985), it is characteristic of magmas formed in the supra-subduction mantle wedge (Duclaux et al., 2006). Pearce et al. (1984) assumed that the eclectic enrichment of Ba and Sr in comparison to Zr, and Y shown by tholeiitic rocks is typical of a supra-subduction zone (SSZ) setting where tholeiitic and boninitic magma mixing happens.

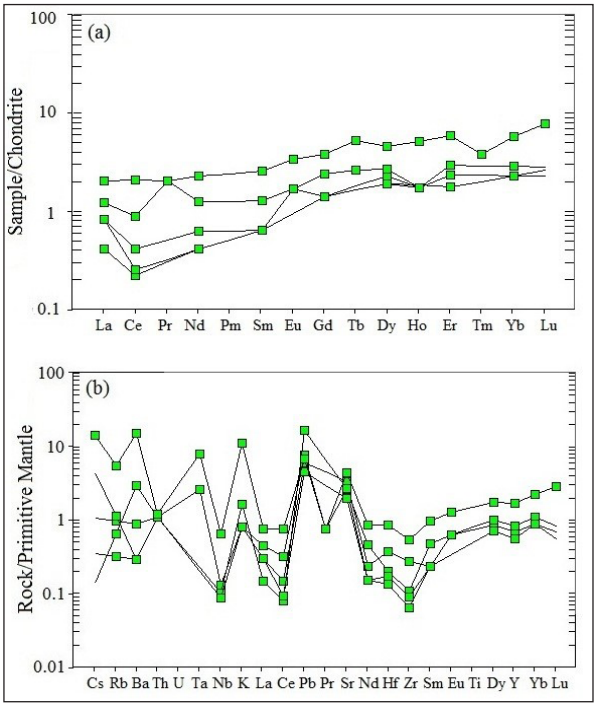

Figure 5. (a) Chondrite-normalized REE patterns of metagabbroic rocks from Penjween ophiolite (Sun and McDonough, 1989); (b) Primitive mantle-normalized spider diagram of metagabbroic rocks of Penjween ophiolite (Sun and McDonough, 1989).

5. Discussion

5.1 Petrogenesis

Magmatic rocks derived from primary magma typically have a high Mg number (Mg# >65) (Winter, 2001; Al Smadi et al., 2018). The samples from the Penjween metagabbro have a high Mg# (68.1), indicating that the metagabbros are the result of primary magma crystallization. REEs and HFSEs are immobile during the weathering and alteration processes (Zhang et al., 2015). As a result, magma origins are determined largely using the ratios and contents of HFSEs and LREEs (Zhao and Zhou, 2007). Most metagabbros fall in the astheno sphere mantle origin in the La/Nb-La/Ba diagram (Figure 6a). The La/Yb ratios have a range of 0.25-0.6, and the Dy/Yb ratios of the metagabbroic rocks are concentrated in a limited range of 1.2-1.5, reflecting shallow source partial melting of spinel-peridotite (Figure 6b) (Thirlwall et al., 1994). Penjween metagabbro mantle metasomatism was also revealed by the La/Sm against Ba/Th diagram (Labanieh et al., 2012) and the Th/Yb against Sr/Nd diagram (Woodhead et al., 1998). As seen in figures (6c, d) the Penjween metagabbros deviate from the sediment melting trend while being consistent with slab dehydration, suggesting that fluids from slab dehydration modified the mantle. The depletion in HFSEs like Zr, Nb, Hf, and Pb refers to the separating of LILE such as Sr, Ba, Rb, and HFSEs during subducting slab dehydration (Shawna et al., 2003). Moreover, the depletion of HFS elements may result from fractionation and metamorphism processes (John et al., 2004). In summary, the Penjween metagabbro formed as a result of partial melting of the mantle spinel peridotite that has been metasomatized by fluids dehydrated from a subducted slab (Wang et al., 2019).

The relation between Y and Cr (Figure 7a) proves that the amount of Cr varies with a nearly constant in Y; which is a characteristic of a mantle source depleted (Shinjo et al., 2000). The relationship between Ni and Cr is significant in determining ferromagnesian mineral fractionation (Leeman, 1976). Figure (7b) shows that clinopyroxene is the main ferromagnesian phase existing in Penjween metagabbros, based on the positive trend between Ni-Cr and the absence of olivine in all samples. This indicates that it was derived from a previous fractionated origin or a melt that was extensively fractionated mostly by removing olivine (Wilson, 2001). On Ti against Ti/Cr and Ti against Al_2O_3/TiO_2 (Figure 7c, d), the crystallization trends of the main phases parallel the trends of plagioclase and clinopyroxene. As a result, these minerals are the major crystalline phases, as Al-Hassan (1982) demonstrated in the Penjween gabbroic rocks.

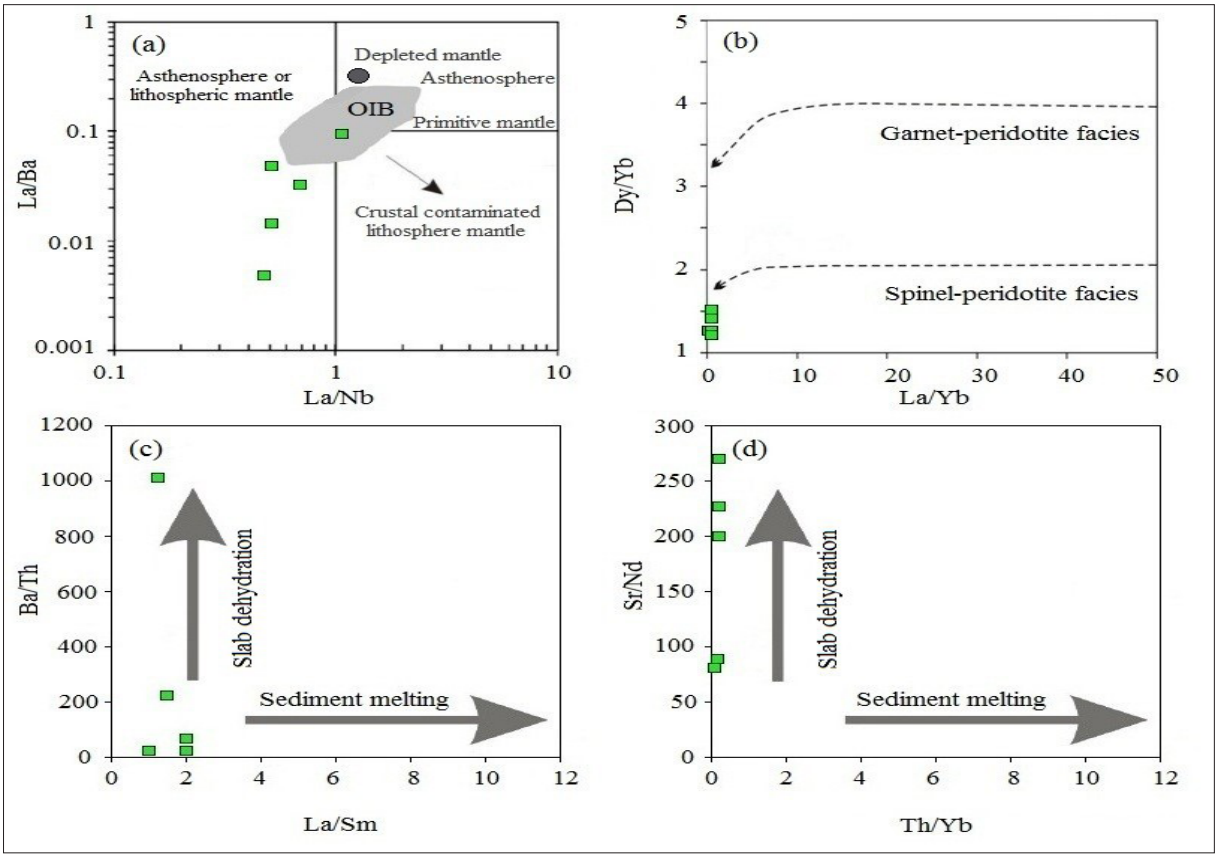

Figure 6. (a) La/Ba vs. La/Nb diagram (Saunders et al., 1992); (b) La/Yb vs.Dy/Yb diagram (Jung et al., 2006); (c) La/Sm vs. Ba/Th for the Penjween metagabbros (Labanieh et al., 2012); (d) Th/Yb vs. Sr/Nb for the Penjween metagabbros (Woodhead et al., 1998).

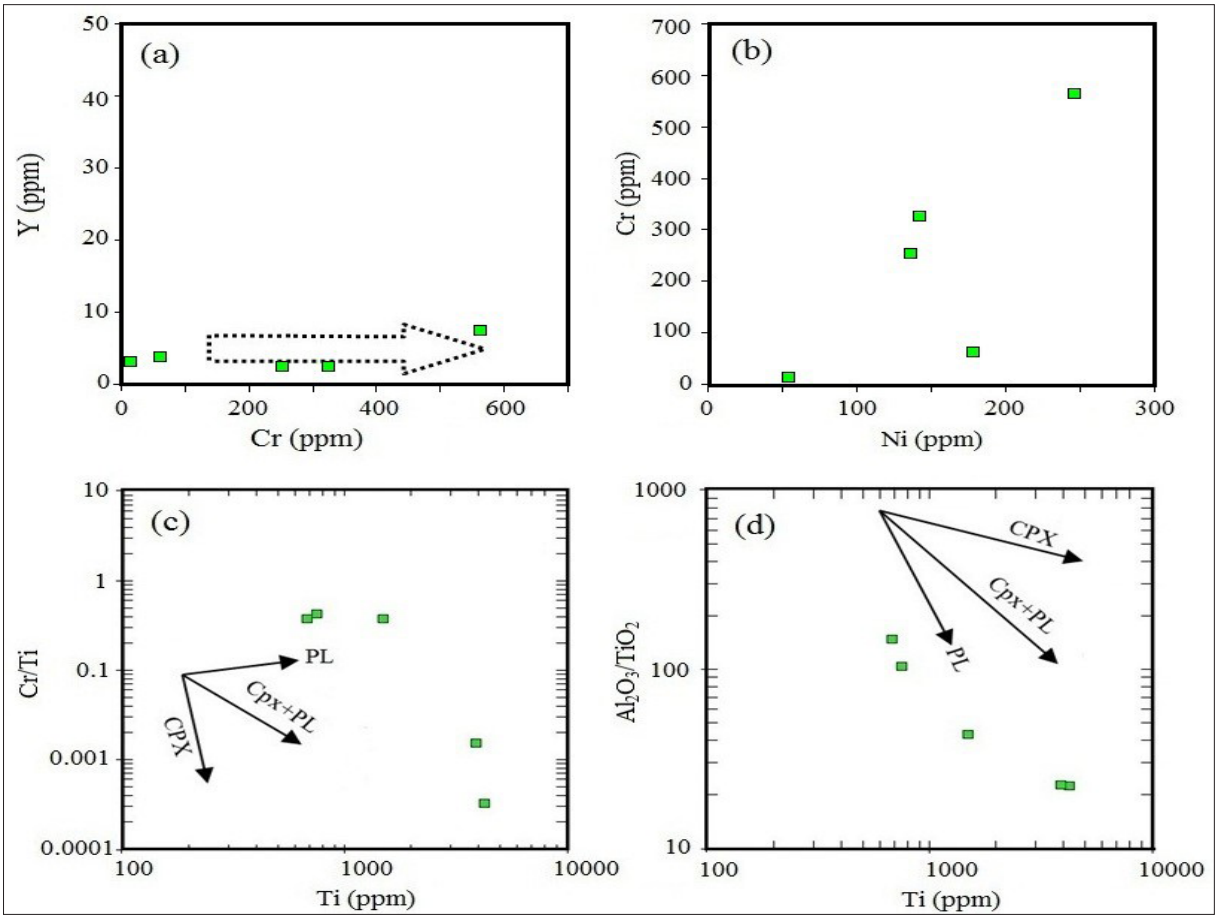

Figure 7. (a) Cr vs. Y diagram shows a depleted mantle source (Shinjo et al., 2000); (b) Ni vs. Cr; (c) Ti vs. Cr/Ti diagram (Pearce and Flower, 1977); (d) Ti vs. Al2O3/TiO2 diagram (Pearce and Flower, 1977).

5.2 Tectonic Setting

In general, all studied metagabbros of the Penjween ophiolite are geochemically related and have a tholeiitic character. Zr-Nb-Th diagram classifies these metagabbros as Island Arc Tholeiite (IAT) (Figure 8a). Therefore, maybe these metagabbroic rocks have been created in the extensional environment (low pressure) by fractional crystallization directly in the supra-subduction zone or above a subduction zone (Kakar et al., 2013). The AFM diagram shows the Penjween metagabbro rocks occur into the arc-related mafic cumulate rock (Figure 8b), this is confirmed that these rocks are created from fractionation of the primary magma via depleted mantle in the magma chamber (Sarifakioglu et al., 2009). All these indicate that Penjween ophiolite metagabbroic rocks are created in a supra-subduction zone environment (Beard, 1986).

The IAT nature of the metagabbroic rocks from the Penjween ophiolite is further evidenced by their REE and spider diagrams (Figure 5a, b). Generally, the chondrite-normalized REE patterns in Penjween metagabbroic rocks exhibit LREE depletion and flat MREE and HREE patterns, with patterns that are nearly flat in general, and these patterns are similar to rocks generated in IAT and subduction-related environments (Shamim et al., 2005). The features exhibited on the spider diagram show enrichments of Sr and Ba and the relative depletion of Y, Zr, and Hf these patterns as well as HFSEs variances in the tholeiitic rocks represent the SSZ setting (Pearce et al., 1984). The depletion in HFSEs with enrichment in LILEs and the strong negative Nb anomaly (Figure 5b) are typical of a magma formed in the supra-subduction zone (Whattam et al., 2004).

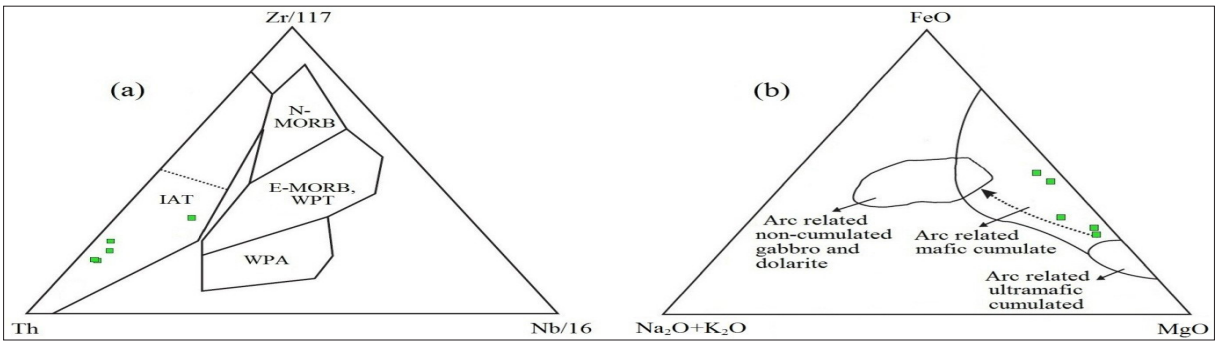

Figure 8. Tectonomagmatic diagrams of the Penjween ophiolite metagabbroic rocks: (a) Zr-Nb-Th diagram (Wood, 1980); (b) AFM compositions of metagabbros in Penjween ophiolite. The non-cumulate and cumulate rocks are from Beard (1986).

The al_2O_3-TiO_2 diagram shows these metagabbros are located in the arc-related magma setting (Figure 9a), whereas all metagabbroic rocks show that the magma is related to subduction on the Zr-Th-Nb diagram (Figure 7a). Figures (9b, c) show that metagabbroic rocks are generally low-Ti and very low-Ti Island Arc Tholeiitic (IAT), indicating that they are generated in a subduction zone. Penjween ophiolite metagabbros contain very low to low-TiO_2 (0.11-0.69%) concentrations and were probably derived from IAT magmas, which are formed in supra-subduction zone environments (Beccaluva et al., 1989). In conclusion, the low and very low Ti concentration strongly suggests that the metagabbroic rocks of the Penjween Ophiolite Complex are linked to Island Arc Tholeiite, which has a link to the supra subduction zone, as Mirza (2008) demonstrated in the Mawat gabbros.

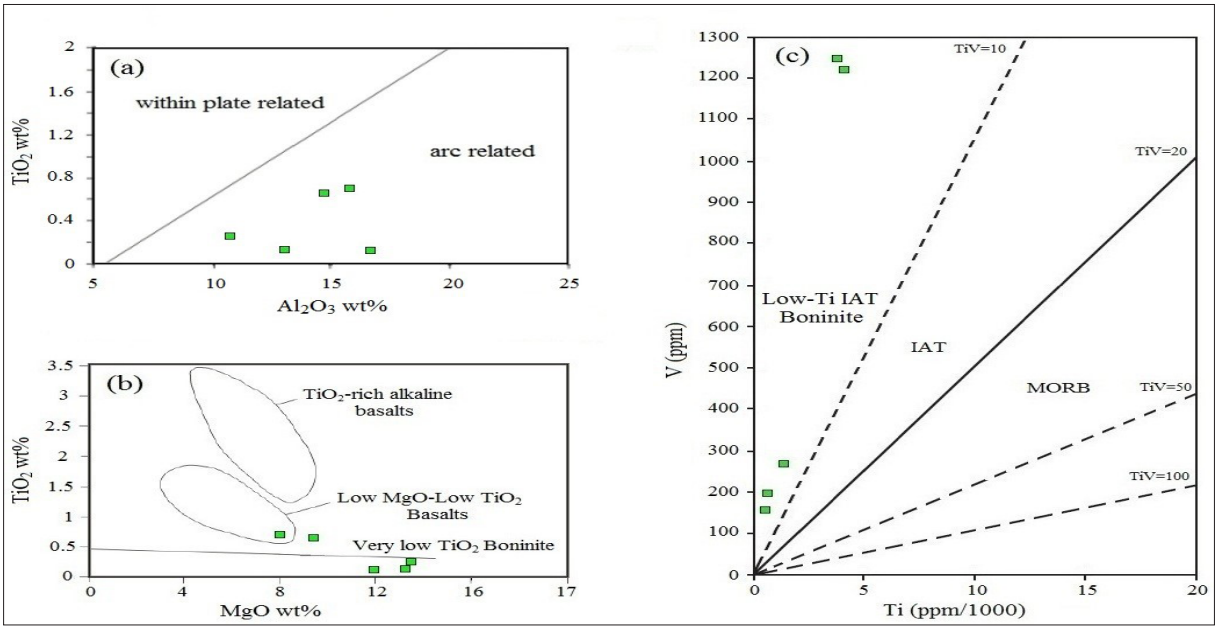

Figure 9. Tectonomagmatic diagrams of the Penjween ophiolite metagabbroic rocks: (a) Al_2O_3 vs. TiO_2 diagram (Muller and Groves, 1997); (b) MgO vs. TiO_2 diagram (Laurent and Hebert, 1989); (c) Ti vs. V petrogenetic discrimination diagram (Shervais, 1982)

6. Conclusion

Penjween ophiolite complex consists of ultramafic rocks followed by gabbros and minor occurrences of diorites, granodiorites, and pegmatites. The metagabbros are composed of saussuritized plagioclase, amphibole with relict pyroxene, chlorite, and opaque minerals. Some metagabbros have been deformed, showing granular and porphyroclastic textures, also these rocks show a schistosity texture. The mineral and textures are typical of metagabbros, which can form from gabbros under low-grade conditions. The geochemical indicators exhibit a substantial variance in major elements content, modest variations in SiO_2, low contents of TiO_2, and P_2O_5, with high contents and wide ranges of MgO, FeO, Fe_2O_3, Al_2O_3, and CaO. Penjween metagabbro rocks have tholeiitic igneous characteristics and are mostly low-K rocks with very low total alkali concentrations. Penjween metagabbro has a high Mg#, indicating that it formed from primary magma crystallization. Geochemical characteristics of the Penjween ophiolite metagabbros demonstrate that these rocks were generated by partial melting of the mantle spinel peridotite that has been metasomatized by fluids dehydrated from a subducted slab. The IAT nature and supra-subduction zone environments of the Penjween ophiolite metagabbroic rocks are confirmed by their REE and HFSEs patterns. The tectonic environment diagrams confirm that the metagabbroic rocks have island arc-related, and also that the TiO_2 concentrations in the Penjween ophiolite metagabbros are very low to low. As concluded, the low and very low Ti content suggests that the Penjween Ophiolite Complex metagabbroic rocks are linked to Island Arc Tholeiite, which is linked to the supra subduction zone.

Acknowledgments

The authors are very grateful to the College of Sciences, University of Mosul for providing facilities, which help to improve the quality of this work. So, we would like to thank Dr. Azzam H. Al-Samman for his helpful and constructive review, which improved the manuscript. The authors are very grateful to the Editor in Chief, the Secretary of the Journal. and the Technical Editors for their great efforts and valuable comments.

References

Al Smadi, A., Al-Malabeh, A., Odat, S. (2018). Characterization and Origin of Selected Basaltic Outcrops in Harrat Irbid (HI), Northern Jordan. Jordan Journal of Earth and Environmental Sciences 9(3): 185-196.

Al-Fugha, H., El-Hasan, T., Al-Malabeh, A., Hamaideh, A., El-Mezayen, A. (2013). Mineralogy, Geochemistry, and Origin of Felsic Dike Swarms in Aqaba Complex (Wadi Al-Yutum), South Jordan. Arabian Journal of Geosciences 6(10): 3979-3987.

Al-Hassan, M.E. (1982). Petrology, Mineralogy, and Geochemistry of Penjwin Igneous Complex, Northeast Iraq, Ph.D. Thesis, University of Dundee.

Al-Hassan, M.E. (1987). Rare-Earth Element Pattern of Layered Gabbro, Penjwin Complex, NE Iraq, In Geochemistry of Ophiolites, edited by Delaloye, M. and Bechon, F., Ofioliti, pp. 437-444.

Al-Hassan, M.E., and Hubbard, F.H. (1985). Magma Segregations in a Tectonic Remnant of Basalt Ophiolite, Penjween, NE Iraq. In: Ophiolites through Time; Proceedings, edited by Desmons, J., Ofioliti. pp. 139-146.

Ali, S.A., Ismail, S.A., Nutman, A.P., Bennett, V.C., Jones, B.G., Buckman, S. (2016). The Intra-Oceanic Cretaceous (˜108 Ma) Kata-Rash Arc Fragment in the Kurdistan Segment of Iraqi Zagros Suture Zone: Implications for Neotethys Evolution and Closure. Lithos 260: 154-163.

Ali, S.A., Nutman, A.P., Aswad, K.J., Jones, B.G. (2019). Overview of the Tectonic Evolution of the Iraqi Zagros Thrust Zone: Sixty Million Years of Neotethyan Ocean Subduction. Journal of Geodynamics 129: 162–177.

Al-Malabeh, A., Al-Fugha, H., El-Hasan, T. (2004). Petrology and Geochemistry of Late Precambrian Magmatic Rocks from Southern Jordan. Neues Jahrbuch fur Geologie und Palaeontologie 233(3): 333-350.

Aswad, K.J. (1999). Arc-Continental Collision in Northeastern Iraq as Evidence by the Mawat and Penjwen Ophiolite Complex. Rafidain Journal of Science 10: 51-61.

Aswad, K.J. and Elias, E.M. (1988). Petrogenesis, Geochemistry, and Metamorphism of Spilitized Subvolcanic Rocks of the Mawat Ophiolite Complex, NE Iraq. Ofioliti 13: 95-109.

Aswad, K.J., Aziz, N.R., Koyi, H.A. (2011). Cr-spinel Compositions in Serpentinites and their Implications for the Petrotectonic History of the Zagros Suture Zone, Kurdistan Region, Iraq. Geological Magazine 148(5–6): 802-818.

Aziz, N.R., 2008. Petrogenesis, Evolution, and Tectonics of the Serpentinites of the Zagros Suture Zone, Kurdistan Region, NE Iraq, Ph.D. Thesis, University of Sulaimani.

Aziz, N.R., Aswad, K.J., Koyi, H.A. (2011). Contrasting Settings of Serpentinite Bodies in the Northwestern Zagros Suture Zone, Kurdistan Region, Iraq. Geological Magazine 148: (5-6), 819-837.

Beard, J.S. (1986). Characteristic Mineralogy of Arc Related Cumulate Gabbros: Implications for the Tectonic Setting of Gabbroic Plutons and Andesite Genesis. Geology 14: 848-851.

Beccaluva, L., Maccciotta, G., Piccardo, G.B., Zeda, O. (1989). Clinopyroxene Composition of Ophiolite Basalts as Petrogenetic Indicator. Chemical Geology 77: 165-182.

Beccaluva, L., Maccciotta, G., Piccardo, G.B., Zeda, O., 1984. Petrology of Lherzolitic Rocks from the Northern Apennine Ophiolites. Lithos, 17, 299-316.

Bonatti, E., Hamlyn, P.R., Ottonello, G. (1981). The Upper Mantle Beneath a Young Oceanic Rift: Peridotites from the Island of Zabargad (Red Sea). Geology 9: 474-491.

Buday, T. and Jassim, S.Z. (1987). The Regional Geology of Iraq: Tectonism, Magmatism, and Metamorphism edited by Kassab, I.M. and Abass, M.J., Geological Survey, and Mineral Investigation, Baghdad.

Colleman, R.G. (1977). Ophiolites: Ancient Oceanic Lithosphere. Springer-Verlag, New York.

Cox , K.G., Bell, J.D., Pankhurst ,R.J. (1979). The Interpretation of Igneous Rocks. George Allen & Unwin, London.

Dilek, Y. and Furnes, H. (2011). Ophiolite Genesis and Global Tectonics: Geochemical and Tectonic Fingerprinting of Ancient Oceanic Lithosphere. Geological Society of America Bulletin 123: 387-411.

Duclaux, G., Menot, R.P., Guillot, S., Agbossoumonde, Y., Hilairet, N. (2006). The Mafic Layered Complex of the Kabye' Massif (North Togo and North Benin): Evidence of a Pan-African Granulitic Continental Arc Root. Journal of Precambrian Research 151: 101-118.

El-Hasan, T. and Al-Malabeh, A. (2008). Geochemistry, Mineralogy and Petrogenesis of El-Lajjoun Pleistocene Alkali Basalt of Central Jordan. Jordan Journal of Earth and Environmental Sciences 1(2): 53-62.

Hassan, D.K. and Ridha, A.H. (2018). Petrography and Mineralogy of Amphibolite Rocks in Penjween Complex, Northeastern Iraq. International Journal of Advanced Engineering

Research and Science. 5(2): 146-157.

Irvine T.N. and Baragar W.R. (1971). A Guide to Chemical Classification of the Common Volcanic Rocks. Canadian Journal of Earth Sciences, 8, 523-548.

Jassim, S.Z. and Al-Hassan, M.I. (1977). Petrography and Origin of the Mawat and Penjwin Igneous Complexes: A Comparison. Journal of Geological Society of Iraq Special Issue: 169-210.

Jassim, S.Z. and Goff, J.C. (2006). Geology of Iraq. Dolin, Prague and Moravian Museum, Brno.

Jeffery, P.G. and Hutchison, D. (1981). Chemical Methods of Rock Analysis. Pergamon Series in Analytical Chemistry. Pergoman Press, Oxford.

John, T., Schherer, E.E., Haase, K., Schenk, V. (2004). Trace Elements Fractionation During Fluid. Incluced Eclogitization in a Suducting Slab: Trace Element and Lu-Hf-Sm-Nd Isotope Systematics. Journal of Earth and Planetary Science Letters 227: 441-456.

Jung, C., Jung, S., Hoffer, E., Berndt, J. (2006). Petrogenesis of Tertiary Mafic Alkaline Magmas in the Hocheifel, Germany. Journal of Petrology 47: 1637-1671.

Kakar, M.I., Mahmood, K., Khan, M., Kasi, A.K., Abdul Manan, R. (2013). Petrology and Geochemistry of Gabbros from the Muslim Bagh Ophiolite: Implications for their Petrogenesis and Tectonic Setting. Journal of Himalayan Earth Sciences, 46(1): 19-30.

Klein, E.M. (2004). Geochemistry of the Igneous Oceanic Crust, In Treatise on Geochemistry, edited by Holland, H.D. and Turekian, K.K., Elsevier Pergamon, Oxford, pp. 433-464.

Koyi, A.M.A., Sofyissa, M.M., Jameel, N.M. (2010). Geochemistry of Metagabbros from Southern Mawat Ophiolite Complex, NE Iraq. Journal of Pure and Applied Sciences. 22(4): 30-46.

Labanieh, S., Chauvel, C., Germa, A., Quidelleur, X. (2012). Martinique: A Clear Case for Sediment Melting and Slabdehydration as a Function of Distance to the Trench. Journal of Petrology 53: 2441-2464.

Laurent, R. and Heberi, R. (1989). The Volcanic and Intrusive Rocks of the Quebec Appalachian Ophiolites (Canada) and their Island Arc Setting. Chemical Geology 77: 287-302.

Le Maitre, R.W. (2002). Igneous Rocks: A Classification and Glossary of Terms. Cambridge University Press, Cambridge, and New York.

Leeman, W.P. (1976). Petrogenesis of Mckinney (Snake River) Olivine Tholeiite in the Light of Rare-Earth Elements and Cr/Ni Distributions. Geological Society of America Bulletin 87: 1582-1586.

Mahmood, L.A. (1978). Petrology of the Ultramafics Around Penjwin, Northeast of Iraq with Special References to the Genesis of the Chromites Associated with them, M.Sc. Thesis, University of Mosul.

Menzies, M.A. and Dupuy, C. (1991). Orogenic Massifs: Protolith, Process, and Provenance. Orogenic Lherzolite and Mantle Processes. Journal Petrology Special: 1-16.

Mirza, T.A. (2008). Petrogenesis of the Mawat Ophiolite Complex and Associated Chromitite, Kurdistan region, NE Iraq, Ph. D. Thesis, University of Sulaimani.

Mohammad, Y.O., Cornell, D.H., Qaradaghi, J.H., Mohammad, F.O. (2014). Geochemistry and Ar-Ar Muscovite Ages of the Daraban Leucogranite, Mawat Ophiolite, Northeastern Iraq: Implications for Arabia–Eurasia Continental Collision. Journal Asian Earth Science 86:151-165.

Muller, D. and Groves, D. (1997). Potassic Igneous Rocks and Associated Gold-Copper Mineralization. Springer-Verlag, Berlin, Heidelberg.

Nicolas, A. and Boudier, F. (2003). Where Ophiolite Come From and What Do They Tell us? Geological Society of America, Boulder, USA, Special Paper 373: 137-152.

Pearce, J.A. (2008). Geochemical Fingerprinting of Oceanic Basalts with Applications to Ophiolite Classification and the Search for Archean Oceanic Crust. Lithos 100: 14-48.

Pearce, J.A. and Flower, M.F.J. (1977). The Relative Importance of Petrogenetic Variables in Magma Genesis at Accreting Plate Margins: a Preliminary Investigation. Journal of the Geological Society, London 134: 103-127.

Pearce, J.A., Lippard, S.J., Roberts, S. (1984). Characteristics and Tectonic Significance of Supra-Subduction Zone Ophiolites, In Marginal Basin Geology, edited by Kokelaar, B.P. and Howells, M.F., Geological Society, London. pp. 77-89.

Sarifakioglu, E., Ozen, H., Winchester, J.A. (2009). Petrogenesis of the Refahiye Ophiolite and its Tectonic Significance for Neotethyan Ophiolites Along the İzmir-Ankara-Erzincan Suture Zone. Turkish Journal of Earth Sciences 18: 187-207.

Saunders, A.D., Storey, M.; Kent, R.W., Norry, M.J. (1992). Consequences of Plume-Lithosphere Interactions, In Magmatism and the Causes of Continental Break-up, edited by Alabaster, T., Storey, B.C., Pankhurst, R.J., Geological Society, London, UK. pp. 41-60.

Shamim, K.M., Smith, T.E., Raza, M., Huang, J. (2005). Geology, Geochemistry and Tectonic Significance of Mafic-Ultramafic Rocks of Mesoproterozoic Phulad Ophiolite Suite of South Delhi Fold Belt, NW Indian Shield. Journal of Gondwana Research, 8(4): 553-566.

Shawna, M., Leatherdale, Maxeiner, R.O., Ansdell, K.M. (2003). Petrography and Geochemistry of Love Lake Lecogabbro, Swan River Complex, Peter Lake Domain, Northern Jour. Saskatchewan, Saskatchewan Geological Survey 2: 1-17.

Shervais, J.W. (1982). Ti-V Plots and the Petrogenesis of Modern and Ophiolitic Lavas. Earth and Planetary Science Letters 59: 101-18.

Shervais, J.W. (2001). Birth, Death, and Resurrection: the Life Cycle of Suprasubduction Zone Ophiolites. Geochemistry, Geophysics, Geosystems 2: 1010.

Shinjo, R., Woodhead, J.D., Hergt, J.M. (2000). Geochemical Variation within the Northern Ryukyu Arc: Magma Source Compositions and Geodynamic Implications. Contributions to Mineralogy and Petrology 140: 263–282.

Snow, J.E. and Dick, H.J.B. (1995). Pervasive Magnesium Loss by Marine Weathering of Peridotites. Geochim. Geochimica et Cosmochimica Acta 59: 4219-4235.

Staudigel, H. (2003). Hydrothermal Alteration Processes in the Oceanic Crust, In Treatise on Geochemistry, edited by Holland, H.D., Turekian, K.K., Elsevier Pergamon. Oxford. pp. 511-535.

Sun, S. and McDonough, W. (1989). Chemical and Isotopic Systematics of Oceanic Basalts: Implications for Mantle Composition and Processes, In Magmatism in the Ocean Basins, edited by Saunders, A.D., Norry, M.J., Geological Society London. pp. 313-345.

Taylor, S.R. and McLennan, S.M. (1985). The Continental Crust: Its Composition and Evolution. Blackwell, Oxford.

Thirlwall, M.F., Upton, B.G.J., Jenkins, C. (1994). Interaction between Continental Lithosphere and the Iceland Plume: Sr–Nd–Pb Isotope Chemistry of Tertiary Basalts, NE Greenland. Journal of Petrology 35: 839-897.

Wang, J.P., Wang, X., Liu, J.J., Liu, Z.J., Zhai, D.G., Wang, Y.H. (2019). Geology, Geochemistry, and Geochronology of Gabbro from the Haoyaoerhudong Gold Deposit, Northern Margin of the North China Craton. Minerals 9(63): 1-18.

Whattam, S., Malpas, J., Ali, J., Smith, I.E.M., Hualo, C. (2004). Origin of the Northland Ophiolite, Northern New Zealand: Discussion of New Data and Reassessment of the Model. Journal of Geology and Geophysics 47: 383-389.

Williams, H., Turner, F.J., Gillbert, C.M. (1954). Petrography:

An Introduction to the Study of Rocks in Thin Sections. Freeman and Company, San Francisco.

Wilson, S.A. (2001). The Geochemical Analysis of Siluro-Devonian Mafic Dikes in the 15' Woodsville Quadrangle, East-Central Vermont, Senior Thesis, Middlebury College, Middlebury, Vermont.

Winter, J. (2001). Introduction to Igneous and Metamorphic Petrology; Prentice Hall: Upper Saddle River, New Jersey, USA.

Wood, D.A. (1980). The Application of a Th-Hf-Ta Diagram to Problems of Tectono-Magmatic Classification and to Establishing the Nature of Crustal Contamination of Basaltic Lavas of the British Tertiary Volcanic Province. Earth and Planetary Science Letters, 50(1): 11-30.

Woodhead, J.D., Eggins, S.M., Johnson, R.W. (1998). Magma Genesis in the New Britain Island Arc: Further Insights into Melting and Mass Transfer Processes. Journal of Petrology 39: 1641-1668.

Zhang, B.L., Lv, G.X., Su, J., Shen, X.L., Liu, R.L., Liu, J.G., Hai, L.F., Zhang, G.L. (2015). A Study of the Tectono-Lithofacies Mineralization Regularities of the Gejiu tin Polymetallic Orefield, Yunnan, and Prospecting in its Western Part. Earth Science Frontiers 22: 078-087.

Zhao, J.H. and Zhou, M.F. (2007). Geochemistry of Neoproterozoic Mafic Intrusions in the Panzhihua District (Sichuan Province, SWChina): Implications for Subduction-Related Metasomatism in the Upper Mantle. Precambrian Research 152: 27-47.

JJEES

JJEES (2023) 14 (2): 158-174
ISSN 1995-6681

Jordan Journal of Earth and Environmental Sciences

Integrated Evaluation of Soil Erosion-prone Areas Based on the GIS Technique and the Analytic Hierarchy Process on Hillside Slopes, Northwest of Jordan

Noah Mohammad Ali Al-Sababhah[1,2], Mohammad Mahmoud Al maqablah[1]

[1] Department of Geography, Yarmouk University, 21163 Irbid, Jordan
[2] Corresponding author: Noah Al-Sababhah, Associate Professor, Department of Geography, Yarmouk University, Irbid, Jordan.

Received 7th February 2022; Accepted 17th October 2022

Abstract

This study aimed to create maps of areas at risk of soil erosion by integration between GIS and the analytic hierarchy process on hillside slopes, northwest of Jordan. For that, it relied on five factors, which included soil erosion contributing ones; thus, slope degree, land use/land cover, soil texture, rainfall, and stream power index (SPI) were integrated into ArcGIS 10.4.1 tools for identifying the areas affected by the risk of soil erosion. Multi-criteria decision analysis (MCDA) method is used to create maps risk of soil erosion. The results of the study showed, based on the erosion risk map classified into five risk levels, including very high, high, medium, low, and very low, that the areas with high and very high erosion risk represented about 8.5% and 16.3%, respectively. The areas with low and very low soil erosion risk formed about 36.6% and 8.9%, respectively, of the total area of the study area. The findings of this study will help decision-makers to plan and carry out effective soil and soil conservation practices in

Areas were highly vulnerable to soil erosion.

Keywords: *Soil Erosion, GIS, Jordan, AHP, MCDA. SPI.*

1. Introduction

Soil erosion is related to human activities and natural problems, such as irresponsible land-use practices, inappropriate soil conservation methods, overgrazing, severe rainstorms, significant slope...etc. It also affects the degradation and desertification of the lands on the slopes of sloping hills, (Mhiret et al. 2018., Andualem et al. 2020). It equally affects the storage, filtering, and cleaning of water. (Zhu et al. 2014., Addis and Klik. 2015). Water erosion in the world is intensified because of different climatic conditions and land use impacting various natural conditions, (Garc´ıa et al. 2021).

The MCDA method depends on multiple factors for effective decision-making for natural resource management, land-use planning, and identification of environmental hazards. (Aher et al. 2013). The analytic hierarchy process (AHP) is considered one of the most important methods that are relied upon in making important decisions due to the efficiency of its use. Also, this method includes multiple levels of spatial decision-making, where the factors related to the suitability of the site are weighted to prepare a pairwise comparison matrix that depends on the relative importance scale. (Al Raisi et al.2014, Chaudhary et al.2016., Yasser et al.2013., Al-Sababhah 2022). The AHP is studied extensively and used in applications where problems related to multiple criteria decision-making are fateful. Many researchers have widely used the AHP method to make critical decisions regarding soil erosion, which saved time and effort in preparing these environmental studies. (Saaty 2008., Aikhuele et al, 2014., Ribeiro, 1996).

Finally, erosion is a natural and/or anthropogenic phenomenon affecting all regions of the world; it is very accentuated, especially in regions with arid and semi-arid climates like the Mediterranean zone, of which Jordan is a part. In the current study, the MCDA method was used to analyze a series of criteria to be ranked from the most preferable to the least preferable using a structured approach. Often the result of the MCDA is several weights related to the various alternatives. The weights express the importance of the different alternatives to each other. The selected factors that govern the fit of the site are weighted using AHP assisted by a pairwise comparison matrix that uses a relative importance scale.

2. Methods and Materials:

In Jordan, as everywhere in the world, soil erosion is the result of various natural and human factors and has many environmental impacts with social, economic, and environmental consequences.

2.1 Study area:

The study area is located in the northwestern district of Jordan and geographically lies between 35°88’ E and 35°54’ E longitude and 32°26’ N and 32°66’N latitude covering an area of 1077.6 km² from the total area of Jordan. The study area can be subdivided into five drainage basins including Al-Arab, Ziqlab, Al-Rayan, Al-taybeh, and Kufr Anja

* Corresponding author e-mail: noah.h@yu.edu.jo

valleys. Figure 1a. In terms of geomorphology, the study area watershed is a complex relief. Indeed, all the rivers have their source in the high mountains on the east bank of the northern Jordan Valley at elevations reaching 1226 m. It ends up below sea level in the Jordan River at elevation (- 332) m. Figure 1b. In the northern Jordan Valley sub-catchment, six slope classes are identified, and calculated in degrees. Drainage basins for the study area are considered permanent water sources to supply the northern regions of Jordan for agricultural and other domestic purposes. Hydrologically, there are three main dams and 177 groundwater wells in the study area. Figure 1c. Climatologically, the long-term temperature analysis showed that the area's average temperature was approximately 19.6°C, with a mean annual minimum and maximum temperature between 14.6 °C and 23 °C, respectively. Figure 1d. Also, the long-term analysis observed a regional rainfall average of 431 mm per year (i.e., approximately 245 mm minimum to 580 mm maximum). Figure 1e. Finally, the study area can be subdivided into three climate regions, including the semi-arid, semi-humid, and humid regions. Figure 1f. The study area also includes 12 soil units according to the USDA classification. Figure 1g. Also, chert-limestone and sand-limestone dominated about 53% of the area of the study area. Figure 1h.

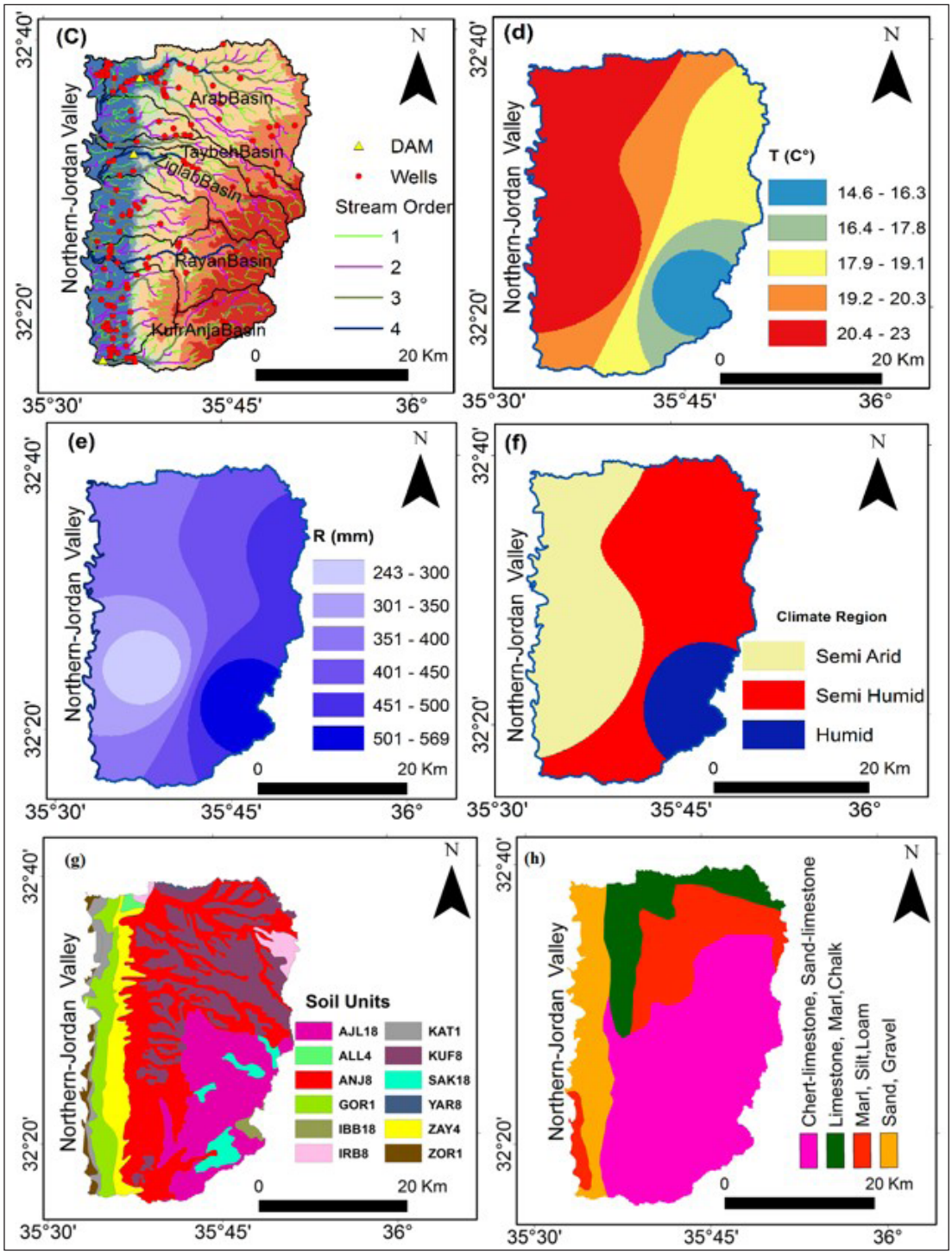

Figure 1. (a) Study Area Location, (b) Elevation (m), (c) Hydrological Properties, (d) Temperature (C°), (e) Rainfall (mm), (f) Climate Regions, (g) Soil Units, (h) Geology Texture.

Also, the study area includes the parts of the eastern bank of the Jordan River, which are: The first is ZOR, which is the narrow range of the flood plain of the Jordan River. The second section is Katar which occurs as a thin stream running along the channel of the Jordan River; its characteristics are generally moderate to high salinity, difficulty in leaching salts, very low permeability, and high erosivity along margins. The third section is Gor, which extends along the eastern edge of the Jordanian river, is highly suitable for irrigation, and is already intensively used for irrigated production of orchard crops and horticultural crops. The fourth part is the escarpments of Jordan Valley; the escarpments are in calcareous rocks, very steep, rocky slopes with rock faces. The major limitations to agrarian culture in this area are the very steep slopes and the stony, often shallow soils that occupy the upper part of the area. Figure 2.

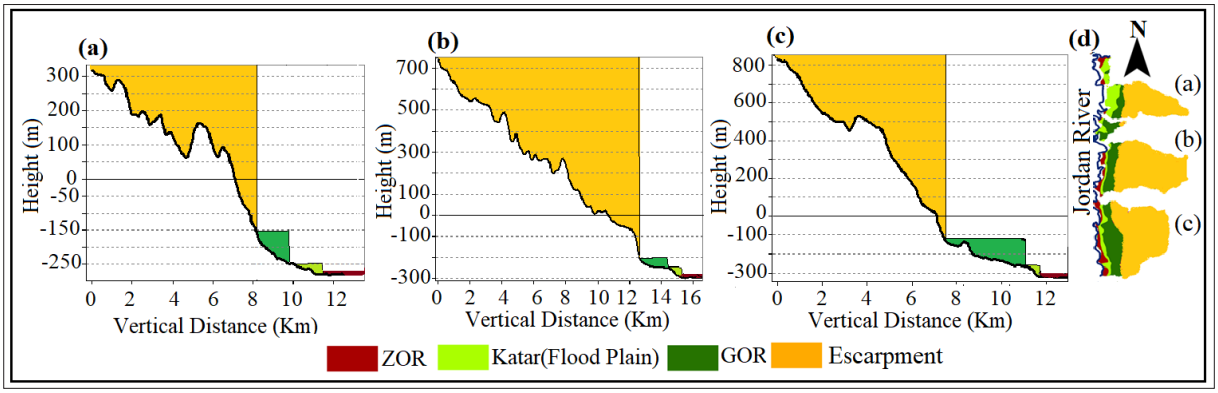

Figure 2. Vertical profile showing the distribution of the parts of the eastern bank of the Jordan Valley according to the change in elevation: (a) the northern part, (b) the middle part, (c) the southern part, (d) a map of the parts of the eastern bank of the Jordan River

2.2 Study Data:

This work is also based on two remote sensing datasets that were obtained: (i) Landsat-8 surface reflectance data freely available from the United States Geological Survey ((USGS (http://www.usgs.gov/)) during the period 2017-2021; and (ii) ASTER GDEM (https://asterweb.jpl.nasa.gov/gdem.asp) data freely available from NASA. As for the soil texture data, it was obtained from the soil survey records of the Jordanian Ministry of Agriculture for the period from 1993 – 2020. The spline interpolation method in GIS has been selected because it is the most appropriate one for studies involving a small number of cases. Also, the long-term (1990-2021) climatic data used in this assessment constitute the monthly and annual rates of rainfall rates for 11 climatic stations. Table 1.

Table 1. Table 1. List of Climatic stations used in this study.

Climate Station	Lat (N)	Long (E)	Ele (m)	Climate Station	Lat (N)	Long (E)	Ele (m)
Kufr Anjah	35°39’	32°16’	190	Taybeh	35°42’	32°32’	360
Wahadna	35°38’	32°19’	560	Dir Abi Saeed	35°40’	32°30’	310
Ruhaba	35°47’	32°25’	970	Kufr Asad	35°42’	32°35’	330
Kufryouba	35°48’	32°32’	570	Rayan	35°35’	32°23’	(-230)
Mazar	35°47’	32°28’	800	Baqura	35°37’	32°39’	(-228)
Irbid	35°51’	32°33’	560				

2.3 Measurement of Stream Power Index (SPI):

The SPI index is one of the most important factors controlling slope erosion processes. Since the erosive power of running water directly influences river cutting and slope toe erosion, (Nefeslioglu et al. 2008., Al-Sababhah 2018) the areas with high stream power indices have an excessive potential for erosion because it represents the potential energy procurable to entrain sediment, (Kakembo et al. 2009). Assuming that discharge is associated with the specific catchment area, the erosive power of water flow can be measured by the stream power index) SPI (, (Moore et al. 1991), as follows:

$$SPI = As \times \tan\sigma \quad (1)$$

where, As represents the specific catchment area in meters and σ is the slope gradient in degrees. Also, ArcGis can be used to measure SPI by the equation:

$$SPI = Ln((\text{"facc\_dem"} + 0.001) * ((\text{"slope\_dem"} / 100) + 0.001)) \quad (2)$$

By following these steps: Launch the Raster Calculator by clicking on click on Spatial Analyst Tools -Map Algebra - Raster Calculator, and Enter the formula, the result looks exactly like the formula above, Output Raster, thumb-drive\terrain\spi, and click ok to run the calculation. For more details, please refer to the website: https://www.wrc.umn.edu/randpe/agandwq/tsp/lidar

2.4 The Analytic hierarchy process (AHP) Method:

The AHP continues to be one of the most popular analytical techniques for complex decision-making problems and is widely used due to its flexibility and ease to use. An AHP hierarchy can have many levels to characterize a decision condition. The selected factors governing the suitability of the site’s suitability are weighted using the AHP which is aided by a pairwise comparison matrix that uses a

scale of relative importance, (Al Raisi et al. 2014, Chaudhary et al. 2016, Yasser et al. 2013., Al-Adamat et al.2010). This method consists of a weighting of the factors adopted by a comparison. In pairs of factors that control erosion in this area, (Tairi et al. 2013) the main factors considered in this study are slope, land use/land cover, soil texture, rainfall, and SPI. The AHP process may be subdivided into three steps Including standardization, weight assignment, and weighted linear combination. Figure 3 indicates the overall procedures employed to create a model that enables us to identify zones of erosion risk.

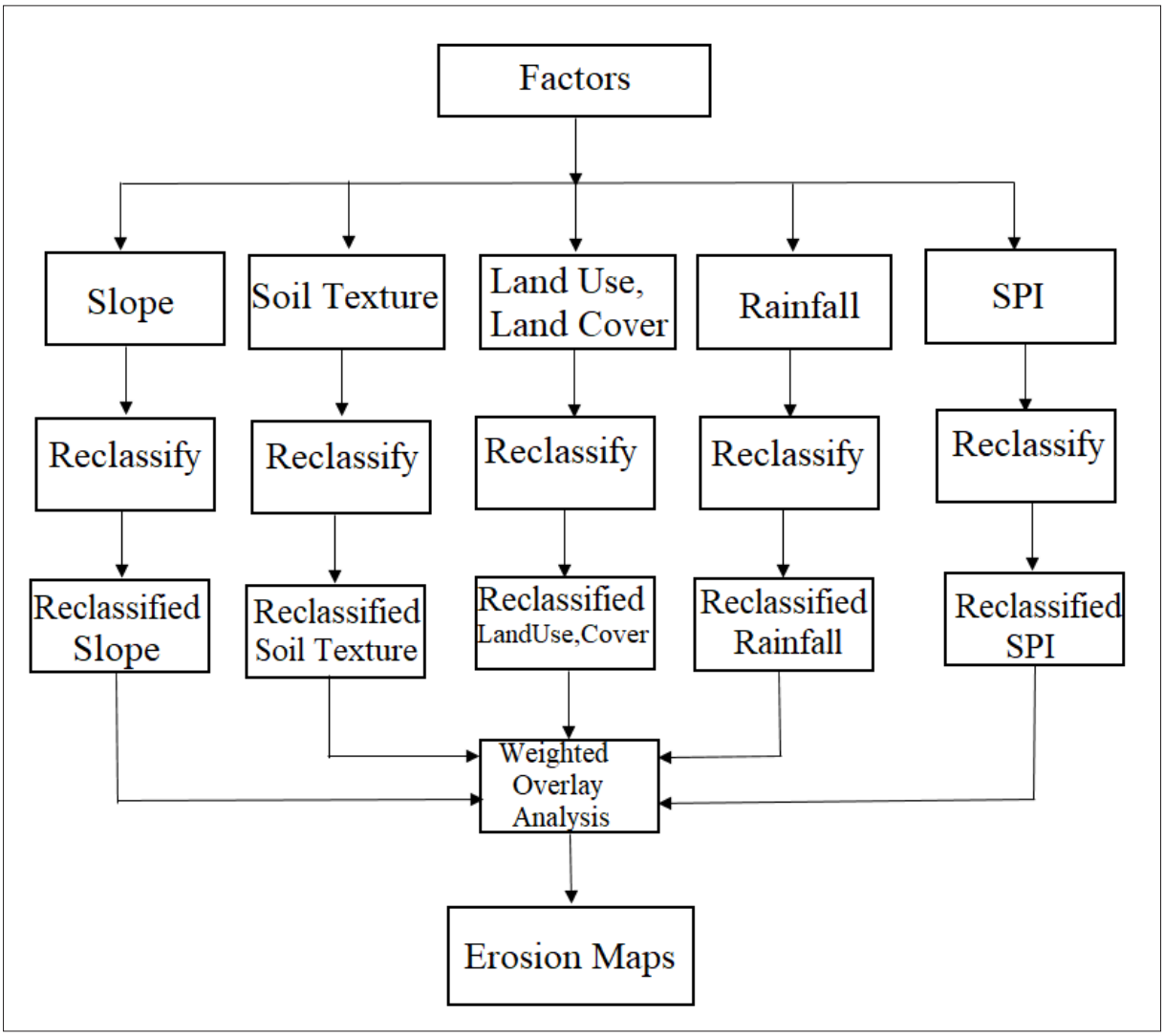

Figure 3. Overall procedures used for erosion risk mapping using MCDA in ArcGIS 10.4.1.

2.4.1 Multi-criteria decisional analysis mapping (MCDA):

Different methods to determine the risk zones of soil erosion, which calculate the amount of erosion and require a lot of data and criteria (Wischmeier and Smith, 1978), can be applied to characterize the erosion phenomenon in the study area. The MCDA is used to analyze a series of alternatives or objectives to rank them from the most preferable to the least preferable using a structured approach. The result of MCDA is often a set of weights linked to the various alternatives. The weights indicate the preference of the alternatives relative to each other. They may also be seen as an advantage or disadvantage when changing from one alternative to another. The choice of methodologies for calculating these weights varies from text to text. Several authors (Stewart and Scott 1995., Joubert et al. 1997., Jankowski et al. 2001., Ayalew and Yamagishi 2005., Kourgialas and Karatzas., 2011) have used the methods highlighted by Malczewski (1999) when calculating weights in MCDA. The AHP developed by Saaty (1977,1984), is the simplest of the multicriteria methods. It is based on the synthesis and aggregation of weights assigned to the criteria of the different levels of the hierarchy. The weights and ranks of each parameter were assigned after the pair-wise comparison using the rating scale. Table 2.

Table 2. Scale of comparisons of criteria (Saaty 1984).

Important	Verbal definition of the importance of one factor over the other	Scale
More Important	Extremely	9
	Very strongly	7
	strongly	5
	Moderately	3
	Equally important	1
Equally Important	Moderately	1/3
	Strongly	1/5
	Very Strongly	1/7
Less Important	Extremely	1/9

2.4.2 Pair-wise comparison matrix:

The application of AHP requires the development of a pairwise comparison matrix between the five factors affecting soil erosion, and this depends on the importance of each factor in the occurrence of erosion. The pairwise comparison of each pair of elements in each level is made to corresponding elements in the above level, depending on their importance. Where the comparisons can then be represented by multiple square matrices, (Chen 2006), as follows:

$$\mathbf{C = (Cij)n * n} \quad (3)$$

where C consistency ratio, each matrix of order n as the matrix. Table 3 shows a multiple square matrix.

Table 3. Multiple Square Matrix.

Factors	Slope	Land Use/ Land Cover	Soil Texture	Rainfall	SPI
Slope	C11	C12	C13	C14	C15
Land Use/ Land Cover	C21	C22	C23	C24	C25
Soil Texture	C31	C32	C33	C34	C35
Rainfall	C41	C42	C43	C44	C45
SPI	C51	C52	C53	C54	C55

Matrices that have reciprocal properties can be expressed., (Saaty 1980), by the following equation,

$$\mathbf{C = (1/Cij)n * n} \quad (4)$$

After the pairwise comparisons have been completed, a weight value is assigned to the element with a higher importance in the pair. As for the lesser important element in the pair, a reciprocal of the value will be assigned to it. Normalization followed by averaging the weights is then done to obtain the relative weight for each of the elements in the hierarchical model, (Kasperczyk and Knickel 2006). Based on equation (4), we arrive at the matrix. Table 4.

Table 4. The representation of matrices that have reciprocal properties.

Factors	Slope	Land Use/ Land Cover	Soil Texture	Rainfall	SPI
Slope	1/C11	1/C12	1/C13	1/C14	1/C15
Land Use/ Land Cover	1/C21	1/C22	1/C23	1/C24	1/C25
Soil Texture	1/C31	1/C32	1/C33	1/C34	1/C35
Rainfall	1/C41	1/C42	1/C43	1/C44	1/C45
SPI	1/C51	1/C52	1/C53	1/C54	1/C55

Then, the pairwise comparison matrix will be normalized by dividing each element in the matrix by the sum of its columns, (Bunruamkaew 2012) to get the following matrix. Table 5.

Table 5. Decision matrix.

Factors	Slope	Land Use/Land Cover	Soil Texture	Rainfall	SPI
Slope	C10/10	C10/5	C10/3.33	C10/2.5	C10/2
Land Use/Land Cover	C5/10	C5/5	C10/5	C10/3.33	C10/2.5
Soil Texture	C3.33/10	C5/10	C3.33/3.33	C10/5	C10/3.33
Rainfall	C2.5/10	C3.33/10	C5/10	C2.5/2.5	C10/5
SPI	C2/10	C2.5/10	C3.33/10	C5/10	C2/2

researcher's vision and referring to previous studies within the same field, pair-wise comparisons, and ranking of factors were done. Table 6. Analyzing

soil erosion areas, the slope was considered the most Weights of all factors in the hierarchical model based on the influential factor (highly sensitive to erosion), whereas SPI was considered less sensitive to contributing soil erosion. The values in each cell represent the scale of relative importance for the given paired factors. The diagonal has a value of "1" throughout because the diagonal represents factors being compared to itself with a scale of "1" (equal importance). On the lower diagonal, the scale values are infractions because the factors are being paired in the reverse order and the scale of relative importance is given as the reciprocal of the upper diagonal pair-wise comparisons. Hence, to identify the erosion Hotspot areas in the north Jordan Valley basin, factors are ranked as follows: slope first; land use second; soil texture third; rainfall fourth; and SPI fifth. For more details, refer to Andualem 2020).

Table 6. Comparison matrix of the five factors adopted.

Factors	Slope	Land Use/Land Cover	Soil Texture	Rainfall	SPI
Slope	1	2	3	4	5
Land Use/Land Cover	0.50	1	2	3	4
Soil Texture	0.33	0.50	1	2	3
Rainfall	0.25	0.33	0.50	1	2
SPI	0.20	0.25	0.33	0.50	1
Sum	2.28	4.08	6.83	11	15

These verbal judgments are based on a good expert knowledge of the field and the importance of each factor in the phenomenon of erosion. To calculate the weights of each factor, we will need to convert each value in the table of the comparison matrix in Table 6, to a percentage of the sum per column. Then the weight of each factor is the average of each row of the standardized matrix multiplied by 100%, Table 7.

Table 7. Standardized Matrix of Erosion Factors.

	Slope	Land Use/Land Cover	Soil Txt	Rainfall	SPI	Total	Average	Weight %
Slope	0.44	0.49	0.44	0.38	0.33	2.08	0.42	41.64
Land Use/Land Cover	0.22	0.25	0.29	0.29	0.27	1.31	0.26	26.18
Soil Txt	0.15	0.12	0.15	0.19	0.20	0.81	0.16	16.10
Rainfall	0.11	0.08	0.07	0.10	0.13	0.49	0.10	9.84
SPI	0.09	0.06	0.05	0.05	0.07	0.31	0.06	6.23
Total	1	1	1	1	1	5	1	100

2.4.3 Consistency analysis:

In the AHP, the pair-wise comparisons in a judgment matrix are considered to be adequately consistent if the corresponding consistency ratio (CR) is less than 10% (Saaty 1980). First, the consistency index (CI) needs to be estimated. This is done by adding the columns in the judgment matrix and multiplying the resulting vector by the vector of priorities (i.e., the approximated eigenvector) obtained earlier. This yields an approximation of the maximum Eigenvalue, denoted by λmax. Table 8 refers to the consistency matrix used to calculate the consistency ratio.

Table 8. Consistency measurement matrix.

Factors	Slope	Land Use/Land Cover	Soil Txt	Rainfall	SPI	Total	Average	Weight %	Consistency Measure
Slope	0.44	0.49	0.44	0.38	0.33	2.08	0.42	41.40	5.11
Land Use/ Land Cover	0.22	0.25	0.29	0.29	0.27	1.32	0.26	26.30	5.10
Soil Txt	0.15	0.12	0.15	0.19	0.20	0.81	0.16	16.10	5.06
Rainfall	0.11	0.08	0.07	0.10	0.13	0.49	0.10	9.80	5.02
SPI	0.09	0.06	0.05	0.05	0.07	0.32	0.06	6.40	5.03
Total	1	1	1	1	1	5.02	1	100	Average 5.06=
	CI=0.02				RI = 1.12				CR=1.45

Then, the CI value is calculated by using the formula:

$$\mathbf{CI} = (\boldsymbol{\lambda}\mathbf{max} - \mathbf{n})/(\mathbf{n} - \mathbf{1}) \quad (5)$$

where is calculated using the formula:

$$\boldsymbol{\lambda}\mathbf{max} = \sum_{i=0}^{n}(\boldsymbol{Xij}) \times (\mathbf{Wij}) \quad (6)$$

Next, the consistency ratio CR is calculated by using the formula:

$$\mathbf{CR} = (\mathbf{CI}/\mathbf{RI}) \times \mathbf{100} \quad (7)$$

where RI refers to the mean of an Index of Consistency, the matrix Order and CI refer to the Index of Consistency as expressed.

A randomly generated pairwise comparison matrix is used to obtain the random consistency index, RI. The values of $\boldsymbol{RI}$ for matrices of order 1 to 15 (1 to 10 elements in one level). Table 9, (Saaty 2016., Satty 1984). The RI value in this study was 1.12.

Table 9. Random indices for matrices of comparisons (Saaty 1984).

Size	1	2	3	4	5	6	7	8	9	10
RI	0	0	0.58	0.9	1.11	1.24	1.32	1.41	1.45	1.49

If λ max is the most massive value of the matrix of its own, the matrix can be determined easily; "n" is the matrix sequence. The CR is a ratio of the random index to the matrix consistency index.

The value is from 0 to 1. A CR of 0.1 or less is considered a respectable level, and over 0.1 implies a revision is required because the individual factor ratings are not being handled uniformly (Malczewski 1999). When these approximations are applied to the previous judgment matrix, it can be verified that the following are derived: λmax = 5.11; CI = 0.02, and CR =0.014. Once the weighting is done, the different factors adopted and the coherence ratio value is acceptable CR = 0.01, the superposition of the 5 input factors adopted will be carried out under ArcGIS software 10.4.1 according to the following equation:

Risk of Erosion = (0.42 * Slope) + (0.26 * Land Use/Land Cover) + (0.16 * Soil Txt) + (0.10 * Rainfall) + (0.06 * SPI).(8)

2.4.4 Field Study:

As an important step for the study, field visits were made to different areas within the study area to verify the accuracy of the results in determining the sites most affected by the risk of soil erosion in the field, in addition to the accuracy of the selection and the importance of (GIS and RS) as effective tools in evaluating soil erosion sites and thus matching the results reached using (GIS and RS) with the field reality. Figure 4 shows the sites of the field verification visits.

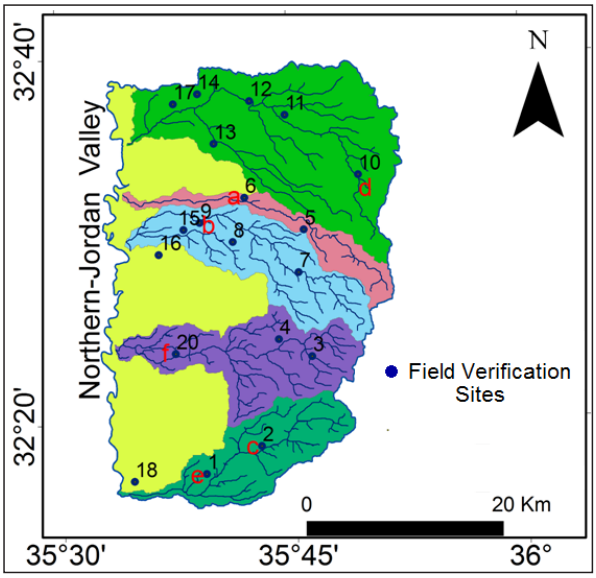

Figure 4. The sites of the field verification visits are shown in numbers. (a, b, c, d, e, f) represent the sites of soil erosion types in Figure 11.

3. Results and discussion:

After the factors of soil erosion are compared with each other by developing a comparison matrix, they are also compared regarding the importance of one concerning another and accordingly given a rating as per the Saaty scale. The present study was conducted to determine the zones of a Northern Jordan valley that contribute to a large amount of soil erosion.

3.1 Soil erosion contributing factors:

To estimate the spatial distribution of soil erosion-hazard areas in the Northern Jordan Valley, five factors are used: Slope, land use/land cover, soil texture, rainfall, and SPI.

3.1.1 Slope:

The slope gradient is a crucial factor that affects soil erosion from the land surface. The slope is one of the most important topographical features that cause soil degradation, (Andualem 2020). The slope ranges from (0 to 58.2°) in Northern Jordan Valley (Figure 5a).

3.1.2 Land use / Cover:

land use/cover changes were considered significant factors in soil erosion in the study region. Land/cover was one of the critical factors influencing surface flux, and decay in land use, (Sinshaw et al. 2021). In this regard, nine types of land use/land cover were recognized in the study area. Land use/land cover classes were investigated and computed as presented in Figure 5b.

3.1.3 Soil Texture:

Soil is an important element in conserving soil watershed moisture. The soil characteristics also control surface water in an aquifer system and are directly linked to absorption, percolation, and permeability levels. Soil texture affects the water content and drainage ability of soils. This is because texture controls the nature of soil pores, thus increasing the possibility of soil erosion, (Burke et al. 1999, Hook and Burke 2000). The soil texture of the study area showed about six major soil texture classes. Figure 5c.

3.1.4 Rainfall:

The effect of rainfall characteristics as a major determining factor is crucial to deal with observed variability in soil erosion, (Ran et al. 2012). Among storm characteristics, rainfall intensity is a very important factor. The close relationship between water erosion and rainfall intensity is due to the impact of raindrops on the soil surface in high-intensity storms which causes increased soil particle detachment and higher rainfall intensity results in higher rates of infiltration excess runoff, and a much greater transport of suspended sediment load, (Van Dijk et al. 2002., Falkland 1993., Al-Sababhah and Alomari 2020). The rainfall ranges from (243 mm to 569 mm). Figure 5d.

3.1.5 Stream Power Index (SPI):

Soil erosion by water is directly linked to slope morphology in the areas (Danielson 2013). SPI determines the erosive water flowing capacity, assuming the flow is proportional to the catchment area and the pitch. The potential energy for sediment is also an indicator (Kakembo et al. 2009). The highest focus on soil erosion has been the higher range of SPIs based on 'researchers' and 'experts' expertise. The SPI ranges from (-13.8 to 11.4). Figure 5e.

3.2 Reclassification of Soil erosion contributing factors:

The model applied in this study allows for determining the zones sensitive to soil erosion in the study area. Based on the sensitivity classes of the factors that control soil erosion, we have established the reclassification maps of the risk of soil erosion in the northern Jordan Valley.

3.2.1 Slope:

The slope map was reclassified into five major slope classes depending on the Food and Agriculture Organization (FAO) slope classification and susceptibility to erosion, Areas that are found on flat and gentle slopes were taken as very low and low susceptible to erosion, and vice versa, Figure 6a.

3.2.2 Land Use / Land Cover:

Land use and land cover changes are also considered as one of the major factors which cause soil erosion in an area, thus leading to land degradation. The northern Jordan Valley basins have five major types of land use and land cover. The land use and land cover types were reclassified according to their susceptibility to erosion where agricultural and bare land areas were considered very highly vulnerable to erosion, due to the soil structure disturbance. At the same time, water and urban areas were considered very lowly vulnerable to erosion. Figure 6b.

3.2.3 Soil Texture:

The susceptibility of soil texture to erosion was reclassified based on the characteristics of soil concerning soil erosion, where silt clay was considered very highly vulnerable to erosion, while clay loam was considered as low vulnerable to erosion, Figure 6c.

3.2.4 Rainfall:

The classified rainfall map was prepared based on areas with high rainfall values assigned to very high and high susceptibility to erosion. Figure 6d.

3.2.5 Stream Power Index (SPI):

Areas with high SPI values are considered highly erosive, whereas areas with low SPI values are classified as low, and susceptible to erosion. Figure 6e.

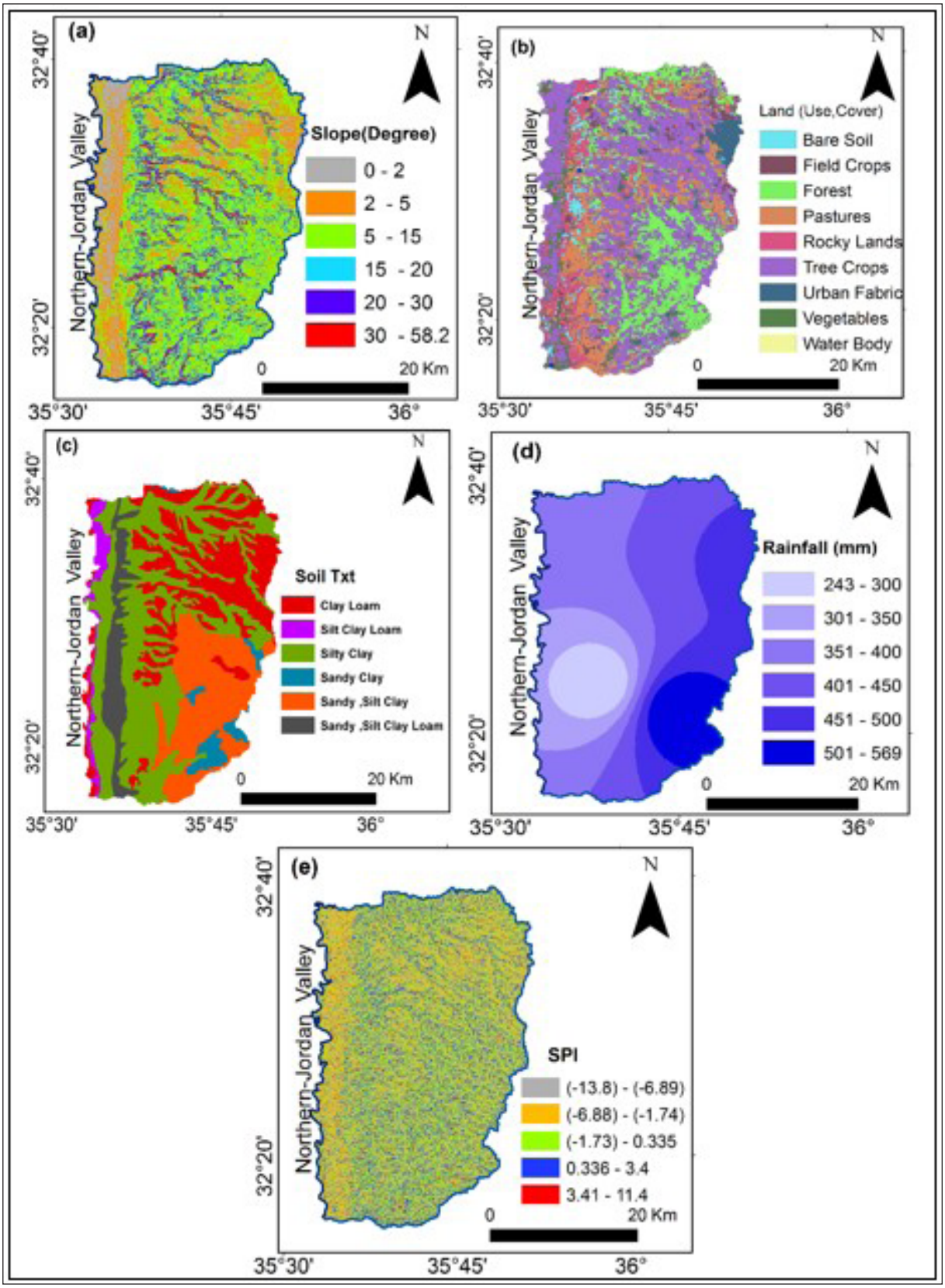

Figure 5. Soil erosion contributing factors: (a) Slope(Degree), (b) Land Use/Land Cover, (c) Soil Texture, (d) Rainfall (mm), (e) SPI.

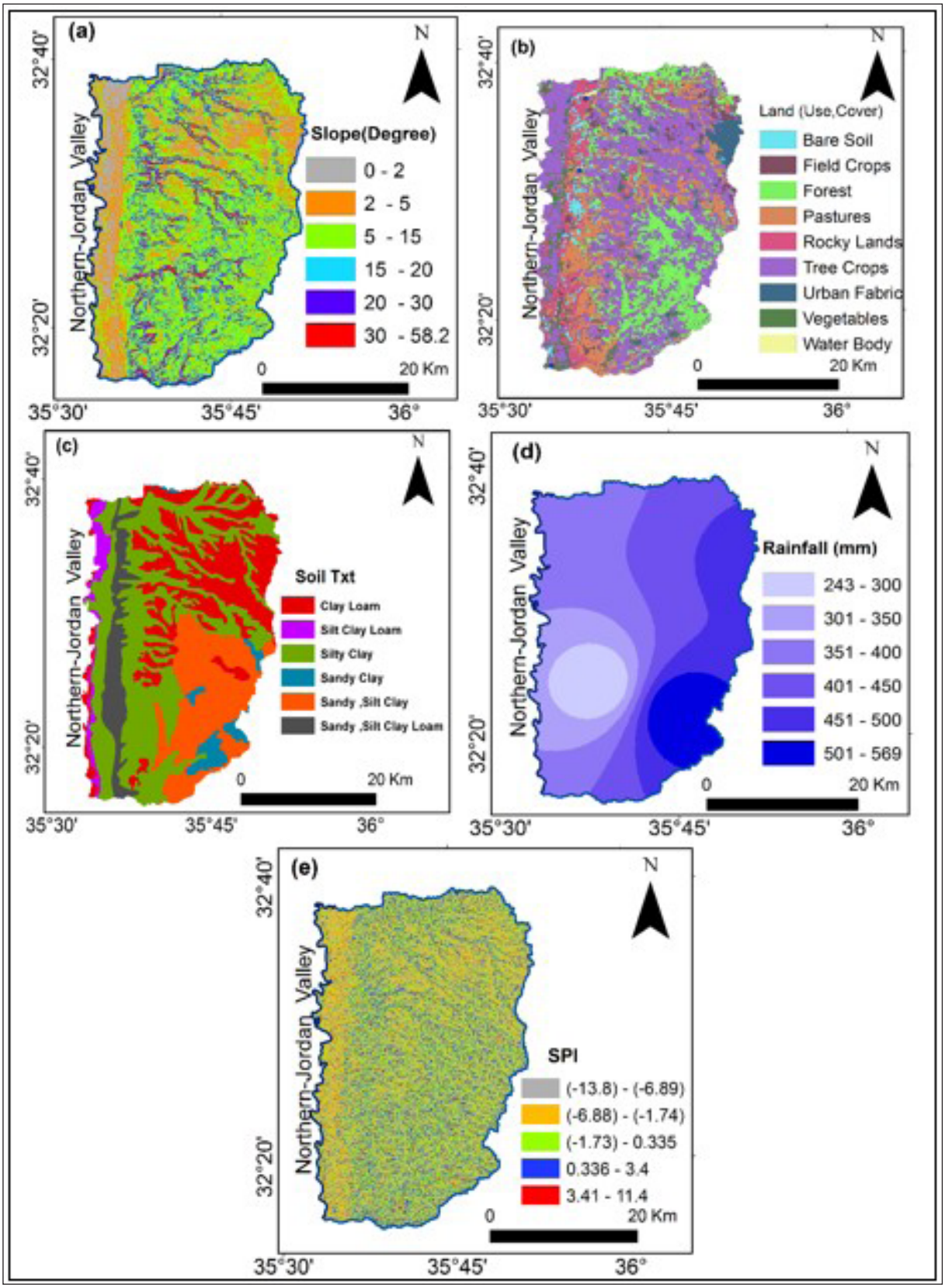

Figure 6. Classified soil erosion contributing factors: (a) Slope(Degree), (b) Land Use/Land Cover, (c) Soil Texture, (d) Rainfall (mm), (e) SPI.

3.3 Weighting of soil erosion contributing factors:

All soil erosion contributing factors were classified into five categories representing the degree of risk scale of that category on the possibility of soil erosion within the same factor. A standard scale of 1-9 according to the Saaty (1984) system was used to determine the degree of impact, with a value of 9 indicating a higher degree of risk.

Referring to the above, these verbal judgments are based on a good expert knowledge of the field and each factor's importance in the erosion phenomenon. To calculate the weights of each factor, we will need to convert each value in the table of the comparison matrix in Table 6, to a percentage of the sum per column. Table 8. Then the weight of each factor is the average of each row of the standardized matrix. Table 7 indicates the weights of the factors, the percentage of weights for each factor, the levels of erosion risk, and the classification of factors. Table 10.

Table 10. Classification and Weighting of Factors.

Factor	Domain	Risk Level	Proposed Weight	Weighting Rate	Total Weight	Percentage (%)
Slope	0-5	Very low	2	0.33	2.08	41.4
	5-10	Low	2.5	0.38		
	10-15	Moderate	3.33	0.44		
	15-20	High	5	0.49		
	20-58.2	Very high	10	0.44		
Land Use/Land Cover	Agricultural and Bare Land	Very low	2	0.27	1.32	26.3
	Forests	Low	2.5	0.29		
	Pastures	Moderate	3.33	0.29		
	Tree Crops	High	5	0.25		
	Water and Urban Areas	Very high	10	0.22		
Soil Texture	Clay Loam	Very low	2	0.20	0.81	16.1
	Sandy Clay	Low	2.5	0.19		
	Sandy Silt Clay Loam	Moderate	3.33	0.15		
	Silty Clay	High	5	0.12		
	Silt Clay Loam	Very high	10	0.15		
Rainfall	243-315	Very low	2	0.13	0.49	9.8
	315-368	Low	2.5	0.10		
	368-420	Moderate	3.33	0.07		
	420-488	High	5	0.08		
	488-569	Very high	10	0.11		
SPI	(- 13. 6)-(- 6. 9)	Very low	2	0.07	0.32	6.4
	(- 6. 9)-(- 1. 75)	Low	2.5	0.05		
	(- 1. 75)-0.34	Moderate	3.33	0.05		
	0.34-3.40	High	5	0.06		
	3.40-11.4	Very high	10	0.09		
Total					5.02	100 %

The risk classes were assigned to the five selected factors. Then the AHP pair-wise comparison matrix was constructed based on the preferences of each factor relative to the others. As input, it takes pair-wise comparisons of the factors and produces their relative weights as output. All soil erosion contributing factors were classified into five levels that represent the degree of risk scale of that category on the possibility of soil erosion to create a weighting map for the five factors. Figure 7.

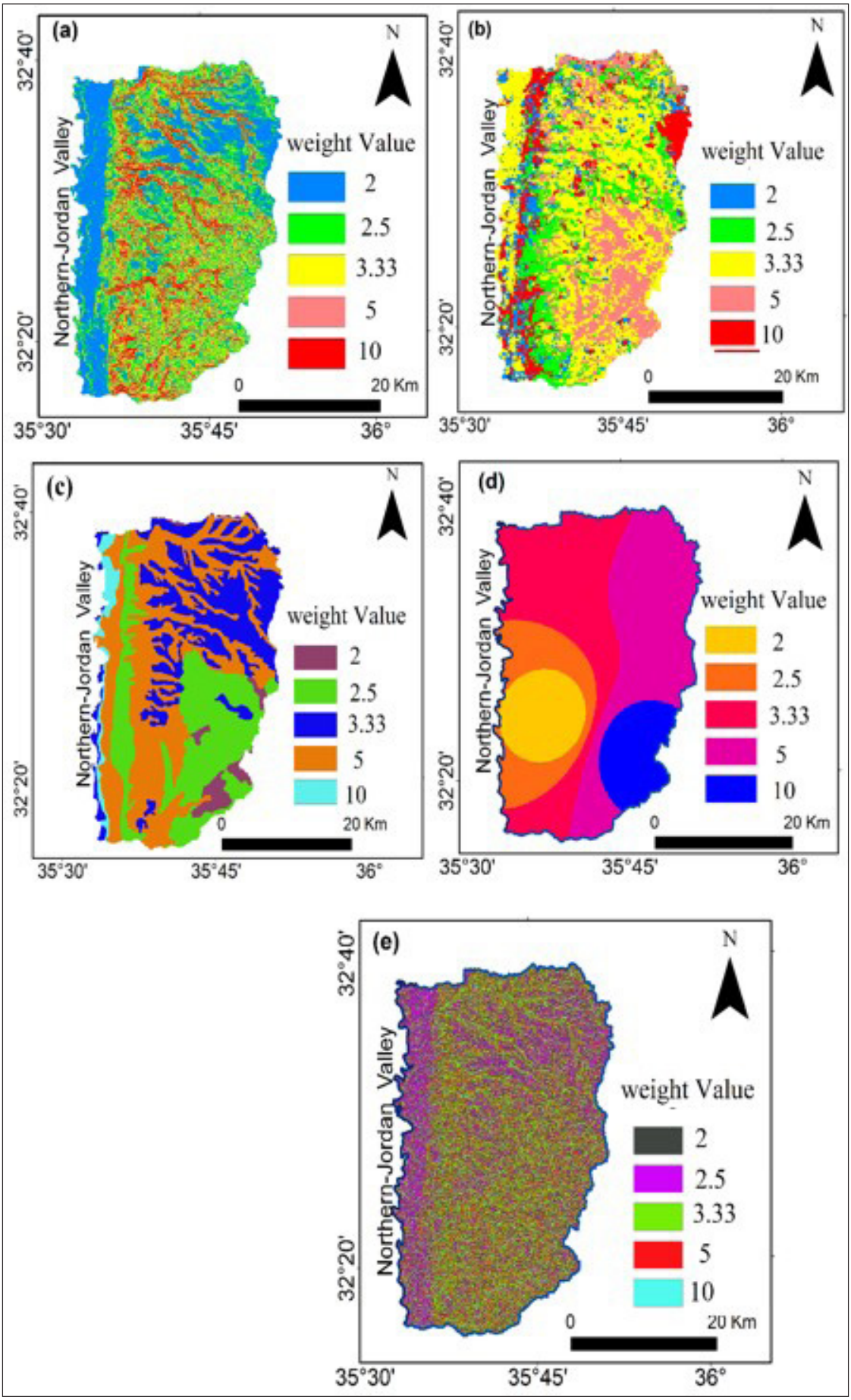

Figure 7. Weighted soil erosion contributing factors: (a) Slope(Degree), (b) Land Use/Land Cover, (c) Soil Texture, (d) Rainfall (mm), (e) SPI.

3.4 Risk levels for soil erosion contributing factors:

Soil erosion risk areas are classified into five risk levels according to the severity of erosion. The spatial distribution of each class of soil erosion risk in percent was developed by the AHP method. Figure 8.

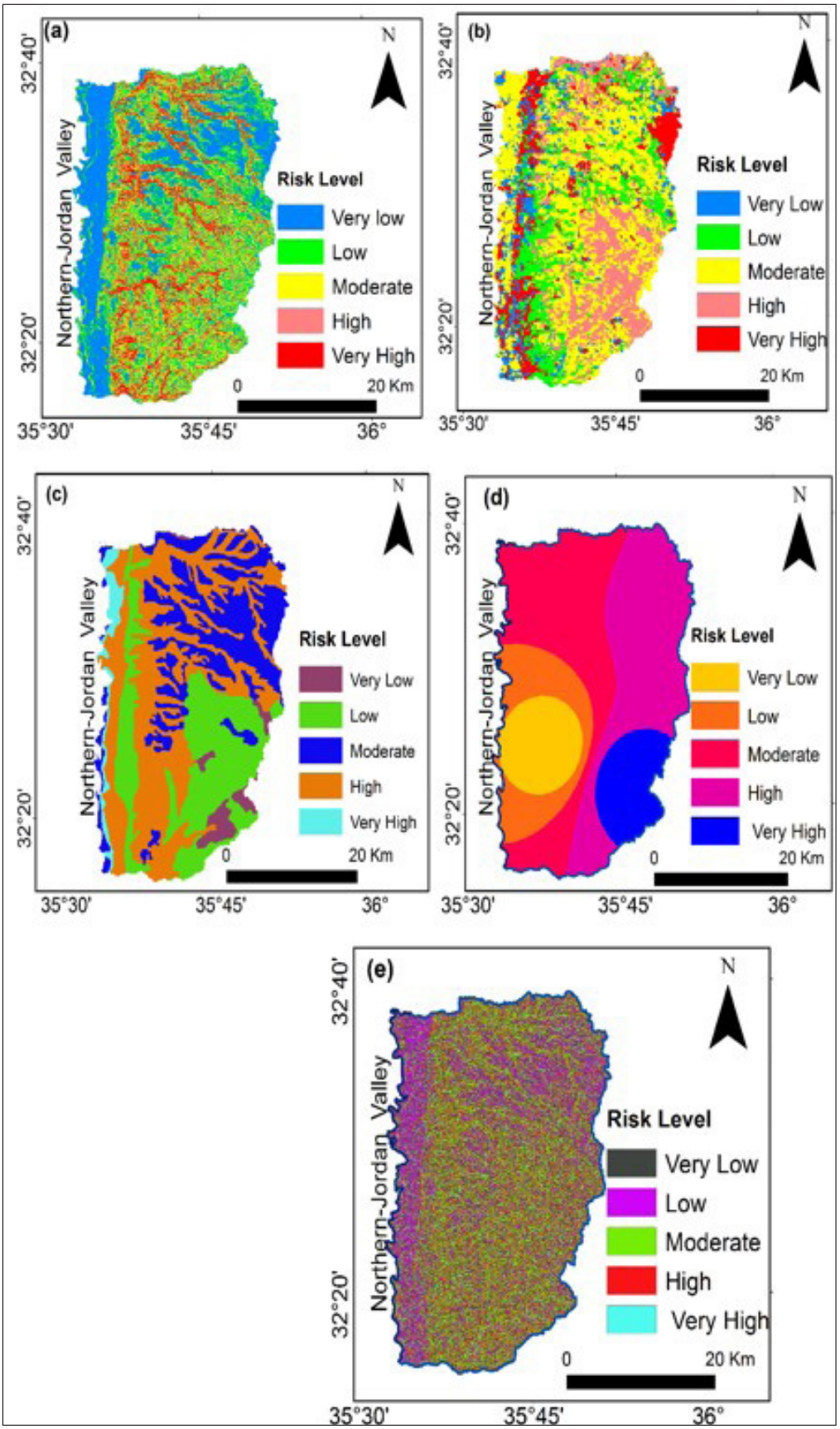

Figure 8. Risk levels for soil erosion contributing factors: (a) Slope(Degree), (b) Land Use/Land Cover, (c) Soil Texture, (d) Rainfall (mm), (e) SPI.

Areas found on flat and less than 10 degrees, were taken as having very low and low, susceptibility to erosion. About 30 % of the area lay in very low erosion risk; on the other hand, about 11.4 % lay in very high erosion. Figure 8 a. Areas that are found in agricultural and bare land were found as very highly susceptible to erosion. Their area constituted 9.7%. As for the areas covered by water and urban areas, which represent areas with a very low risk of erosion, they constituted a percentage of 11.44%. However, it can be considered that pastures with moderate impact on the risk of erosion constituted the highest percentage of the area at around 43.1 %. Figure 8 b. Northern-Jordan valley basin is dominated by Silty Clay with an area coverage of 441.2 km^2 or about 40.9% of the total area, which constitute areas of high risk of erosion, while the areas covered by clay loam have an area of 32.7 km^2 with a percentage of 3% of the total area and represent areas of very low risk of soil erosion. Figure 8 c. Areas with high rainfall/rainfall erosivity values were assigned to very high and high risk of erosion. About 117.6 km2 and 340.7 km2 area were found in a very high and high erosive area, respectively, while, about 124.5 km2 area was found in a very low erosive area, Figure 8 d. Finally, areas with high SPI values were considered highly erosive, whereas areas with low SPI values were classified with low susceptibility to erosion. As seen from the spatial distribution map of SPI, 15.5 % and 2.9 % of the area have been found in high and very high susceptibility to soil erosion. Figure 8 e. Table 11 shows the distribution of risk levels for soil erosion contributing factors.

Table 11. Distribution of risk levels for soil erosion contributing factors.

Factors	Domain	Risk Level	Area (Km)	Percentage (%)
Slope	0-5	Very low	355.6	33
	5-10	Low	287.2	26.7
	10-15	Moderate	196.7	18.3
	15-20	High	115.6	10.7
	20-58.2	Very high	122.5	11.37
Land Use/Land Cover	Agricultural and Bare Land	Very high	105	9.7
	Forests	High	175.6	16.3
	Pastures	Moderate	464.5	43.1
	Tree Crops	Low	209.2	19.4
	Water and Urban Areas	Very low	123.3	11.44
Soil Texture	Clay Loam	Very low	32.7	3
	Sandy Clay	Low	285.8	26.5
	Sandy Silt Clay Loam	Moderate	284.3	26.4
	Silty Clay	High	441.2	40.9
	Silt Clay Loam	Very high	33.6	3.1
Rainfall	243-315	Very low	124.5	11.6
	315-368	Low	150.3	13.9
	368-420	Moderate	344.5	32
	420-488	High	340.7	31.6
	488-569	Very high	117.6	10.9
SPI	(- 13. 6)-(- 6. 9)	Very low	301.3	28
	(- 6. 9)-(- 1. 75)	Low	219.9	20.4
	(- 1. 75)-0.34	Moderate	358.1	33.2
	0.34-3.40	High	167.5	15.5
	3.40-11.4	Very high	30.9	2.9

A final soil erosion map was created for the Northern-Jordan Valley basin to show the spatial distribution of erosion hazard sites. In addition to developing the soil erosion maps which are laid in erosion, potential areas have been identified to notify the respective officials at all levels of decision-makers and planners for providing sustainable soil and water conservation practices. Figure 9.

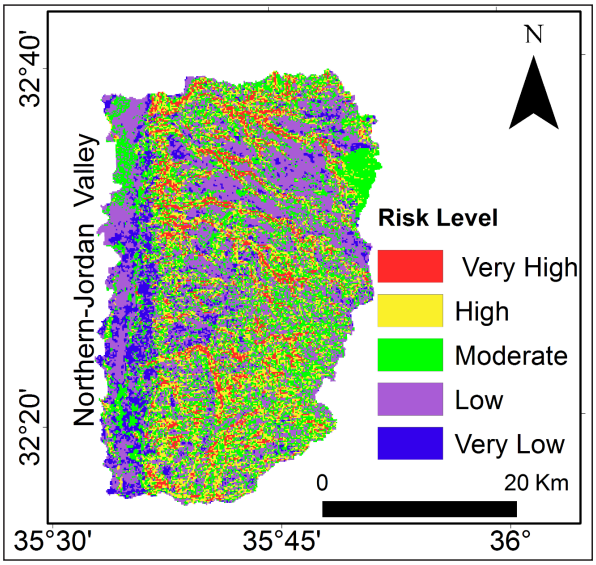

Figure 9. Soil erosion hazard map for the study area.

Where, the areas with high and very high erosion risk in the northern Jordan Valley basin are about 8.5% and 16.3%, respectively. As for the areas with low and very low soil erosion risk, they form about 36.6% and 8.9%, respectively, of the total area of the study area, Table 12

Table 12. Distribution of risk levels for soil erosion in the Northern-Jordan Valley.

Risk level	Area (km²)	percentage (%)
Very High	91.6	8.5
High	175.6	16.3
Moderate	319.8	29.7
Low	394.8	36.6
very Low	95.8	8.9
Total	1077.6	100

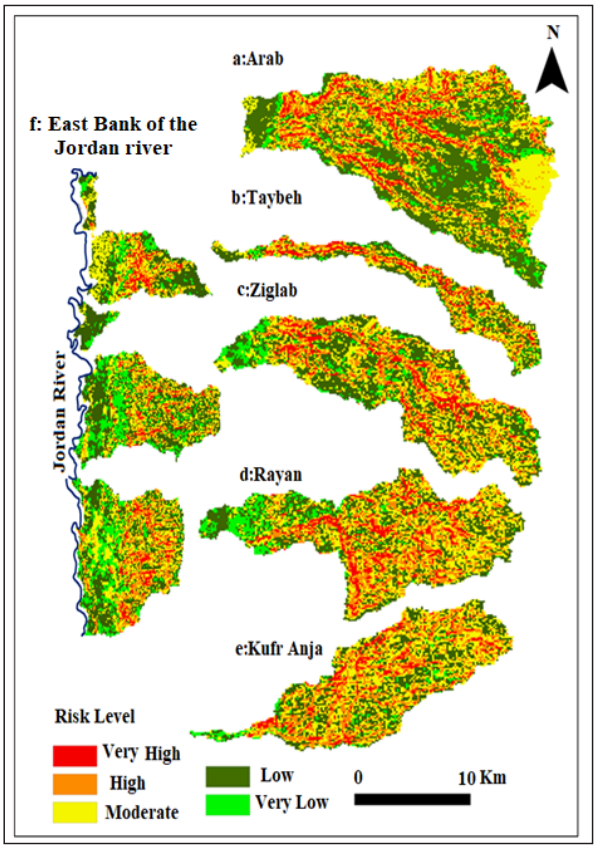

Figure 10. Soil erosion risk map for sub-basins.

3.5 Risk levels for sub-basins:

Likewise, the analysis for soil erosion was conducted for the sub-basins, including Al-Arab, Ziqlab, Al-Rayan, al-taybeh, Kufer Anja, and the areas located on the eastern bank of the Jordan River. Figure 10.

In the analysis of soil erosion, it has been found that the Arab basin has a high and very high erosion area of about 69.8 km², with a percentage of about 6.5% of the total area. Hence, that catchment can be considered the most topographically-complex basin in the study area, resulting in more steep morpho-metric characteristics. Also, it has been found that this catchment has the highest slope ratio even though it is the largest watershed, which is considered a hazardous indication since it means that soil erosion could reach great volume over a small area. The low and very low area of soil erosion, was in the lands of the eastern bank of the Jordan River, covering about 191.3 km². This is related to the spread of favored plain areas to cash crop production and intensive agriculture which can lead to low-erosion soil. Table 13.

Table 13. Distribution of risk levels for sub-basins.

Basin	Risk Level	Area (Km²)	Percentage (%)
Arab	Very high	27.4	9.40
	High	42.4	14.5
	Moderate	86.95	29.8
	Low	117.6	40.3
	Very low	17.2	6
	Total	291.55	100
Taybeh	Very high	8.1	13.5
	High	11.4	19.0
	Moderate	17.2	28.7
	Low	20.7	34.5
	Very low	2.6	4
	Total	60	100
Ziglab	Very high	13.6	9.54
	High	26.2	18.4
	Moderate	42.6	29.9
	Low	50.3	35.3
	Very low	9.92	7.0
	Total	142.62	100
Rayan	Very high	16.2	11.1
	High	31.3	21.4
	Moderate	44.9	31
	Low	43	29.5
	Very low	10.6	7.3
	Total	146	100
Kufr Anja	Very high	10.2	9.2
	High	28.8	25.9
	Moderate	37.1	33.4
	Low	30.8	27.7
	Very low	4.2	3.8
	Total	111.1	100
East Bank of the Jordan River (Gor,Zor, Katar, and escarpment)	Very high	15.5	4.7
	High	37.8	11.6
	Moderate	81.7	25.0
	Low	134.4	41.2
	Very low	56.93	17.4
	Total	326.33	100

3.6 Field study:

Fieldwork is used while investigating soil erosion areas. Also, field visits are an important tool for investigating spatial scale, the scenarios of interaction between the various environmental factors, and the surfaces they act upon to cause soil erosion. The types of soil erosion were distributed within the study area and were limited in the field visits to six types as their locator in Figure 3: The first type is Raindrop or splashes erosion due to the impact of falling raindrops on the soil surface leading to the destruction of the crumb structure, also known as the raindrop or splash erosion. Figure 11a. The second type of sheet erosion is the uniform removal of soil in thin layers from the land surface caused by water. Land areas with loose, shallow topsoil overlying compact soil are most prone to sheet erosion. Figure 11b. The third type of rill soil erosion is a form of water erosion in which the erosion takes place through numerous narrow and more or not-so-straight channels called streamlets, or head cuts. Rill is the most common form of erosion, which you can also observe during heavy rain. Figure 11c. The fourth type of gully erosion occurs due to the runoff of surface water causing the removal of soil with drainage lines. When started once, gullies will move by headward erosion or even by slumping of side walls unless and un-till proper steps will be taken to stabilize the disturbance. Figure 11d. The fifth type of stream bank erosion is nothing but washing away from the banks of a stream or a river. It is different from the erosion of the bed of a watercourse, which is referred to as scouring. This type of erosion is also termed Stream Bank Erosion. Figure 11e. The sixth type of soil flow frosion is the movement of water-saturated soils towards the lowest slopes, and it is active in wet regions where it transports large quantities of soil during sufficient amounts of rainfall. Figure 11f.

Figure 11. The types of soil erosion: (a) raindrop or splash erosion, (b) sheet soil erosion, (c) rill soil erosion, (d) gully soil erosion, (e) stream bank soil erosion, (f) soil flow erosion.

Overall, the area most susceptible to soil erosion has a low potential for agriculture and forestry unless soil erosion and soil maintenance were installed to make maximum use of the dominant environmental system in the study area. The potential for grazing and browsing is constantly decreasing due to active soil erosion processes, specifically with deforestation and fires, apart from stream channels and slopes, where high and very high soil erosion occurs. Soil erosion is more evident in the semi-humid and humid regions with rainfall of more than 350 mm, the degree of a steep slope, and mostly silty loam and silty clay loam, as well as in the regions of agriculture, forests, and poor pastures where the thickness of the soil is more than 25 cm to allow rainwater saturation and increase the possibility of soil erosion, Table 14.

Table 14. Data of soil erosion sites selected in Figure 11.

Variables \ Sites	a	b	c	d	e	f
Coordinates	35°42′E 32°32′N	35°39′E 32°31′N	35°42′E 32°18′N	35°49′E 32°33′N	35°39′E 32°17′N	35°37′E 32°23′N
Basin	Taybeh	Ziglab	KufrAnja	Arab	KufrAnja	Rayan
Climate Region(Iar-DM)	Semi-Humid	Semi-Humid	Semi-Humid	Semi-Humid	Semi-Arid	Semi-Humid
Rainfall(mm)	427	426	490	463	350	453
SPI Value	3.5	4.03	6.4	1.6	5.2	4.1
Temperature (C°)	18.8	19.2	17.8	18.4	21.4	20.1
Elevation (m)	330	43	700	520	410	453
Slope(Deg)	10.6	6.2	34.4	22.9	39.8	35.2
Soil Texture	Silty Clay Loam	Silty Clay	Silty Clay Loam	Silty Clay	Silty Clay	Silty Clay
Soil Depth (cm)	72	80	30	120	25	140
Land Use/Land Cover	Pasture	Tree Crops	Forest	Pasture	Forest	Pasture
Erosion Type	Raindrop	Sheet	Rill	Gully	Stream Bank	Soil Flow
Erosion Class	Very High	Very High	Very High	High	Very High	Very High

4. Conclusion

The application of the Analytical Hierarchy Process (AHP), integrated into Geographic Information Systems (GIS) is one of the most important methods for creating soil erosion risk maps. On the one hand, assessing and analyzing soil erosion risk areas in different regions of the world, especially where soil erosion is a dominant phenomenon that has economic, social, and environmental effects. On the other hand, the method used provides a strong database for decision-makers to simulate scenarios of erosion in the region and to plan erosion control interventions. To achieve this goal, the study relied on five factors, slope, land use/land cover, soil texture, rainfall, and SPI for the northern Jordan Valley basin. It was found that the areas with a very high and high risk of soil erosion are about 24.8%, and those with low and very low risk of erosion form about 45.5 % of the total area of the study area.

References

Addis, K., Klik, A. 2015. "Predicting the spatial distribution of soil erodibility factor using USLE nomograph in an agricultural watershed, Ethiopia", International Soil and Water Conservation Research, 3(4):282–290. DOI:10.1016/j.iswcr.2015.11.002

Aher, P., Adinarayana, J., Gorantiwar, S. 2013. "Prioritization of watersheds using multi-criteria evaluation through the fuzzy analytical hierarchy process", Agric Eng Int CIGR J,15(1):11–18.

Aikhuele, D., Souleman, F., Amir, A .2014. "Application of Fuzzy AHP for Ranking Critical Success Factors for the Successful Implementation of LeanProduction Technique", Australian Journal of Basic and applied sciences, 8 (18):399-407.

Al-Adamat, R., Diabat, A., Shatnawi, G.H. 2010. "Combining GIS with multi-criteria decision making for sitting water harvesting ponds in northern Jordan", Journal of Arid Environments, 74, 1471-1477.

Al Raisi, S., Sulaiman, H., Abdallah, O., Suliman, F .2014. "Landfill suitable analysis using AHP method and state of heavy metals pollution in selected landfills in Oman", European Scientific Journal,10(17). DOI: 10.19044/esj.2014.v10n17p%25p

Al-Sababhah, N. 2018 "Assessment of Flood Vulnerability in Arid Basins from a Geomorphological Perspective (Wadi Musa in Southern Jordan: Case Study", Journal of the Faculty of Arts (JFA),78 (7), 267-296.

Al-Sababhah, N., and Alomari, A. 2020. " Runoff Estimation by Using the (SCS-CN) Method with GIS and RS for Wadi Shuieb Watershed", ", Association of Arab Universities Journal for Arts,1 (19), 191-218.

Al-Sababhah, N. 2022. "Development of Landslide Susceptibility Mapping Using GIS Modeling in Jordan's Northern Highlands" Environment and Ecology Research, 10(6): 701-727. DOI: 10.13189/eer.2022.100607.

Andualem, T., Hagos, Y., Kefale, A., Zelalem, B .2020. "Soil erosion-prone area identification using multi-criteria decision analysis in Ethiopian highlands", Modeling Earth Systems and Environment, 6:1407–1418. DOI:10.1007/s40808-020-00757-2

Ayalew, L., Yamagishi, H. 2005. "The application of GIS-based logistic regression for landslide susceptibility mapping in the Kakuda–Yahiko Mountains, Central Japan", Geomorphology,65(2):15–31. DOI: 10.1016/j.geomorph.2004.06.010

Bunruamkaew K (2012) Division of Spatial Information Science, University of Tsukuba, 1 (3).

Burke, I., Lauenroth, W., Riggle, R., Brannen, P., Madigan B., Beard, S., .1999. "Spatial variability of soil properties in the shortgrass steppe: the relative importance of topography, grazing, microsite, and plant species in controlling spatial patterns", Ecosystems, 2(5):422-438. DOI:10.1.1.477.2806&re

p=rep1&type=pdf

Chaudhary, P., Chhetri, S., Joshi K, Shrestha, B., Kayastha, P. 2016. “Application of an Analytic Hierarchy Process (AHP in the GIS interface for suitable fire site selection: A case study from Kathmandu Metropolitan City, Nepal”, Socio-Economic Planning Services: 60 –71. DOI: org/10.1016/j.seps.2015.10.001

Chen, Ch. 2006. “Applying the analytical hierarchy process (AHP) approach to convention site selection”, Journal of Travel Research, 45(2):167 – 174. DOI: org/10.1177/0047287506291593

Danielson, T. 2013. “Utilizing A High-Resolution Digital Elevation Model (Dem) To Develop a Stream Power Index (Spi) For The Gilmore Creek Watershed in Winona County”, Minnesota. Papers in Resource Analysis,15.

Garc´ıa, A. et al. 2021. “Geospatial Analysis of Soil Erosion including Precipitation Scenarios in a Conservation Area of the Amazon Region in Peru”, Applied and Environmental Soil Science, Article ID 5753942, 21 pages. DOI: org/10.1155/2021/5753942

Hook, P., and Burke, I. 2000. “Biogeochemistry in a shortgrass landscape: control by topography, soil texture and microclimate”, Ecology, 81(10):2686-2703. DOI: org/10.1890/0012-9658(2000)081[2686:BIASLC]2.0.CO;2

Jankowski, P., Andrienko, N., Andrienko, G. 2001 “Map-centred exploratory approach to multiple criteria spatial decision making”, International Journal of Geographical Information Science, 15(2):101–127. DOI: org/10.1080/13658810010005525

Joubert, A., Leiman, A., de Klerk, H., Katu, S., Aggenbach, J. 1997. “Fynbos (fine bush) vegetation and the supply of water: a comparison of multi-criteria decision analysis”, Ecological Economics, 22(2):123–140. DOI:org/10.1016/S0921-8009(97)00573-9

Kakembo, V., XangaW., Rowntree, K. 2009. “Topographic Thresholds in Gully Development On the Hillslopes of Communal Areas in Ngqushwa Local Municipality, Eastern Cape, South Africa”, Geomorphology, 110:188–194. DOI: org/10.1016/j.geomorph.2009.04.006

Kasperczyk, N., and Knickel, K. 2006. “The Analytic Hierarchy Process (AHP)”, Available at: www.ivm.vu.nl/en/Images/MCA3_tcm53-161529.pdf

Kourgialas, N., Karatzas, G. 2011. “Flood management and a GIS modeling method to assess flood-hazard areas: A case study”, Hydrological Sciences Journal, 56(2): 212–225. DOI: or g/10.1080/02626667.2011.555836

Malczewski, J. 1999. “GIS and Multi-Criteria Decision Analysis, John Wiley and Sons, New York.https://www.wiley.com/en-us/search?pq=%7Crelevance%7Cauthor%3AJacek+Malczewski

Mhiret, D., Dagnew, D., Assefa, T., Tilahun, S., Zaitchik, B., Steenhuis, T. 2018. “Erosion hotspot identification in the sub-humid Ethiopian highlands”, Ecohydrol Hydrobiol, 19(1):146–154. DOI: org/10.1016/j.ecohyd.2018.08.004

Moore, I., Rodger B., Grayson. 1991. “Terrain-based catchment partitioning and runoff prediction using vector elevation data”, Water Resour, Res,27(6):1177–1191. DOI: org/10.1029/91WR00090

Nefeslioglu, H., Gokceoglu, C., Sonmez, H. 2008. “An assessment on the use of logistic regression and artificial neural networks with different sampling strategies for the preparation of landslide susceptibility maps”, Eng. Geol, 97:171–191. DOI:org/10.1016/j.enggeo.2008.01.004

Ran, Q., Su, D., Li, P., He, Z. 2012. Experimental study of the impact of rainfall characteristics on runoff generation and soil erosion”, Journal of Hydrology 424: 99-111. DOI: org/10.1016/j.jhydrol.2011.12.035

Ribeiro, R. 1996. “Fuzzy Multiple Criterion Decision Making: A Review and New Preference Elicitation Techniques”, Fuzzy Sets and Systems,78(2):155-181. DOI: org/10.1016/0165-0114(95)00166-2

Falkland, A. 1993. “Hydrology and water management on small tropical islands, Hydrology of Warm Humid Regions”,16:263-303.

Saaty, T. 1977. “A scaling method for priorities in hierarchical structures”, Journal of Mathematical Psychology, 15,234-281.

Saaty, T.L. 1984. “The Analytic Hierarchy Process: Decision Making in Complex Environments” In Avenhaus, R., Huber, R.K. (eds) Quantitative Assessment in Arms Control. Springer, Boston, MA.:pp285-308. DOI: org/10.1007/978-1-4613-2805-6_12

Saaty, T. 2008. “The Analytic Hierarchy and Analytic Network Measurement Processes: Applications to Decisions under Risk”, European journal of pure and applied mathematics, 1(1):122-196. DOI:org/10.29020/nybg.ejpam.v1i1.6

Saaty, T. 2008. “Decision making with the analytic hierarchy process”, Int. J. Services Sciences, 1(1):83-98.

Saaty, R. 2016. “Decision making in complex environments: the analytic network process (anp) for dependence and feedback, Katz graduate school of business university of Pittsburgh, Including a Tutorial for the SuperDecisions Software and Portions of the Encyclicon of Applications, Vol. I. https://www.superdecisions.com/sd_resources/v28_man02.pdf

Sinshaw, B et al. 2021. “Prioritization of potential soil erosion susceptibility region using fuzzy logic and analytical hierarchy process, upper Blue Nile Basin, Ethiopia”, Water-Energy Nexus,4:10–24. DOI: org/10.1016/j.wen.2021.01.001

Stewart, T., and Scott, L. 1995. “A Scenario-Based Framework for Multicriteria Decision Analysis in Water Resources Planning”, Water Resources Research, 31(11):2835–2843. DOI: org/10.1029/95WR01901

Tairi, A., Elmouden, A., Aboulouafa, M. 2013. “Soil Erosion RiskMapping Using the Analytical Hierarchy Process (AHP) and GeographicInformation System in the Tifnout-Askaoun Watershed, Southern Morocco”, European Scientific Journal, 15(30):338. DOI:org/10.19044/esj.2019.v15n30p338

Van Dijk, A., Bruijnzeel, L., Rosewell, C. 2002. “Rainfall intensity-kinetic energy relationship: Acritical literature appraisal”, Journal of Hydrology, 261(1–4): 1–23. DOI:org/10.1016/S0022-1694(02)00020-3

Wischmeier, W., Smith, D. 1978. Predicting rainfall erosion losses. A guide to conservation planning”, Trans. Am. Geophys, Union. https://books.google.jo/books?hl=ar&lr=&id=rRAUAAAAYAAJ&oi=fnd&pg=PA5&ots=cvowuRsvSX&sig=wbOIvjkrBLtooBPmESCj9a3D7YE&redir_esc=y#v=onepage&q&f=false

Yasser, M., Jahangir, K., Mohmmad, A. 2013. “Earth dam site selection using the analytic hierarchy process (AHP): A case study in the west of Iran”, Arabian Journal of Geoscience, 6 (9):3417–3426. DOI: org/10.1007/s12517-012-0602-x

Zhu, A., Wang, R., Qiao, J., ZhiQin, Ch., Chen, Y., Liu, J., Du, F., Lin, Y., Zhu, T. 2014 “An expert knowledge-based approach to landslide susceptibility mapping using GIS and fuzzy logic”, Geomorphology,214:128–138. DOI: org/10.1016/j.geomorph.2014.02.003

المملكة الأردنية الهاشمية

صندوق دعم البحث العلمي

الجامعة الهاشمية

المجلة الأردنية
لعلوم الأرض والبيئة

JJEES

مجلة علمية عالمية محكمة

المجلد (١٤) العدد (٢)

http:// jjees.hu.edu.jo/

ISSN 1995-6681

المجلة الأردنية لعلوم الأرض والبيئة

مجلة علمية عالمية محكمة

المجلة الأردنية لعلوم الأرض والبيئة: مجلة علمية عالمية محكمة ومفهرسة ومصنفة، تصدر عن عمادة البحث العلمي في الجامعة الهاشمية وبدعم من صندوق البحث العلمي - وزارة التعليم العالي والبحث العلمي، الأردن.

ترسل البحوث إلكترونيا إلى البريد الإلكتروني التالي:

رئيس تحرير المجلة الأردنية لعلوم الأرض والبيئة

jjees@hu.edu.jo

لمزيد من المعلومات والأعداد السابقة يرجى زيارة موقع المجلة على شبكة الانترنت على الرابط التالي:

www.jjees.hu.edu.jo

المملكة الأردنية الهاشمية صندوق دعم البحث العلمي الجامعة الهاشمية

JJEES

المجلة الأردنية لعلوم الأرض والبيئة

Indexed by Scopus ELSEVIER

المجلد (14) العدد (2)

مجلة علمية عالمية محكمة تصدر بدعم من صندوق دعم البحث العلمي

ISSN 1995-6681 jjees.hu.edu.jo حزيران 2023